Energy Research and Development Division

FINAL PROJECT REPORT

Building a Climate Change-Resilient Electricity System for Meeting California's Energy and Environmental Goals

California Energy Commission

Gavin Newsom, Governor

February 2019 | CEC-500-2019-015

PREPARED BY:

Primary Author(s):

Brian Tarroja
Scott Samuelsen
Amir AghaKouchak
David Feldman
Kate Forrest
Felicia Chiang

Advanced Power and Energy Program
114 Engineering Lab Facility, Bldg. 323
Irvine, CA 92697-3550
949-824-7302
www.apep.uci.edu

Contract Number: EPC-14-074

PREPARED FOR:

California Energy Commission

David Stoms
Project Manager

Aleecia Gutierrez
Office Manager
ENERGY GENERATION RESEARCH OFFICE

Laurie ten Hope
Deputy Director
ENERGY RESEARCH AND DEVELOPMENT DIVISION

Drew Bohan
Executive Director

ACKNOWLEDGEMENTS

The authors acknowledge the following individuals and organizations who contributed to strengthening the analyses in this report:

Daniel Cayan at the Scripps Institution of Oceanography for providing the California downscaled climate inputs for the IPCC AR5 climate scenarios.

Dr. Colin Williams at the United States Geological Survey for providing data on geothermal potential capacities in California.

The LTES team from Lawrence Berkeley National Laboratory and UC Berkeley for providing input on the modeling of residential and commercial buildings.

Energy and Environmental Economics (E3) for providing the year 2050 technology base case to which climate impacts are applied in this study.

PREFACE

The California Energy Commission's Energy Research and Development Division supports energy research and development programs to spur innovation in energy efficiency, renewable energy and advanced clean generation, energy-related environmental protection, energy transmission and distribution and transportation.

In 2012, the Electric Program Investment Charge (EPIC) was established by the California Public Utilities Commission to fund public investments in research to create and advance new energy solutions, foster regional innovation and bring ideas from the lab to the marketplace. The California Energy Commission and the state's three largest investor-owned utilities – Pacific Gas and Electric Company, San Diego Gas & Electric Company and Southern California Edison Company – were selected to administer the EPIC funds and advance novel technologies, tools, and strategies that provide benefits to their electric ratepayers.

The Energy Commission is committed to ensuring public participation in its research and development programs that promote greater reliability, lower costs, and increase safety for the California electric ratepayer and include:

- Providing societal benefits.
- Reducing greenhouse gas emission in the electricity sector at the lowest possible cost.
- Supporting California's loading order to meet energy needs first with energy efficiency and demand response, next with renewable energy (distributed generation and utility scale), and finally with clean, conventional electricity supply.
- Supporting low-emission vehicles and transportation.
- Providing economic development.
- Using ratepayer funds efficiently.

Building a Climate Change Resilient Electricity System for Meeting California's Energy and Environmental Goals is the final report for the Building a Climate Change Resilient Electricity System for Meeting California's Energy and Environmental Goals project (Grant Number EPC-14-074) conducted by the University of California, Irvine. The information from this project contributes to Energy Research and Development Division's EPIC Program.

For more information about the Energy Research and Development Division, please visit the Energy Commission's website at www.energy.ca.gov/research/ or contact the Energy Commission at 916-327-1551.

ABSTRACT

Responding to concerns regarding the environmental effects of the current energy resource mix, significant research has focused on determining the future energy resources to meet emissions reduction and environmental sustainability goals. Many of these studies focus on various constraints, such as costs, grid operability requirements, and environmental performance, and develop different plans for the rollout of energy resources between the present and future years. However, these planning studies have not yet taken into account the potential impact that changing climate may have on the availability and performance of key energy resources that compose these plans. This project investigated climate change impacts on three aspects of the energy system: 1) changes in hydropower generation due to altered precipitation, streamflow, and runoff patterns; 2) changes in the availability of solar thermal and geothermal power plant capacity due to shifting water availability; and 3) changes in the residential and commercial electric building loads from increased temperatures. These impacts would cause the proposed resource scenario for meeting 80 percent reduction in greenhouse gas emissions by 2050 developed by the Energy and Environmental Economics PATHWAYS study to deviate from meeting California's emissions target and renewable energy resources. The study found that the impacts of climate change on energy system performance could be reduced by increasing the flexibility of the system to make more effective use of otherwise excess renewable generation. This project collaborated with two related studies led by Energy and Environmental Economics and Lawrence Berkeley National Laboratory, who used the outputs of these analyses to develop energy resource scenarios that are more resilient against the impacts of climate change.

Keywords: Climate change, greenhouse gas reduction, electric grid, hydropower, renewable energy, electric demand

Please use the following citation for this report:

Tarroja, Brian, Scott Samuelsen, Amir AghaKouchak, David Feldman, Kate Forrest, Felicia Chiang. University of California, Irvine. 2019. *Building a Climate Change Resilient Electricity System for Meeting California's Energy and Environmental Goals*. California Energy Commission. Publication: CEC-500-2019-015

TABLE OF CONTENTS

LIST OF FIGURES

Page

LIST OF TABLES

Page

EXECUTIVE SUMMARY

Introduction

California has set goals to reduce emissions of greenhouse gases that cause climate change and the many related consequences for the economy, public health and safety, and the environment. The most ambitious of these goals at the time of this study calls for reducing these emissions to 80 percent below 1990 levels by 2050. The energy sector (including transportation fuel) is a major contributor of greenhouse gas emissions. Significant progress has been made in reducing the emissions in California's energy sector; however, this progress must accelerate if the 2050 goal is to be achieved. Other studies have modeled alternative scenarios of the mix of energy resources that can meet future electricity load demand and the 2050 goal. These scenarios involve significant use of renewable energy and storage, great improvements in efficiency, and electrification of energy services that are carbon-intensive, such as transportation and space heating. Such studies have helped set a vision for the long-term evolution of the energy system.

Even with rapid reductions in greenhouse gas emissions, the effects of past and current emissions are being experienced and will continue. In the energy sector, climate change is expected to change the amount and timing of some low-carbon energy resources such as hydropower, thermally based renewable resources that require water for cooling, and energy demands associated with heating and cooling buildings. These past energy scenario studies, however, were limited because they did not account for the effects of climate change on the energy system and may have underestimated the additional changes required to achieve the 2050 emissions goal.

Project Purpose

The long-term energy scenarios project resulted in a coordinated portfolio of studies funded by the California Energy Commission and conducted by Energy and Environmental Economics (E3, EPC-14-069), Lawrence Berkeley National Laboratory with University of California (UC) Berkeley (EPC-14-072), and UC Irvine (this study). The teams produced scenarios for the state's electricity sector to achieve the state's goal of reducing GHG emissions to 80 percent below 1990 levels by 2050, while taking into account the potential effects of climate change to the energy system. The UC Irvine group estimated climate impacts on renewable generation and evaluated the effectiveness of adaptation strategies to offset those impacts. The team harmonized assumptions with the other two studies using different modeling tools. E3 provided most of the assumptions to be as compatible as practical with the California Air Resources Board Scoping Plan, while Lawrence Berkeley National Laboratory provided input on the modeling of residential and commercial buildings. The teams investigated whether differences in modeling approaches would result in significantly different outcomes. At the end, the three groups reached similar conclusions with complementary insights. Analysis from the Energy and Environmental Economics PATHWAYS study was used as a key input into a study by a team from Berkeley Economic Advising and Research, which evaluated potential costs and benefits of

these deep decarbonization scenarios to low-income and disadvantaged communities in California.

This project provided an understanding of the specific effects of climate change on the electricity system by midcentury and the implications of those effects for the ability of the system to satisfy California's greenhouse gas reduction target. In the case that an energy scenario does not account for climate change and may fall short of meeting that target, the project team also explored a set of energy technologies and resource management strategies to determine whether they could offset the shortfall. The project generated a more realistic energy scenario for achieving the 2050 target at the lowest cost and provided this information to use in future energy system planning studies for California.

Project Process

First, the researchers interpreted climate change projections relevant to the energy system, in particular, changes in precipitation, runoff, streamflow, and temperature. Water is essential for many types of energy generation. The amount and timing of runoff into hydroelectric reservoirs affect the capacity of these reservoirs to generate electricity and how much can be held back for when that electricity is urgently needed to meet demand (known as spinning reserve). Using knowledge of the climate impacts on hydrology and evaporation, the researchers determined how that would change total hydropower generation, generation profiles through time, and resources for ancillary services such as spinning reserve. Water must also be available to include additional solar thermal and geothermal resources as components of a low-carbon, renewable-based electricity portfolio. The research team used climate-induced changes in water supply to analyze how much these energy technologies could be constrained in the future. Warming temperatures are expected to change electricity demand through a combination of increased demand for cooling buildings in summer and a decreased demand for heating in winter. The research team developed advanced models of the electricity loads of different building types in each climate zone across the state so that the magnitude and profile over time of the electric load demand in 2050 could be estimated more accurately.

This information on changes in electricity supply and demand allowed the research team to model the impacts of these climate-driven effects on greenhouse emission reductions relative to climate and renewable energy goals. A base case scenario without climate impacts was developed in the companion project by E3, designed to achieve the 2050 greenhouse gas emission reduction target. This study applied the existing Holistic Grid Resource Integration and Deployment model, which models the hourly operation of the electricity system and simulates the response of the system to changes in energy technology or environmental-forcing factors such as climate change. The model was run using the assumptions and parameters of that base case scenario to identify differences in results due just to the structure of the two models. The climate change-based effects were then incorporated in the Holistic Grid Resource Integration and Deployment model to determine whether this modified scenario could still achieve the 2050 target. The project team evaluated options for overcoming the effects of climate change on the ability of the electricity system to meet its greenhouse gas goal for 2050. This evaluation focused on two options: 1) increasing the use of battery energy storage and 2)

enabling the electric vehicle fleet to charge the grid when required. These options were selected because they can increase the flexibility of the electricity system by being instantly adjusted to meet the needs of the grid. Increasing renewable energy beyond what the base case scenario proposed was not considered as an option because that scenario had selected the optimal mix of energy generation.

Project Results

Climate Change Impacts on Hydropower Generation

The operational rules for surface water reservoirs with hydropower facilities require sufficient water storage capacity to 1) provide flood control during future storms, 2) manage water releases to ensure year-round water availability, and 3) comply with regulations for environmental flow limits. The climate change analysis indicates a shift in snowmelt and mountain runoff from spring and summer to winter and spring when electricity demand is low. The hydropower modeling showed this early season inflow would tend to increase the amount of water that managers would need to "spill" to avoid dangerous overflow. This shift in the timing of runoff increases the generation earlier in the year by an average of about 10 percent and decreases generation in the summer during the annual peak demand by about 2 percent on average across climate models. The loss of low-carbon electricity must be replaced with more generation from other energy sources. In addition to providing electricity generation, large hydropower units also play a significant role in the ancillary service markets for spinning reserve, for which they are paid. The analysis found that hydropower facility spinning reserve bidding is expected to decrease on average about 13 percent under the climate scenarios and close to 40 percent during a long drought. This potential loss of spinning reserve must also be made up through other energy resources. The study did not consider potential changes in operational procedures for water management that might allow greater or more reliable generation.

Climate Change Effects on Thermally Based Renewable Generation

Certain renewable energy conversion technologies such as solar thermal and geothermal power plants require water for cooling and other facility needs. In almost all cases, the study found that a lack of available water would limit future installable capacity for solar thermal and geothermal electricity generation compared to the base case scenario without climate change effects. For California, the high-quality solar thermal and geothermal resources are concentrated in the Colorado River and South Lahontan regions, so the water balance of these two arid regions is fundamental; however, climate change is projected to intensify the dry conditions of these regions. More potential electricity generating capacity could be installed if generators were to use a more efficient cooling system (that is, dry cooling), but only in regions where there will be some surplus water supply to provide the small amount of water necessary for operations at these generating plants. Future scenarios incorporating water conservation and reductions in regional water demand were shown to increase solar thermal and geothermal capacities than either the business-as-usual case with climate change or the base case without climate change.

Climate Change Impacts on Electricity Demand

Impacts on demand were based on physical modeling of heat loading on residential and commercial buildings. Increased temperatures would increase annual (1-4 percent) and peak electricity demands (3-8 percent) to meet the loads for space cooling, especially for commercial buildings. Overall, however, the total site-level energy demand including electricity and fuel will increase only slightly because the increases for space cooling in summer would be partially offset by 17-22 percent decreases in space heating in winter, the latter of which is met mostly by natural gas in California. The perturbations to the electric load profile will be strongest in Southern California, where the largest populations will experience the largest increases in electric loads under climate change.

Combined Impacts on Electricity System Greenhouse Gas Emissions

These climate change impacts of decreased electricity generation and increased demand mean that strategies to meet the long-term greenhouse gas reduction goal are likely to underestimate the requirements of a midcentury energy system. Making up the difference could increase emissions by about 6 million metric tons of carbon dioxide equivalent per year above the economy-wide target of about 87 million metric tons, or 6.5 percent. This study found lack of available water in geothermal resource areas would be a major driver of emissions increases relative to the no-climate change base scenario, as other energy resources would have to make up this difference in midcentury generation capacity. Climate impacts on hydropower generation and on electricity loads in commercial and residential buildings would lead to relatively small increases in greenhouse gas emissions. This would occur because the increases in electric loads tend to occur during the periods of the day when solar generation is at its peak, and, therefore, these additional loads could be met by the uptake of otherwise excess renewable generation.

Climate Change-Resilient Grid Resource and Technology Portfolios

Whereas the previous step identified the potential shortfall in meeting the 2050 greenhouse gas emission reduction goal, this step focused on evaluating two strategies to determine whether they could make up for the shortfall. The study showed a tenfold increase in the installed capacity of battery energy storage over the base case level could successfully make up this shortfall. Vehicle-to-grid management for all light-duty vehicles could reduce greenhouse gas emissions from the electricity sector to below the no-climate change base case and would enable integration of more renewable energy resources onto the grid. Although a complete adoption of electric vehicles and vehicle-to-grid charging by 2050 seems unlikely, even partial adoption could significantly contribute to increasing the robustness of greenhouse gas emissions reduction strategies against climate change into the electricity system. Estimating the costs of these strategies remains a task for future research.

Benefits to California

The primary benefit of this study was addressing a knowledge gap that has hampered energy planners and policy makers. Previous energy planning studies for the state assumed that future climate would be the same as historical or that climate change would have no impact on the

energy system. This study revealed that feedback from climate change could disrupt strategies designed to meet California's greenhouse gas reduction and renewable energy goals for 2050. The study also found that the potential shortfalls caused by climate change could be overcome with existing technologies, perhaps aided by policy changes. Accounting for the effects of climate change, and finding potential solutions to undesirable outcomes of these effects, are necessary steps for developing energy plans that effectively overcome these effects.

The study provides policy makers and ratepayers a clearer understanding of the importance of water resources, and therefore water conservation and management, in supporting a low-carbon energy system. The effects of water availability on hydropower generation and on the potential expansion of solar thermal and geothermal capacity have implications for grid operation (such as ancillary services) and greenhouse gas emission levels. Strategies for reducing water demand and managing water resources to maximize year-round availability can be important for developing a robust low-carbon energy system.

CHAPTER 1: Introduction

1.1 Background

Significant research efforts have focused on determining the future energy resource mix to meet emissions reduction and environmental sustainability goals, in response to concerns regarding the environmental effects of the current energy resource mix. Relevant policies in California on the response to these concerns at the time of this study include, but are not limited to:[1]

- Senate Bill 350 (De León, Chapter 547, Statutes of 2015) - Clean Energy and Pollution Reduction Act of 2015
- Senate Bill 32 (Pavley, Chapter 249, Statutes of 2016) - State Targets for Climate Pollution
- Executive Order B-30-15 - establish a California greenhouse gas reduction target of 40 percent below 1990 levels by 2030

Many studies have focused on various constraints, such as costs, grid operability requirements, and environmental performance, and developed plans for the rollout of energy resources between the present and future years. Examples include the Energy and Environmental Economics (E3) PATHWAYS study [1], which examined economy-wide technology transformation scenarios for meeting the 80 percent reduction in greenhouse gases (GHG) target by 2050, and studies conducted by University of California Berkeley [2] using the SWITCH model to determine cost-optimal energy technology investments under different policy and technical constraints.

One aspect not yet systematically accounted for in these studies, however, is the set of potential effects that the changing climate may have on the availability and performance of key energy resources that compose these plans. The effectiveness of many components or resources that these plans depend on may be compromised by shifting climate. In particular, this study examines three effects: hydropower resources, regional water availability, and electric load demand. This report follows scientific convention in referring to these as *climate change impacts*.

First, climate change is projected to affect the timing and availability of hydropower resources. Hydropower generation is a key component of a low-carbon and high-renewable electricity

[1] In 2018, Senate Bill 100 (de León, Chapter 310, Statutes of 2018) set a planning target of 100 percent zero-carbon electricity resources by 2045 and increased the 2030 renewables target from 50 percent to 60 percent. On the same day of signing SB 100, Governor Brown signed Executive Order B-55-18 with a new statewide goal to achieve carbon neutrality (zero-net GHG emissions) by 2045 and to maintain net negative emissions thereafter. These goals were established after the analysis for this study was completed.

system because of its ability to provide low-cost electricity; balance the variability of certain renewable resources such as wind and solar; and provide ancillary services that are critical for the reliability and resilience of electricity service. The availability and timing of hydropower generation, however, depend on the long-term trends for precipitation, runoff, and competing needs for water resources and flood control management. Climate change can affect the seasonal timing of precipitation and runoff, as well as the overall availability of water for hydropower generation. Therefore, the potential changes must be accounted for to enable more accurate planning.

Second, the shifts in precipitation from climate change can affect regional water availability, which influences the ability to use renewable resources that depend on water resources for cooling, such as solar thermal and geothermal power plants. Using solar thermal and geothermal can be an important part of a low-carbon energy strategy; however, adequate access to water resources is needed to sustain plant operations. Therefore, the change in availability of usable water for supporting thermally based renewable deployment must be investigated.

Third, climate change is projected to cause increases in average and extreme ambient air temperatures. These temperature shifts have strong implications for the shape and magnitude of electric load demand in the future. Higher ambient air temperatures may cause increases in electric loads due to increased space cooling in hot regions. Furthermore, an increase in temperatures in historically cooler regions will cause more occupants to begin using air conditioning and add to space cooling loads. This change in demand for space cooling units will in turn increase the magnitude and peaks of the electric loads that low-carbon energy resources must meet and, therefore, the scale to which they must be used.

This project focused on addressing the following research questions:

- How might climate change affect the ability of the future electricity system to support California's year 2050 GHG emissions reduction goal?
- What adjustments can be made in planning the future electricity system to increase the robustness of the electricity system to support long-term GHG emissions reductions in the state?

1.2 Project Overview

This study focuses on assessing and characterizing these impacts and the effects they will have on the ability of the electricity system to meet the associated long-term goals for greenhouse gas (GHG) emissions reduction and renewable resource use. The study determined climate change impacts for the electricity system and the steps necessary for building resilience against these impacts on the system. This project included: (1) identifying, characterizing, and quantifying the impacts of climate change-affected atmospheric and hydrological conditions on electricity system generation, renewable potential, and demand; (2) determining the implications for meeting GHG reduction and Renewables Portfolio Standard (RPS) targets; and (3) developing solutions to address these impacts.

1.2.1 Project Goals, Objectives, and Approach

The primary goals of this project were to:

- Provide an advisory understanding regarding the specific impacts of climate change on the electricity system, the extent of these impacts, and related implications for the ability of the system to satisfy the state's GHG reduction and RPS targets.
- Provide a base of information for utilities and policy makers to build an electricity system that is resilient to the impacts of climate change and capable of meeting the state's environmental and energy targets.

To achieve these goals, the research conducted under this effort is composed of meeting several objectives, each corresponding to a primary technical task of the project:

1) **Identify projected spatially and temporally resolved changes in precipitation, runoff, streamflow, and ambient temperature due to climate change.**
   The study identified projected changes to these atmospheric conditions in 2050 by examining the output of global climate models as downscaled to California for climate change scenarios outlined in the IPCC 5th Assessment Report [3].

2) **Develop projected impacts of climate change on the performance and behavior of the hydropower electric generation fleet.**
   Using knowledge of the projected impacts of precipitation, runoff, and streamflow changes on hydropower reservoir inflows, the study assessed the projected relationship of temperature on reservoir evaporation and minimum fill levels for these reservoirs and the projected impact of climate change on total hydropower generation, temporal generation profiles, and ancillary service provision.

3) **Develop projected impact of climate change on the capacity potential and behavior of solar thermal and geothermal renewable resources.**
   Using projections of the climate change-affected precipitation and runoff in combination with the drought model, the team developed projections of the maximum allowable water consumption in high solar thermal and geothermal resource areas. Combining this with knowledge of power plant water consumption, the researchers identified the water-constrained capacity potential of solar thermal and geothermal resources in California. The team also used information about lands where energy development is allowed and land-use requirements by different power plant types to determine land-use-constrained solar thermal and geothermal resources.

4) **Develop projections of the impact of climate change on electricity demand for California.**
   The research team developed representative models of residential and commercial buildings and simulated the related electric loads in response to climate change-affected temperature anomalies. This was carried out for different climate zones across the state. With knowledge of the electric loads in these population centers and the contribution of residential and commercial loads to this total, the team developed projections of the change in the magnitude and profile of the electric load demand.

5) **Assess the combined effect of the identified impacts on statewide electricity system GHG emissions and renewable use performance of currently projected strategies for meeting GHG reduction and RPS targets.**
Using the Holistic Grid Resource Integration and Deployment (HiGRID) model, the team evaluated the performance of the base case grid resource and technology portfolios that are able to meet GHG and RPS targets for 2050 without taking into account climate change, under the combined effects of climate change on different components of the electricity system. The researchers then quantified performance in terms of greenhouse gas emissions and renewable penetration level. *Renewable penetration level* refers to the percentage of the yearly electric load that is satisfied by renewable energy resources.

6) **Identify and evaluate modifications to strategies for meeting GHG reduction and RPS targets that resist the impacts of climate change on the electricity system.**
From the understanding gained in the previous objective, the researchers developed scenarios with modifications to the grid resource and technology portfolio such that GHG and RPS targets can be met for 2050 based on objectives including minimum cost.

The overall approach to the project is presented in Figure 1.

Figure 1: Overall Project Approach

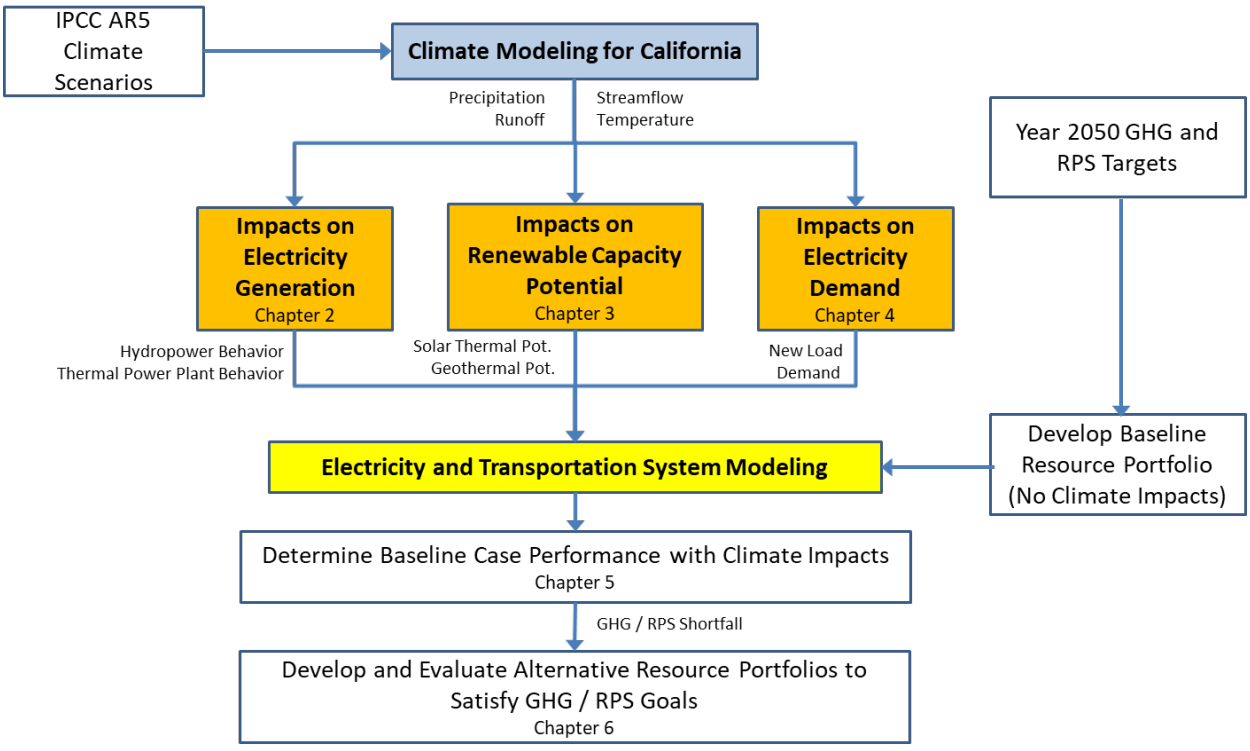

Source: Advanced Power and Energy Program, University of California Irvine

It is important to note that for all of the analyses presented here, it is assumed that California's electric load is primarily met by in-state resources, with the exception of a fixed amount of unspecified imports as defined by the E3 PATHWAYS study. The effects of climate change are examined over California's geographic boundary only, and the amount of imported electricity utilized by the California electricity system is assumed to not change between the different climate scenarios (under historical climates and under each of the climate change models and Representative Concentration Pathways (RCPs).

1.2.2 Coordination With Other Research Groups

This project is one of three awarded by the California Energy Commission as part of the Long-Term Energy Scenarios (LTES) effort, which seeks to understand the effect of climate change on the planning of California's energy system to meet long-term environmental goals. As such, this project is part of the larger LTES framework and interacts with parallel but complementary efforts from Lawrence Berkeley National Laboratory (LBNL) and E3. The coordination among the three research teams is presented in Figure 2.

Figure 2: Coordination Among LTES Research Teams

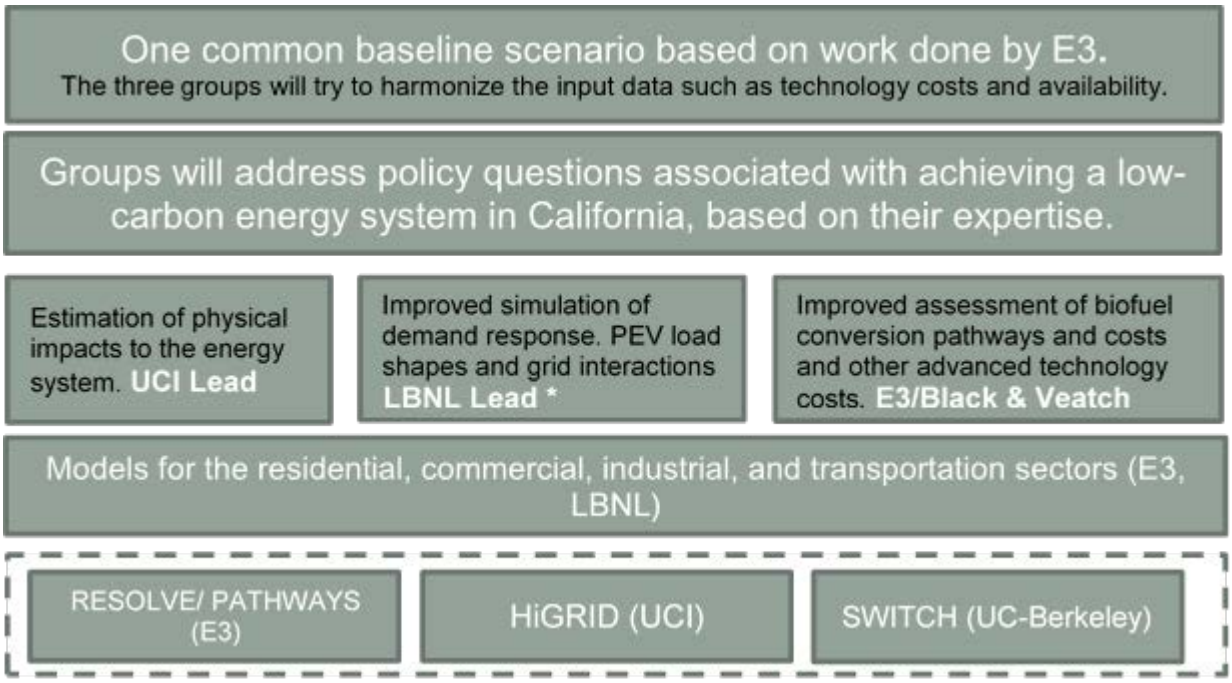

Source: California Energy Commission

In addition, analysis from the Energy and Environmental Economics PATHWAYS study was used as a key input into a study by a team from Berkeley Economic Advising and Research, which evaluated potential costs and benefits of these deep decarbonization scenarios to low-income and disadvantaged communities in California.

The UC Irvine (UCI) team in particular focused on estimating the physical impacts to the energy system due to climate change and provided that information to LBNL and E3 for energy system planning studies. While the three teams conducted energy system modeling studies, the

perspective of the UCI research focused on quantifying the effects of climate change on the performance of the system and potential options to address them. The LBNL and E3 teams incorporated this information to determine optimal or preferred planning of the energy system, taking into account other factors such as energy cost.

1.3 Summary of Atmospheric Conditions Under Climate Change

The onset of climate change is projected to alter the magnitude and spatiotemporal patterns of atmospheric conditions such as precipitation and temperature across the state. A short summary of these changes is included to place the main results of this study into context. For detail on this topic, refer to Appendix B.1. These results are derived from the Localized Construction Analogs (LOCA) downscaled Coupled Model Intercomparison Project 5 (CMIP5) projections for California.

Total precipitation in 2045-2055 in the state is expected to increase relative to the reference period 2010-2020, but impacts to individual regions of the state will vary. The northern areas of California are projected to experience statistically significant increases in precipitation. The Central Coast and Central Valley areas of the state are projected to have relatively unchanged total precipitation, while the southern regions of the state are projected to have slightly decreased precipitation on the coasts and relatively unchanged precipitation in the inland areas (summarized from [62]). However, the form of precipitation is expected to shift to less snowfall and more rainfall. The spatial distribution of precipitation changes, along with changes in its form, will have implications for impacts on hydropower generation, described in Chapter 2, and water availability for thermal renewable power plants, described in Chapter 3. Regarding temperature, the average daily temperature is expected to increase in all regions of the state by about 1.6 to 2 degrees Celsius by midcentury, with the largest increases occurring in the southern inland areas of California summarized from [62]).

The projected temperature increases, however, introduce spatially disproportionate effects on cooling degree days and heating degree days in different regions of California (summarized from [62]). Specifically, while heating degree days are expected to decrease significantly in all regions of the state, the inland northern regions, which have historically experienced the coldest temperatures, are projected to experience the largest decrease. In general, the northern regions are projected to experience larger decreases in cooler temperature days, while the southern regions are projected to experience smaller decreases. For cooling degree days, however, the spatial trend is the opposite. The southern regions of the state, particularly the inland areas, are projected to experience significant increases in cooling degree days from the increased temperatures. Generally, the southern regions experience higher cooling degree days than the northern regions of the state. The changes in cooling and heating degree days will have implications for building energy demand, as described in Chapter 4.

1.4 Key Findings of the Project

The major analyses and results for the different aspects of this project are presented in Chapters 2 through 6. The main takeaways that can be abstracted from these results and conclusions are summarized into overall key findings presented here.

1. Climate change may only have small effects on annual California hydropower generation potential, but it will increase seasonal hydropower generation variability and limit the ability of the hydropower system to provide ancillary services.

2. Climate change effects on water availability could constrain the capacity of new solar thermal and geothermal resources that could be installed in California.

3. Climate change impacts on ambient weather conditions will significantly increase residential and commercial electric loads on both an annual and peak load basis in California but will cause little to no change in total site level (combined electricity and natural gas) energy use.

4. Climate change impacts on the electricity system are projected to cause current electricity resource use strategies for meeting the 2050 greenhouse gas reduction goal to fall short of achieving the intended reductions by 3.94 million to 5.94 million metric tons (21.8% to 32.9% of the emissions in the 2050 case without climate change) of carbon dioxide equivalent (CO_2e) per year.

5. The shortfall in greenhouse gas reductions in current electricity resource use strategies when accounting for the effects of climate change can be addressed by increasing the flexibility of the electricity system. Strategies to do so include capturing more effectively otherwise excess renewable generation through increased deployment of energy storage and intelligent electric vehicle integration.

Overall, the analyses summarized in this report suggest that climate change will impact the effectiveness of electricity system operation and planning efforts for meeting California's 2050 greenhouse gas reduction goal. However, these impacts can be addressed through slight adjustments of electric grid resource mix scenarios. The following chapters of this report and the supporting appendices present details of the analyses that give rise to these key findings.

CHAPTER 2:
Assessing Climate Change Impacts on Hydropower Electricity Generation

2.1 Introduction and Background

Climate change is projected to shift the availability of water in both timing and location. In California, where hydropower provides roughly 7 to 24 percent of in-state electricity generation [4], shifts in regional hydrology may have a significant impact on electricity generation and achieving statewide emission reduction targets.

Most of California's hydroelectric capacity originates from the Sierra Nevada, with inflow to reservoirs historically regulated by the melting snowpack. The slow release of water, peaking in spring, allows hydropower plants to deliver important load-following and peak support throughout the year, most critically during the summer months when electricity demand is high. This support has become increasingly important as the portion of variable renewable generation on the grid has grown [5]. Hydropower also provides key ancillary services, such as spinning reserve [6]. *Spinning reserve* refers to available capacity that power plants (such as a hydropower facility) commit to providing additional electricity generation that can be called upon to compensate for the impacts of a contingency event (e.g., a failure or removal from operational service) that compromised the functionality of a major generation facility or transmission line on the electric grid.

Projected temporal and spatial shifts in hydrology may jeopardize the ability of hydropower to provide these services. Simulations of climate warming have shown a wide range of potential impacts on precipitation depending on climate model assumptions, particularly concerning wet versus dry warming; however, climate projections tend to agree that warming will result in seasonal shifts in runoff, a decreased snowpack, and increased winter runoff in California [7-9]. Under this new regime, reservoirs are expected to reach capacity earlier in the year, and the faster-paced fill may result in increased spilling for reservoirs with limited storage capacities. Higher inflow in winter may yield higher hydropower generation during those months. However, shifts in precipitation may require dam operators to spill more water in the spring to avoid dangerous overflow, leaving less water available in summer months for hydropower generation.

In the case of wet warming, increased spill events, or controlled releases of water, may be offset by overall increases in precipitation; however, in the case of dry warming, where total runoff is projected to decrease, summer hydropower generation is at greater risk [7]. Where generation from hydropower declines, other dispatchable resources such as natural gas will need to make up the difference. During the most recent drought, California relied heavily on cheap natural gas to provide load-following, peaking, and ancillary services in the absence of hydropower potential [10, 11]. Increased reliance on fossil fuels during droughts may affect efforts to

achieve the state's objective to reduce emissions from these resources. The effect of hydropower changes combined with other climate impacts to the generation portfolio is discussed in Chapter 5.

Several studies have previously examined the potential impact of climate change on hydropower in California [12-15]. Most of the previous studies focused on single or select regions in California. Comparing these studies, it can be observed that the magnitude of change varies spatially, with some regions being more susceptible to climate forcing. Madani et al (2014) [12] found that high-elevation hydropower with low reservoir capacities and high hydraulic heads are sensitive to small shifts in runoff, leading to notable impacts on hydropower operations under climate change conditions. Vicuna, Dracup, and Dale (2011) [15] found that Northern and Southern California hydropower experience different degrees of warming and changes in precipitation under climate change, with Southern California experiencing greater annual reduction in runoff.

Predictions on total runoff changes varies between studies, with some climate models projecting reduced total runoff [15], whereas other models project increased total runoff [7]. Nevertheless, earlier runoff peaks are predicted in both wet and dry warming scenarios [15]. Shifts toward earlier runoff have implications for hydropower as they lead to a greater likelihood of spill events.

The effect of climate change on regional hydrology does not directly translate to impacts on hydropower. Hydropower units have varying degrees of flexibility to capture, store, and dispense available water based on demand. Systems with large storage capacities see little to no impact to increased runoff during winter and spring [16], as they have the ability to manage the increase in inflow into the reservoirs. On the other hand, systems with small storage capacities can see a greater impact, with higher rates of spillage leading to decreased generation potential, especially during summer [12].

In addition to providing electricity generation, large hydropower also plays a significant role in the ancillary service markets such as spinning reserve. Data on the contribution of individual hydropower plants to ancillary services are limited [6, 17, 18]. In general, hydropower plants associated with large reservoirs fully participate in ancillary service markets since these facilities often have enough water volume that can be dispensed on demand without compromising the ability of these facilities to perform the intended role for the water infrastructure (that is, flood control, long-term water storage). In contrast, plants with small reservoirs have limited participation because releasing water on demand may significantly decrease reservoir levels and, therefore, the ability of these plants to perform the intended function for the water infrastructure. Furthermore, run-of-the-river plants, which have no storage capacity, cannot participate in ancillary service markets since these facilities do not have control over when water is released through them [19]. Available data for the hydropower units owned by the U.S. Bureau of Reclamation support this generalization, showing Trinity (large storage capacity) participating, while Keswick (small reservoir) has no participation in the spinning reserve markets [18]. Restrictions for participating in ancillary services include, but are not limited to outflow constraints, reservoir capacity, and pricing versus operating costs

[17]. Reservoir conditions, which can change daily, seasonally, and annually, affect participation in ancillary services. California Independent System Operator (California ISO) market reports indicate that high hydropower production in spring can result in reduced ancillary market participation in summer [11].

Previous studies examining the future of hydropower participation in ancillary services focus mostly on new management and market strategies to increase hydropower participation in ancillary service markets without modeling or, in most cases, even considering potential climate forcing changes to hydropower dispatch [19-23]. There is a gap in understanding how climate change impacts may influence ancillary service participation, assuming historical market strategies.

To carry out the analysis in this chapter, the team developed a model of large hydropower plants in California. This model consists of a water reservoir fill-and-release module, which determines the operation of hydropower reservoirs based on inflow, reservoir constraints, and water demand, and an electric dispatch module, which determines the response of a hydropower plant to grid conditions while constrained by water release concerns. This two-part simulation model is applied to large (P > 30 MW) hydropower plants in the state and the corresponding reservoirs, under historical inflow conditions and those altered by climate change to determine the response of California's hydropower system to climate change. For large hydropower plants not associated with a reservoir, these are simulated as run-of-the-river. Detail on the method described is presented in Appendix A.1.

2.2 Results and Analysis

The primary results presented in this report focus on climate change impacts associated with the RCP 8.5 climate scenario set. Results for the RCP 4.5 climate scenario set are presented in Appendix B.2.

2.2.1 Hydrology Shifts Under Climate Change Conditions

The average annual total inflow for years 2046-2055 increased compared to the historical time range (2000-2009) for all models. CanESM2 and CNRM-CM5 saw the most significant increase at 60% and 87% higher, respectively. Average annual inflow under the HadGEM2-ES and MIROC5 models also increased but to a lesser degree. Again, these increases did not occur uniformly across the year. Looking purely at the average seasonal inflow compared to the historical baseline, the greatest increase occurred in winter, followed by spring (Figure 3). Inflow decreased for half the models, namely HadGEM2-ES and MIROC5, during the summer and fall. The CanESM2 and CNRM-CM5 scenarios for RCP 8.5 show higher average inflow compared to their counterparts for RCP 4.5; however, HadGEM2-ES and MIROC5 show lower average inflow for RCP 8.5 than for RCP 4.5.

Figure 3: Projected Average California Seasonal Inflow for 2046-2055 as a Percentage of Historical (2000-2009) Inflow (100%) for All RCP 8.5 Scenarios

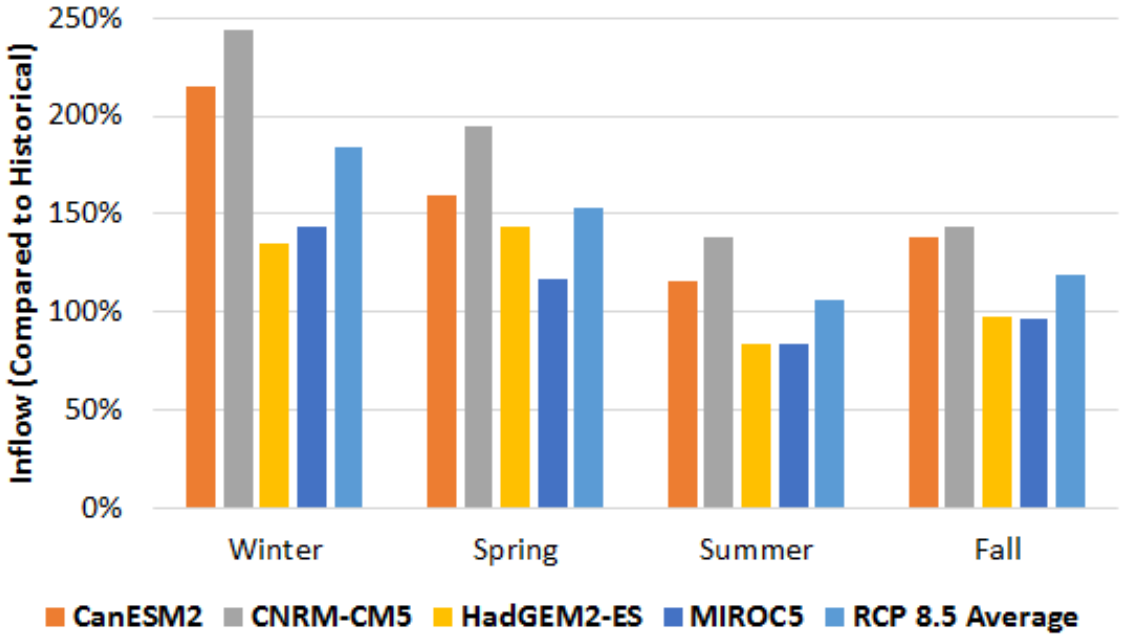

Source: Advanced Power and Energy Program, University of California Irvine

All the RCP 8.5 scenarios show that, on average, projected inflow (2046-2055) increased during the first part of the year, extending into May (Figure 4). CanESM2 and CNRM-CM5 show increased inflow during the summer, although to a lesser degree than during the winter months. HadGEM2-ES and MIROC5 show a slightly decreased inflow on average during the summer compared to the historical baseline (2000-2009).

Figure 4: Projected Average California Monthly Inflow for All RCP 8.5 Scenarios for 2046-2055 Compared to Historical Inflow (2000-2009)

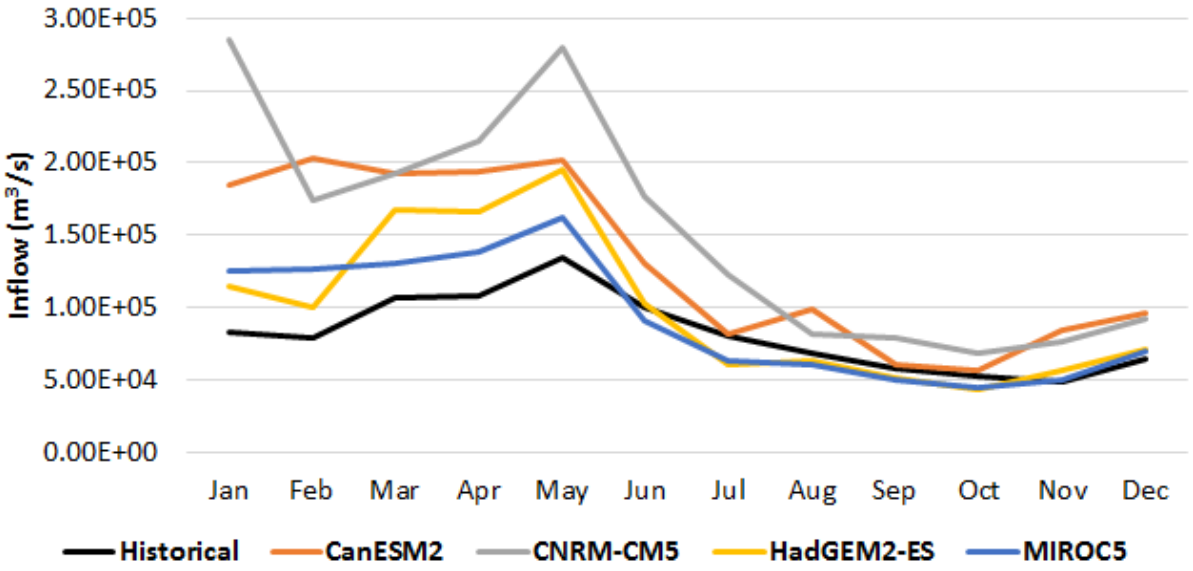

Source: Advanced Power and Energy Program, University of California Irvine

There remains significant inter-annual variability in the magnitude of inflow under climate change, especially during the winter and spring. In fact, differences in projected California seasonal inflow across years increase for most RCP 8.5 scenarios (Figure 5). All RCP 8.5 scenarios show increased variability (as characterized by range, interquartile range, variance, and standard deviation) during spring and fall. CanESM2, CNRM-CM5, and HadGEM2-ES RCP 8.5 scenarios have variability increasing in winter as well, and half the scenarios, CanESM2 and CNRM-CM5, have variability increasing in summer. The greatest variability occurs in winter for the CanESM2 and CNRM-CM5 RCP 8.5 scenarios. The most pronounced example is CNRM-CM5, in which one winter receives only 40% of the 10-year average winter inflow, while another winter receives 300%.

Figure 5: Boxplots for California Historical Inflow (2000-2009) and Projected Inflow (2046-2055) for All RCP 8.5 Scenarios

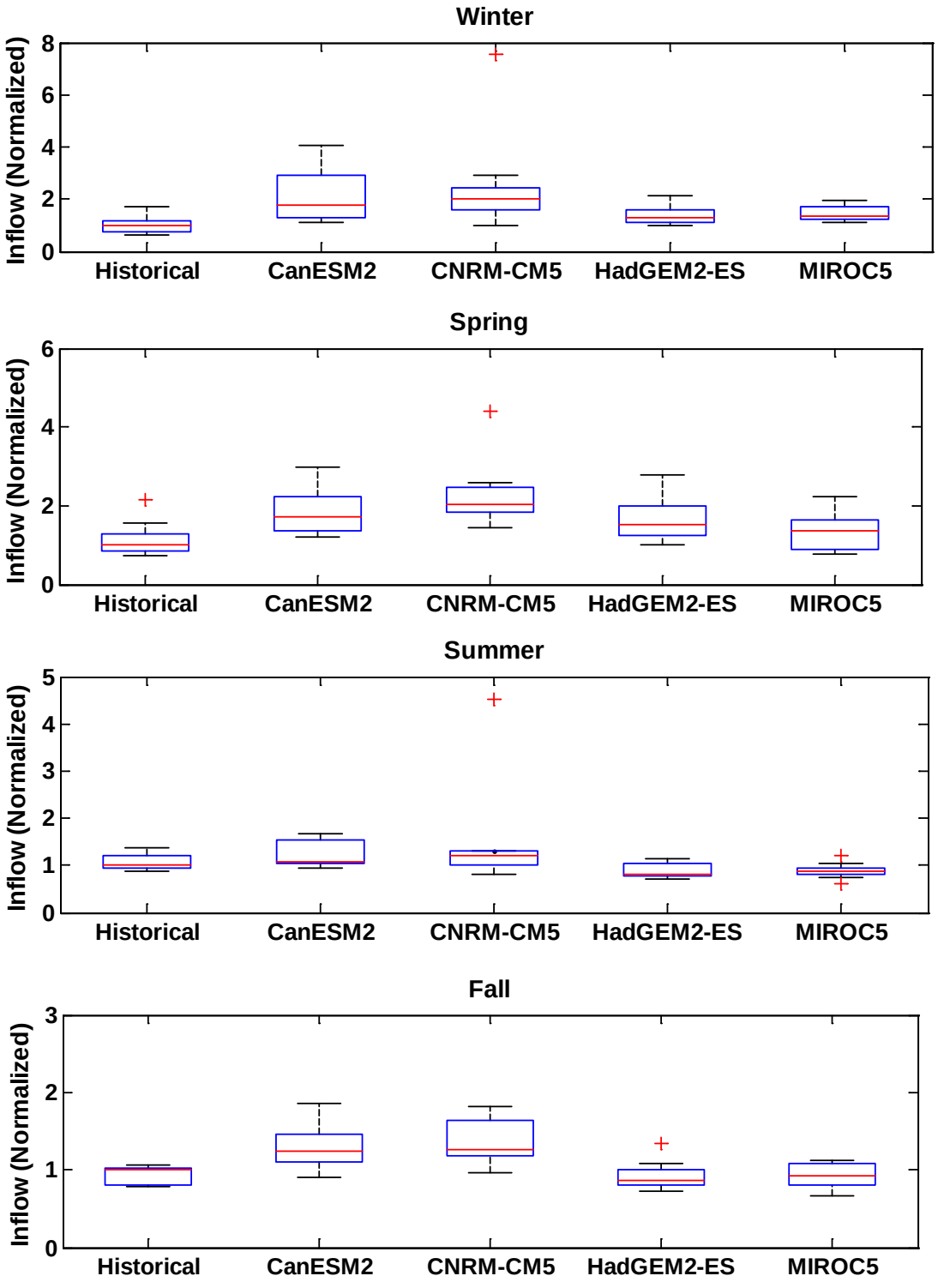

Each season is normalized based on the historical median for that season.

Source: Advanced Power and Energy Program, University of California Irvine

2.2.2 California Hydropower Generation Trends Under Climate Change

Despite average annual inflow increasing for all climate models, this trend does not necessarily translate into increased hydropower generation in California. CanESM2 and CNRM-CM5 show higher average annual generation for 2046-2055 compared to historical (both up 15%), and HadGEM2-ES and MIROC5 show slightly lower (down 4% and 3%, respectively) (Figure 6). There is increased spilling for all RCP 8.5 scenarios. Despite increased total inflow for HadGEM2-ES and MIROC5, net generation is lower than the historical period due to increased spill events. This is due to the increase in inflow during winter and spring compared to later in the year. The increased concentration of inflow during these months leads to a greater number of events in which outflow levels exceed hydropower capacity; specifically, spills occur, and not all flow through the hydropower unit can be used for electricity generation. This pattern is most significant for the RCP 8.5 scenario CNRM-CM5, in which only slightly more than half of potential generation is actually realized.

Figure 6: Projected RCP 8.5 California Hydropower Generation (2046-2055) Compared to Historical (2000-2009) Generation (100%) for Theoretical Generation Based on Total Inflow Versus Net Generation

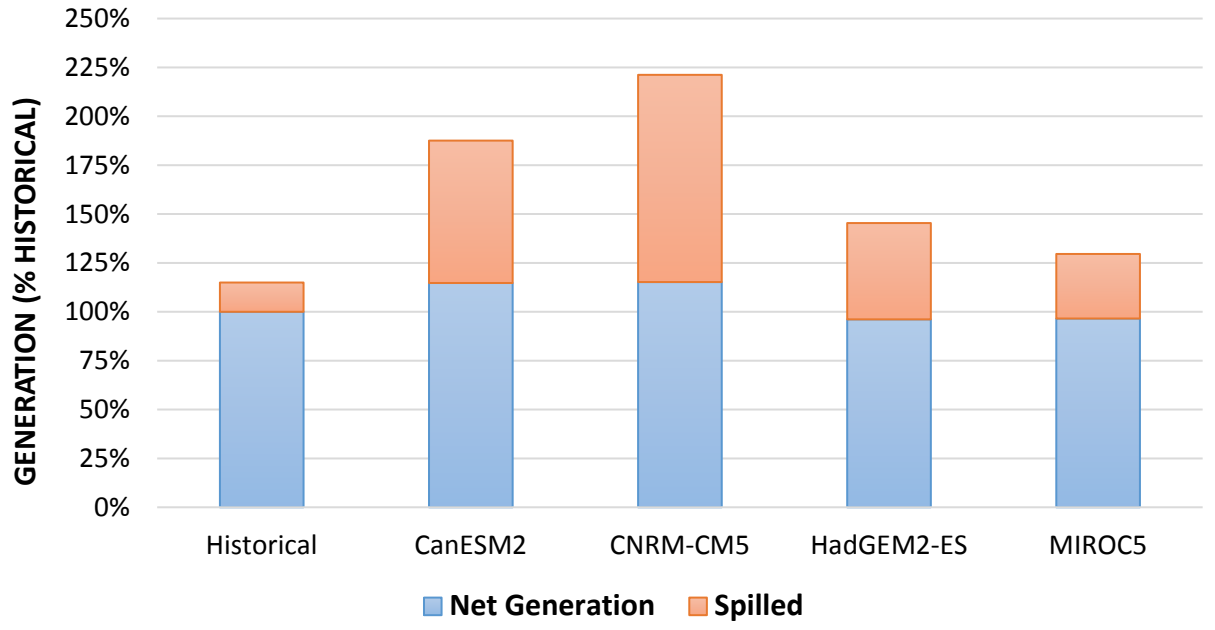

Spilled is the amount of generation lost due to spills. Total theoretical generation is the sum of net generation and spilled if total available inflow was used for electricity generation.

Source: Advanced Power and Energy Program, University of California Irvine

Figure 7 depicts projected California seasonal generation (2046-2055) for all models under the RCP 8.5 scenario. When comparing seasonal inflow versus generation, in general, higher inflow results in higher generation, while lower inflow results in lower generation. However, the effect of increased inflow during winter and spring on generation is limited by maximum outflow/hydropower capacity constraints. Increased inflow during these seasons also results in increased outflow through spillways, meaning that increased flow does not directly translate

into increased generation. For example, for the RCP 8.5 scenarios HadGEM2-ES and MIROC5, projected average inflow during winter and spring increases by 20-40% compared to the historical period (2000-2009), but average generation stays very close to historical (increases less than 2%).

For the RCP 8.5 scenarios CanESM2 and CNRM-CM5, projected average California hydropower generation during winter and spring increases by roughly 20% compared to historical for both CanESM2 and CNRM. CanESM2 and CNRM-CM5 also show increased California hydropower generation during summer and winter, while HadGEM2-ES and MIROC5 show decreased generation during the same period.

Figure 7: Projected Average California Seasonal Hydropower Generation (2046-2055) for All RCP 8.5 Scenarios Compared to Historical (2000-2009) Hydropower Generation (100%)

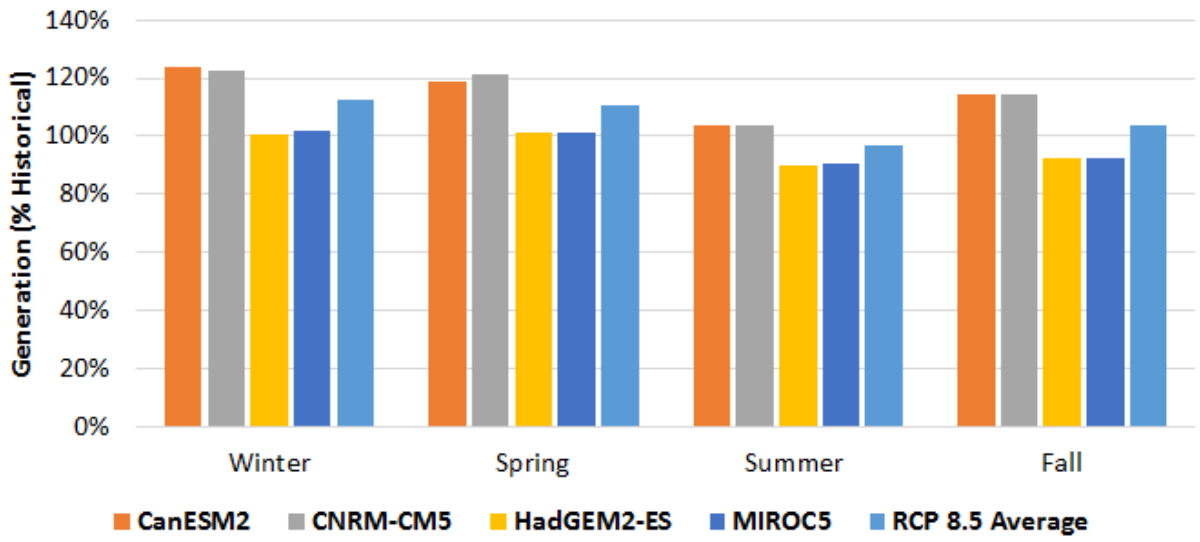

Source: Advanced Power and Energy Program, University of California Irvine

Examining total projected (2046-2055) California monthly hydropower generation for the different models shows that CanESM2 and CNRM-CM5 predict higher monthly generation on average. HadGEM2-ES and MIROC5 predict similar generation levels compared to historical (2000-2009) for December to May but a decrease in generation for the latter half of the year (Figure 8).

Figure 8: Projected Monthly California Hydropower Generation for All RCP 8.5 Scenarios-Mean and Range for Years 2046-2055

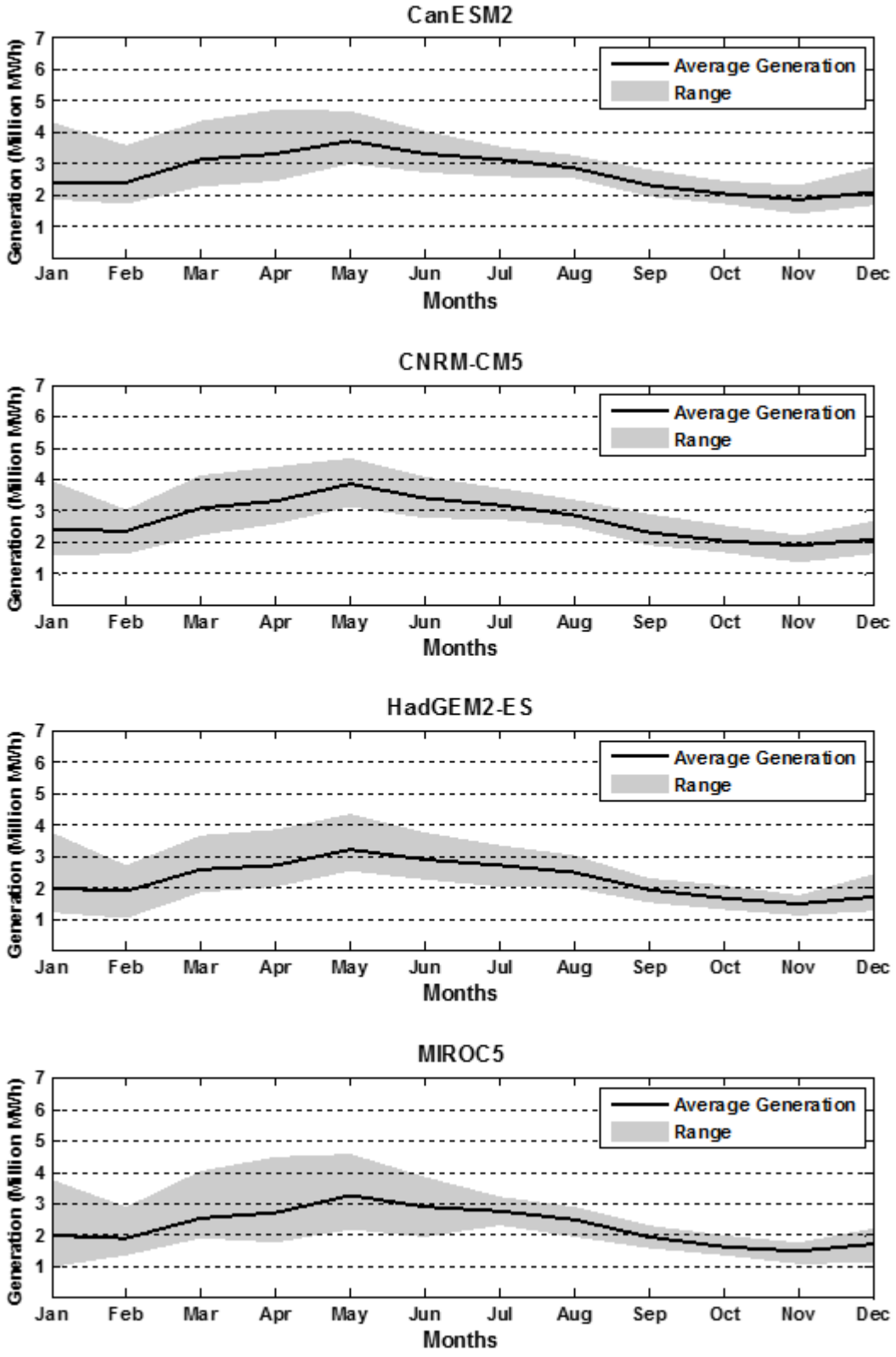

Source: Advanced Power and Energy Program, University of California Irvine

Under the different model projections for 2046-2055, peak hydropower generation still occurs around May on average, as it does under the historical (2000-2009) baseline. However, the model projections differ in that the generation then drops off quickly throughout the summer (Figure 9). Projected California hydropower generation output drops to about 75% of peak generation by August for all models, while in the historical period, generation remains around 95% of peak through July and above 85% by August. Lower percentages compared to peak generation persist through December. This behavior switches around the beginning of the year, with monthly average generation between January and May slightly exceeding the historical generation levels.

Figure 9: Projected Average California Monthly Hydropower Generation (2046-2055) as a Percent of Annual Peak for Historical Hydropower Generation (2000-2009) and All RCP 8.5 Scenarios

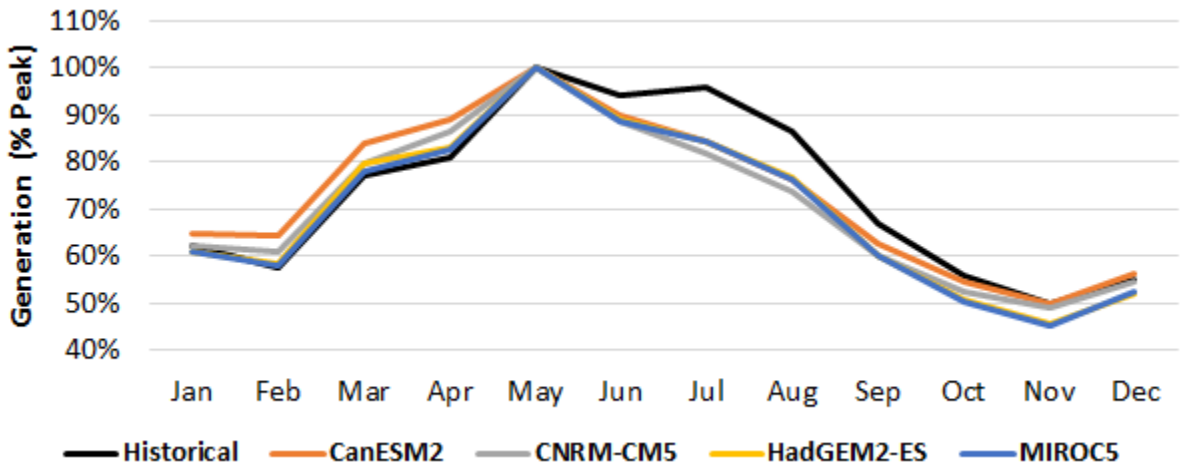

Source: Advanced Power and Energy Program, University of California Irvine

This overall trend occurs for all RCP 8.5 scenarios, even though CanESM2 and CNRM-CM5 project higher average peak California hydropower generation for May, and HadGEM2-ES and MIROC5 project lower average peak California hydropower generation for May. All scenarios have a greater portion of the year's inflow occurring in the beginning of the year. For CanESM2 and CNRM-CM5, inflow during the summer remains around historical levels; this shift correlates to a net lower ratio of average hydropower generation during the summer months versus the May peak. For HadGEM2 and MIROC5, winter hydropower generation remains around historical levels due to increased spilling, and summer generation decreases, related to decreased inflow during those months. The net effect is lower projected California hydropower generation compared to the peak in the later summer months, as inflow from earlier in the year is not retained.

2.2.3 Projected California Ancillary Service Trends Under Climate Change

Changes in projected (2046-2055) spinning reserve bidding for the dispatchable California hydropower units were found for all RCP 8.5 scenarios. Higher generation bids result in decreased spinning reserve potential, limited by both maximum capacity and reservoir

constraints. Projected increases in California hydropower generation and shifting precipitation and runoff, especially during spring, would result in a net decrease in hydropower spinning reserve bids for RCP 4.5 and RCP 8.5.

Projected (2046-2055) average California hydropower spinning reserve bidding decreases for all RCP 8.5 scenarios across all seasons, with spring having the greatest average reduction (-21% to -14%), followed by summer (Figure 10). The projected average annual bidding for spinning reserve decreased about 13% compared to the historical period (2000-2009). Spinning reserve bidding is similar among the different RCP 8.5 scenarios, showing similar levels of decline for each season.

Figure 10: Projected Average California Hydropower Spinning Reserve Bidding (2046-2055) as a Percent of Historical (2000-2009) for All RCP 8.5 Scenarios

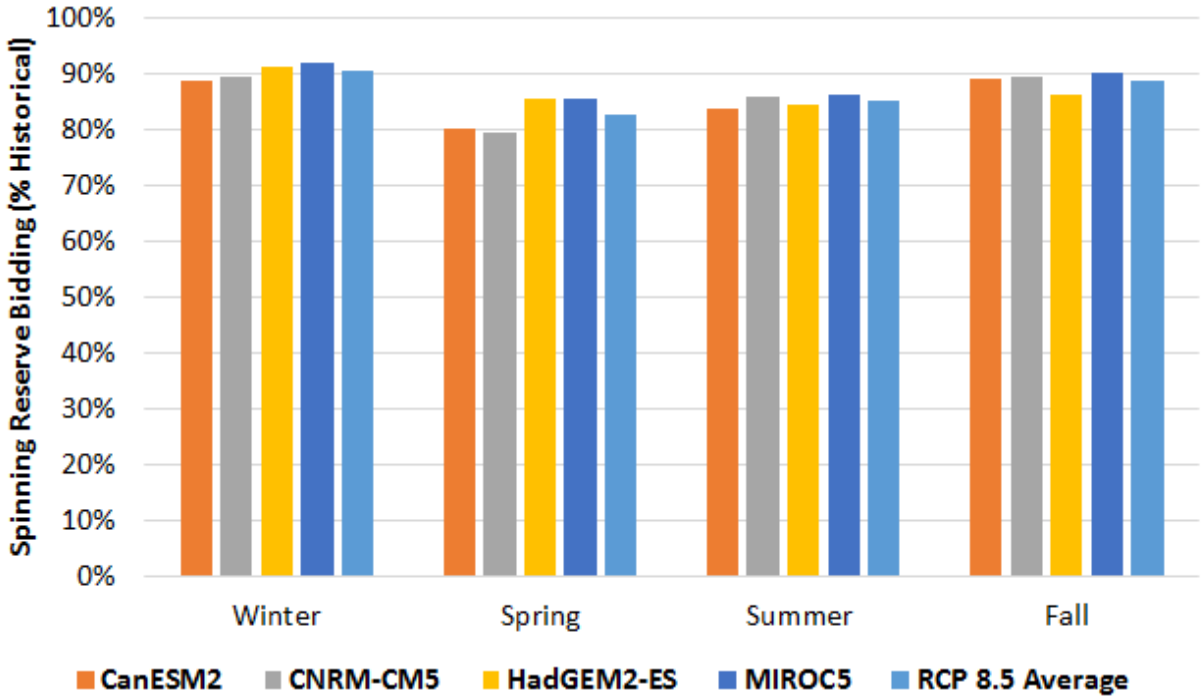

Source: Advanced Power and Energy Program, University of California Irvine

All RCP 8.5 scenarios project an increase in the number of days for which the bids for generation and spinning reserve were less than the combined rated capacity of the participating hydropower units (Figure 11). In addition to an increase in the number of days for which one or more hydropower units exhibit decreased spinning reserve, there is an increase in the number of hydropower units that simultaneously experience reservoir constraints that limit spinning reserve potential.

Comparing the different scenarios for RCP 8.5, CanESM2 and CNRM-CM5 project an average increase in generation bids, resulting in a net decrease in spinning reserve potential. This increase in projected California hydropower generation has the greatest impact during spring. Projected spinning reserve bids are further decreased due to increased frequency of hydropower units experiencing reservoir constraints limiting spinning reserve bids.

For the RCP 8.5 scenarios HadGEM2-ES and MIROC5, however, projected (2046-2055) average California hydropower generation and spinning reserve bids decrease (compared to 2000-2009), indicating that diminished bids are the result of increased frequency of periods in which hydropower units would experience decreased outflow and decreased reservoir storage. This combination results in projections for decreased generation and decreased spinning reserve bids.

Figure 11: Projected Daily Average California Hydropower Spinning Reserve Bids Versus Generation Bids for All RCP 8.5 Scenarios (2046-2055)

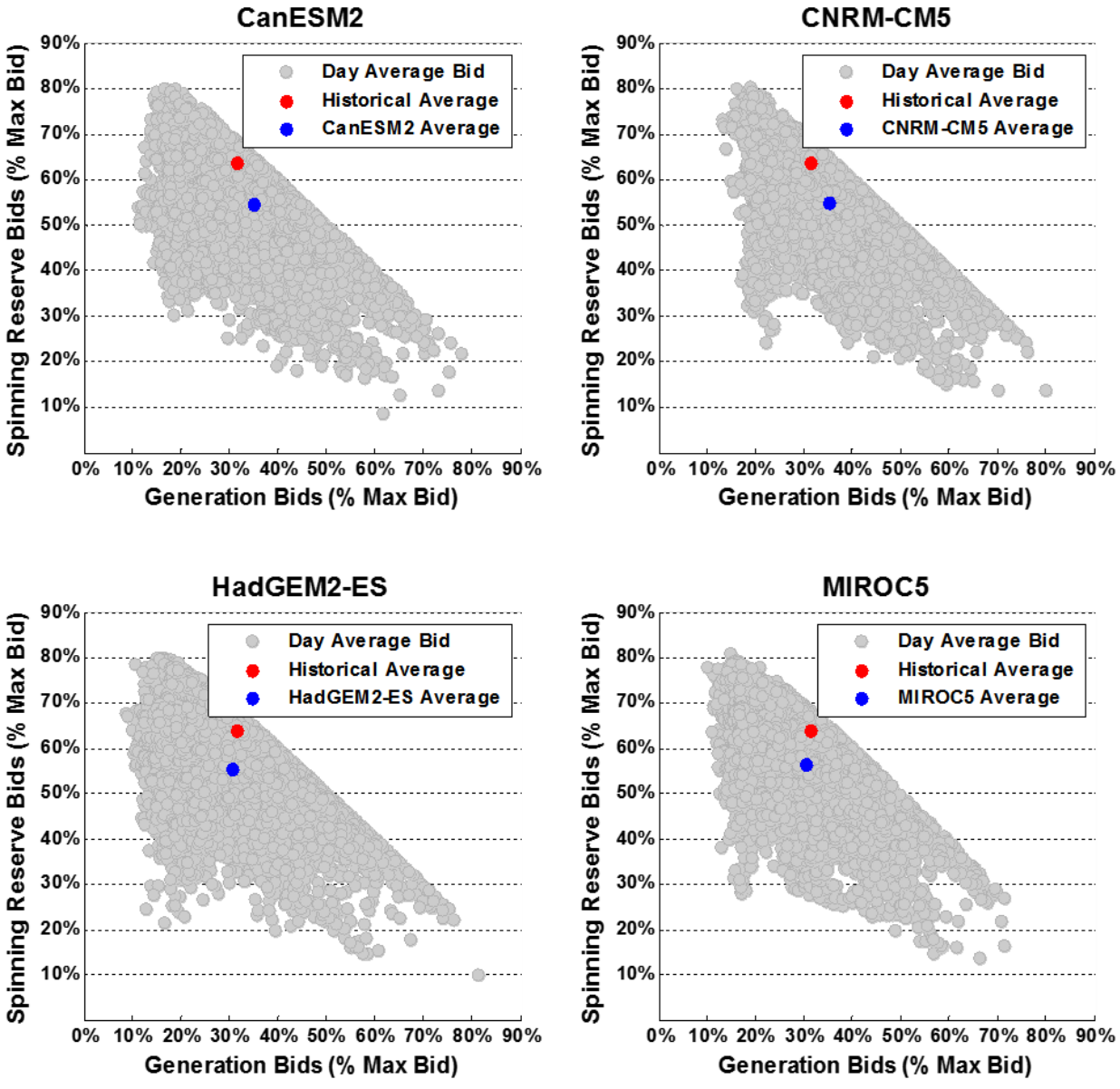

Source: Advanced Power and Energy Program, University of California Irvine

2.2.4 Extended Drought Impacts on California Hydropower Under Climate Change

The team conducted a supplemental analysis to examine the effect of an extended drought under climate change (RCP 8.5) on California hydropower generation and ancillary services. While *most* California hydropower units are projected to experience decreased runoff for the drought period selected, not all hydropower units experience this. Some hydropower units will experience increased inflow compared to the historical baseline (2000-2009). Nevertheless, the overall trend observed is a net decrease in runoff and inflow into hydropower units across the 10-year period, which results in lower reservoir levels and decreased hydropower bidding for generation and ancillary services.

All years during the drought period scenario are projected to experience reduced runoff, and the resultant total inflow into California hydropower units also decreases by 5-12% compared to historical (2000-2009), depending on the year. Inflow increases slightly during the fall and winter compared to the historical baseline, and it decreases during the spring and summer (Figure 12). This is in line with predictions that under climate change conditions, more precipitation will fall as rain in California, resulting in a shift in runoff to earlier in the year compared to historical. This trend parallels the results found for the RCP 4.5 and RCP 8.5 scenarios. The difference between this scenario and the scenarios in section 2.2.1 is that, in this case, the total inflow into reservoirs decreases, and there is a notable reduction in inflow during spring and summer, tied to the net reduction in total runoff.

Figure 12: Projected Average California Seasonal Inflow as a Percentage of Historical (2000-2009) Inflow (100%) for RCP 8.5 Drought Scenario (2046-2055)

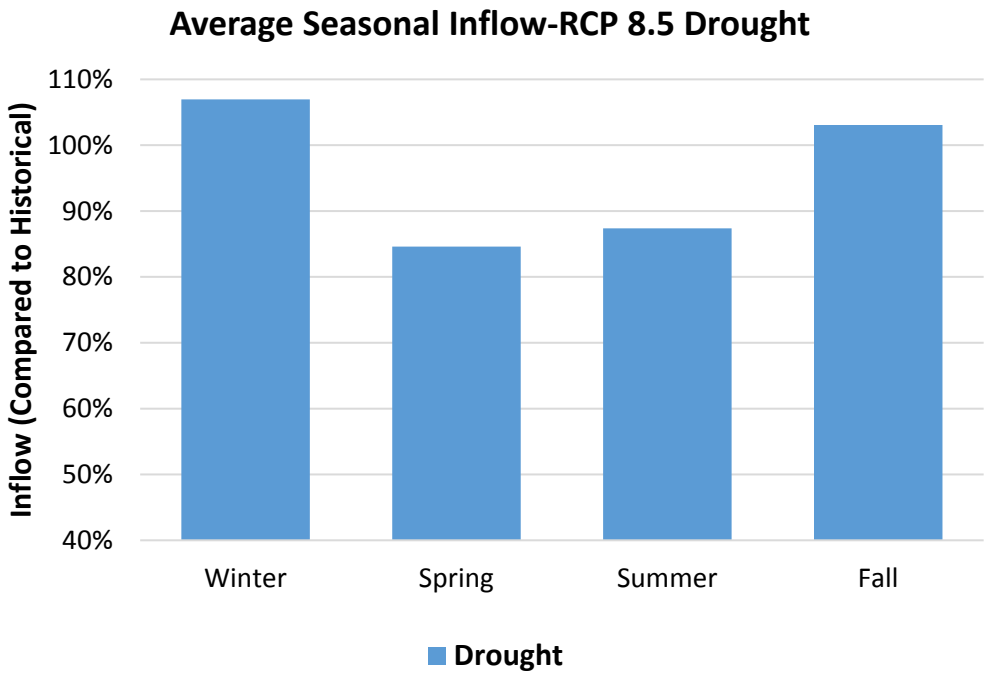

Source: Advanced Power and Energy Program, University of California Irvine

Examining shifting flow patterns more closely, the team plotted projected average California monthly inflow for the period under drought in comparison to the historical baseline (2000-2009) in Figure 13. On average, increased inflow compared to the historical baseline is observed for November to February. Most years are projected to experience higher inflow during these months compared to the historical counterparts. The remainder of the year, from March to October, has decreased inflow into the hydropower units compared to the historical baseline. Almost all years have decreased inflow during the spring and summer, as discussed, and, in particular, all years have reduced inflow into hydropower units for May through August.

Figure 13: Average California Monthly Inflow for Historical Baseline (2000-2009) and Projected RCP 8.5 Drought Scenario (2046-2055)

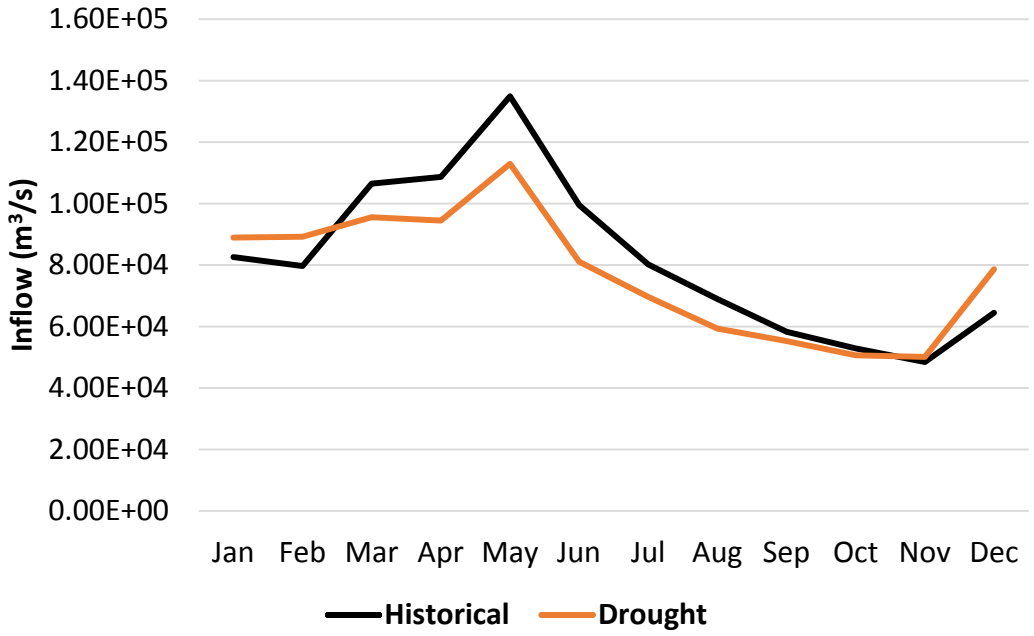

Source: Advanced Power and Energy Program, University of California Irvine

Unlike the scenarios in section 2.2.1 explored for RCP 4.5 and RCP 8.5, the drought scenario under RCP 8.5 shows similar inter-annual variability in inflow compared to the historical baseline (Figure 14). Examples of the corresponding impacts on reservoir fill profiles are presented in Figure 15. The exception is the fall, in which a larger range of values is observed. The range for the remaining seasons remains similar to historical. The median inflow value under drought for each season decreases compared to the historical baseline. This result illuminates the fact that the mean inflow value is skewed by years with higher seasonal inflow than the historical average.

For the RCP 8.5 drought scenario, there is an observed trade-off between meeting water demands and maintaining reservoir levels. While reservoirs are partially able to reduce the decline in inflow by releasing stored water to meet water demands, this contribution can lower reservoir storage levels over time if inflow does not increase. In fact, the RCP 8.5 drought scenario showed reservoir levels across several major reservoirs declining across the 10-year

period. (Nondispatchable hydropower units also experienced more, greater magnitude high-flow events; however, because they do not have significant storage capacity to retain the flow, they were unable to use this increase in flow).

Figure 14: Boxplots for California Historical Inflow (2000-2009) and Inflow for Projected RCP 8.5 Drought Scenario (2046-2055)

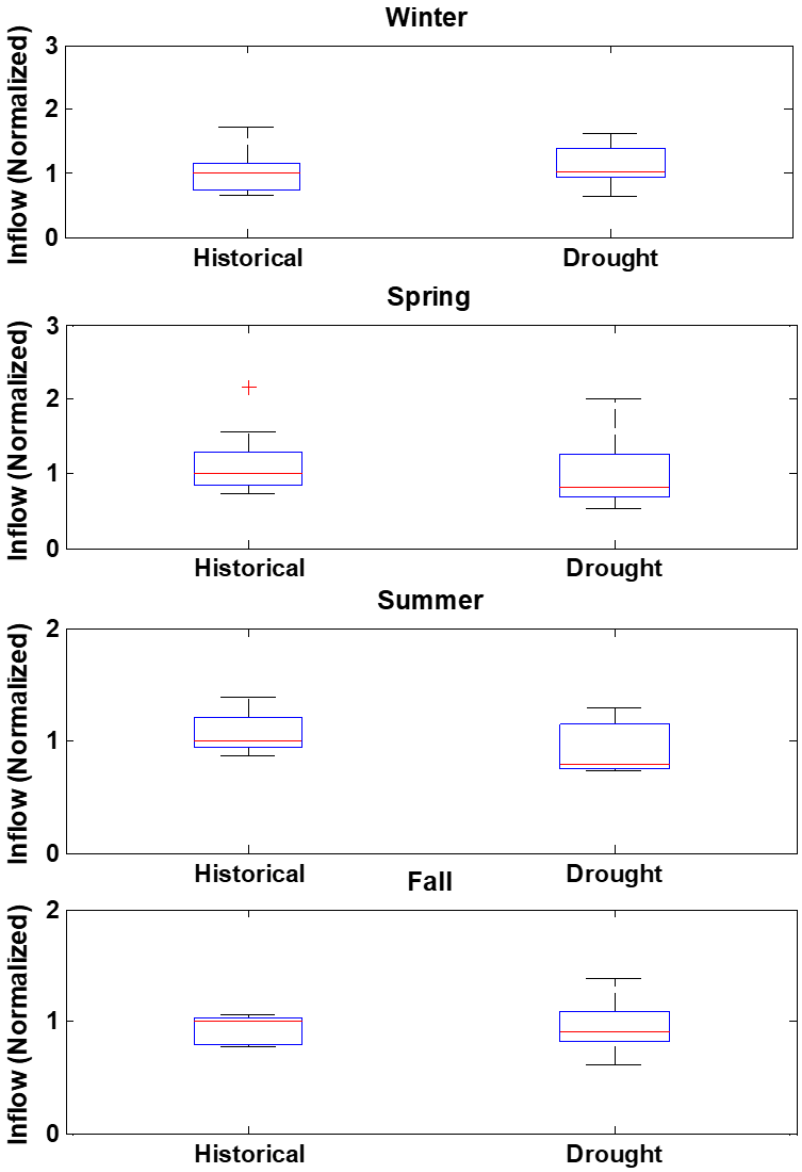

Each season is normalized based on the historical (2000-2009) median for that season.

Source: Advanced Power and Energy Program, University of California Irvine

Figure 15: California Reservoir Fill Profiles for the Historical Baseline (2000-2009) and the Projected RCP 8.5 Drought Period (2046-2055)

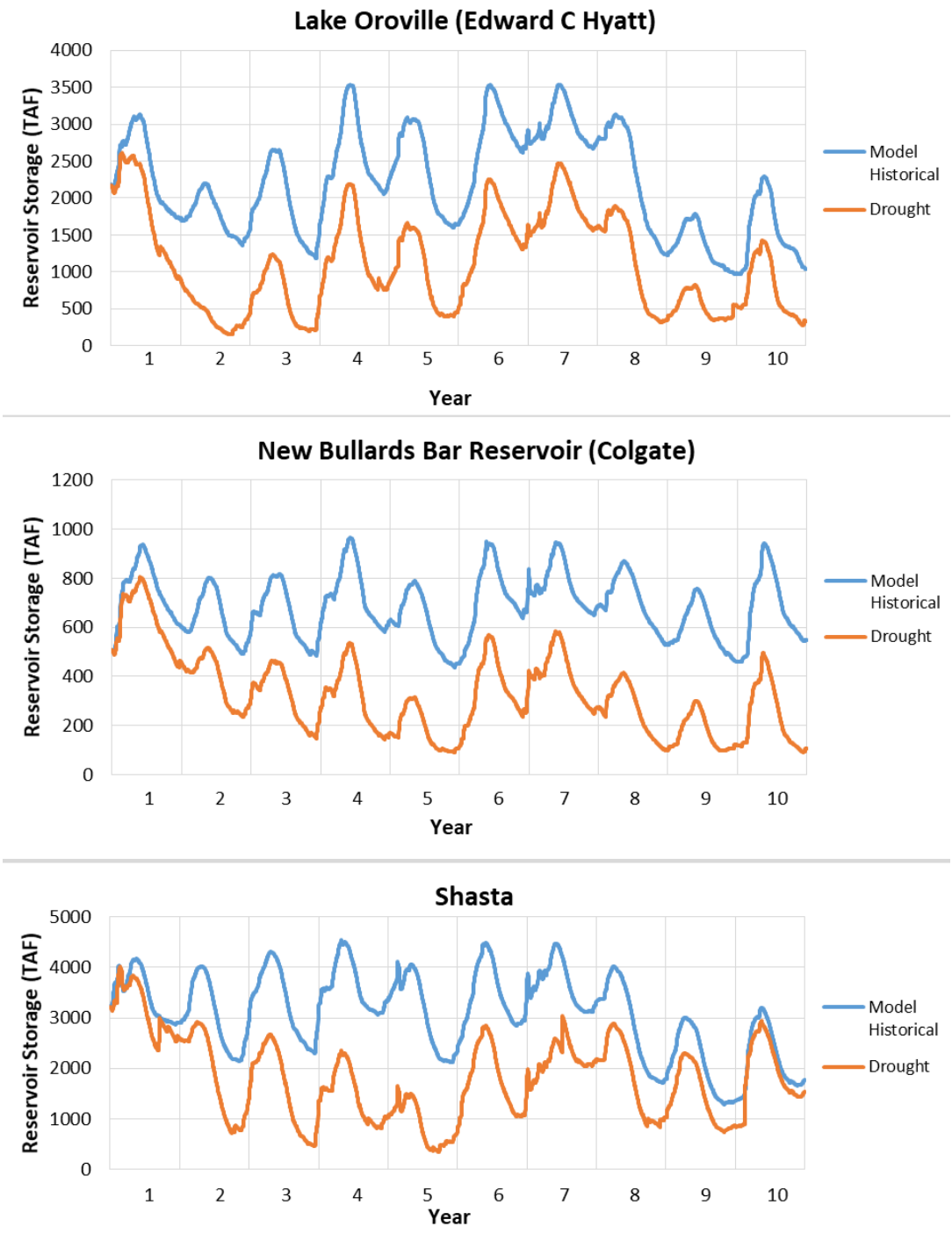

Source: Advanced Power and Energy Program, University of California Irvine

Dispatchable hydropower refers to hydropower plants that have the ability to control the profile of water releases. These facilities typically have large water reservoirs and controllable floodgates. *Nondispatchable hydropower* refers to hydropower facilities that have little to no control over the temporal profile of water releases, such as run-of-the-river facilities or those with very limited reservoir storage. For most years, inflow during the wet season in the drought scenario is projected to be insufficient to replenish the reservoir, and over time, the reservoir level continues to decline as water demands are addressed. Lower reservoir levels would result in greater restrictions on water usage for generation and bidding into ancillary service markets. In some cases, such as at Shasta Lake, the reservoir is able to recover in part or fully by the end of the 10-year period by retaining water during high-flow events, but there is still a reduced reservoir level for most of the years.

The previous scenarios for RCP 4.5 and RCP 8.5 discussed in section 2.2.1 and Appendix B.2 had more frequent, greater magnitude high-flow events, resulting in projections showing reservoirs would not experience the same level of reservoir decline that was observed for the RCP 8.5 drought scenario. For the previous scenarios, reservoirs experience increased projected constraints and lower reservoir levels during the summer, but they were able to recover during wet years enough so that there was not the long-term drop in reservoir levels that was observed for the drought scenario under RCP 8.5.

The model projected that nondispatchable hydropower units would also experience more, greater magnitude high-flow events; however, because they do not have significant storage capacity to retain the flow, they were unable to use this increase in flow.

There is a 19% reduction in projected California hydropower generation for the drought period investigated compared to the historical baseline (2000-2009). All years have a reduction in hydropower generation, and all years but one result in lower annual generation than the historical average. The driest year during the drought period generates 20% less electricity from hydropower compared to the driest year during the historical period.

While the projected average and median California inflows decrease during the investigated period, peak inflow increases. Similar to the previous RCP 4.5 and RCP 8.5 scenarios, there are several events with higher-than-historical runoff, with the resultant inflow into reservoirs being above the capacity to retain or directly use. This leads to increased spillage (Figure 16). In addition, nondispatchable hydropower units with extremely limited or no storage were unable to retain any excess flow and, therefore, experienced projected spillage to a greater degree than hydropower units with associated reservoirs.

Figure 16: RCP 8.5 Drought (2046-2055) California Hydropower Generation Compared to Historical (2000-2009) Hydropower Generation (100%)

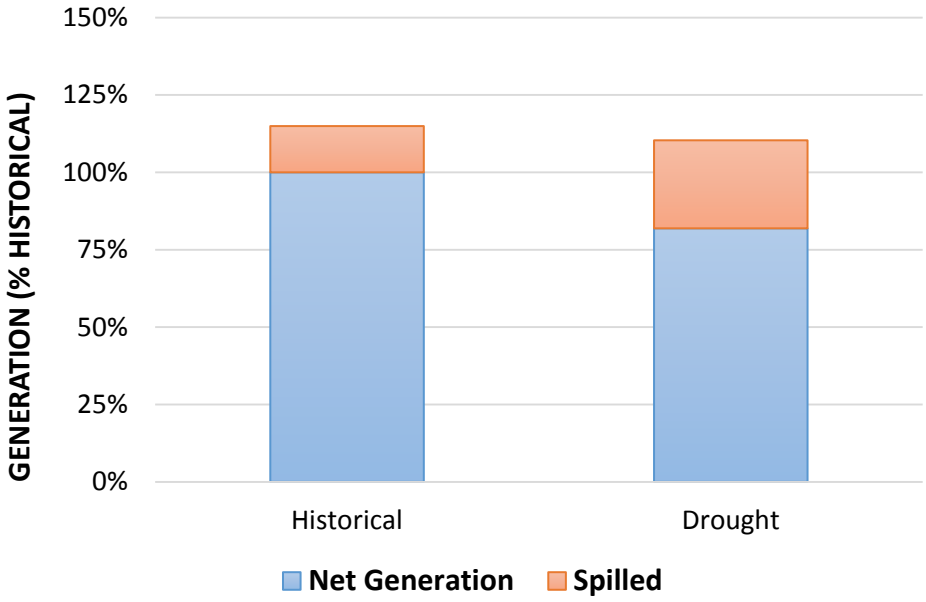

For theoretical generation based on total inflow versus net generation. Spilled is the amount of generation lost due to spills. The sum of net generation and spilled is the total theoretical generation if available inflow was utilized for electricity generation.

Source: Advanced Power and Energy Program, University of California Irvine

Figure 17depicts the average seasonal difference in generation across the 10-year drought period.

Figure 17: Average California Projected Seasonal Hydropower Generation Compared to Historical (2000-2009) for RCP 8.5 Drought Period (2046-2055) Scenario

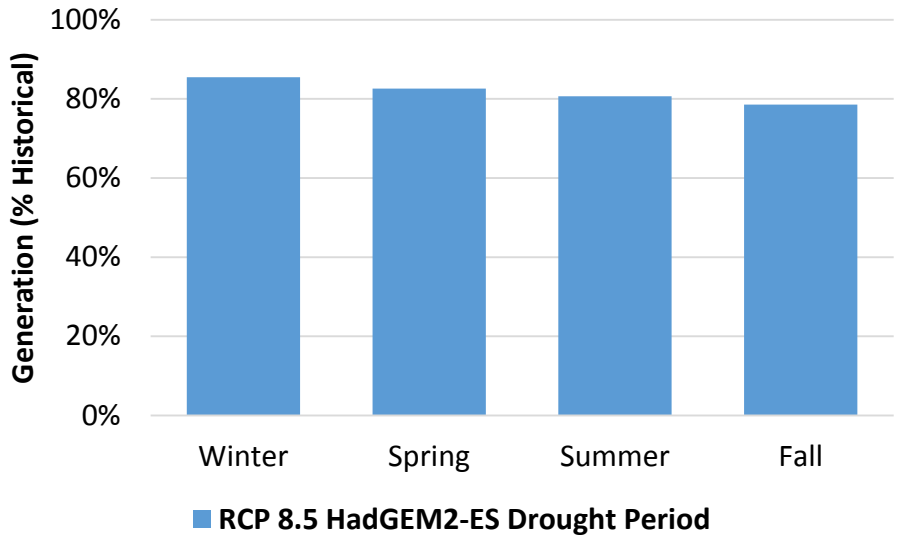

Source: Advanced Power and Energy Program, University of California Irvine

All seasons across all years show a reduction in electricity generation. The average seasonal reduction is 15% to 21% below historical, depending on the season. Most years have the greatest reduction in generation during the fall. This conclusion correlates to the observed decline in reservoir levels across the year/ between years, as well as reduced inflow during the months leading up to the fall. On the other hand, nondispatchable hydropower units, which do not have significant storage capacity, are not able to retain water during high-flow events and are, therefore, more susceptible to periods of low inflow. The net result is that nondispatchable hydropower units show a greater reduction in generation potential than large hydropower as a whole, showing a 23% reduction compared to the 19% reduction overall.

Not only does the projected average hydropower generation value decrease across the year, the range of projected values shifts lower under drought conditions (Figure 18). Hydropower generation still peaks in May, as it does in the historical (2000-2009) case, but the wettest year during the extended drought peaks at 14% lower than the historical peak. Projected California hydropower generation for some months for the driest year during the drought scenario is 10-32% less electricity compared to the driest year during the historical period and 38% to 55% less than the historical average. Lastly, the projected average California monthly generation is 12-22% less than the historical average.

Figure 18: Projected Monthly California Hydropower Generation for RCP 8.5 Drought Period Scenario–Mean and Range

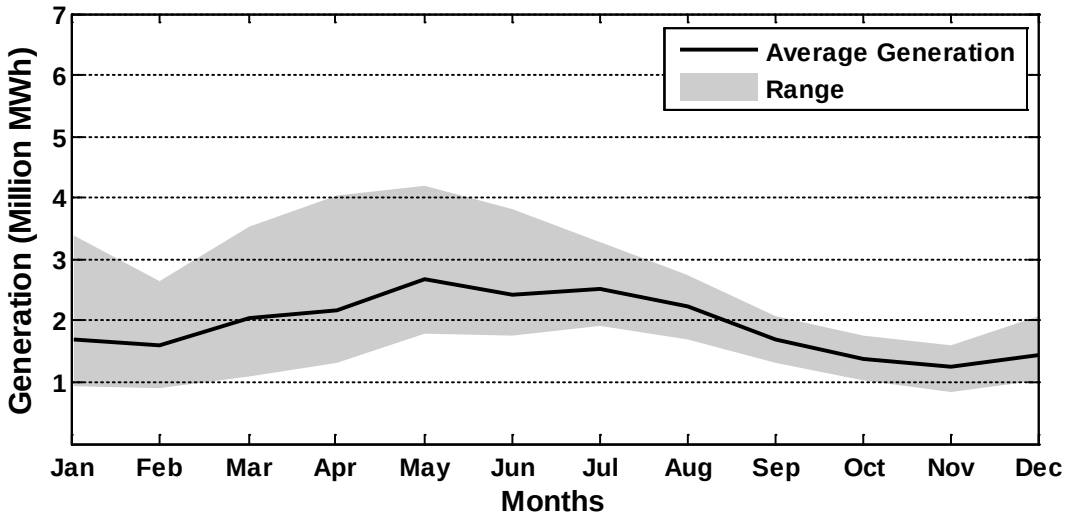

Source: Advanced Power and Energy Program, University of California Irvine

Examining average monthly generation for the RCP 8.5 drought scenario as a function of peak generation, the team found that there is less generation compared to the peak during the summer under the projected drought scenario than the historical (2000-2009) period (Figure 19). This is in part due to 1) a shift in inflow to earlier in the year and 2) the overall reduction in inflow, which lowers the peak value. The projected trend observed in Figure 19 is similar to that observed for the RCP 4.5 and RCP 8.5 scenarios in section 2.2.2 and Appendix B.2; however, in this case, the drop as a percentage of peak is smaller (on the scale of a few percentage points versus roughly 15% for RCP 8.5 as a whole). The reduction in generation during the drought

scenario is also more uniform across the year than the reduction observed under the modeled years 2046-2055 under RCP 8.5 for the HadGEM2-ES and MIROC5 scenarios. However, there is still a marked projected shift toward more of the California hydropower generation being supplied earlier in the year and less electricity being generated across the latter part of the year.

Figure 19: Average California Monthly Hydropower Generation Compared to the Annual Peak for Historical (2000-2009) and RCP 8.5 Projected Drought Scenario (2046-2055)

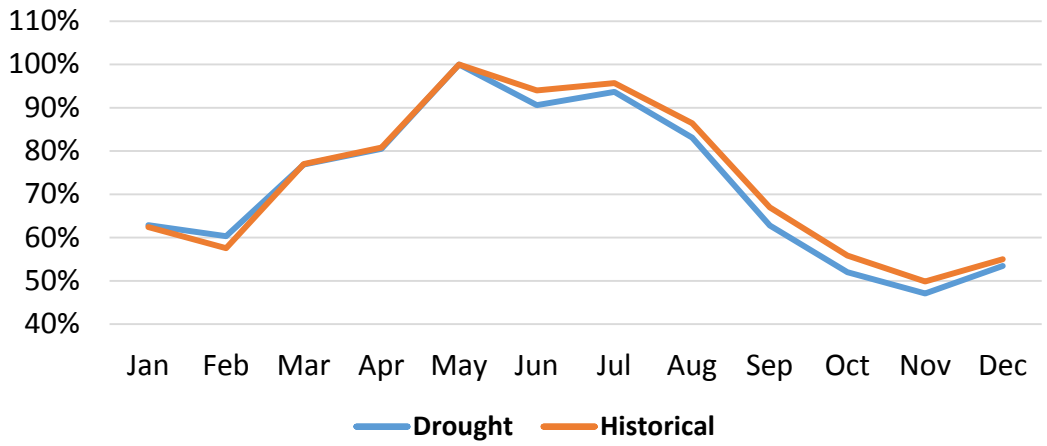

Source: Advanced Power and Energy Program, University of California Irvine

Projected spinning reserve bidding decreases across all years compared to the historical (2000-2009) average. Each season sees an average reduction of 38% to 44% compared to the historical baseline. This is driven primarily by lower reservoir levels. For example, for reservoirs like Shasta, peak reservoir levels reached during the drought period are comparable to the mid- to low levels observed during the historical period. Moreover, over the year as water is dispatched to meet generation demands (and auxiliary water requirements), reservoir levels decrease, and there are then greater bidding constraints during the summer and fall (Figure 20).

Figure 20: Projected Average California Hydropower Seasonal Spinning Reserve Bidding As a Percent of Historical (2000-2009) for the RCP 8.5 Drought Period (2046-2055) Scenario

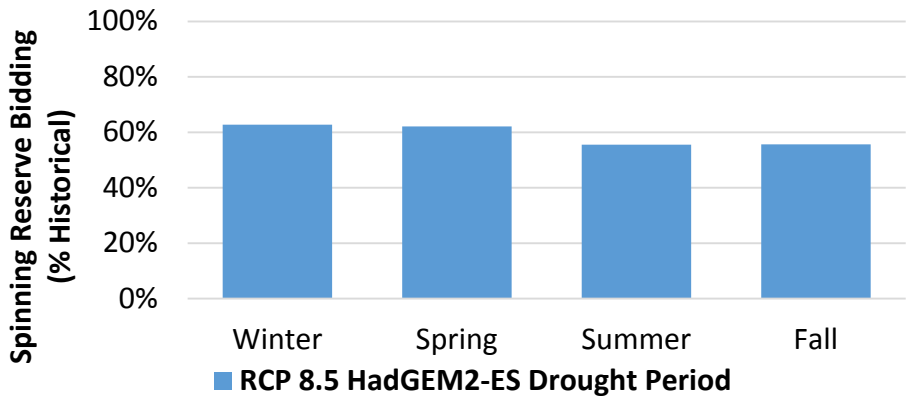

Source: Advanced Power and Energy Program, University of California Irvine

Examining projected daily bid averages for California hydropower spinning reserve bids versus generation for the drought scenario, the researchers found a large projected increase in the number of days in which one or more reservoirs experience constraints on bidding into the spinning reserve markets (Figure 21). There are also numerous days in which most reservoirs have reservoir level constraints, resulting in average overall spinning reserve bids being 58% lower than the historical average. Balancing the decrease in inflow while maintaining historical water demands not only decreases water releases for generation, but decreases the reservoir storage available to bid into the spinning reserve market. Even for days when most dispatchable hydropower units are running at high part load, a large portion of the reservoirs demonstrate reduced capacity to bid into the spinning reserve market due to low reservoir levels.

Figure 21: Projected Daily Average California Hydropower Spinning Reserve Bids Versus California Hydropower Generation Bids for the RCP 8.5 Drought Period (2046-2055) Scenario

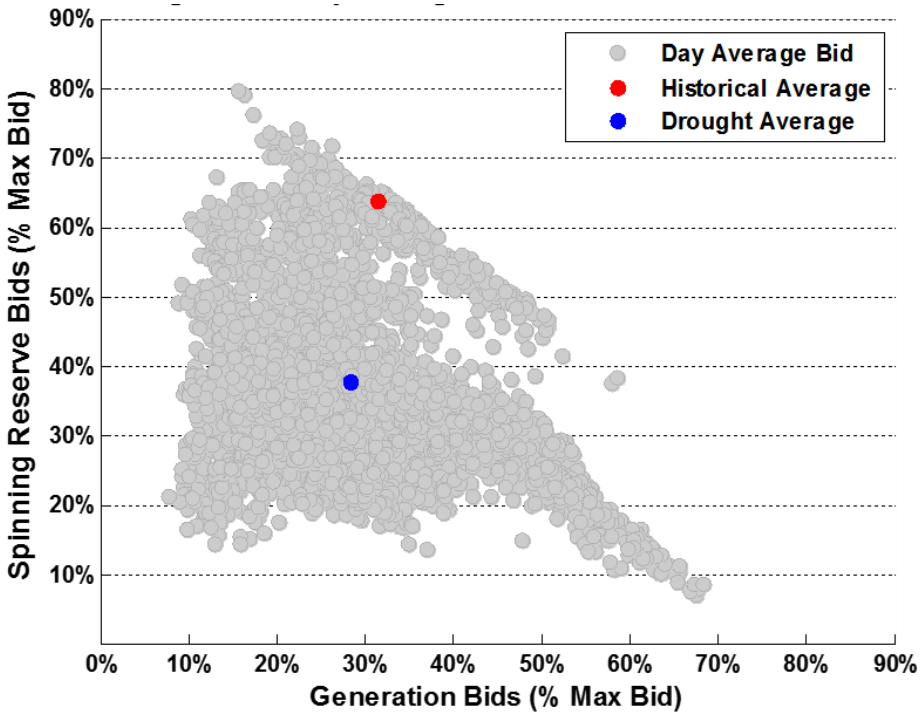

Source: Advanced Power and Energy Program, University of California Irvine

2.3 Conclusions

This chapter examined the potential climate change impacts on California hydropower generation and the contribution of hydropower to ancillary services for 2046-2055 and a drought scenario compared to an historical baseline (2000-2009). This was accomplished by modeling the historical behavior of large hydropower units, both dispatchable and nondispatchable. Climate change conditions were used to model perturbed historical inflow into these hydropower units to evaluate projected shifts in hydropowerelectricity generation and spinning reserve bidding.

1. **Winter and spring runoff is projected to increase in California, leading to increased risk of reservoir overflow and spill events.** Increased inflow into hydropower units when storage is already high can overwhelm the capacity of these units to hold and dispense water in correspondence with demand, leading to increased spill events. This risk is greater for small reservoirs with high minimum storage constraints. The delivery of water into reservoirs earlier in the year decreases the probability that the water can be retained into the summer months, when hydropower supports peak electricity demand.

2. **Increased runoff does not necessarily translate to increased California hydropower generation, due to the temporal shift in inflow and operational constraints of the hydropower units.** Despite significant inflow increases into hydropower units during winter, projected generation did not increase for all scenarios compared to the historical

baseline. More concentrated runoff in winter instead led to increased spill events in which water releases surpassed hydropower capacity. Increased spillage resulted in a loss in generation potential. Because reservoirs were able to retain some of the increased inflow, average annual generation did increase for the scenarios with a large increase in inflow, but for scenarios for which inflow was at or only slightly above historical, the temporal shift in the runoff led to a net decrease in generation due to spilling.

3. **The projected temporal shift in runoff leads to increased California hydropower generation earlier in the year and decreased generation in the summer compared to the annual peak.** Increased projected inflow during the winter and spring leads to a shift in the hydropower generation profile. High hydropower generation levels are reached earlier in the year. During the 2000-2009 period, higher generation levels occurred during May into the late summer. This shift in projected California hydropower generation has planning implications, as high inflow during winter and spring may give an overly generous idea of water available for generation in the summer, unless climate change is taken into account.

4. **California hydropower spinning reserve bidding potential is expected to decrease.** All scenarios, except the drought scenario, projected increased generation bidding during the winter and spring, leading to decreased availability to provide spinning reserve during those times of year. The model also projected that reservoir constraints would impose greater limitations on California hydropower spinning reserve bidding due to spilling and minimum storage requirements. These two factors led to a net decrease in projected California hydropower spinning reserve potential across the year for the 2046-2055 period compared to the 2000-2009 period. During the drought scenario, projected spinning reserve bidding potential is further constrained by lower reservoir levels.

5. **Extended drought periods in California under climate change are exacerbated by shifting precipitation patterns.** The climate change scenarios modeled in this study project that extended droughts would reduce hydropower reservoir levels and decrease hydropower bidding into markets in California. This trend is made more severe by changing precipitation patterns. Episodes of high-flow conditions observed under projected climate change scenarios are challenging to manage and result in greater spillage from hydropower units. The net impact is even lower generation during the drought than if the inflow could be otherwise captured, stored, and used throughout the year.

CHAPTER 3:
Assessment of Climate Change Impacts on Solar Thermal and Geothermal Capacity

3.1. Introduction and Background

As parts of the portfolios modeled in studies to reach the year 2050 GHG reduction goal, solar thermal and geothermal resources fulfill varying roles in contributing to the renewable resource mix. In addition, solar thermal and geothermal resources also have certain advantages for dispatchability (that is, the power output of these resources can be adjusted as needed) and use of available and mature components for steam-cycle power plants.

Solar thermal and geothermal power plants are based on Rankine-cycle steam turbine power plant configurations. These power plants require external cooling of the working fluid to carry out the heat rejection in the condenser. This is typically accomplished in two ways. The most conventional way is by heat rejection from the working fluid to an external loop of cold water. The cold water is warmed and subsequently releases heat to the atmosphere by being sprayed into a cooling tower, where cooler ambient air receives heat and moisture and rises into the environment. This is referred to as *wet-tower cooling*. This method is efficient, since it allows power plants to use the latent heat capacity of the cooling water; however, since some water evaporates into the atmosphere in cooling towers, a continuous supply of water must be brought in to compensate for these losses.

An alternate method is heat rejection from the working fluid directly to ambient dry air by blowing ambient air at high velocity across a water-to-air heat exchanger. This configuration is referred to as *dry cooling* and can significantly reduce the water consumption of a solar thermal or geothermal power plant. Dry cooling, however, does not eliminate water consumption in a steam-turbine based power plant. Other uses of water include, but are not limited to, make-up water for the main working fluid loop and for cleaning solar thermal collectors.

In California, much of the solar thermal and geothermal potential is in the southeastern desert areas of the state. These regions, however, tend to be limited in water availability for use in these power plants due to local climate, which can potentially constrain the installable capacity of these resources. This limitation can be exacerbated under climate change depending on the shifts in future water availability in the region.

Therefore, this analysis examines how future changes in water availability affect the installable capacity of solar thermal and geothermal resources in California and the role of these resources as a component of the portfolio to meet the state's emissions reduction and renewable use goals.

The solar thermal and geothermal capacity potential is first determined without consideration of water constraints. These are based on resource estimates provided from various sources (National Renewable Energy Laboratory, U.S. Geological Survey); then constraints are applied in

geographic information system software (ArcGIS™) to determine the land area suitable for solar thermal power plant installation, and the sites suitable for geothermal power plant installation are determined and translated to capacity levels. Lands were excluded based on factors such as protected areas, land use and cover, and steep slopes (see Appendix A.2. for details). Next, a water balance is performed in each of California's hydrologic regions under historical conditions and climate change altered conditions to determine the net available supply, which is the amount of water available to be devoted toward supporting solar thermal and geothermal power plants. Third, the water constraints are applied to the unconstrained potential to determine how water availability constraints affect installable solar thermal and geothermal potential, and the water-constrained capacity potential for each resource is calculated. Finally, the sensitivity of this result to population growth and water demand trends are analyzed. Treated wastewater was not considered in the analysis. Details on these steps are presented in Appendix A.2.

3.2 Results and Analysis

3.2.1 Solar Thermal – Isolated Climate Change Impacts

The team first determined the impact of climate change on the installable solar thermal electric capacity under a scenario with no change in water demand in each hydrologic region from current levels to isolate the impact of climate change affected water availability. Figure 22 presents the results for solar thermal use. Each entry represents a unique combination of climate model, climate scenario, and cooling system. For comparison, the water unconstrained installable solar thermal capacity is also plotted.

Without any change in water demand, the installable solar thermal electric capacity varies widely between scenarios. Since most of the unconstrained installable potential (with daily direct normal insolation [DDNI] > 7 kWh/m^2/day) is in the South Lahontan and Colorado River regions in the southeastern corner of the state, the water balance of these two regions are the drivers for determining installable solar thermal capacity from the perspective of technical potential.

A first observation is that nine of the 24 climate affected scenarios exhibit no installable solar thermal electric capacity. In these cases, the water balance yielded zero net available supply due to the water balance showing a zero or negative storage change for the considered hydrologic regions. The E3 no-climate-change compliance scenario did not rely on solar thermal to begin with; therefore, projecting zero solar thermal with climate change has no effect. The spatial aspect is important to consider. Even if net available supply is positive in a given region, if it is not a region where there are not significant solar thermal resources to begin with, then that supply does not contribute to installable solar thermal capacity. An example of this effect is presented in Figure 23, which shows the projected net available supply requirements to support 100% of the unconstrained potential with wet cooling, hybrid cooling, and dry cooling compared against the projected net available water supply for the RCP 4.5 climate scenario and the MIROC5 climate model.

Figure 22: Projected (2046-2055) California Water Constrained Installable Solar Thermal Capacity, Historical (2001-2010) Regional Water Demand Levels

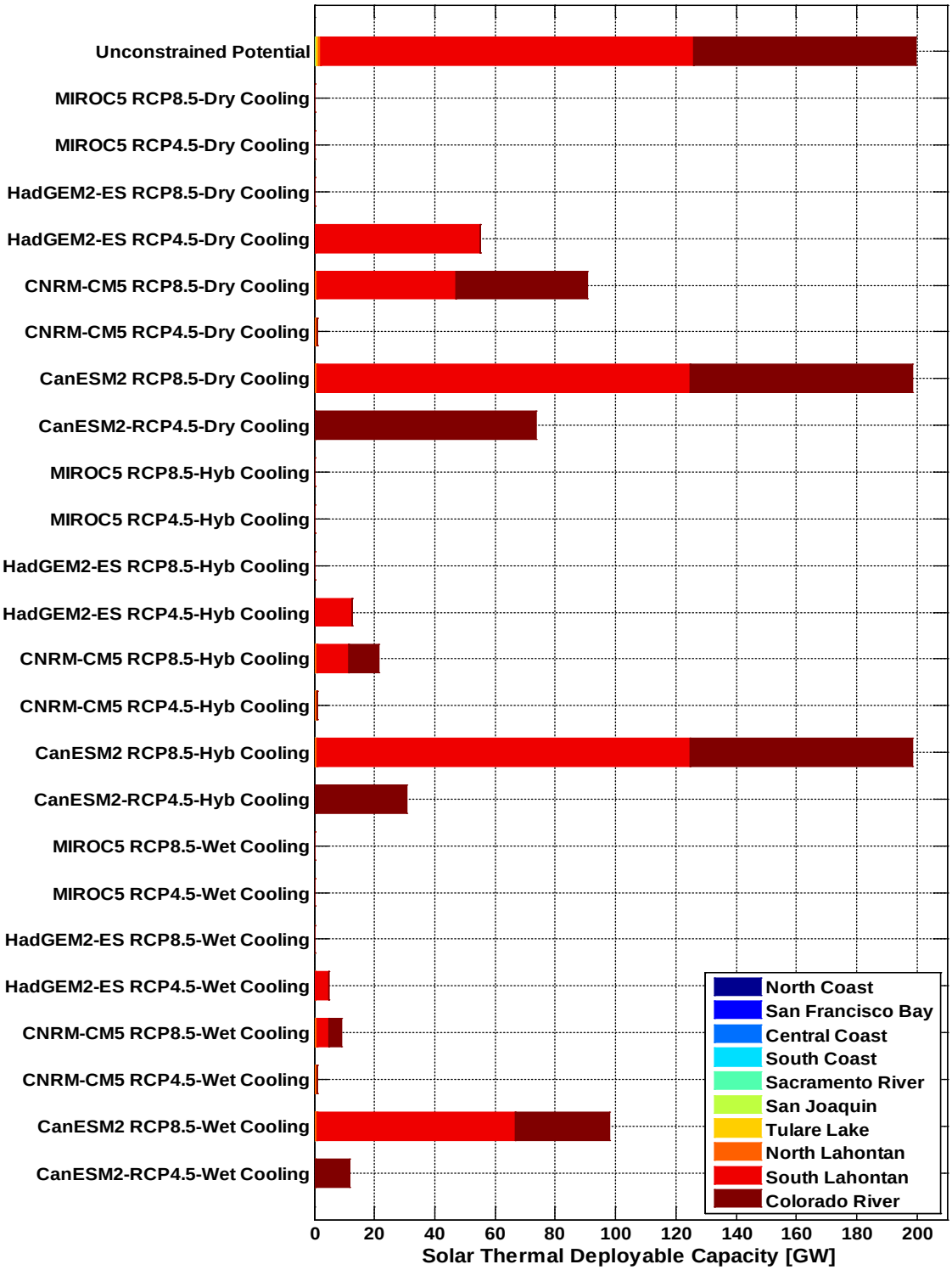

Source: Advanced Power and Energy Program, University of California Irvine

Figure 23: Projected (2046-2055) Net Available Water Supply Requirements for Supporting Potential California Solar Thermal Electricity Generation vs. Projected (2046-2055) Net Available Water Supply. MIROC5 Climate Model/RCP 4.5 Climate Scenario With Historical (2001-2010) Water Demand Amounts

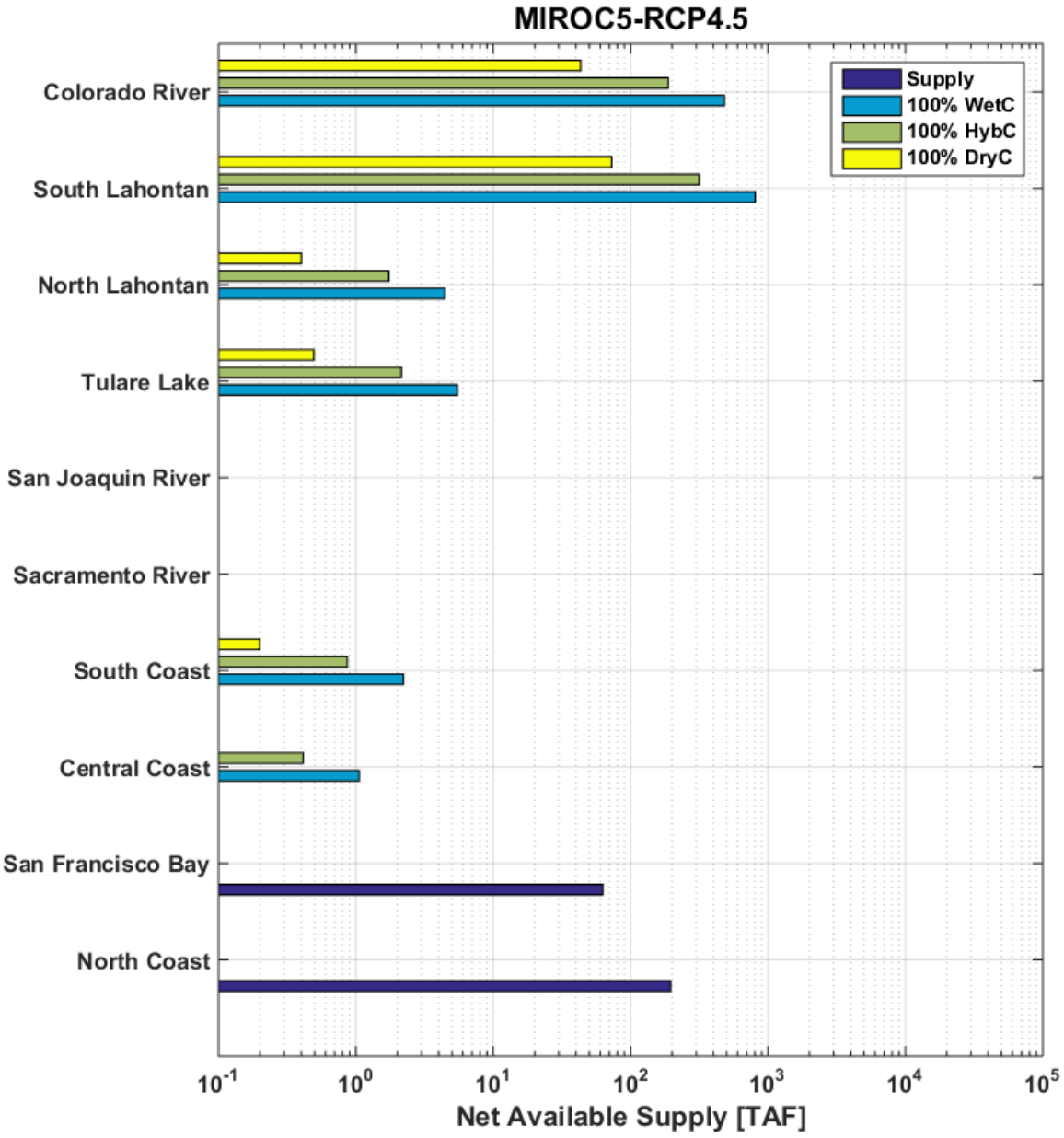

Supply = Projected Net Available Supply for a given region, 100% WetC = Net Available Supply Requirement to Support 100% of Installable Solar Thermal Capacity with Wet Cooling, 100% HybC = Net Available Supply Requirement to Support 100% of Installable Solar Thermal Capacity with Hybrid Cooling, 100% DryC = Net Available Supply Requirement to Support 100% of Installable Solar Thermal Capacity with Dry Cooling.

Source: Advanced Power and Energy Program, University of California Irvine

In Figure 23, a positive net available water supply is projected for the San Francisco Bay and North Coast hydrologic regions; however, the solar thermal electric resource potential is located

only in other hydrologic regions of the state. The areas where solar thermal electric potential is available do not correspond with a positive projected net available water supply, which gives rise to a zero potential installable capacity for these resources. On the other hand, scenarios that have significant projected net available water supply in regions where solar thermal electric resources are present allow full or near-full use of the unconstrained installable solar thermal capacity regardless of cooling resources. This can be seen for the CanESM2 RCP 8.5 scenario, where the hybrid and dry cooling cases allow full use of the installable solar thermal electric potential. The projected net available water supply requirement and projected net available water supply in each region for this scenario are presented in Figure 24.

Figure 24: Projected (2046-2055) Net Available Water Supply Requirements for Supporting Potential California Solar Thermal Electricity Generation vs. Projected (2046-2055) Net Available Water Supply. CanESM2 Climate Model/RCP 8.5 Climate Scenario With Historical (2001-2010) Water Demand Amounts

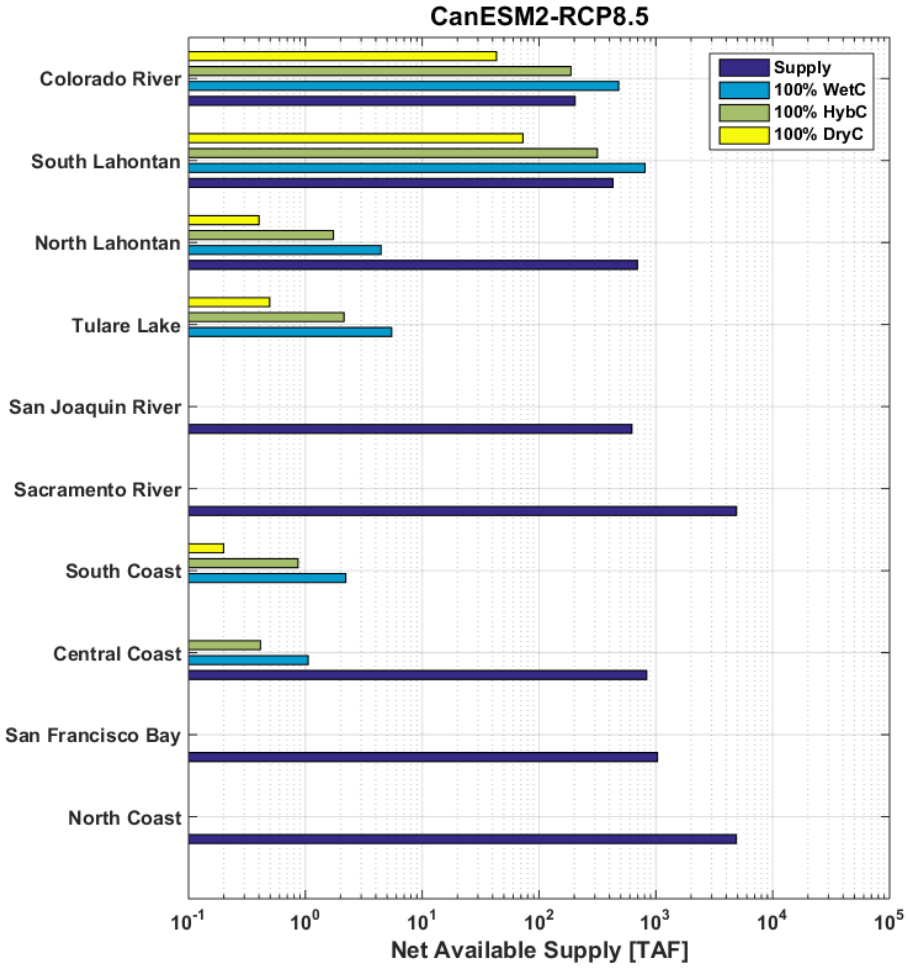

Supply = Projected Net Available Water Supply for a given region, 100% WetC = Net Available Supply Requirement to Support 100% of Installable Solar Thermal Capacity with Wet Cooling, 100% HybC = Net Available Supply Requirement to Support 100% of Installable Solar Thermal Capacity with Hybrid Cooling, 100% DryC = Net Available Supply Requirement to Support 100% of Installable Solar Thermal Capacity with Dry Cooling.

Source: Advanced Power and Energy Program, University of California Irvine

In this case (CanESM2 RCP 8.5 scenario), there is sufficient projected net available water supply to meet the water requirements using 100% of the installable solar thermal electric potential for the dry and hybrid cooling cases in the two major regions with solar thermal electric capacity in California– Colorado River and South Lahontan. For the wet cooling case, the projected net available water supply is almost sufficient to support the water use requirements. The only shortfall in projected net available water supply in this scenario is in the South Coast and Tulare Lake regions; however, these regions have a very low potential for installable solar thermal electric capacity to begin with and are small contributors to the total capacity potential.

A second key observation is that the cooling system type does not have much effect on the installable solar thermal electric capacity. The selection of power plant cooling system only has a major effect when the climate scenario and climate model dictate that a positive net available supply is present in the hydrologic regions where solar thermal resources are available. Using a more water-efficient cooling system, such as hybrid or dry cooling, will allow the net available water supply projected to be present in a hydrologic region to support larger installable solar thermal electric capacities. An example of this impact is the CNRM-CM5 RCP 8.5 scenario, where use of hybrid cooling and dry cooling increases the installable solar thermal electric capacity. Specifically, projected net available water supply with wet cooling allows about 9 gigawatts (GW) of installable capacity, hybrid cooling allows about 22 GW of installable capacity, and dry cooling allows 90 GW of installable capacity. The projected net available water supply requirements and projected water availability for this scenario (CNRM-CM5 Climate Model / RCP 8.5 Climate Scenario, 2046-2055) are presented in Figure 25.

Figure 25: Projected (2046-2055) Net Available Water Supply Requirements for Supporting Potential California Solar Thermal Electricity Generation vs. Projected (2046-2055) Net Available Water Supply. CNRM-CM5 Climate Model / RCP 8.5 Climate Scenario With Historical (2001-2010) Water Demand Amounts

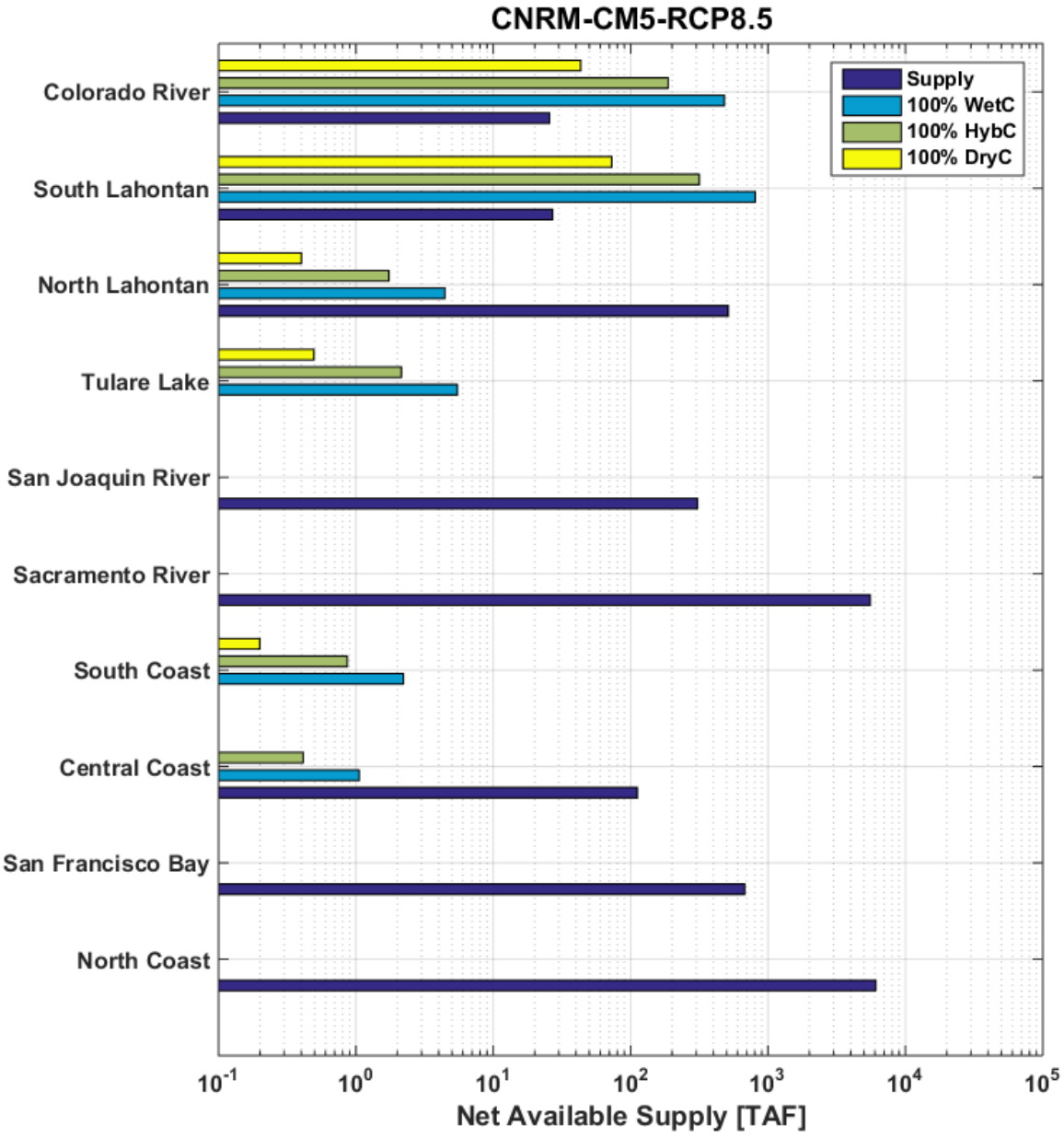

Supply = Projected Net Available Supply for a given region, 100% WetC = Net Available Supply Requirement to Support 100% of Installable Solar Thermal Capacity with Wet Cooling, 100% HybC = Net Available Supply Requirement to Support 100% of Installable Solar Thermal Capacity with Hybrid Cooling, 100% DryC = Net Available Supply Requirement to Support 100% of Installable Solar Thermal Capacity with Dry Cooling.

Source: Advanced Power and Energy Program, University of California Irvine

The projected (2046-2055) net available water supply is enough to meet a larger fraction of the projected water requirements for dry cooling and hybrid cooling versus wet cooling in the Colorado River and South Lahontan hydrologic regions. In this scenario (CNRM-CM5 Climate

Model / RCP 8.5 Climate Scenario, 2046-2055), there are also significant projected amounts of water available in other hydrologic regions of California, but they do not have significant solar thermal electric resources. With such significant projected water availability, however, the prospect of transporting water toward the regions where solar thermal electric resources are available could be investigated on an economic basis. This is beyond the scope of this work.

From a planning standpoint, however, these results indicate that there is potential for water availability to limit the use of solar thermal electric resources during the 2046-2055 period in California. There is a wide variability in the results of cases due to the differences in the behavior of the climate models, and the calculated value of the water constrained installable solar thermal capacity ranges from zero to full use. This indicates that strategies to ensure water availability – through imports or unconventional local resources in each hydrologic region – must be considered for solar thermal electric resources to be a reliable component of a renewable energy resource portfolio in the future. Furthermore, other measures to potentially reduce demand in other sectors and free allocations of water that can be used for supporting solar thermal electric resources need to be investigated.

3.2.2 Solar Thermal – Combined Climate Change and Demand Change Impacts

The impact on the water-constrained installable solar thermal capacity is presented in Figure 26, based on projected changes in climate and water demand in each hydrologic region up to 2050. This figure corresponds to the current trends population + current population density trends demand growth scenario from the *California Water Plan Update* [51].

Figure 26: Projected (2046-2055) California Water Constrained Installable Solar Thermal Capacity, with Projected Year 2050 Population Growth and Water Demand Trends

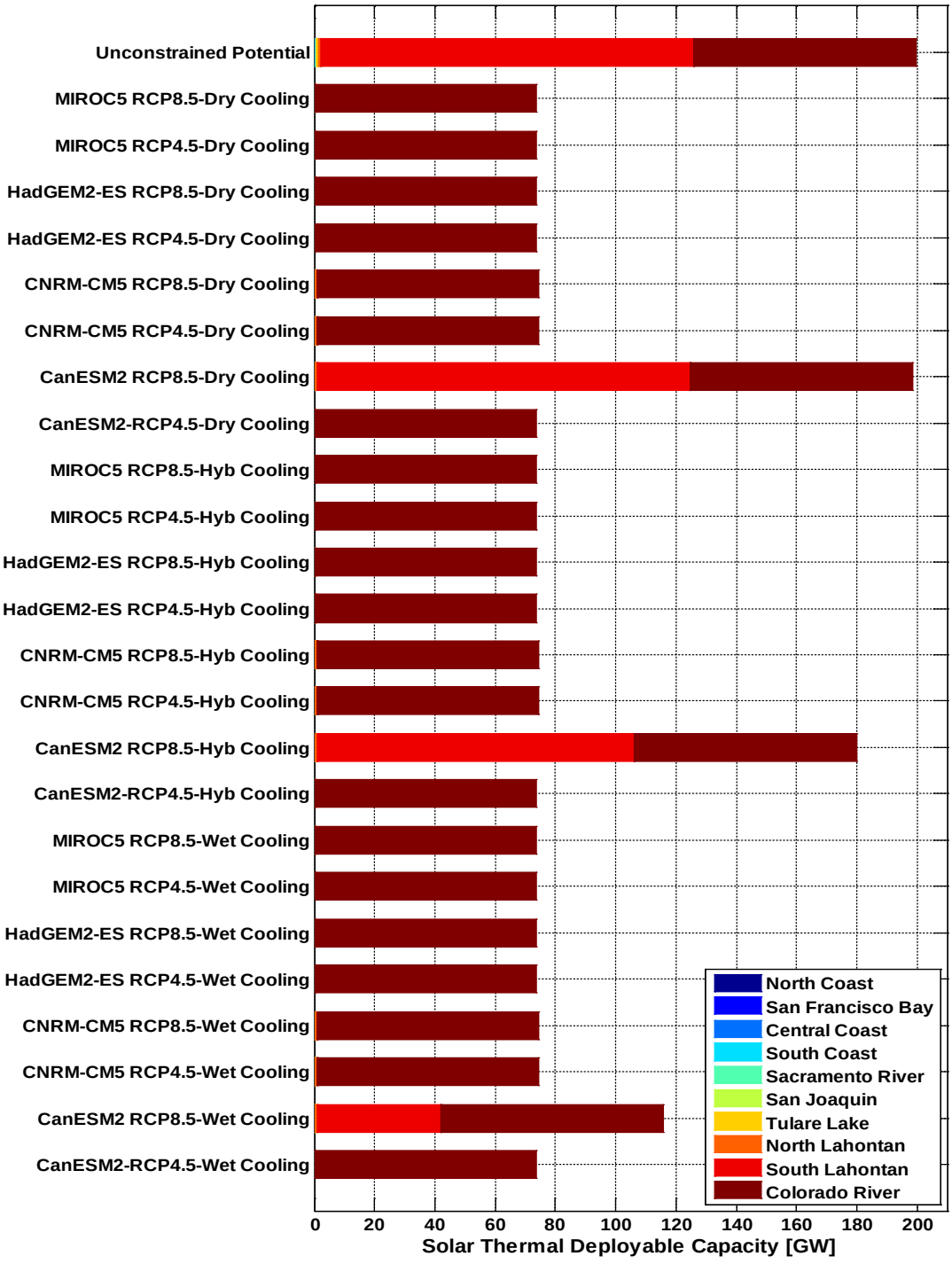

Regional water demand levels using current population growth and current population density growth trends.

Source: Advanced Power and Energy Program, University of California Irvine

From Figure 26, all scenarios with the exception of the CanESM2 RCP 8.5 scenario set show a water-constrained installable solar thermal capacity of 73-74 GW, regardless of cooling system. For these scenarios, comparing the regional breakdown to that for the unconstrained installable solar thermal capacity shows that each scenario allows full use of the potential capacity in the Colorado River region, which corresponds to about 73.6 GW. The CNRM-CM5 scenarios additionally allow a very small use of the South Lahontan potential.

These results occur due to a combination of the spatial profile of the net available supply under these scenarios and the spatial profile of the changes in total water demand by hydrologic region. The urban water demand in all hydrologic regions tends to increase, but the agricultural water demand in all California hydrologic regions tends to decrease. Reducing the agricultural water use in most cases exceeds the increase in urban water use, causing net reductions in total water use in the California hydrologic regions. Comparing Figure 26 to Figure 22, this reduction in agriculture water use results in more installable solar thermal capacity when demand changes are taken into account. This tends to hold no matter the growth scenario for total population and population density.

The reductions in total water demand for the Colorado River region are very significant, since this region has a large agricultural water demand that is projected to decrease significantly by 2050 as a result of urbanization and background water conservation [51]. This reduction occurs at a larger scale than the impacts on the water balance due to climate change alone in certain cases and frees water supply that can be used to support the water needs of solar thermal power plants. For comparison, the net available supply breakdown for the MIROC5 RCP 4.5 scenario with the projected change in water demand using the current population and population density growth trends is presented in Figure 27.

Figure 27: Projected (2046-2055) Net Available Water Supply Requirements for Supporting Potential California Solar Thermal Electricity Generation vs. Projected (2046-2055) Net Available Water Supply. MIROC5 Climate Model/RCP 4.5 Climate Scenario With Year 2050 Population Growth Trends.

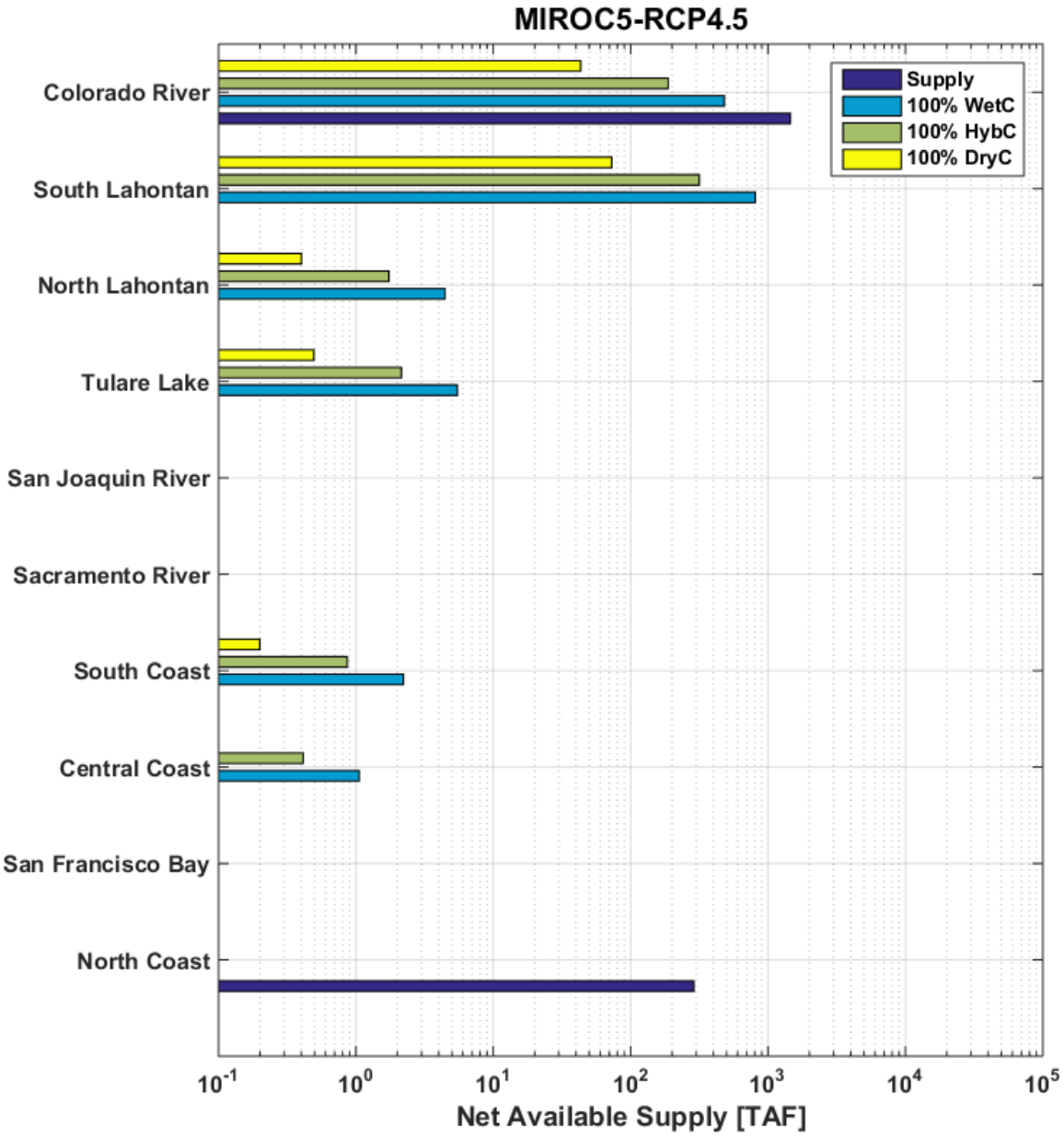

Projected water demand amounts for potential solar thermal electric power plants in California using current trends for population growth and population density growth. Supply = Actual Net Available Supply for a given region, 100% WetC = Net Available Supply Requirement to Support 100% of Installable Solar Thermal Capacity with Wet Cooling, 100% HybC = Net Available Supply Requirement to Support 100% of Installable Solar Thermal Capacity with Hybrid Cooling, 100% DryC = Net Available Supply Requirement to Support 100% of Installable Solar Thermal Capacity with Dry Cooling.

Source: Advanced Power and Energy Program, University of California Irvine

Comparing Figure 23, Figure 24, Figure 25, and Figure 27, the team made a few observations. First, projections for 2050 show the San Francisco Bay hydrologic region is not expected to have any net available water supply available for solar thermal electric power plants since this region exhibits an increase in total water demand for other uses. Note that this analysis did not consider the extent to which technological advancements for solar thermal generation can affect the feasibility of solar thermal resources in the San Francisco Bay region. The water demand in the San Francisco Bay region is largely urban-based, which is projected to increase. Second, with projected changes in water demand taken into account, the Colorado River region in California is projected to have net available water supply that significantly exceeds the water required to use the full installable solar thermal electric capacity technical potential; projected net available water supply in this region far exceeds the amount needed for potential quantities of wet, hybrid, and dry cooling types of solar thermal electric power plants. The projections for the South Lahontan region of California, however, still do not have any net available water supply to be allocated to support any fraction of the large solar thermal electric capacity potential in that region.

The CanESM2 RCP 8.5 scenario set is the only one that projects significant net available water supply to meet water required for installable solar thermal electric capacity in the South Lahontan region. As a result, this scenario projects higher amounts of potential solar thermal electric capacity than the 73.6 GW present in the other scenarios. The net available supply breakdown for this scenario set is presented in Figure 28.

Figure 28: Projected (2046-2055) Net Available Water Supply Requirements for Supporting Potential California Solar Thermal Electricity Generation vs. Projected (2046-2055) Net Available Water Supply. CanESM2 Climate Model/RCP 8.5 Climate Scenario With Year 2050 Population Growth Trends.

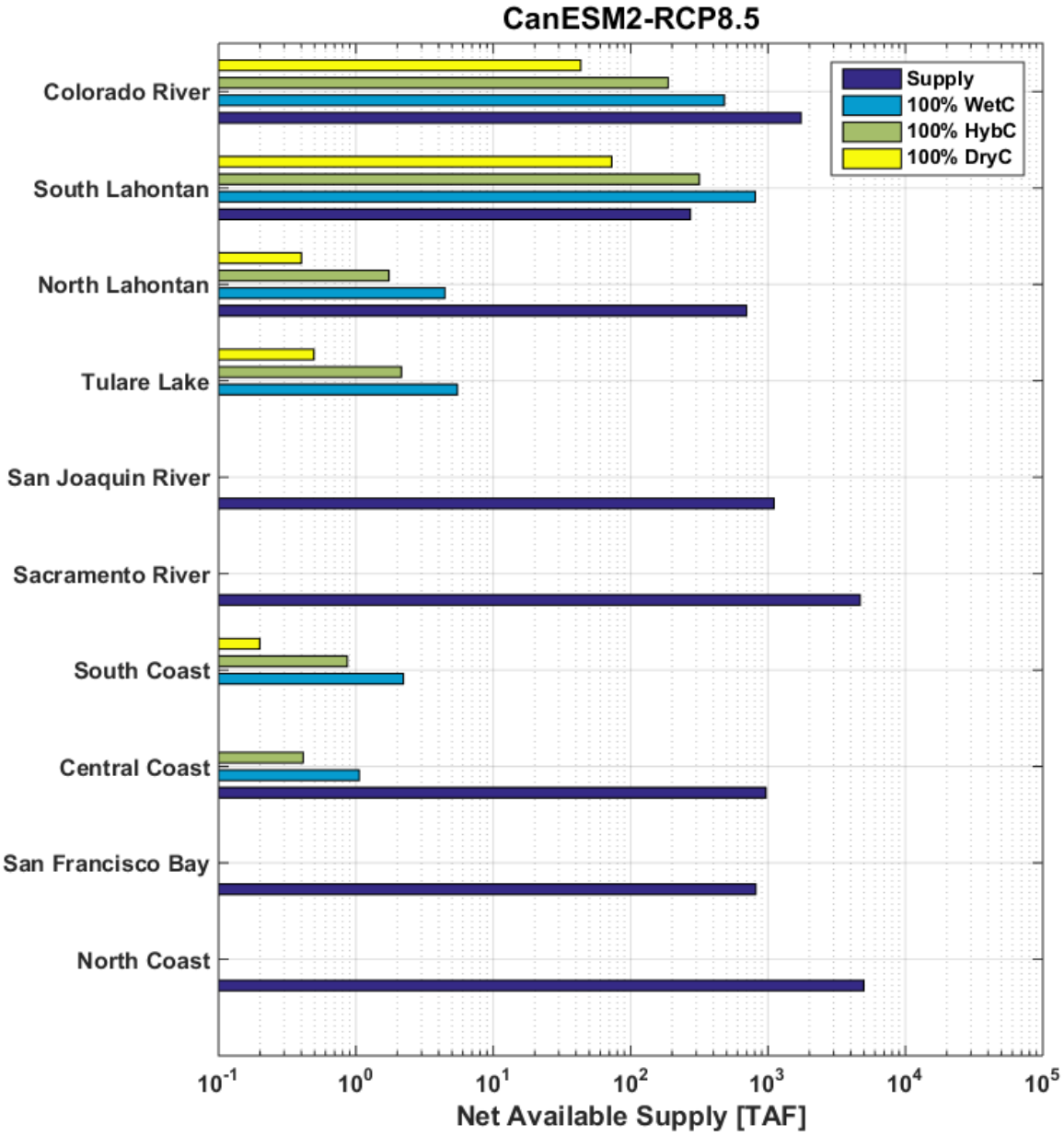

Projected water demand amounts for potential solar thermal electric power plants in California using current trends for population growth and population density growth. Supply = Actual Net Available Supply for a given region, 100% WetC = Net Available Supply Requirement to Support 100% of Installable Solar Thermal Capacity with Wet Cooling, 100% HybC = Net Available Supply Requirement to Support 100% of Installable Solar Thermal Capacity with Hybrid Cooling, 100% DryC = Net Available Supply Requirement to Support 100% of Installable Solar Thermal Capacity with Dry Cooling.

Source: Advanced Power and Energy Program, University of California Irvine

There are two key observations arising from a comparison of Figure 28 to Figure 24. First, the change in net available supply when projected water demand changes are taken into account is

relatively small in all regions except the Colorado River region. In the Colorado River region, the net available supply increased by almost an order of magnitude in the case where demand changes are taken into account, from 203,000 acre-feet to 1,851,000 acre-feet. This shows that the projected reduction in agricultural water demand is significant and can have a significant effect on installable solar thermal capacity.

From a planning standpoint, these results indicate that reduction in water demand due to either agriculture water use efficiency or reduction in agriculture use in the Colorado River region can provide significant benefits for using potential solar thermal electric resources. This shows another aspect of the water-energy nexus. Water use efficiency not only saves energy through reducing the energy usage of the water infrastructure, but it can also free water allocations, which can be used to support larger capacities of thermally based renewable energy resources.

3.2.3. Geothermal – Isolated Climate Change Impacts

The effect of climate change on the installable solar thermal electric capacity is first determined under a scenario with no change in water demand in each hydrologic region from current levels to isolate the impact of climate change-affected water availability. The results for geothermal deployment are presented in Figure 29. Each axis entry represents a unique combination of climate model, climate scenario, and cooling system. For comparison, the water-unconstrained installable geothermal capacity is also plotted.

Without any change in water demand, the installable geothermal capacity also varies widely between scenarios. Compared to solar thermal electric resources, geothermal resources are more distributed across the 10 hydrologic regions, but the total is still dominated by one region. Most geothermal resources in the state are in the Colorado River hydrologic region, with about 4.5 GW of the total 16.7 GW distributed across other hydrologic regions.

Since nontrivial amounts of geothermal resources are present in many hydrologic regions, there are no cases where the water-constrained installable geothermal capacity is zero. There are some cases where it can be considered as small (specifically, less than 1 GW), but geothermal capacity is slightly more resilient than solar thermal electric resources against spatial variability in net available water supply. Geothermal resources are subject to the same hierarchy of effects, however, as that for solar thermal electric. Spatial availability of net available water supply is a larger factor than cooling system type – if water is not available in the regions with large geothermal potential, then it will not contribute to larger installable geothermal capacities, even if sufficient water is available in other regions.

Figure 29: Projected (2046-2055) Water Constrained Installable Potential Geothermal Capacity in California, Historical (2001-2010) Regional Water Demand Levels.

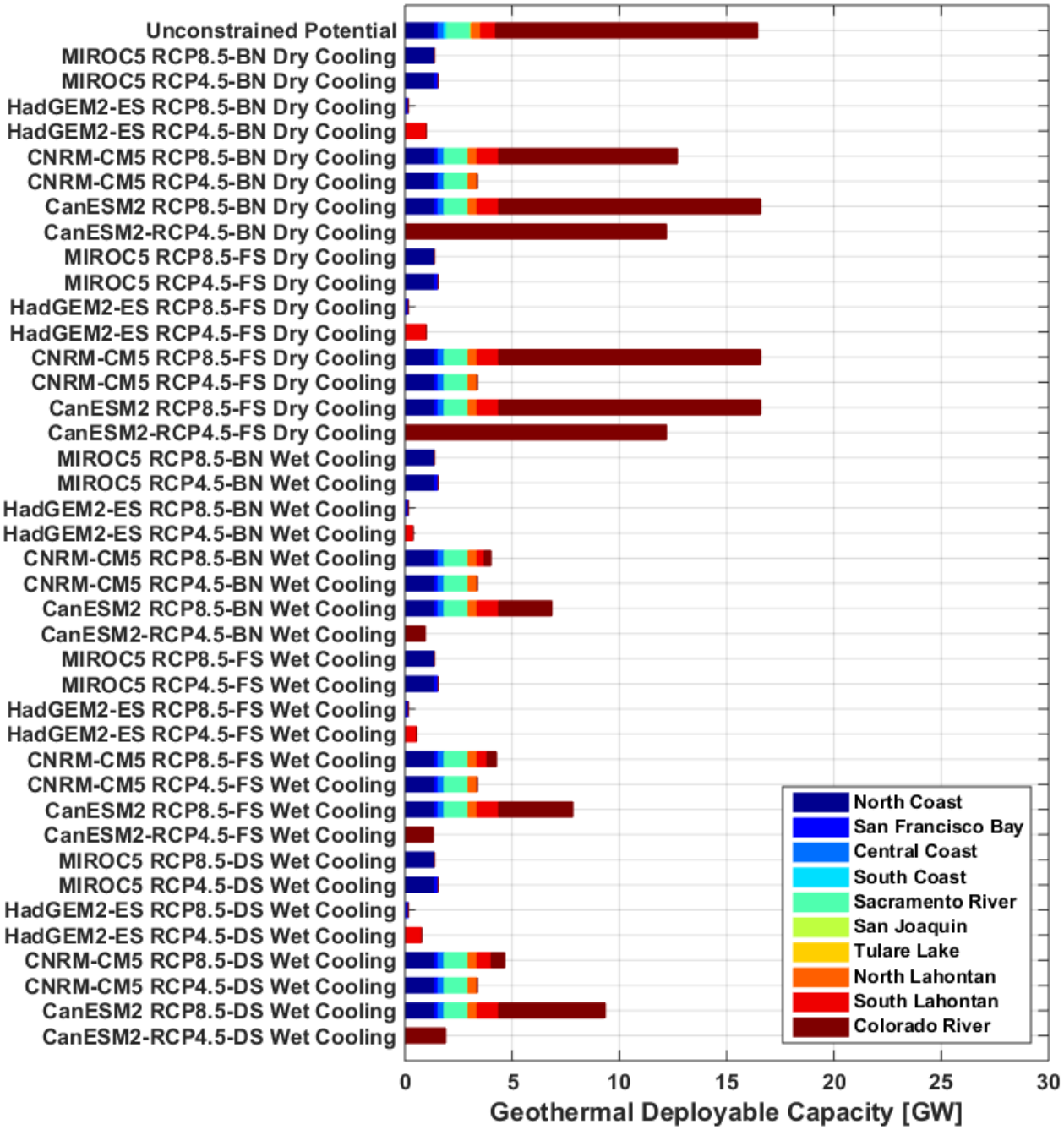

DS = Dry Steam, FS = Flash Steam, BN = Binary.

Source: Advanced Power and Energy Program, University of California Irvine

Since there is some geothermal resource in every hydrologic region, however, cooling system type fulfills a larger role for geothermal power than it does for solar thermal power. Transitioning from wet cooling to dry cooling makes a large difference for many of the scenario sets, including CanESM2 RCP 4.5 and RCP 8.5, and CNRM-CM5 RCP 8.5. The projected net

available water supply breakdown for the CanESM2 RCP 8.5 scenario set is presented in Figure 30.

Figure 30: Projected (2046-2055) Net Available Water Supply Requirements for Supporting Potential Geothermal Deployment in California vs. Projected (2046-2055) Net Available Water Supply. CanESM2 Climate Model/RCP 8.5 Climate Scenario With Historical (2001-2010) Water Demand Amounts

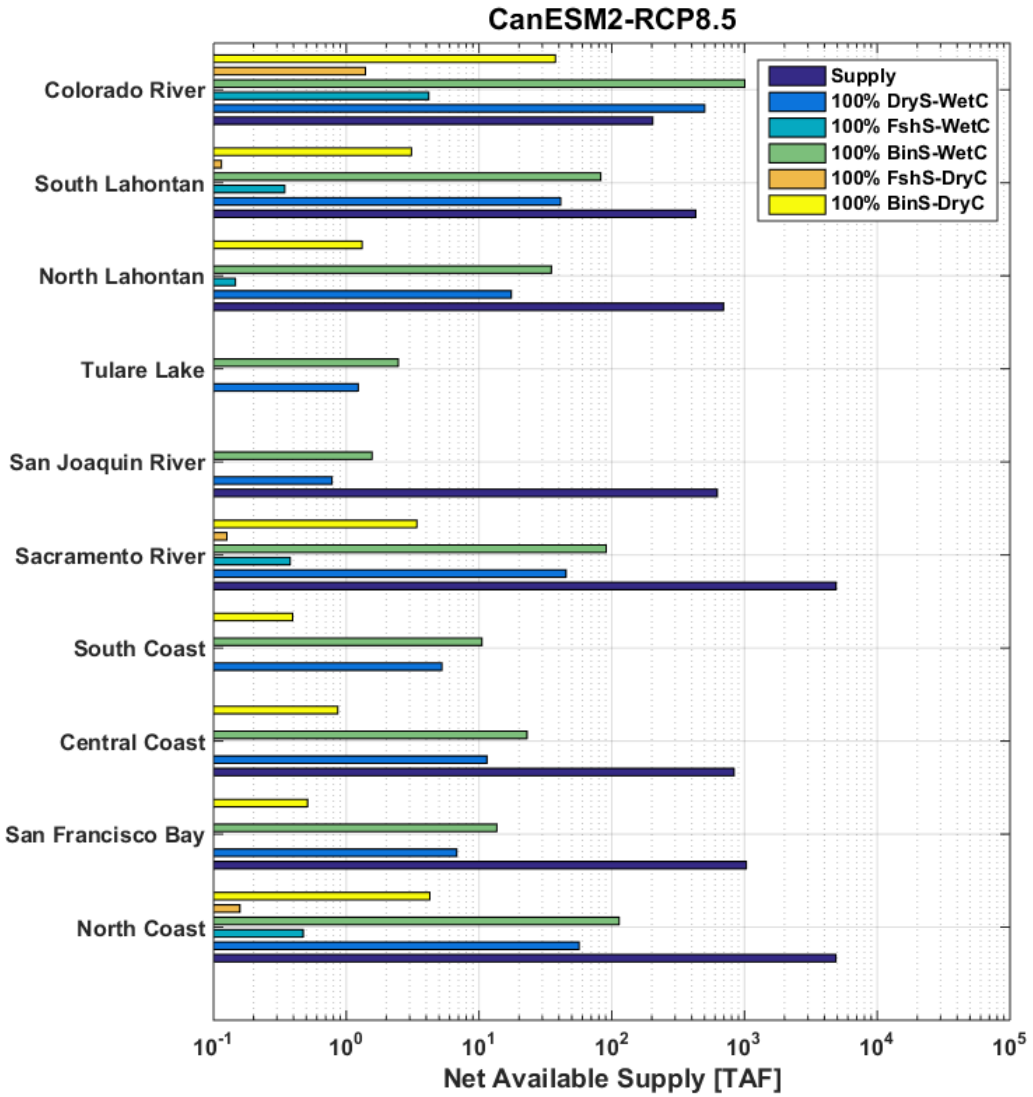

Supply = Projected Net Available Water Supply for a given region, 100% DryS-WetC = Net Available Supply Requirement to Support 100% of Installable Geothermal Dry Steam Capacity with Wet Cooling, 100% FshS-WetC = Net Available Supply Requirement to Support 100% of Installable Geothermal Flash Steam Capacity with Wet Cooling, 100% BinS-WetC = Net Available Supply Requirement to Support 100% of Installable Geothermal Binary Capacity with Wet Cooling, 100% FshS-DryC = Net Available Supply Requirement to Support 100% of Installable Geothermal Flash Steam Capacity with Dry Cooling, 100% BinS-DryC = Net Available Supply Requirement to Support 100% of Installable Geothermal Binary Capacity with Dry Cooling.

Source: Advanced Power and Energy Program, University of California Irvine

The projected net available water supply in the Colorado River region exceeds the water supply requirements for all the dry cooling cases but only for portions of the wet cooling cases. The projected net available water supply also exceeds water supply requirements in supporting potential geothermal power plants in regions with geothermal potential such as South Lahontan, North Lahontan, Sacramento River, San Francisco Bay, and North Coast.

Figure 29 also shows the cooling system not affecting certain cases due to the spatial distribution of projected net available water supply not aligning with the spatial distribution for geothermal resource potential. Scenario sets including MIROC5 RCP 4.5, MIROC5 RCP 8.5, HadGEM2-ES RCP 4.5 and HadGEM2-ES RCP 8.5 are not affected by cooling system type. In each case, projected net available water supply is present in only one or two hydrologic regions, but no scenario has significant projected net available water supply in regions that have a significant amount of geothermal resources. In the regions where net available water supply is projected, water supply tends to exceed the requirements for full use of geothermal resources regardless of cooling system type. Therefore, for these scenarios, cooling system type does not affect installable potential geothermal capacity.

From a planning standpoint, these results provide similar lessons to the results for solar thermal electric resources. The availability of water to support geothermal resources can potentially be a limiting factor for the extent to which geothermal resources can be used in each region. This indicates that strategies to ensure water availability – through imports or unconventional local resources in each hydrologic region – must be considered for geothermal resources to be a reliable component of a renewable resource portfolio in the future. This aspect must also be considered for the long term viability of current geothermal resources to continue operating in the future. Furthermore, other measures to potentially reduce water demand in other sectors and free allocations of water that can be used for supporting geothermal resources may need to be investigated.

3.2.4 Geothermal – Combined Climate Change and Demand Change Impacts

The combined impact of climate change and projected water demand changes in each hydrologic region up to 2050 on the water-constrained installable geothermal capacity is presented in Figure 31. This particular figure corresponds to the current trends population + current population density trends demand growth scenario from the *California Water Plan Update* 2013.

Figure 31: Projected (2046-2055) Water Constrained Installable Potential Geothermal Capacity in California, Projected Year 2050 Regional Water Demand Levels With Population Growth Trends

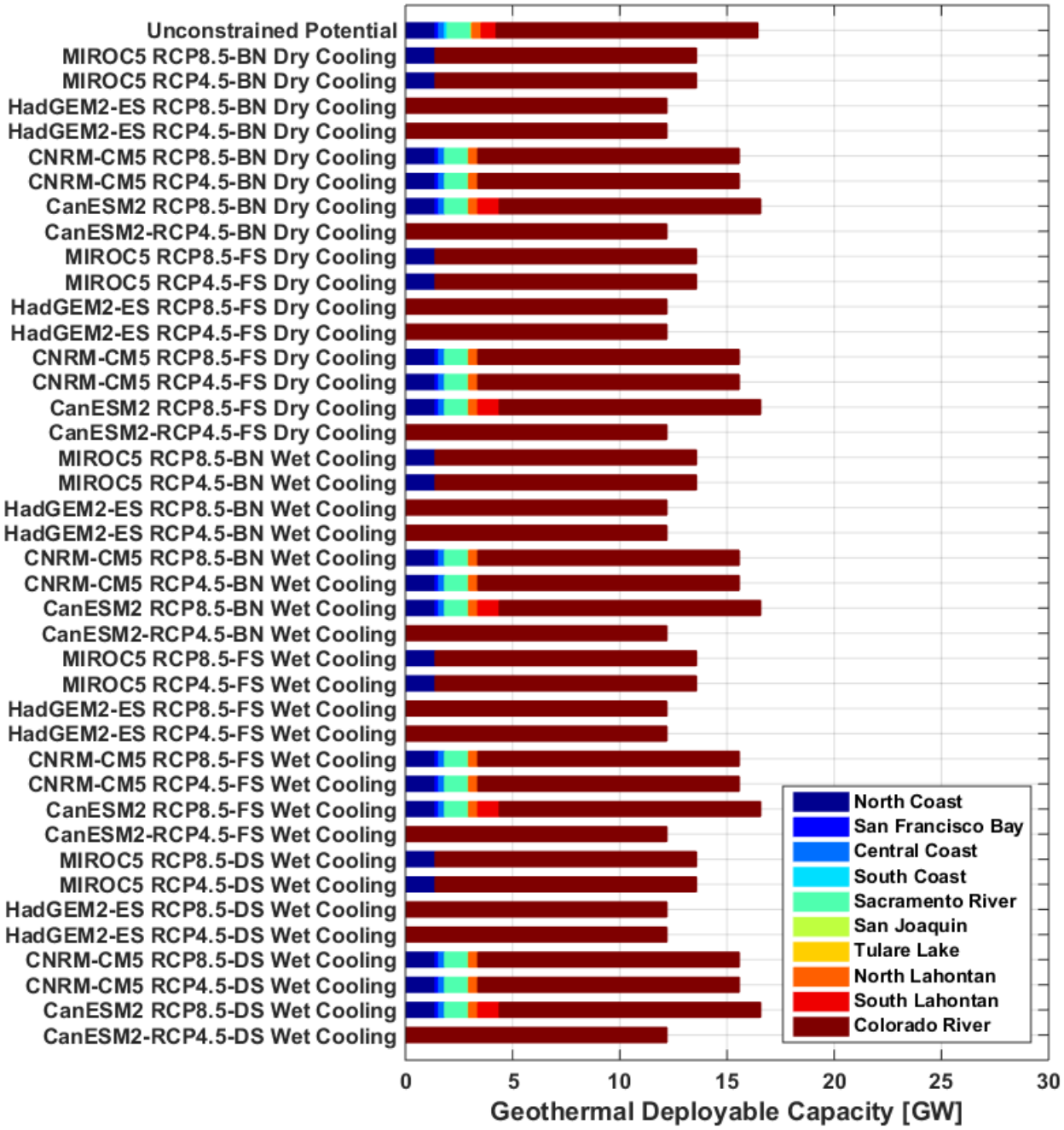

Using current population growth and current population density growth trends.

Source: Advanced Power and Energy Program, University of California Irvine

With projected demand changes taken into account, all the scenarios allow the use of large fractions of the unconstrained installable geothermal capacity. The water-constrained installable capacity ranges from 11.5 GW to the full 16.7 GW resource potential, with the lower end corresponding to the full resource availability in the Colorado River region. Variability

between the minimum and maximum depends on how much use is allowed in other hydrologic regions.

As described for solar thermal electric resources, the projected water demand changes for the Colorado River region are negative and significant in magnitude due to the projected reduction in agricultural water usage. From the data used for this analysis, the reduction in water use in the Colorado River region overcomes the effects of climate change and the increase in urban water use. Since the geothermal resource potential is dominated by the Colorado River region, these water demand dynamics have significant implications for the installable geothermal capacity. This impact is more significant for geothermal than for solar thermal electric.

The net available water supply breakdowns for the HadGEM2-ES RCP 8.5 scenario and the CanESM2 RCP 8.5 scenario, which represent the minimum and maximum capacity, respectively, in this case, are presented in Figure 32 and Figure 33, respectively.

Figure 32: Projected (2046-2055) Net Available Water Supply Requirements for Supporting Potential Geothermal Deployment in California vs. Projected (2046-2055) Net Available Water Supply. HadGEM2-ES Climate Model/RCP 8.5 Climate Scenario With Year 2050 Population Growth Trends

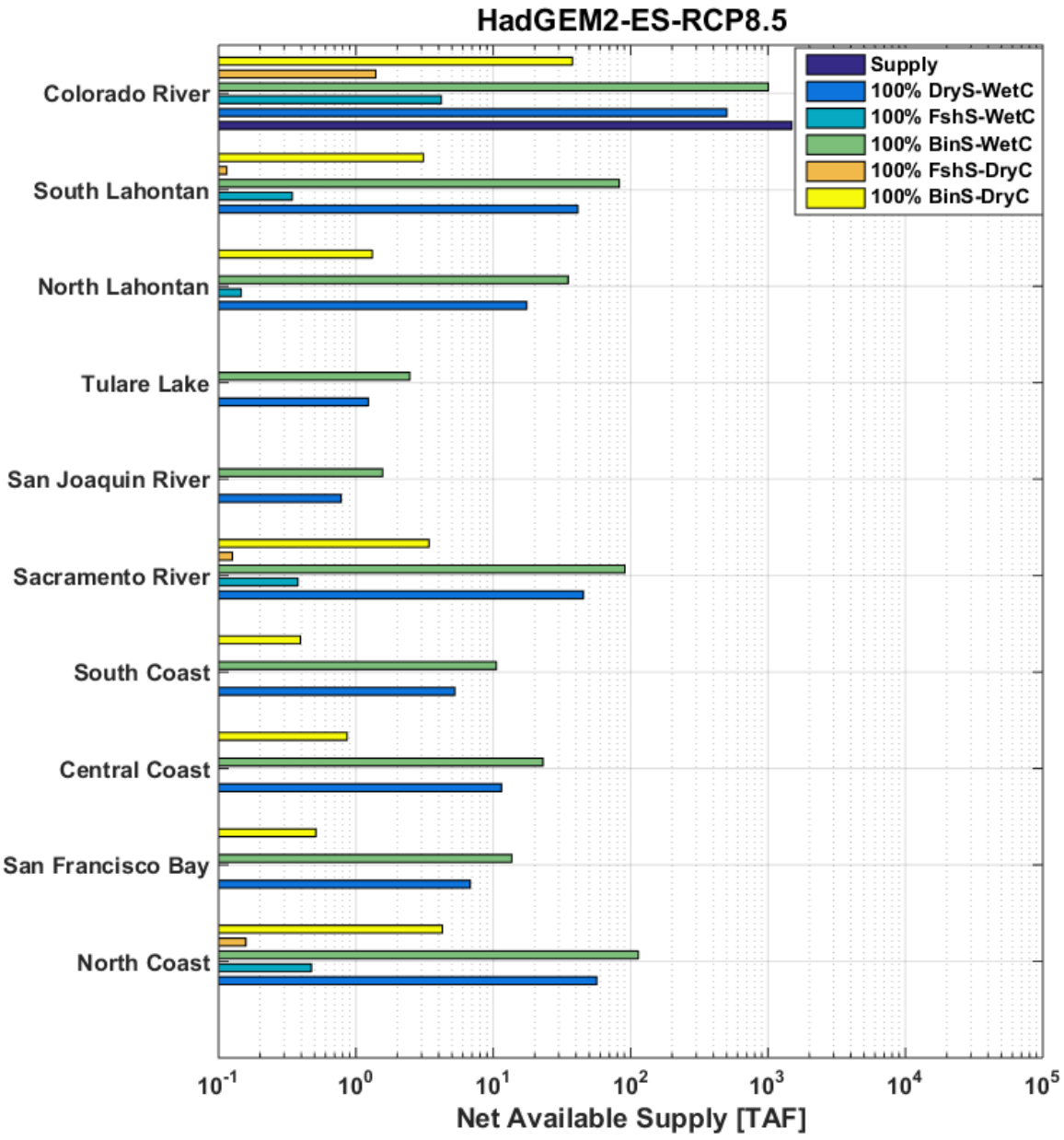

Using current trends for population and population density growth. Supply = Actual Net Available Supply for a given region, 100% DryS-WetC = Net Available Supply Requirement to Support 100% of Installable Geothermal Dry Steam Capacity with Wet Cooling, 100% FshS-WetC = Net Available Supply Requirement to Support 100% of Installable Geothermal Flash Steam Capacity with Wet Cooling, 100% BinS-WetC = Net Available Supply Requirement to Support 100% of Installable Geothermal Binary Capacity with Wet Cooling, 100% FshS-DryC = Net Available Supply Requirement to Support 100% of Installable Geothermal Flash Steam Capacity with Dry Cooling, 100% BinS-DryC = Net Available Supply Requirement to Support 100% of Installable Geothermal Binary Capacity with Dry Cooling.

Source: Advanced Power and Energy Program, University of California Irvine

Figure 33: Projected (2046-2055) Net Available Water Supply Requirements for Supporting Potential Geothermal Deployment in California vs. Projected (2046-2055) Net Available Water Supply. CanESM2 Climate Model/RCP 8.5 Climate Scenario With Year 2050 Population Growth Trends

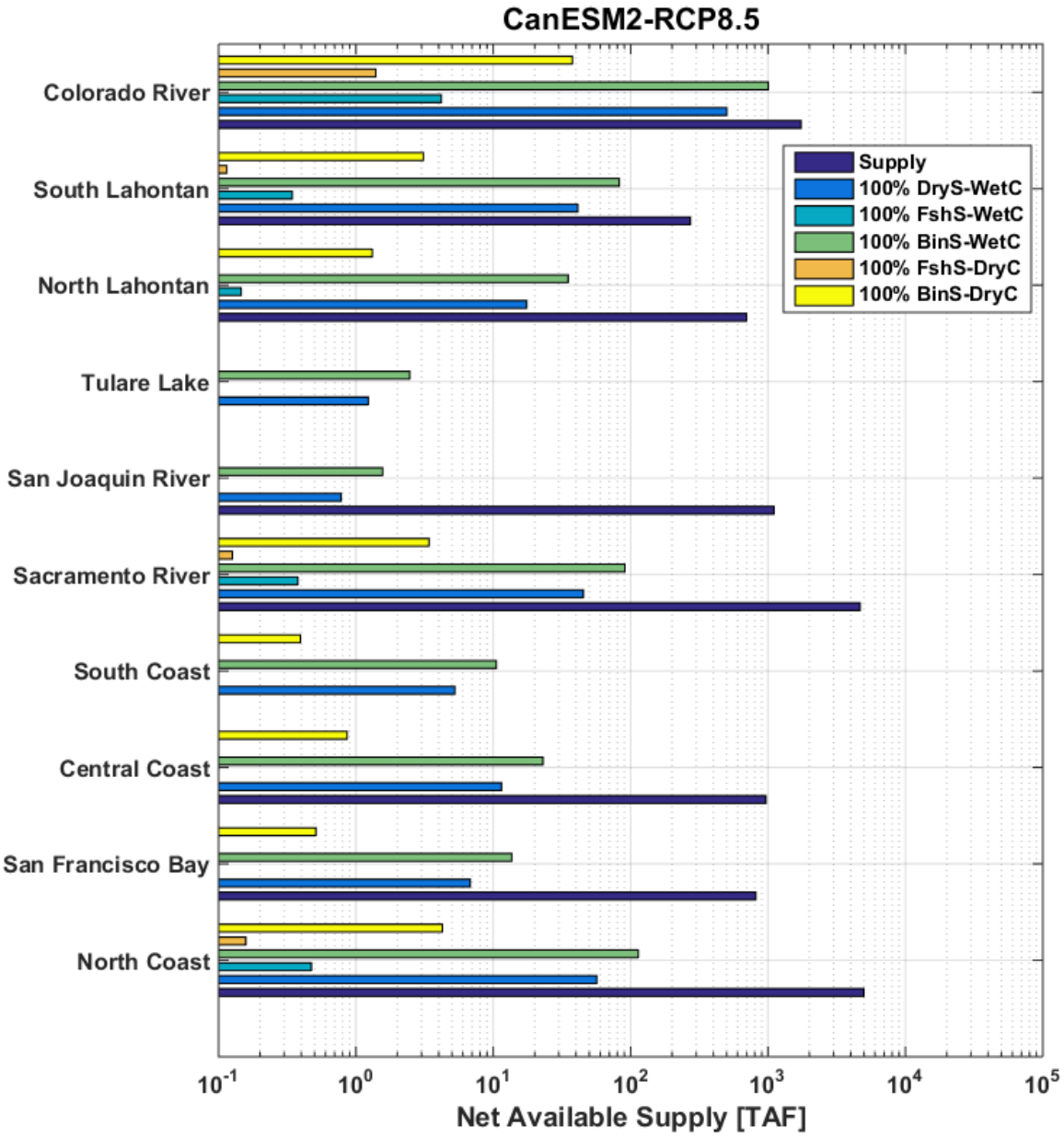

Using current trends for population and population density growth. Supply = Actual Net Available Supply for a given region, 100% DryS-WetC = Net Available Supply Requirement to Support 100% of Installable Geothermal Dry Steam Capacity with Wet Cooling, 100% FshS-WetC = Net Available Supply Requirement to Support 100% of Installable Geothermal Flash Steam Capacity with Wet Cooling, 100% BinS-WetC = Net Available Supply Requirement to Support 100% of Installable Geothermal Binary Capacity with Wet Cooling, 100% FshS-DryC = Net Available Supply Requirement to Support 100% of Installable Geothermal Flash Steam Capacity with Dry Cooling, 100% BinS-DryC = Net Available Supply Requirement to Support 100% of Installable Geothermal Binary Capacity with Dry Cooling.

Source: Advanced Power and Energy Program, University of California Irvine

The HadGEM2-ES RCP 8.5 scenario does not have any net available supply in any hydrologic region except the Colorado River region; however, the net available supply present in that region is large enough to exceed the requirements to support the full geothermal potential for that region regardless of cooling type. This highlights the importance of alignment between the spatial distribution of net available supply and thermally based resource potential. The CanESM2 RCP 8.5 scenario, however, exhibits significant net available supply in all hydrologic regions except Tulare Lake and South Coast. In each of the regions where net available supply is present, the magnitude exceeds the requirements for supporting the full geothermal resource base in those regions, regardless of cooling type. With changes in demand taken into account, the selection of cooling type does not appear to have significant implications for the potential installable capacity of geothermal power plants in California for the projected period.

From a planning standpoint, these results also indicate that reduction in water demand due to either agriculture water-use efficiency or reduction in agriculture usage in the Colorado River region can provide significant benefits for the use of geothermal resources, similar to the results for solar thermal electric resources. Water-use efficiency not only saves energy through reducing the energy usage of the water infrastructure, but it can allow water to be available for supporting larger capacities of thermally based renewable resources.

3.2.5 Impact of Different Population and Population Density Growth Scenarios

The water-constrained installable capacity can also be sensitive to the extent of water demand change. This section examines the sensitivity of those results to using different scenarios for water demand change based on population and population density growth trends. The data from the California Water Plan update [51] included projections for nine demand change scenarios – three population growth scenarios with three population density growth scenarios each. The maximum and minimum water-constrained installable solar thermal capacities calculated from the range of the water demand change scenarios are presented in Figure 34. The results for the no demand change case are also plotted for comparison.

Figure 34: Projected (2046-2055) Water Constrained Installable Solar Thermal Capacity in California – Sensitivity to Water Demand Change from Projected Year 2050 Population and Population Density Growth Scenarios

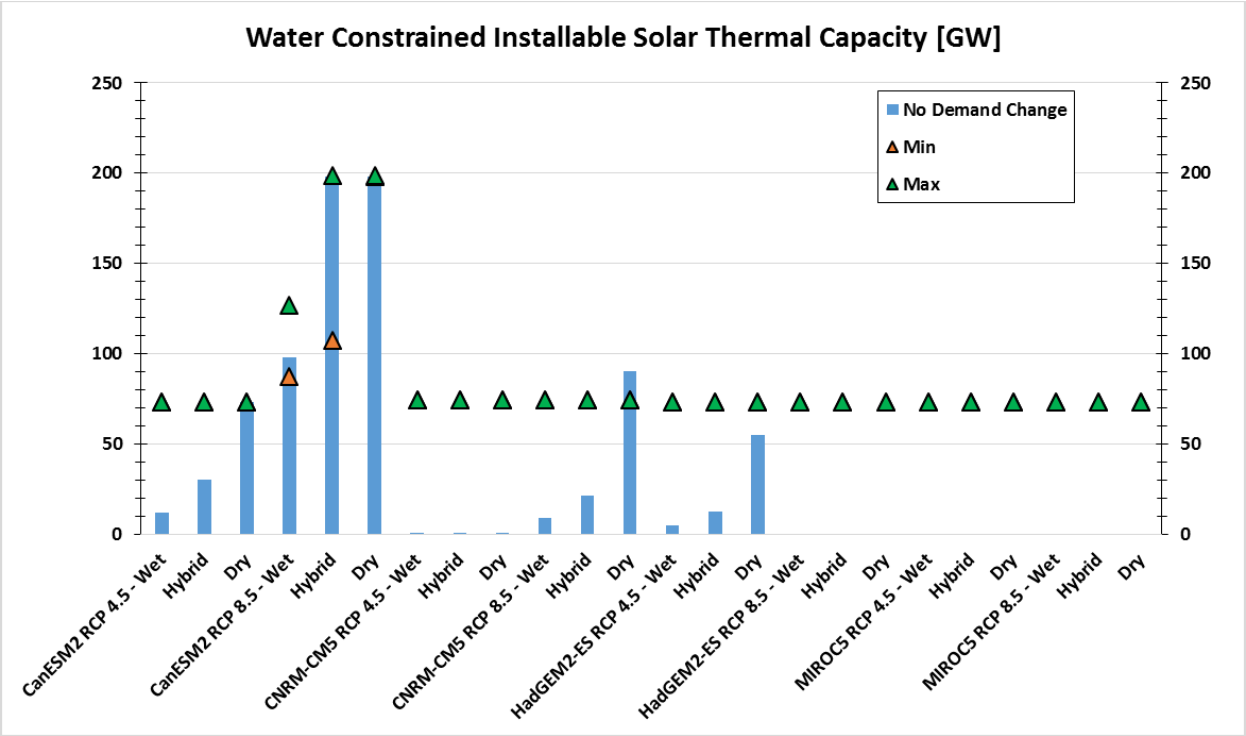

No Demand Change = Historical water demand levels, Min = Minimum installable solar thermal capacity calculated from the range of growth scenarios, Max = Maximum installable solar thermal capacity calculated from the range of growth scenarios.

Source: Advanced Power and Energy Program, University of California Irvine

The selection of water demand change scenario from the California Water Plan Update 2013 did not affect the water-constrained installable solar thermal capacity in any case except for the CanESM2 RCP 8.5 scenario set in the wet and hybrid cooling cases. In all the other scenario sets, the maximum and minimum water-constrained installable solar thermal capacities are effectively the same – being insensitive to the water demand change scenario. This occurs because all the water demand change scenarios project significant reductions in agriculture water use in the Colorado River region and, therefore, allow full use of the 73.6 GW capacity potential in that region. In the CanESM2 RCP 8.5 scenario set, the climate impacts allow a positive net available supply to be present in the South Lahontan region, and, therefore, the growth scenarios and cooling system type affect how much solar thermal capacity that the net available supply can support. In this case, the range is between 83 GW and 125 GW for wet cooling and between 108 GW and the full 199.6 GW for hybrid cooling. Dry cooling allows use of the full 199.6 GW regardless of water demand change scenario. This shows that for solar thermal capacity, the range of water demand change scenarios based on the California Water Plan Update do not significantly affect the results.

The maximum and minimum water-constrained installable geothermal capacities calculated from the range of the water demand change scenarios are presented in Figure 35. The results for the no demand change case are also plotted for comparison.

Figure 35: Projected (2046-2055) Water Constrained Installable Geothermal Capacity in California - Sensitivity to Water Demand Change from Projected Year 2050 Population and Population Density Growth Scenarios

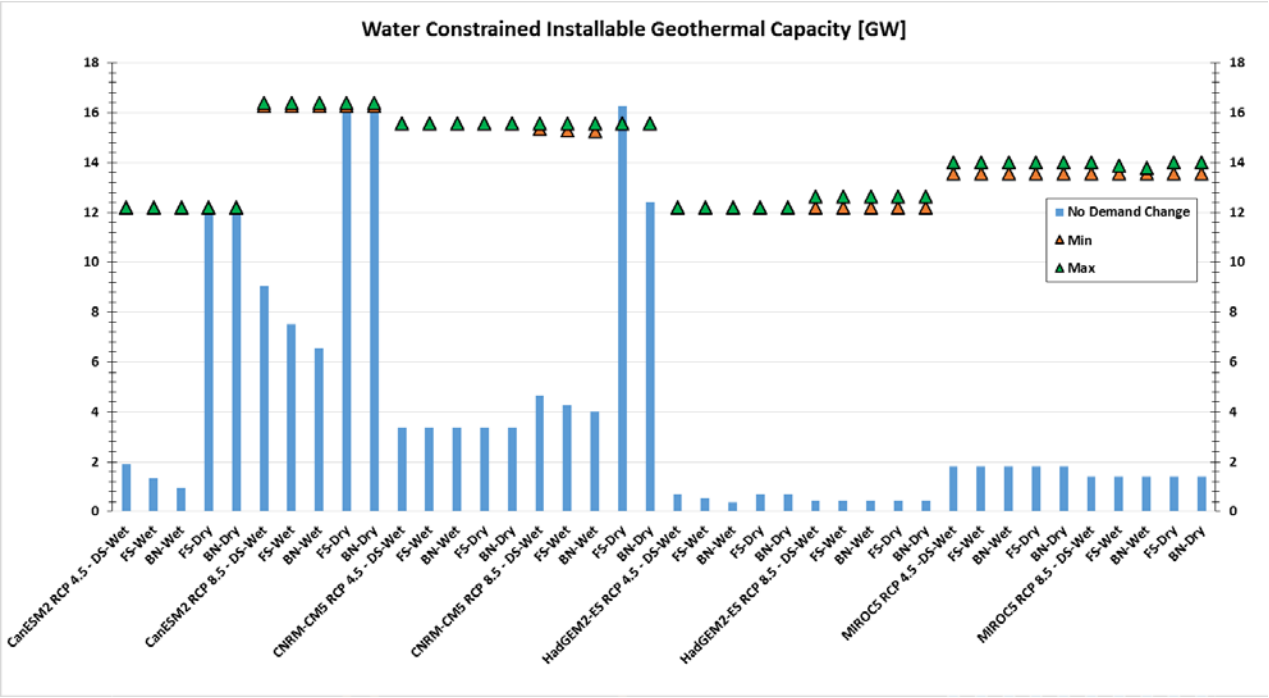

No Demand Change = Historical water demand levels, Min = Minimum installable solar thermal capacity calculated from the range of growth scenarios, Max = Maximum installable solar thermal capacity calculated from the range of growth scenarios.

Source: Advanced Power and Energy Program, University of California Irvine

Similar to the results for solar thermal capacity, the water demand change scenarios did not significantly affect the water-constrained installable geothermal capacity. This occurs due to the large reductions in agricultural water demand in the Colorado River region, where most of the geothermal potential is located. This holds across all scenarios, and the difference between the maximum and minimum installable geothermal capacities due to water demand change scenario is relatively small. Since all water demand change scenarios show large demand reductions in the Colorado River, this allows full use of the capacity potential in this region. The water demand change scenario affects mainly the installable capacity in other regions, which are a smaller portion of the total statewide potential.

3.3 Conclusions

The research team examined the impact of future water availability under climate change on the ability to support solar thermal electric and geothermal resource use in California by 2050. This was accomplished by 1) calculating the water unconstrained potential capacity for solar

thermal and geothermal resources, 2) calculating the available supply of water for supporting the water needs of these power plants under different climate scenarios and models, and 3) determining the capacity that can be supported from the available water supply based on power plant cooling type. The sensitivity to water demand changes was also examined comparing cases with historical water demand levels and a range of water demand change scenarios from the California Water Plan Update 2013. The main insights and implications from this study are as follows:

1. **Water availability can limit the use of solar thermal and geothermal resources as components of a low-carbon, renewable-based electricity portfolio.** The water-constrained installable capacity for both solar thermal and geothermal resources was lower than the unconstrained analogue in almost every scenario. This effect is especially strong for the case without any reductions in water demand from historical levels, where certain scenarios showed zero installable capacity due to unavailability of water.

2. **The spatial distribution of water availability is a main driving factor in determining the extent to which the potential for solar thermal and geothermal resources can be used.** Water availability, as well as the potential for solar thermal and geothermal resources, has a strong spatial component. For solar thermal and geothermal resources to be used, water does not only have to be available, it must be available in the hydrologic regions where significant solar thermal and geothermal resources are present. For California, this is especially important since the high-quality solar thermal and geothermal resources are concentrated in the Colorado River and South Lahontan regions. Therefore, the water-constrained installable capacity will depend mostly on the water balance of these two regions.

3. **When the spatial distributions of water availability and resource potential align, selection of water-efficient power plant cooling type allows a given level of water availability to support a larger portion of the total solar thermal and geothermal resource potential.** The overall results for water-constrained installable solar thermal capacity were less sensitive to cooling system type than climate scenario. This is because while a more efficient cooling system (specifically dry cooling) allows a given level of water availability to support higher solar thermal or geothermal capacities, if the water availability in a given region with solar thermal or geothermal potential is negative or zero, cooling system has no impact. This is because even with dry cooling, steam-turbine based power plants still require small amounts of water for other operations. However, when water is available in a region with solar thermal electric or geothermal potential, dry cooling will make the most effective use of that water.

4. **Reducing water demand in areas with solar thermal electric and geothermal potential is important for allowing large use of the solar thermal electric and geothermal resource potential.** The cases using historical water demand levels for each hydrologic region exhibited very limited water-constrained installable solar thermal electric and

geothermal capacities in most cases. When water demand change scenarios were projected, most of which included water demand reductions for the Colorado River region, all the cases exhibited larger potential for water-constrained installable capacities. Reducing water demands in these key regions can potentially free water allocations for use to support solar thermal electric and geothermal development, highlighting a potential synergy in the water-energy nexus.

Overall, these insights have implications for planning and determining the role of solar thermal electric and geothermal resources in developing renewable-based, low-carbon electricity portfolios for California. Solar thermal electric and geothermal resources may make sense only from a sustainability standpoint when integrated to an extent that does not cause or exacerbate water stress. Moreover, there is a sense of risk involved with solar thermal electric and geothermal deployment: if large solar thermal and geothermal capacities are installed, some of these facilities may be unable to run in later years if water shortage becomes a constant aspect of the regions in which they are located. If solar thermal electric and geothermal resources are to be used, it is important that the operations of these resources are streamlined to require as little water as possible.

Equity is another consideration, whether net available supply in a given hydrologic region should be devoted to solar thermal and geothermal power plants, as opposed to other uses. This discussion must be carried out on a region-by-region basis, taking into account the priority of other water demands in a region and the ability to access these supplies.

CHAPTER 4:
Assessment of Climate Change Impacts on Electricity Demand

4.1 Introduction and Background

Many studies have focused on projecting the potential portfolio of electric grid resource technologies to be deployed for meeting California's long-term GHG reduction goals. Climate change will impact the electric loads on buildings through the related impacts on local atmospheric conditions, most prominently through changes in patterns and magnitudes of average and peak temperatures across the state. These temperature patterns will affect the magnitude of cooling loads through potentially increased air-conditioning use, as well as decreased heating loads through changes in space- and water-heating needs. Furthermore, the changes in electric loads and total site-level building energy demands (electricity and natural gas consumption within buildings) will vary spatially across the state's Title 24 Building Climate Zones.[2]

The impacts of climate change on electric loads and energy demands are important to consider in designing a potential energy resource portfolio that is robust in meeting California's carbon reduction and renewable use goals. Potentially increased electric loads and energy demands due to climate change in excess of those expected from population and other factors can potentially cause demand forecasts based on previous strategies to fall short of the stated goal. Therefore, this work will characterize the impact of future climate conditions on residential and commercial electric loads and energy demands to better inform low-carbon, renewable-based energy resource planning to meet California's energy goals.

This chapter examines the impact of environmental conditions under climate change on the magnitude and profile of residential and commercial building energy use. A suite of residential and commercial prototype buildings was modeled using the EnergyPlus building simulation tool (see Appendix A.3). Environmental weather conditions, under scenarios for historical climate conditions and those imposed by climate change, are imposed onto the yearlong operation of residential and commercial buildings located in different representative climate zones of the state. The changes in the magnitude and profile of electric loads, natural gas usage, and other operational characteristics between historical and climate change conditions are analyzed to characterize the impacts. Further detail on the method is provided in Appendix A.4., with supplemental results provided in Appendix B.

4.2 Analysis and Results

[2] https://www.energy.ca.gov/maps/renewable/building_climate_zones.html

The impact of climate change conditions on the annual California electric load demand of the combined sectors is presented in Figure 36 for percentage change between the climate change conditions and the historical conditions (Base) and in Figure 37 for absolute magnitude of the load.

Figure 36: Projected Year 2050 Climate Change Impacts on Annual California Statewide Electric Load Demand in Percentage Change From the Base Case for Different Climate Models and Climate Scenarios. Climate Modeling Spans 2046-2055.

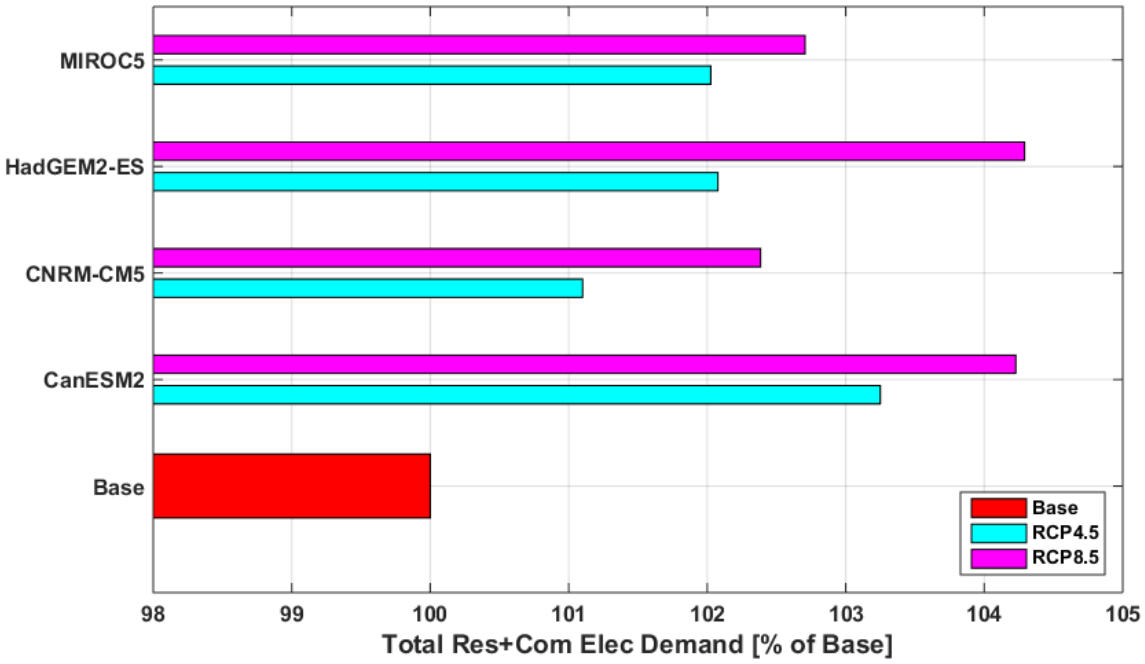

Source: Advanced Power and Energy Program, University of California Irvine

Figure 37: Projected Year 2050 Climate Change Impacts on Annual California Statewide Electric Load Demand in Absolute Magnitude for Different Climate Models and Climate Scenarios. Climate Modeling Spans 2046-2055

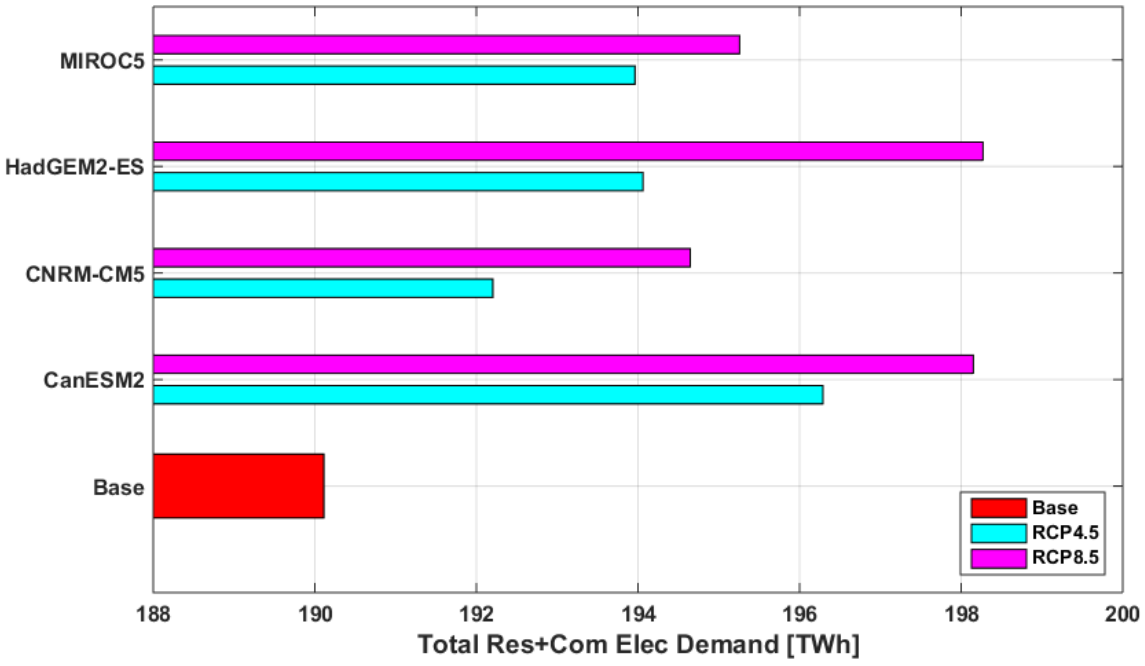

Source: Advanced Power and Energy Program, University of California Irvine

For the combined residential and commercial sectors, the projected California electric load demand by the year 2050 increases due to climate change by between 1.1% to 3.2% for the RCP 4.5 climate scenario and 2.4% to 4.3% for the RCP 8.5 climate scenario, depending on climate model. In absolute terms, this translates to increases of between 2.10 to 6.20 terawatt hours (trillion watt hours, TWh) for the RCP 4.5 cases and between 4.50 to 8.20 TWh for the RCP 8.5 cases. The RCP 8.5 scenarios have warmer temperatures relative to the RCP 4.5 cases due to larger GHG concentrations and radiative forcing in the atmosphere. Across climate models within a given climate scenario, the CanESM2 climate model tends to have the highest increases in electric loads for the RCP 4.5 case, but the HadGEM2-ES climate model has the highest increases in the RCP 8.5 case. These occur due to temperature increases and the different effects described for the commercial and residential sectors, as described in Appendix B.3.

A time series snapshot of the electric load profile of combined buildings under historical climate and climate change-impacted conditions for the RCP 8.5 climate scenario is presented in Figure 38 for each climate model.

Figure 38: Combined Sector California Statewide Electric Load Profiles for the Year 2050 Projected Under Climate Change for Each Climate Model Under the RCP 8.5 Climate Scenario (Five Summer Days). Climate Modeling Spans 2046-2055

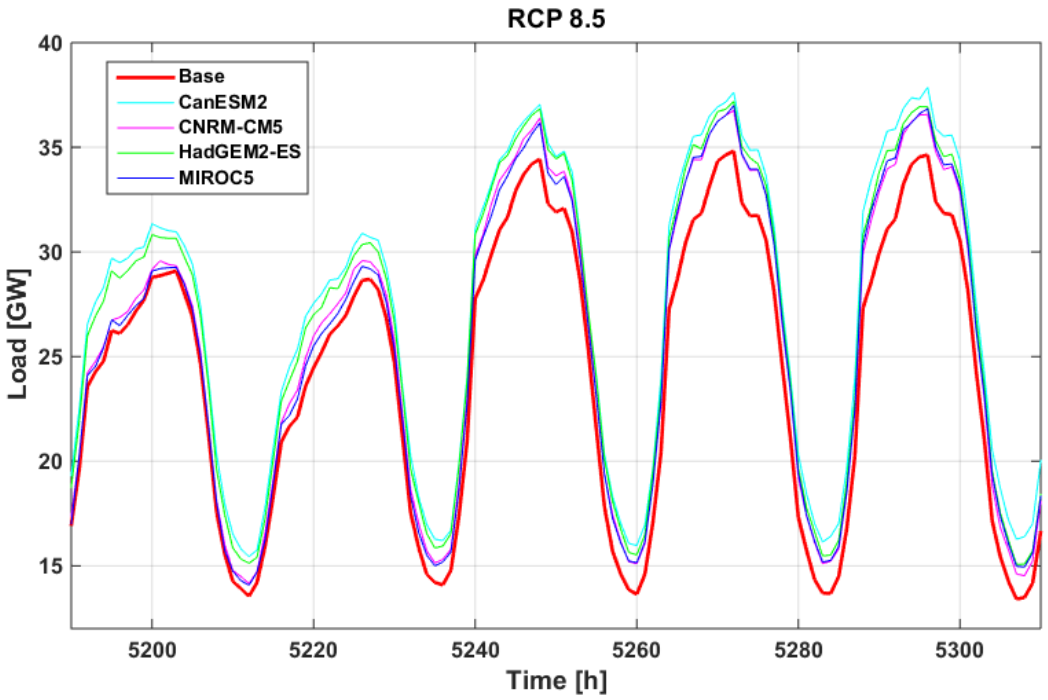

Source: Advanced Power and Energy Program, University of California Irvine

The impact of climate change-affected temperatures on typical combined sector peak hourly electric loads are presented in Figure 39 for percentage change from historical conditions (Base) and in Figure 40 for absolute magnitudes. Since the climate conditions are derived from an average from 2046-2055 in the climate models to derive a representative 2050 profile, these are termed as *typical hourly peak electric demands*.

Figure 39: Projected Year 2050 Climate Change Impacts on California Statewide Peak Hourly Electric Load Demand in Percentage Change From the Base Case for Different Climate Models and Climate Scenarios. Climate Modeling Spans 2046-2055

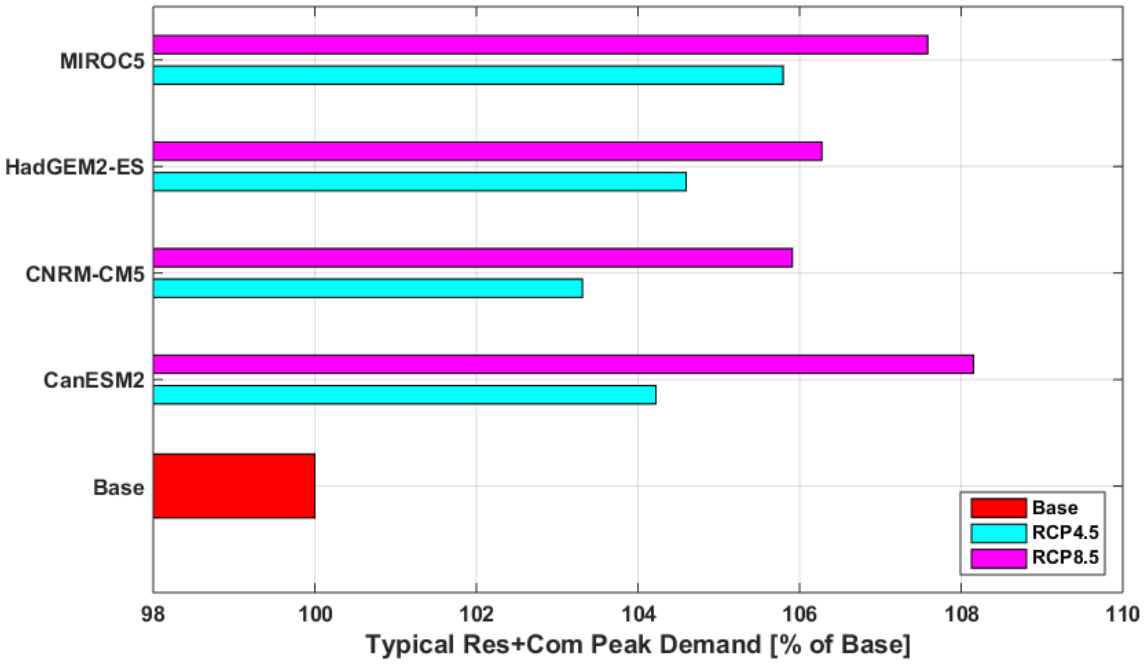

Source: Advanced Power and Energy Program, University of California Irvine

Figure 40: Projected Year 2050 Climate Change Impacts on California Statewide Peak Hourly Electric Load Demand in Absolute Magnitude for Different Climate Models and Climate Scenarios Climate Modeling Spans 2046-2055

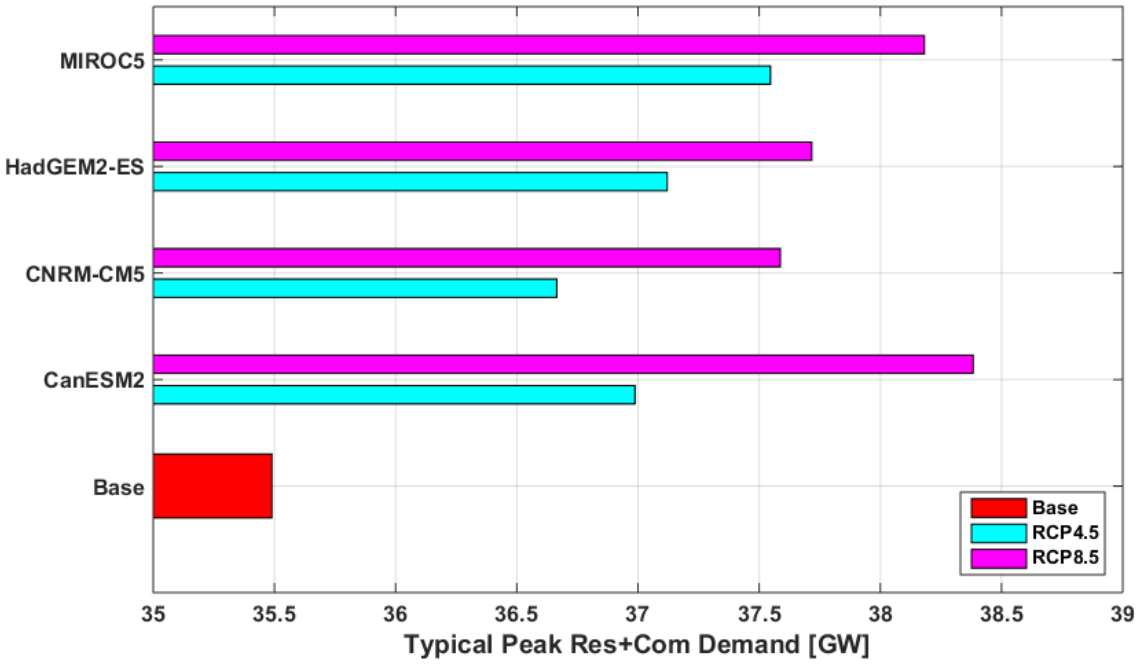

Source: Advanced Power and Energy Program, University of California Irvine

For the combined sector, the projected peak electric load demand for 2050 increases due to climate change between 3.3% to 5.8% for the RCP 4.5 climate scenario and 5.9% to 8.2% for the RCP 8.5 climate scenario, depending on climate model. In absolute terms, this translates to increases of between 1.17 to 2.06 GW for the RCP 4.5 cases and between 2.10 to 2.89 GW for the RCP 8.5 cases.

For the combined sector, the annual site-level energy use under historical (2001-2010) climate conditions and projected climate change-impacted conditions (2046-2055) by end use is presented in Figure 41. The end uses considered are space cooling, space heating, water heating, and other. The “other” category refers to other loads within combined buildings such as appliances and plug loads, which do not vary significantly with external building conditions.

Figure 41: Projected Year 2050 Annual California Statewide Total Combined Energy Demand in Million MMBTU by End Use. Base refers to Historical (2001-2010) Climate Conditions, Each RCP refers to Future (2046-2055) Climate Conditions

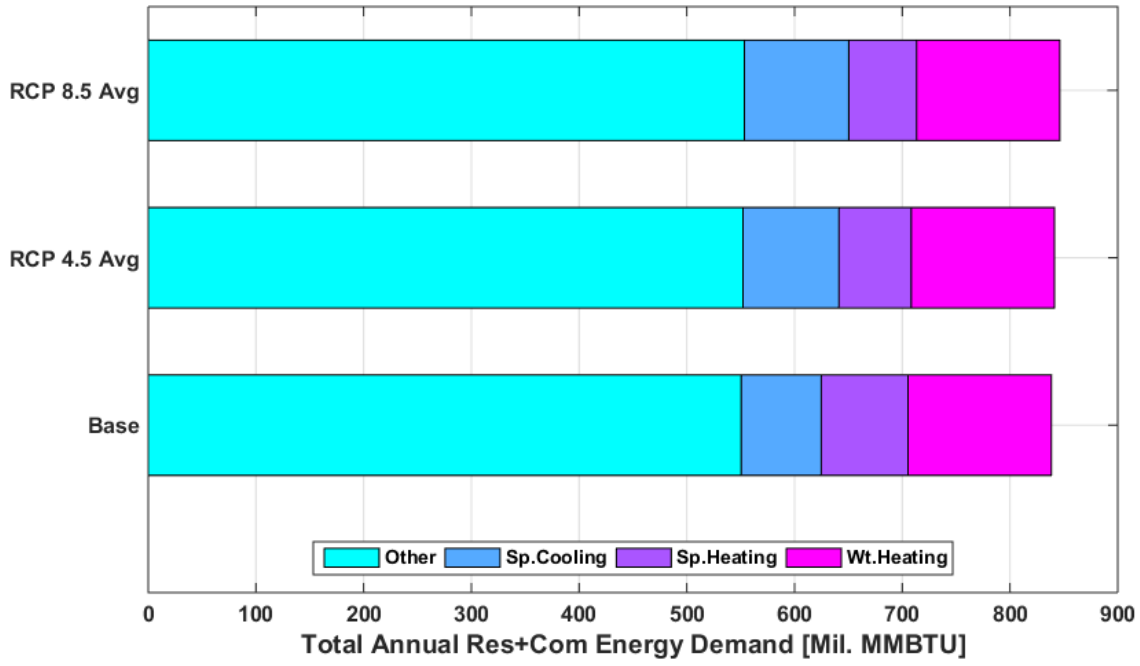

Sp. Cooling = Space Cooling, Sp. Heating = Space Heating, and Wt. Heating = Water Heating.

Source: Advanced Power and Energy Program, University of California Irvine

The values from the individual climate models were averaged with equal weight to provide a representative climate change effect. In general, the hotter models (CanESM2 and HadGEM2-ES) showed larger decreases in space heating demands and increases in space cooling demands compared to the average. For the combined commercial and residential sectors, the annual site-level energy demand increases very slightly. The competing effects of increases in the residential sector and decreases in the commercial sector causes the combined sector annual energy demand under climate change to be similar to the base case. The commercial sector comprises a slightly larger fraction of the total energy demand compared to residential, so the effects on the commercial sector have slightly more influence.

The change of site-level energy demand by end use under climate change is presented in Figure 42 in percentage change from base and in Figure 43 for absolute magnitude changes.

Figure 42: Projected Year 2050 Climate Change Impacts on Annual California Statewide Site-Level Energy Demand by End Use in Percentage Change From the Base Case (2001-2010) for Different Climate Scenarios (2046-2055)

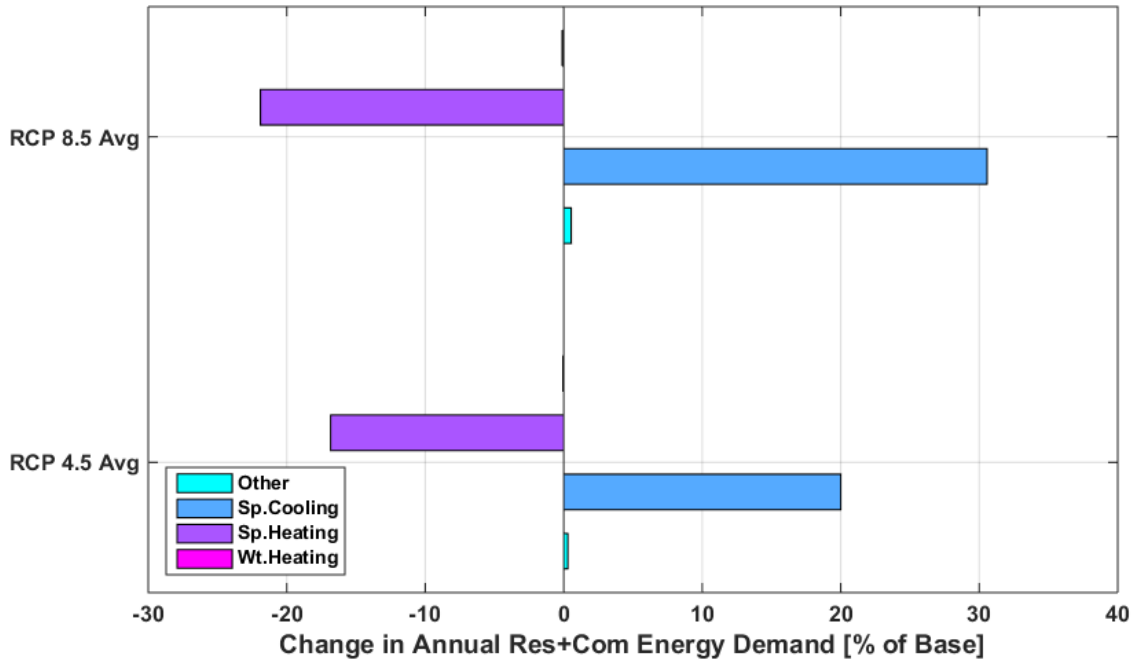

Source: Advanced Power and Energy Program, University of California Irvine

Figure 43: Projected Year 2050 Climate Change Impacts on Annual California Statewide Site-Level Energy Demand by End Use in Absolute Magnitude From the Base Case (2001-2010) for Different Climate Scenarios (2046-2055)

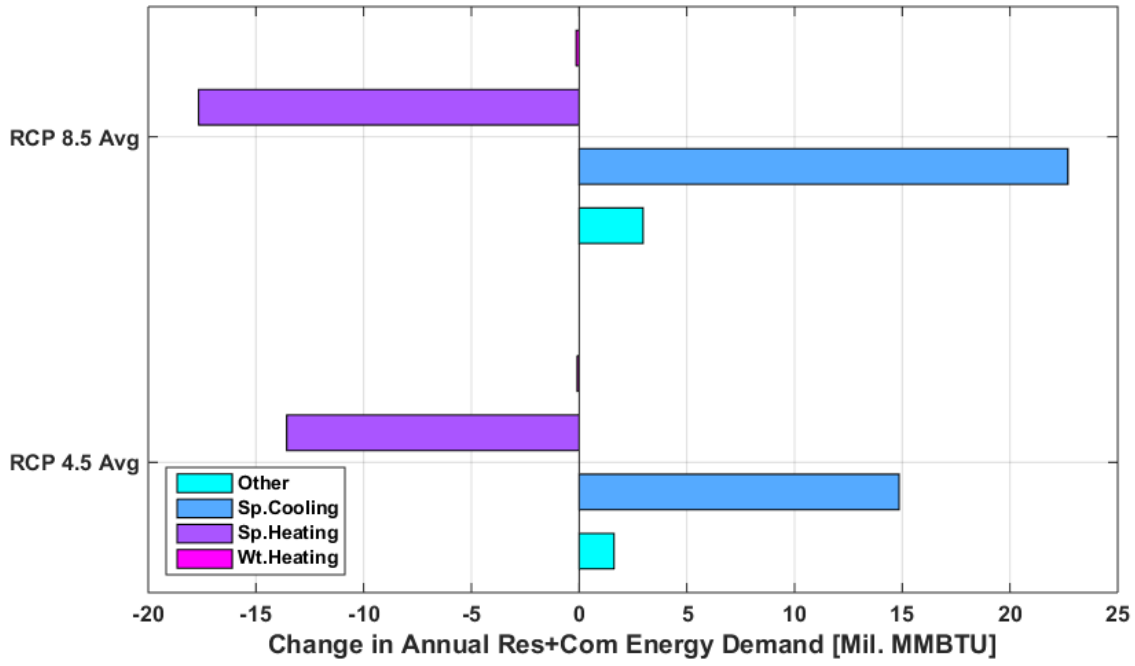

Source: Advanced Power and Energy Program, University of California Irvine

For the combined commercial and residential sectors, the changes in energy demand by end use exhibits decreases in space-heating energy demand (-16.83% to -21.90%), increases in space-cooling energy demand (+20.01% to +30.56%), slight increases in other energy demands (+0.29% to +0.54%), and very small decreases in water-heating energy demands (-0.06% to -0.10%). The decreases in space-heating demands are smaller than the increases for space-cooling demands in absolute terms from the influence of the commercial sector on the combined results.

The increase in space-cooling energy demands and the decrease in space-heating and water-heating demands would shift the distribution of energy use by fuel type toward electricity by the year 2050, compared to that in historical conditions represented by 2001-2010. The effect is slight, but the onset of climate change causes combined buildings to increase reliance on electricity and decrease reliance on natural gas. This occurs since space cooling is solely an electric load, while space heating is met mostly by natural gas.

In addition to the statewide impacts of climate change on the combined sector projections, the impacts of climate change vary across climate zone and location within the state. The annual combined electricity demand for the year 2050 (climate modeling spanning 2046-2055) by climate zone is presented in Figure 44, and the change from historical climate conditions (Base: 2001-2010) is presented in Figure 45.

Figure 44: Projected Year 2050 Annual California Statewide Combined Electric Demand by Climate Zone Under Climate Change – Absolute Magnitude. Climate Modeling Spans 2046-2055 and is Compared to Historical Conditions Spanning 2001-2010

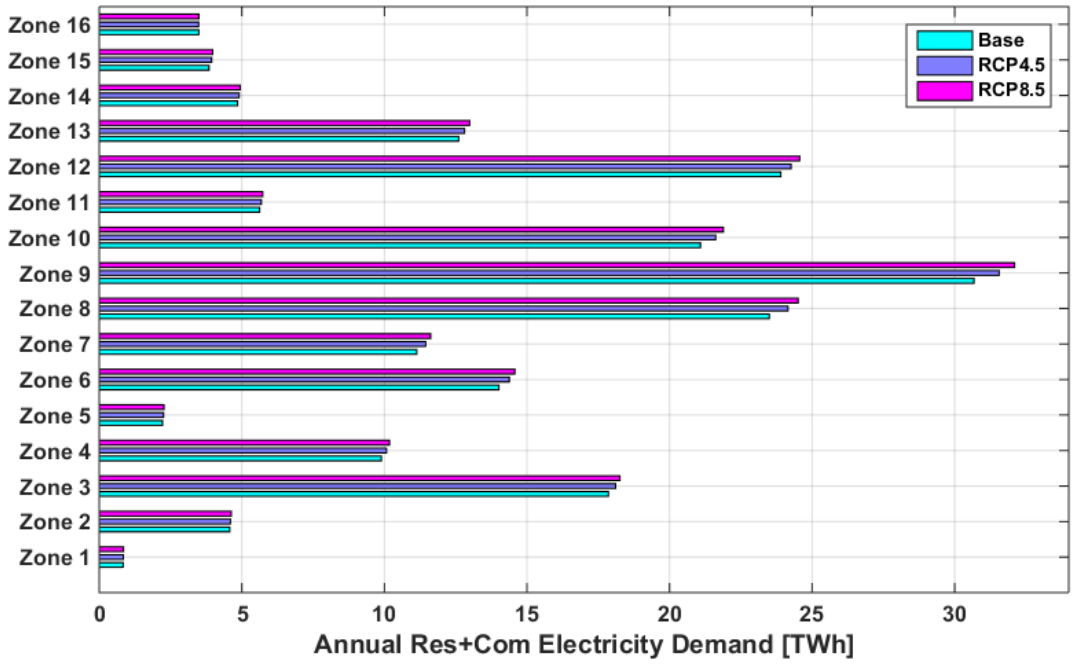

Source: Advanced Power and Energy Program, University of California Irvine

Figure 45: Projected Year 2050 Annual California Statewide Combined Electric Demand by Climate Zone Under Climate Change – Percentage Change from Base. Climate Modeling Spans 2046-2055 and is Compared to Historical Conditions Spanning 2001-2010

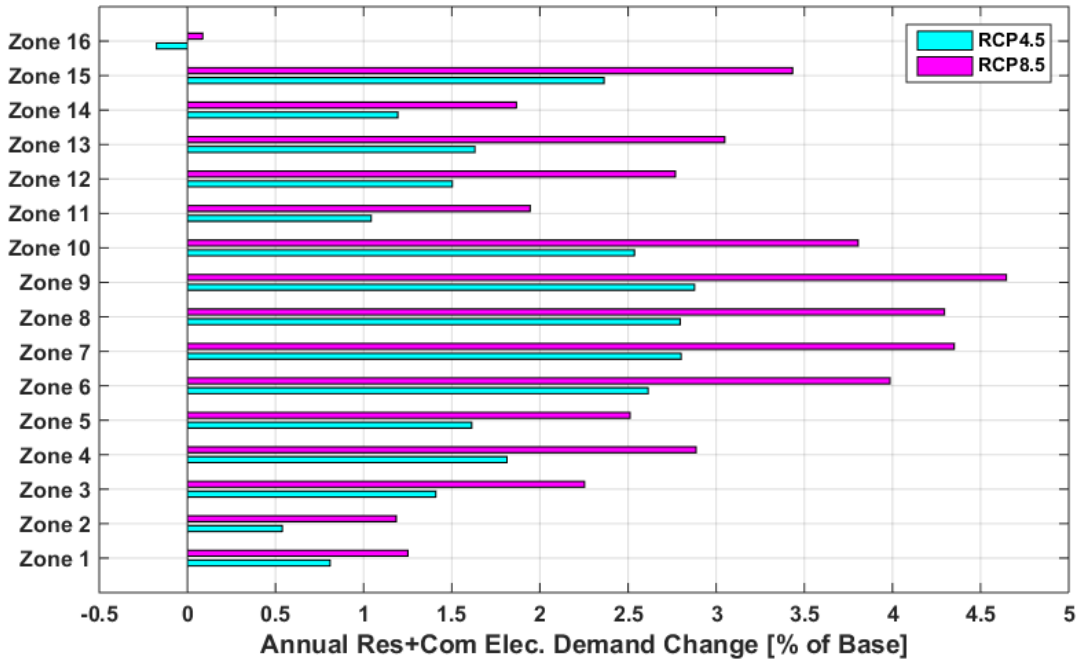

Source: Advanced Power and Energy Program, University of California Irvine

The largest percentage increases in electricity demands occur in Climate Zones 6-10 for RCP 4.5 and RCP 8.5 climate scenarios. Climate Zones 6-10 are all in Southern California, encompassing the heavily populated coastal and slightly inland areas of the southern part of the state. The commercial and residential sectors show the largest percentage increases in Climate Zones 6-10. Results of this analysis indicate these regions will be subject to the largest increases in temperatures due to climate change by 2046-2055 compared to 2001-2010.

4.3 Conclusions

The research team investigated the projected impact of climate change-impacted weather conditions in 2050 on the electric loads and site-level energy demands of the commercial and residential sectors in California. For each sector and the combined commercial and residential sector, impacts on annual electricity demand, peak electric loads, total site-level energy demands, energy demands by end use (space cooling, space heating, water heating, other), fuel type, and the spatial distribution of electricity impacts across the state were assessed. The future year 2050 was represented by climate modeling spanning 2046-2055 and compared to historical climate conditions spanning 2001-2010. This was accomplished by 1) obtaining physical-based representative building prototypes for commercial and residential buildings for simulation in the EnergyPlus building modeling platform, 2) calculating the change in external weather conditions that buildings will be subject to using four climate models and two GHG emissions scenarios, and 3) building up the commercial and residential building stock to obtain

electric loads and energy demands under historical climate conditions and climate change impacted conditions. The main insights and their implications from this study are as follows:

1. **Climate change is expected to increase residential and commercial California electricity demands by increasing space-cooling loads due to increased temperatures.** Across all climate scenarios and climate models, the 2050 annual electric load demand of the commercial and residential sectors increased relative to historical (2001-2010) energy conditions, with the upper end of the range being 4.3%. The RCP 8.5 cases exhibit the largest increases due to higher average temperatures. Variability between climate models is linked to the related average temperatures and seasonality relative to that of distinct residential and commercial electricity demands. For example, the warmer models (CanESM2 and HadGEM2-ES) exhibit higher average temperatures, which drives larger increases in space cooling on an annual basis compared to the CNRM-CM5 and MIROC5 models. On a seasonal basis, space cooling loads are the highest during the summer months, and cooling energy use increases nonlinearly with temperature. Therefore, the seasons where climate models project temperature increases are also important for capturing changes in space cooling energy demand.

2. **The combined residential plus commercial California site-level energy demand is expected to increase only slightly under climate change in 2050 compared to 2001-2010 because increases in space-cooling energy demands are slightly offset by decreases in space-heating energy demands.** Increased temperatures cause increased demands for cooling but decreased needs for heating. Since space-heating needs are typically met using natural gas boilers but space-cooling requirements are met using electrically driven vapor compression systems, providing a given amount of cooling requires less site-level energy input compared to a given amount of heating. Therefore, in the residential sector where space cooling and space heating energy demands are of a similar magnitude, this causes site-level residential energy use to decrease under climate change in 2050. In the commercial sector, however, space cooling is a larger demand than space heating, so site-level commercial energy use increases under climate change. These competing effects cause the combined site-level energy use to increase only slightly.

3. **In 2050 climate change is projected to cause California site-level energy use to depend more on electricity and less on direct fuel inputs.** The increased emphasis on space cooling and decreased emphasis on space heating cause increased electricity consumption but decreased natural gas consumption. These emphases have the potential to align more readily with low-carbon electrification efforts.

4. **In 2050, projections indicate the most populous regions in Southern California will exhibit the largest increases in electric loads under climate change compared to other parts of California.** The largest increases in electricity demand in absolute terms and percentage change occur in the climate zones on the coastal and slightly inland

areas of Southern California. These regions combine large populations with the largest increases in temperatures due to climate change, causing the largest increases in electric demands. This occurs in both the commercial and residential sectors. Therefore, these regions will need to be a focus for implementing more low-carbon electricity generation to offset these increases and potential increases in electricity sector emissions.

Overall, these results have implications regarding the scale and character of the electric loads that must be met in planning of the energy resource mix to satisfy GHG reduction and renewable energy use goals. The increases in electric load magnitude due to climate change impacts alone indicate that a larger capacity of renewable and low-carbon resources must be in place to meet a given emissions reduction goal. Climate change is projected to have important impacts on strategies for managing peak electricity events.

The increasing shift toward dependence on electricity to meet residential and commercial loads at the site level places a heightened emphasis on the necessity to have a significantly decarbonized electricity supply. Finally, the result that the impacts of climate change will most strongly affect heavily populated areas in Southern California indicates that efforts to reduce loads, increase energy efficiency, and implement advanced building codes must be targeted to these areas to reduce the potential impacts of climate change on electric loads. These aspects must be taken into account to develop robust planning strategies and technology portfolios to meet California's statutory energy goals.

This analysis does not account for changes in demand due to population growth, as it focused on isolating the effect of climate change on building energy demands. The effects of population growth on building energy demands will compound the effects analyzed here to produce larger overall increases in building energy use.

CHAPTER 5:
Climate Change Implications of Renewable Use and Greenhouse Gas Emissions Reduction Strategies – Part 1: Impacts

5.1 Introduction and Background

Chapters 2, 3, and 4 of this report investigated the impacts of climate change conditions on hydropower generation, the installable capacity of solar thermal electric and geothermal-based resources, and the magnitude of residential and commercial loads. These impacts, individually and combined, can affect the ability of developed electricity planning scenarios for meeting long-term reductions in electricity system GHG emissions and increases in renewable energy use. This chapter focuses on translating the effects of climate change described in Chapters 2, 3, and 4 to changes in GHG emissions and renewable energy use of the electricity system. The research team also investigated how these impacts affect the effectiveness of scenarios of technology mixes developed to meet these goals that do not take into account climate change. In particular, this chapter focuses on 2050 and the corresponding GHG goal, since 2030 is not expected to exhibit significant climate change impacts. Any shortfalls in the attainment of climate and energy goals must be compensated for by adjustment in the technology mix deployed to meet these goals. Mitigation strategies for any identified shortfalls are discussed in Chapter 6.

The results of climate change impacts on hydropower generation, solar thermal and geothermal potential limits, and building load demands are imposed on operating the electricity system for each climate model under the RCP 8.5 emissions scenario. The year 2050 electric grid resource portfolio is modeled based on the E3 PATHWAYS study for 2050 as resource capacities (before limits are applied), transportation integration, and electric loads [24]. The operation of the electricity system is modeled in the HiGRID model, which is an hourly resolved electricity system dispatch model that captures the response of electric grid resource operation to technology and environmental condition disruptions. The HiGRID model will produce as outputs relevant to this chapter the electricity system GHG emissions and renewable penetration level attained. More details on the methods used to carry out the analyses in this chapter are presented in Appendix A.5, and supplementary results that investigate the isolated effect of each climate change impact type on the electric grid are presented in Appendix B.

5.2 Results and Analysis

The combined impacts of climate change-altered hydropower generation, constrained geothermal capacity, and climate change-altered residential and commercial building loads on electricity sector GHG emissions are presented as a difference from the 2050 case without climate change conditions on a 10-year average in Figure 46. The case without climate change

conditions is represented by 2001-2010 climate conditions, while climate change is represented by 2046-2055 and averaged to develop the year 2050 case.

Figure 46: Projected California Electric Grid Greenhouse Gas Emissions Difference From Historical Climate Conditions – 10-Year Average Representing 2050

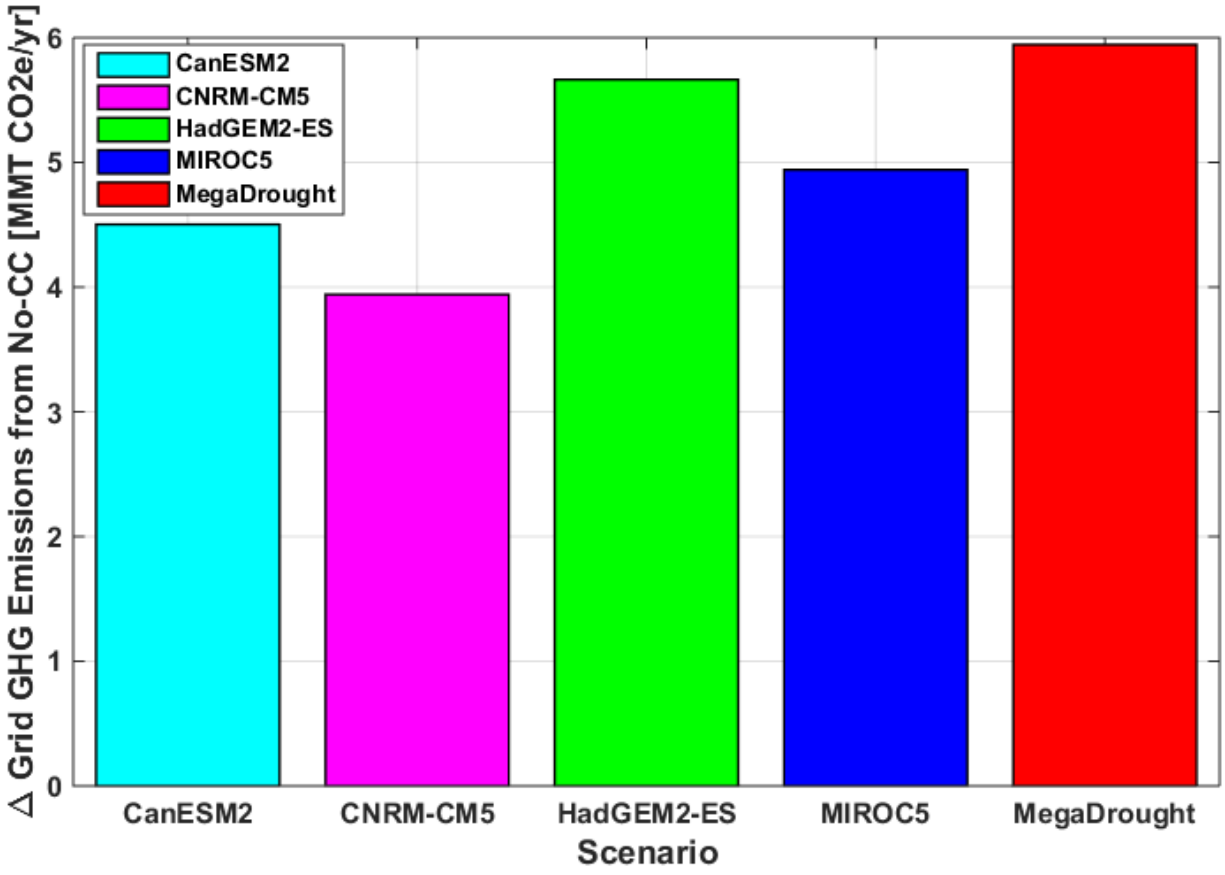

Emissions level without climate change = 18.04 million metric tons (MMT) CO_2e/yr

Source: Advanced Power and Energy Program, University of California Irvine

Each year from 2046-2055, and on average, the California electric grid GHG emissions increase from the effects of climate change. For the 2050 compliance scenario, assuming no change in climate conditions, the electric grid produces 18.04 million metric tons (MMT) of CO_2e greenhouse gases per year primarily due to natural gas power plants performing load balancing and providing ancillary services. In any year, the order of emissions increases for these climate models align with the order of the 10-year average.

To study the causes of these impacts, the research team examined changes in the projected generation profile due to climate change. The distribution of delivered electricity to load taking into account curtailment and losses for each scenario is presented as the changes from the case without climate change by resource for each scenario presented in Figure 47.

Figure 47: Projected Change in California Delivered Electricity Distribution by Resource in 2050 due to Climate Change

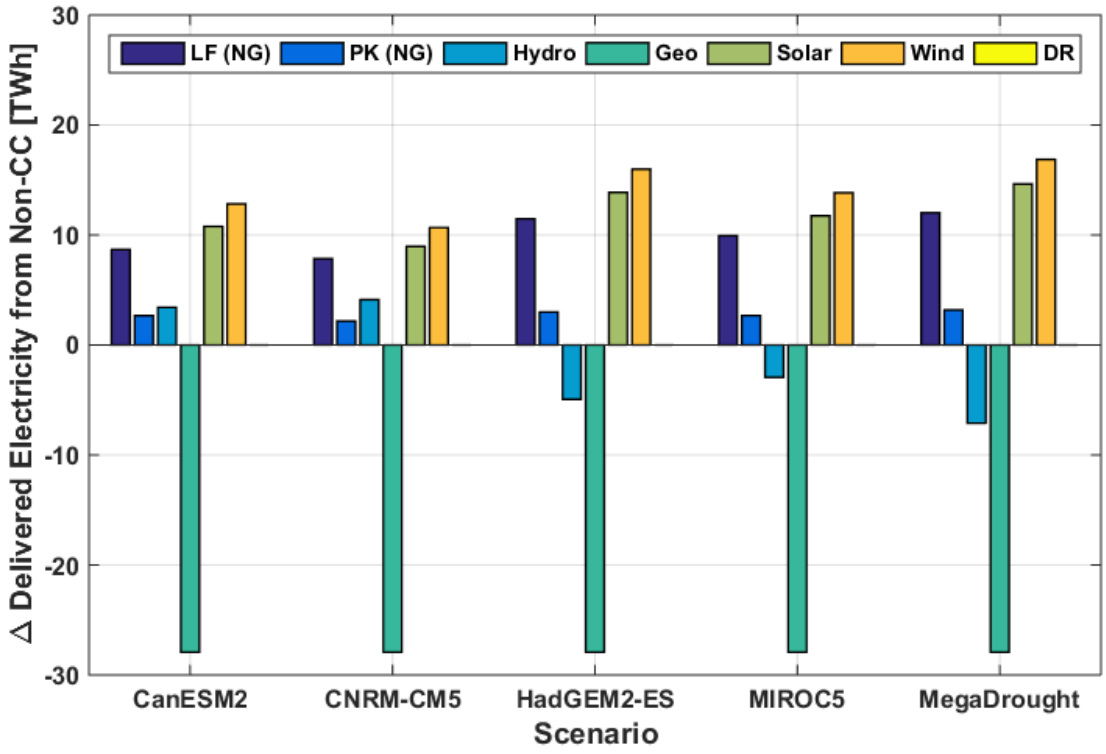

Source: Advanced Power and Energy Program, University of California Irvine

The projected total California delivered electricity values are different for each energy scenario from the change in electricity demand due to climate scenario. Of the different climate models, HadGEM2-ES exhibits the largest increases in GHG emissions. This occurs from the highest magnitudes in annual load increases due to climate change in combination with the largest on-average decreases in water availability and hydropower generation. The MegaDrought case, which is based on the HadGEM2-ES model but with an imposed long-term drought, showed the largest GHG increases of the cases examined. The MIROC5 model also exhibits decreases in hydropower generation, but to a lesser extent than HadGEM2-ES, and has a lower increase in electric loads. The other two climate models show increases in hydropower generation, but lower electric load increases in the CNRM-CM5 model allow that scenario to exhibit the lowest GHG emissions.

Regardless of climate model, however, all climate change scenarios exhibit increases in greenhouse gas emissions compared to the historical climate case. The projected decrease in delivered electricity from geothermal resources due to water constraints on geothermal capacity is compensated by an increase in delivered electricity from natural gas load followers, natural gas peakers, plus solar and wind. The increase in delivered electricity from wind and solar generation is caused by the decrease in base load generation from geothermal. This increase is partially compensated by additional use of wind and solar generation that was curtailed in the historical climate scenario. Since renewable curtailment from wind and solar is not available during all hours of the year to compensate for the constant generation from

geothermal resources, however, the shortfall in generation during some hours is compensated by natural gas load following and peaking power plants. The generation from these units contributes to the increase in GHG emissions of all climate change scenarios compared to the historical climate scenario.

Additional factors contribute to the increase in natural gas power plant generation. The decreases in hydropower generation in the drier climate models – HadGEM2-ES and MIROC5 – exacerbate the amount of generation needed from natural gas power plants to balance the load. This situation is more pronounced in the MegaDrought case. A time series exhibiting the increase in solar and wind use from the additional use of otherwise curtailed renewable generation is displayed by Figure 48.

Figure 48: Ten-Day Snapshot Time Series of Projected Year 2050 California Generation Profile and Load – Historical (2001-2010) Climate Conditions

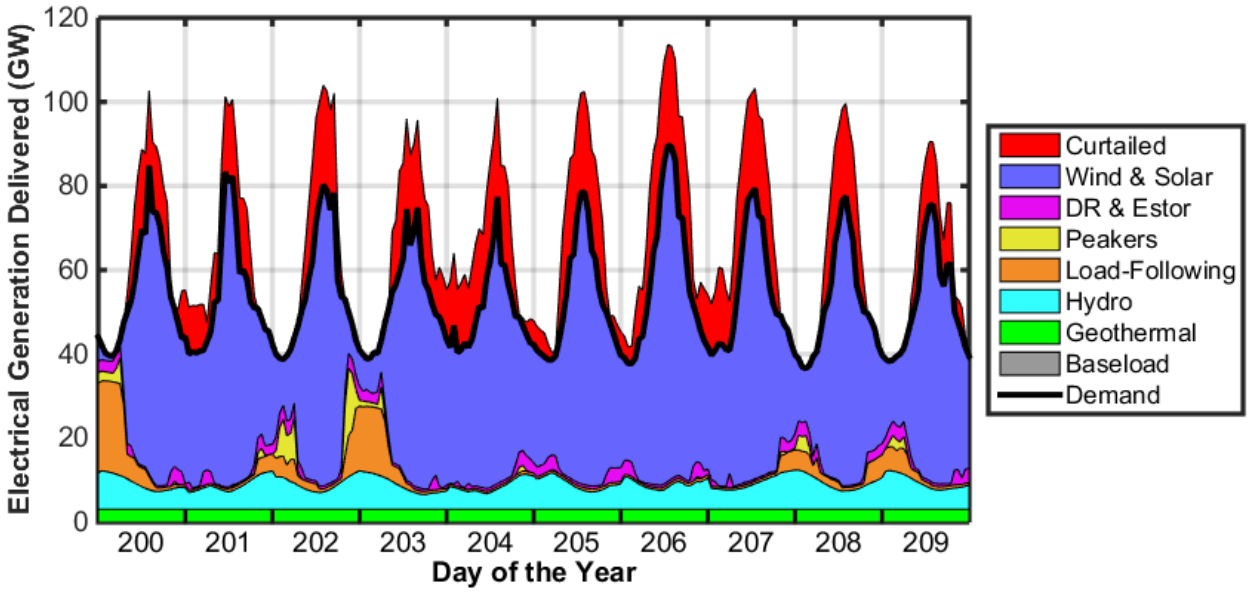

Source: Advanced Power and Energy Program, University of California Irvine

As geothermal and hydropower generation is decreased, additional wind and solar generation that was originally curtailed is then used to balance the electric load, when available. This indicates that with the proposed generation mix, excess generation from wind and solar can be used to provide a redundant means of providing carbon-free generation in case of a shortage of generation due to operational concerns or climate change impacts, as presented in this study.

Figure 49: Ten-Day Snapshot Time Series of Projected Year 2050 California Generation Profile and Load – Climate Change-Affected (2046-2055) Conditions Using the HadGEM2-ES Climate Model

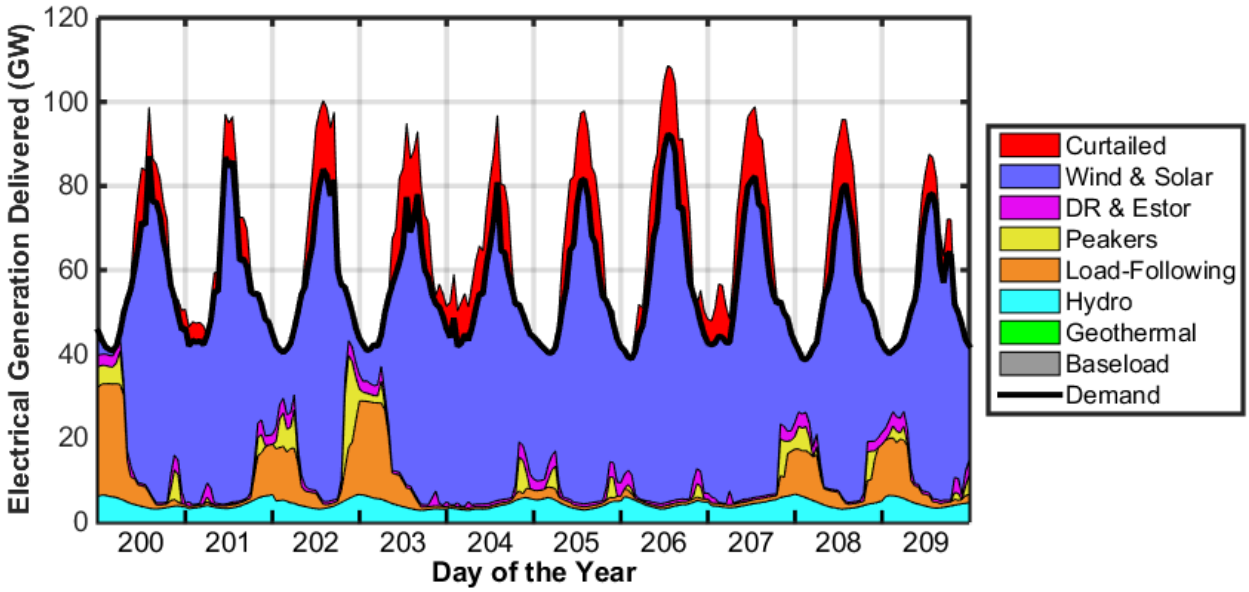

Source: Advanced Power and Energy Program, University of California Irvine

Changes to hydropower generation also affect ancillary services, which in this study are provided only by hydropower and natural gas power plants. This possibility would require increased natural gas power plant generation. The average annual spinning reserve provision from hydropower for historical and climate change-affected conditions is presented in Figure 50.

Figure 50: Projected Ten-Year Average California Hydropower Spinning Reserve Provision Under Historical (2001-2010) and Climate Change (2046-2055) Conditions

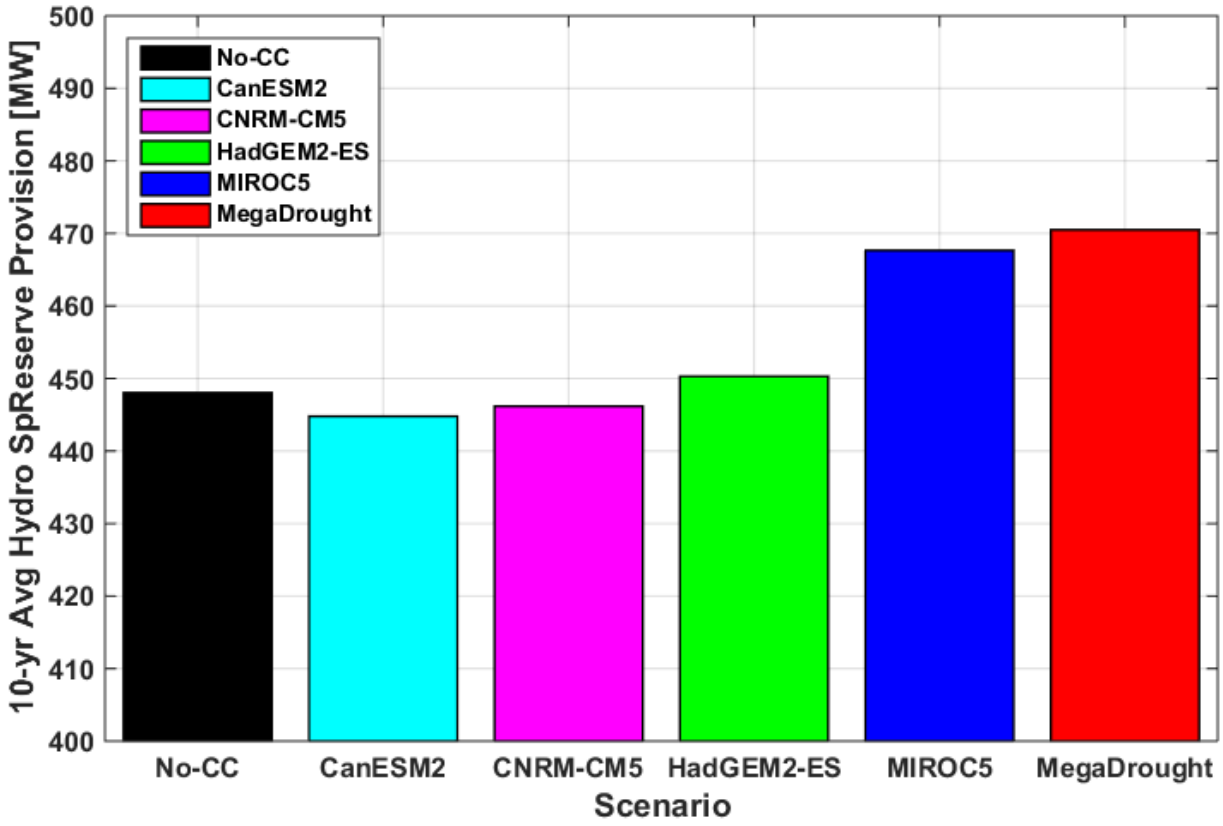

Source: Advanced Power and Energy Program, University of California Irvine

In this particular study applied to California, the 10-year annual average hydropower spinning reserve provision only changes slightly under climate change. Three of the climate models show effectively the same (<1% difference) hydropower spinning reserve provision levels under climate change relative to historical conditions. Within these three models, the wetter models show minor decreases because with more available water resources, the hydropower plants shift to bidding more toward providing generation rather than spinning reserve. The MIROC5 model is the only one to exhibit a noticeable increase in hydropower spinning reserve provision. Technically, the wetter models show slight decreases in spinning reserve provision as reservoirs shift toward providing more generation since it is more valuable, and the drier models show increases in spinning reserve provision as reservoirs recover lost revenue from being unable to provide generation (due to insufficient water resources) by providing spinning reserve. Both HadGEM2-ES and MIROC5 are drier models, but MIROC5 is drier than HadGEM2-ES. This causes reservoirs in the MIROC5 scenario to exhibit lower reservoir levels and shift more toward spinning reserve compared to HadGEM2-ES. The HadGEM2-ES model shows a larger decrease in generation due to increased spillage, not necessarily from low reservoir levels. This trend is exacerbated in the MegaDrought case.

These results indicate that for California under these specific climate models, the change in ancillary services is not a major contributor to the changes in GHG emissions. This is only the

case because the changes in water availability were not very large, and reservoir levels did not drop to the point where there is not enough water to provide spinning reserve. Other regions that experience more significant droughts may show an impact from ancillary services. Moreover, while the overall change in the spinning reserve provision from hydropower is relatively small on an average basis, the changes in any year are highly variable (Figure 51).

Figure 51: Projected Annual Average California Hydropower Spinning Reserve Provision Under Historical and Climate Change Conditions Over the 10-Year Time Frame (2046-2055)

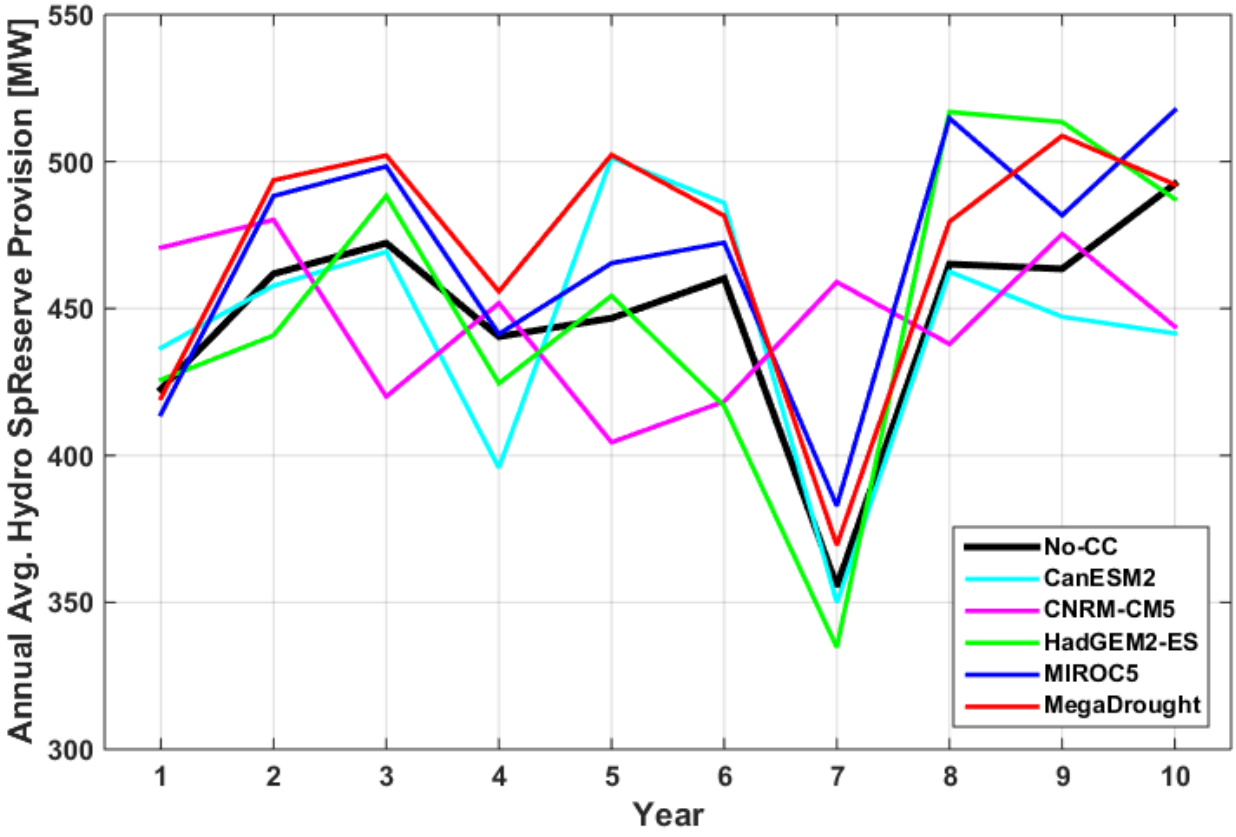

Source: Advanced Power and Energy Program, University of California Irvine

The impacts of climate change also affect the renewable penetration level achieved by the system. The renewable penetration level is the fraction of the electric load demand (by energy) that is satisfied by renewable resources. In this study, renewables encompass wind, solar, geothermal, small hydropower, and biopower resources to be consistent with the definitions used for calculating California's Renewables Portfolio Standard. The combined impacts of climate change-altered hydropower generation, constrained geothermal capacity, and altered residential and commercial building loads on electricity sector renewable penetration are presented as a difference from the case without climate change as a 10-year average in Figure 52.

Figure 52: Projected California Electric Grid Renewable Penetration Level Difference From Historical 10-Year Average Representing 2050

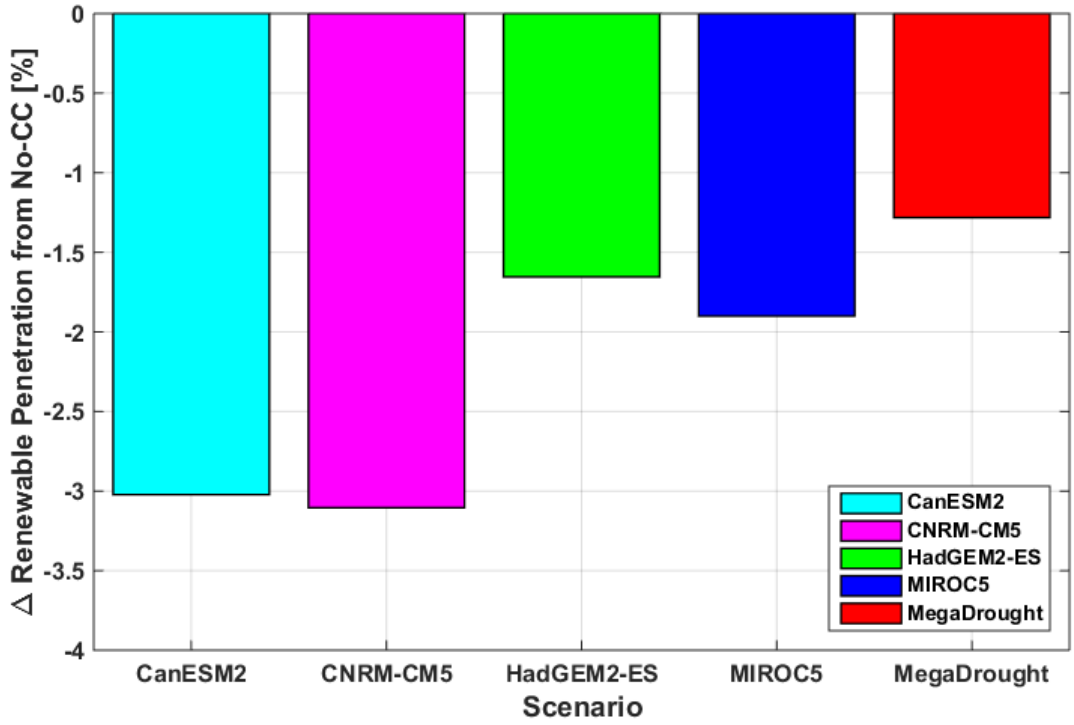

Renewable penetration level without climate change = 83.66%.

Source: Advanced Power and Energy Program, University of California Irvine

For all the climate models, the renewable penetration level decreases under climate change compared to historical levels. On a 10-year average basis, the renewable penetration level drops from 83.66% to between 80.68% and 81.95%. Based on the changes of the generation profile due to climate change, the decrease in the renewable penetration is largely due to the decrease in geothermal generation and partially due to decreases in small hydropower generation in the drier climate models. As discussed, however, this is partially offset by additional use of wind and solar generation that was otherwise curtailed during hours when such excess generation is available. Therefore, the decrease in renewable penetration is not as large as would be predicted by the decrease in geothermal and small hydropower generation alone.

Among the climate models, however, the wetter models (CanESM2 and CNRM-CM5) show a larger decrease in renewable penetration level from the case under historical climate conditions compared to the drier models (HadGEM2-ES and MIROC5). This is the reverse of the trends exhibited for electricity system GHG emissions and indicates that renewable penetration level, which is on a percentage basis, is not necessarily an indicator of GHG emissions, which is measured on an absolute basis. This occurs because in the wetter models, a larger portion of the generation profile consists of large hydropower generation compared to the drier models. Although large hydropower is carbon-free, it is not counted as renewable in the California RPS definition.

Overall, the impacts of climate change have the potential to compromise slightly the effectiveness of technology portfolios in meeting long-term carbon reduction and renewable penetration goals, but in general the impacts are not overly severe on a systemwide level. The maximum overshoot of 5.663 MMT CO_2e/yr must be planned around and avoided, but this deviation is relatively small considering that the economy-wide goal for California GHG emissions in 2050 is 86.6 MMT CO_2e/yr (80% below year 1990 levels). Assuming no other change in other sectors due to climate change, the impacts discussed here will put current strategies on track for a maximum of 6.5% deviation from the target, or 92.1 MMT CO_2e/yr. Chapter 6 will discuss some strategies that can be deployed to compensate for this deviation from the target.

5.2.1 Summary of Impacts on Electricity System Greenhouse Gas and Renewable Penetration

Summary comparisons of the impacts of climate change effects – individually and combined – on electricity system greenhouse gas emissions and renewable penetration of a 2050 low-carbon scenario are presented in Table 1 for GHG and Table 2 for renewable energy generation. The reference case for these comparisons is the base scenario from E3 [24]. The explicit analyses for the impacts are presented in Appendix B.

Table 1: Summary of Climate Change Impact Results for Greenhouse Gas Emissions

Impact Type/Climate Model	Hydropower Impact Only	Constrained Geothermal Impact Only	Electric Load Impact Only	Sum of Individual Impacts	Simultaneous Impacts
	[Δ MMT CO_2e/yr]	[Δ MMT CO_2e/yr]	[Δ MMT CO_2e/yr]	[Δ MMT CO_2e/yr]	[Δ MMT CO_2e/yr]
CanESM2	-0.7518	+3.7100	+0.5993	**+3.5575**	**+4.5030**
CNRM-CM5	-0.8238	+3.7100	+0.1724	**+3.0586**	**+3.9400**
HadGEM2-ES	+0.5019	+3.7100	+0.4594	**+4.6713**	**+5.6640**
MIROC5	+0.1305	+3.7100	+0.1602	**+4.0007**	**+4.9410**
MegaDrought	+0.7542	+3.7100	+0.4594	**+4.9236**	**+5.9440**

Source: Advanced Power and Energy Program, University of California Irvine

Table 2: Summary of Climate Change Impact Results for Renewable Generation

Impact Type/Climate Model	Hydropower Impact Only	Constrained Geothermal Impact Only	Electric Load Impact Only	Sum of Individual Impacts	Simultaneous Impacts
	[Δ %RE]	[Δ %RE]	[Δ %RE]	[Δ %RE]	[Δ %RE]
CanESM2	-0.5073	-2.3300	+0.0540	**-2.7833**	**-3.0230**
CNRM-CM5	-0.6443	-2.3300	+0.0967	**-2.8776**	**-3.1040**
HadGEM2-ES	+0.8869	-2.3300	+0.1425	**-1.3006**	**-1.6550**
MIROC5	+0.5928	-2.3300	+0.1446	**-1.5926**	**-1.9010**
MegaDrought	+1.2890	-2.3300	+0.1425	**-0.8985**	**-1.2820**

Source: Advanced Power and Energy Program, University of California Irvine

The magnitude of the impacts on GHG emissions and renewable energy penetration for the sum of the impacts is different (underestimated) than that for the case where all three were simultaneously modeled. This finding indicates that it is not necessarily accurate to investigate each impact and add the effects of the impacts to estimate the scale of the combined impacts, because there are interactions among these impacts that can exacerbate or limit the overall effects.

5.3 Conclusions

In this study, the research team translated the effects of climate change on hydropower generation, thermally based renewable capacity potential, and residential and commercial electric load demands to the associated impacts on electricity system GHG emissions, and renewable penetration in 2050. This was accomplished by implementing the effects and models described in previous chapters into the HiGRID electric system balancing model. These impacts were applied to a scenario that represented compliance with the goal of 80% below 1990 levels of greenhouse gas emissions without climate change impacts as the baseline developed by E3. The research team investigated deviations in GHG emissions and renewable penetration level of the electricity system due to the combined effect of all three impacts taking place simultaneously and individually. The main conclusions of this study are as follows:

1. **The effects of climate change for California's electricity system in 2050 included in this study have the potential to compromise the effectiveness of strategies to meet the long-term greenhouse gas reduction goal (80% below 1990 levels by 2050) that do not take climate change into account, but the deviation from the target emissions is not overly severe.** Without climate change, the modeled California electricity system produced greenhouse gas emissions of 18.06 MMT CO_2e/yr, and the economy-wide greenhouse gas emissions must meet 86.6 MMT CO_2e/yr by 2050. The combined impacts of climate change can increase emissions from the no-climate-change case by up to 5.663 MMT CO_2e/yr, which translates to a 6.54% deviation from target from an

economy-wide basis. This amount is nontrivial, and strategies to meet the 2050 greenhouse gas reduction goal must plan to reduce this amount of emissions in addition to current plans. The magnitude of this deviation, however, is not very large and is expected to be manageable.

2. **The projected effect of climate change constraining the use of California geothermal resources was found to be a major driver of emissions increases from the no climate change compliance scenario for the year 2050.** Geothermal resources represent high-capacity-factor resources that provide generation that is counted as carbon-free and renewable. These resources represent about 6.3% of overall delivered electricity by energy. The inability to use these resources due to water constraints must be compensated by other resources, such as a combination of otherwise curtailed wind and solar generation and natural gas fired power plants due to the dynamics of load balancing.

3. **The projected effect of climate change on California hydropower generation by 2050 contributes to relatively small changes in emissions using the current IPCC AR5 predictions.** Under the RCP 8.5 pathway, the four climate models used in this study predict precipitation levels that are either much higher than or effectively similar to historical levels. These scenarios produce a high degree of water spillage, but this is overcome by the sheer availability of water resources and the ability of non-reservoir hydropower generation being able to take advantage of the additional streamflow. The drier models exhibited increases in grid emissions due to the small increase in natural gas-fired generation to balance the load, and the wetter models exhibited decreases in grid emissions due to displacing such generation. Furthermore, while spinning reserve levels did change on a yearly basis, on average the spinning reserve provision from hydropower was similar to the no-climate-change case. This occurs because these climate scenarios did not exhibit significant drawdown of reservoir levels to the extent that would have limited spinning reserve provision. This occurred even in the MegaDrought case derived from the HadGEM2-ES model.

4. **The projected effect of climate change in 2050 (compared to 2001-2010) on California commercial and residential buildings also contributes to relatively small changes in greenhouse gas emissions.** While climate change will increase the magnitude and peaks of commercial and residential electric loads by a nontrivial amount due to increases in space cooling needs, the bulk of these increases tend to occur during the daytime hours, where a significant amount of otherwise curtailed solar generation is present. Therefore, the marginal load increase is often met by excess solar generation and does not contribute excessively to increases in GHG emissions. The climate models considered, however, did show differences in the amount by which marginal load increases aligned with excess renewable generation.

5. **The combined effect of different projected climate change impacts underestimated those by modeling them simultaneously.** This study investigated the effect of climate change impacts and the related simultaneous effects on electricity system GHG emissions and renewable penetration level in 2050. The sum of the effects of the cases where impacts were simulated tended to be less than the effects exhibited by the case where all three were simultaneously applied. This finding indicates that different climate change impacts interact with each other to either exacerbate or limit individual effects, and this must be taken into account.

Overall, climate change impacts on the California electricity system as represented by the three types (hydropower resources, regional water availability, and electric load demand) investigated show that additional factors need to be considered to develop a robust technology deployment plan for meeting the 2050 goal of reducing California economy-wide GHG emissions by 80% below 1990 levels. In this case, the scale of the impact is nontrivial but manageable. Chapter 6 investigates different options that could be used to overcome the projected deviation from the target emissions level and discuss their advantages and disadvantages.

CHAPTER 6:
Climate Change Implications of Renewable Use and Greenhouse Gas Emissions Reduction Strategies – Part 2: Evaluating Mitigation Options

6.1. Introduction and Background

Chapter 5 translated the individual and combined projected impacts of climate change in 2050 described in Chapters 2, 3, and 4 to changes in GHG emissions and availability of renewable energy resources of the California electricity system and investigated how they affect the effectiveness of technology mixes developed to meet these goals that do not take into account climate change. The effect of the combined changes in hydropower, water constraints on renewable resources, and increased loads due to temperature shifts was examined, as well as the effects of each of these aspects. The Chapter 5 analysis found that the projected water constraints on renewable resource use, particularly geothermal resources, contributed most to increasing the greenhouse gas emissions of the proposed 2050 electricity mix and caused it to fall short of the emissions target. Moreover, the shortfall was found to be greater under certain climate models (HadGEM2-ES) that projected both high temperatures and decreased water availability compared to others.

The analysis presented in this chapter focuses on evaluating options for reducing the impact of climate change on the ability of the modeled California electricity system to meet the 2050 GHG goal. The goal of these options is to allow the electricity system to reduce GHG emissions back to the levels achieved in the case without the impacts of climate change and raise the renewable penetration level to that of the no-climate-change case. In particular, this analysis focuses on two options: 1) increasing battery energy storage use and 2) enabling vehicle-to-grid charging of the electric vehicle fleet. An auxiliary analysis that examines the possibility of allowing renewable resources to contribute ancillary services to increase flexibility is presented in Appendix B.4.

6.2 Results and Analysis

6.2.1 Increasing the Installed Capacity of Battery Energy Storage by Five

The base case adopted the level of storage assumed in the California Air Resources Board Scoping Plan to meet the State's energy storage mandate (3.7 GW). The increase in storage is only for battery storage from 1.3 GW in the base case to 6.5 GW; the 2.4 GW of pumped hydro storage is assumed to remain constant. The impacts of increasing the installed capacity of battery energy storage by a factor of five compared to the base case (Table A-26) on electric

grid GHG emissions is presented as the difference from the no-climate-change case in Figure 53. Each color represents a different climate model. The label "5xES" denotes the cases with increased energy storage.

Figure 53: Projected California Electric Grid Greenhouse Gas Emissions Difference From Historical (2001-2010) Climate Conditions – 10-Year Average (2046-2055) Representing the Year 2050

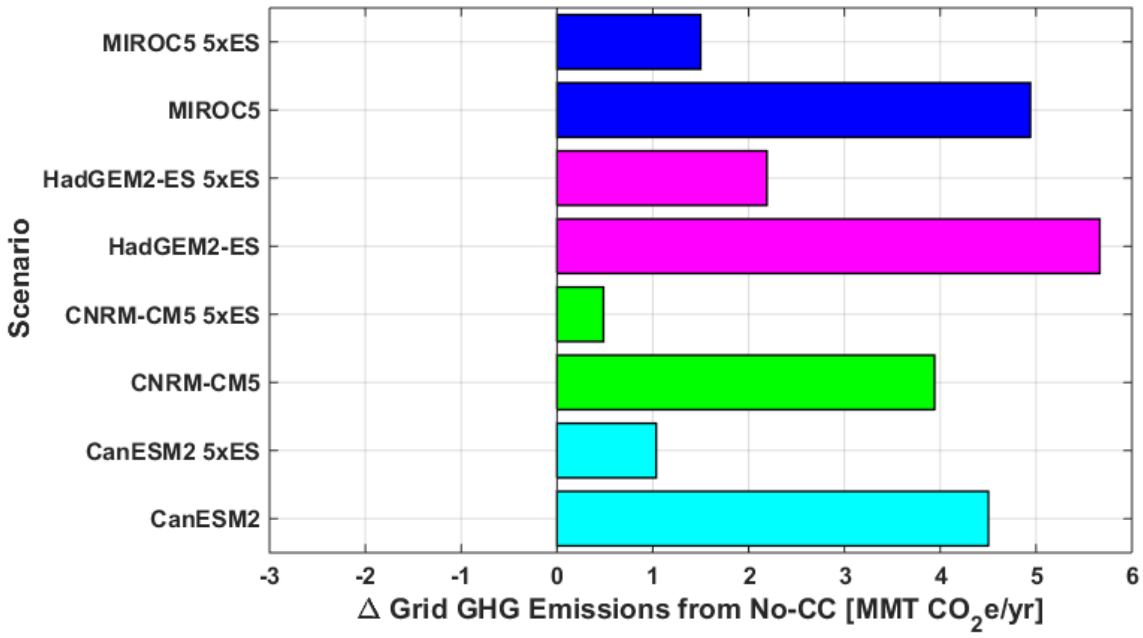

Climate change only vs. climate change + 5x battery storage increase. "5xES" represents the cases with a 5x increase in battery energy storage capacity. Emissions Level Without Climate Change = 18.04 MMT CO_2e/yr

Source: Advanced Power and Energy Program, University of California Irvine

Climate change increases California electricity system GHG emissions under each climate model. Increasing the installed battery energy storage capacity by a factor of five offsets this increase somewhat. As shown by the positive values for the increase from the case without climate change in Figure 53, however, this strategy does not completely offset the projected increases in GHG emissions caused by climate change in 2050.

The CNRM-CM5 climate model, which had the lowest GHG emissions of the different climate models used, exhibited the closest GHG emissions levels to the no-climate-change case when energy storage capacity was increased. Using more energy storage did not change the comparative trends among the climate models. That is, the climate model with the greatest projected GHG emissions without added storage also had the greatest emissions with the added storage.

Although the impact was not enough to reduce GHG emission levels to the no-climate-change case, increasing the energy storage capacity did reduce GHG by a substantial amount for all climate models. Average reductions from the increase of energy storage capacity account for

about 3.0 MMT CO_2e/yr reductions across all the climate models. This shows that increasing the energy storage capacity by a factor of five has a beneficial impact but may not be scaled to a sufficient level in this case to overcome the impacts of climate change.

The impacts of increasing the installed capacity of battery energy storage by a factor of five compared to the base case on the renewable penetration level is presented in terms of the difference from the no-climate-change case in Figure 54. Each color represents a different climate model. The label "5xES" denotes these cases with increased energy storage in the figure.

Figure 54: Projected California Electric Grid Renewable Penetration Level Difference From Historical (2001-2010) Climate Conditions – 10-Year Average Representing the Year 2050

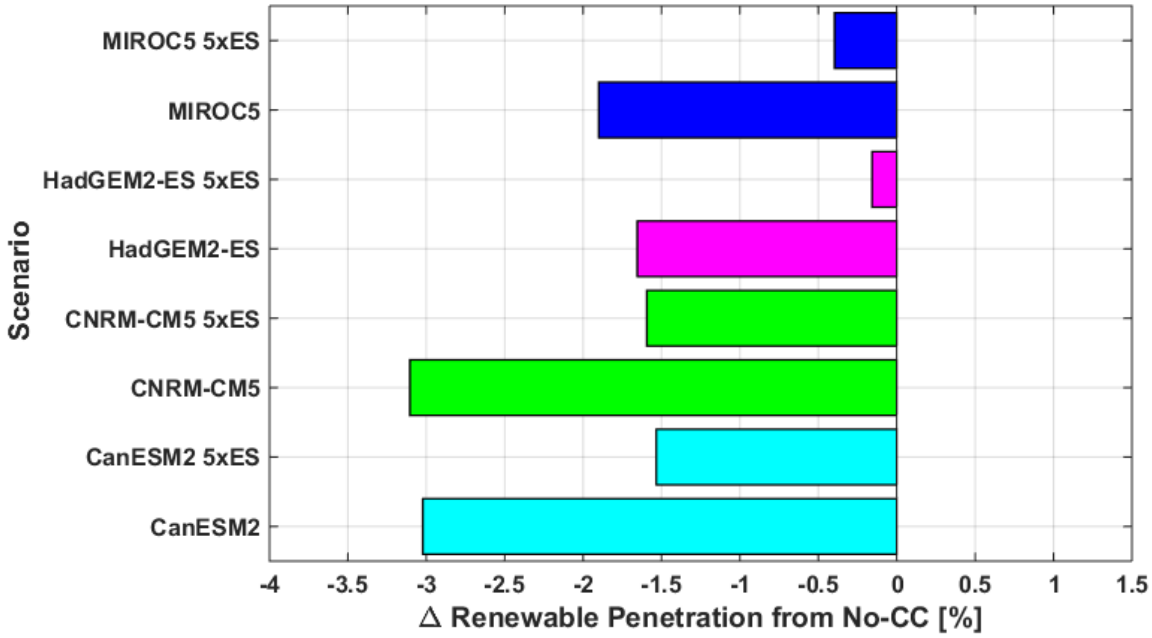

Climate change only vs. climate change + 5x battery storage increase. "5xES" represents the cases with a 5x increase in battery energy storage capacity. Renewable Penetration Level without Climate Change = 83.66%

Source: Advanced Power and Energy Program, University of California Irvine

Increasing the battery energy storage capacity by a factor of five increases the penetration level of renewable energy but does not on average allow the system to overcome the decrease in renewable penetration level due to the impacts of climate change in 2050. For the HadGEM2-ES and MIROC5 climate models, the renewable penetration levels are brought very close to that in the no-climate-change case, with the former meeting or exceeding the no-climate-change case levels in a couple of years in the simulation time frame. The CanESM2 and CNRM-CM5 climate models still show depressed renewable penetration levels but are improved compared to the respective cases without the energy storage increase.

On average, the renewable penetration levels of the HadGEM2-ES and MIROC5 climate model cases for 2050 are brought to within 0.5% of the no-climate-change case. On average, increasing the battery energy storage capacity by a factor of five accounts for an improvement in

renewable penetration level of about 1.4%. In absolute terms, renewable penetration levels are increased into the 81% to 83% range.

The breakdown of delivered electricity by resource to meet the electric load demand is presented for each case in Figure 55 as the difference in delivered electricity by resource from the no-climate-change case.

Figure 55: Projected Change in California Delivered Electricity Distribution by Resource in 2050 Due to Climate Change and 5x Increased Battery Energy Storage

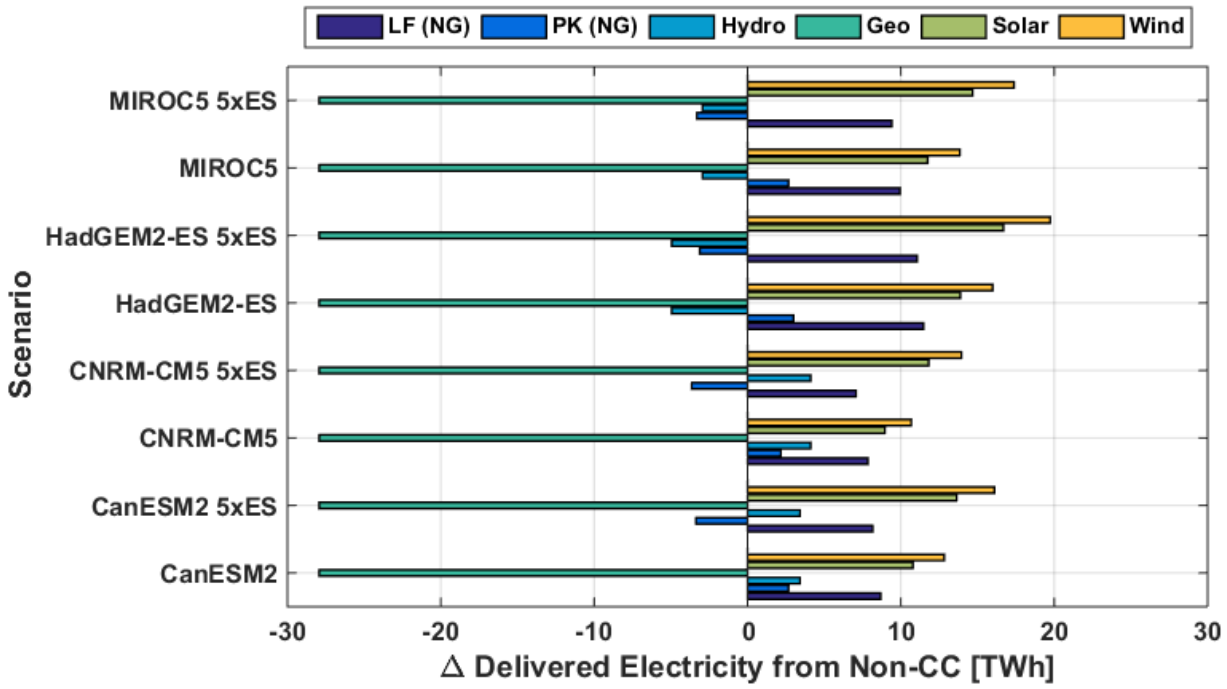

"5xES" represents the cases with a 5x increase in battery energy storage capacity.

Source: Advanced Power and Energy Program, University of California Irvine

The impacts of climate change reduce geothermal (and hydropower for HadGEM2-ES and MIROC5 models) generation, which is compensated by a combination of otherwise curtailed wind and solar generation, as well as increases in natural gas load following and peaking power plant generation. Increasing battery energy storage capacity by a factor of five increases wind and solar use due to the ability to capture otherwise curtailed generation and shift it to times when it can be used. Moreover, the increased energy storage capacity reduces reliance on fast-ramping peaking power plants, since energy storage can smooth out the profiles of the net load demand such that these power plants are not needed to balance the load as much compared to the base cases. An example of this is displayed in the time series snapshot in Figure 56. Note how the use of peakers (yellow) is decreased.

Figure 56: Time Series Snapshot of Projected California Generation Profiles for the CanESM2 Model (2050)

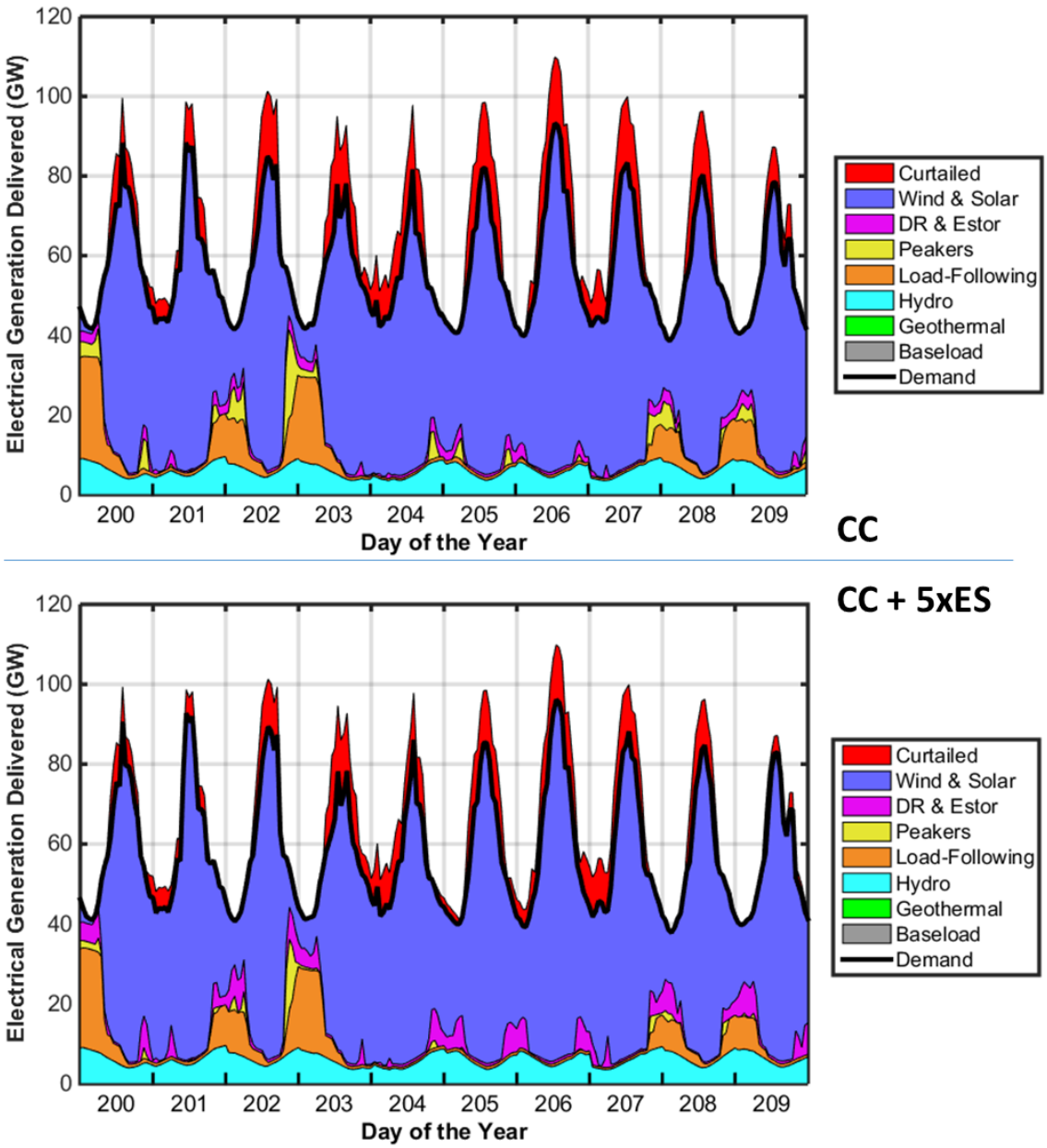

Climate change only vs. climate change + 5x battery storage increase. CC: Climate Change, CC+5xES = Climate Change w/5x Battery Energy Storage Capacity.

Source: Advanced Power and Energy Program, University of California Irvine

The primary reduction in GHG emissions comes from this latter effect. At this scale of energy storage, however, the reliance on load-following generation is relatively unaffected, since the energy storage system addresses the largest peaks in the net load as a higher priority.

6.2.2 Increasing the Installed Capacity of Battery Energy Storage by Ten

The team explored the effect of energy storage scaling, increasing the installed battery energy storage capacity to 10 times of that installed in the base case (Table A-26). The increase in storage is only for battery storage from 1.3 GW in the base case to 13.0 GW; the 2.4 GW of pumped hydro storage is assumed to remain constant. The impacts of the factor of 10 increase in battery energy storage capacity on electric grid GHG emissions compared to the base case on electric grid GHG emissions is presented in terms of the difference from the no-climate-change case in Figure 57. Each color represents a different climate model. The label "10xES" denotes the cases with increased energy storage.

Figure 57: Projected California Electric Grid Greenhouse Gas Emissions Difference From Historical (2001-2010) Climate Conditions – 10-Year Average Representing the Year 2050

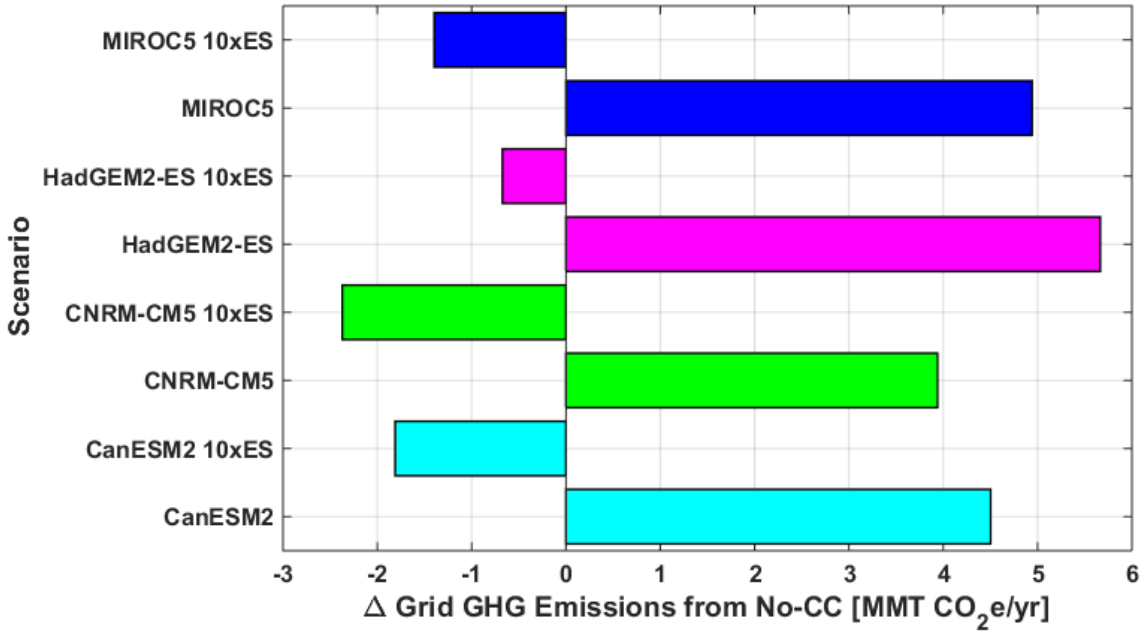

Climate change only vs. climate change + 10x battery storage increase. "10xES" represents the cases with a 10x increase in battery energy storage capacity. Emissions Level without Climate Change = 18.04 MMT CO_2e/yr

Source: Advanced Power and Energy Program, University of California Irvine

With battery energy storage capacity increased by a factor of 10, the electricity system is able to fully reduce the GHG emissions impacts caused by climate change and restore GHG emissions to levels at or below that of the no-climate-change case. On average, this is the case for all climate models. For each of the 10 years in the simulation time frame, only the HadGEM2-ES model shows one year with GHG emissions above the no-climate-change case but only by a small amount.

On an absolute basis, projected California electricity system GHG emissions in 2050 are reduced to between 15.6 MMT and 17.4 MMT CO_2e/yr with battery energy storage capacity increased by a factor of 10, compared to 18.06 MMT CO_2e/yr in the base case.

This shows that appropriate scaling of energy storage is important for building the California electricity system to be resilient against the impacts of climate change while meeting GHG emission reduction goals.

The impacts of increasing the installed capacity of battery energy storage by a factor of 10 compared to the base case on the renewable penetration level is presented in terms of the difference from the no-climate change case in Figure 58. Each color represents a different climate model. The label "10xES" denotes the cases with increased energy storage.

Figure 58: Projected California Electric Grid Renewable Penetration Level Difference From Historical (2001-2010) Climate Conditions – 10-Year Average Representing the Year 2050

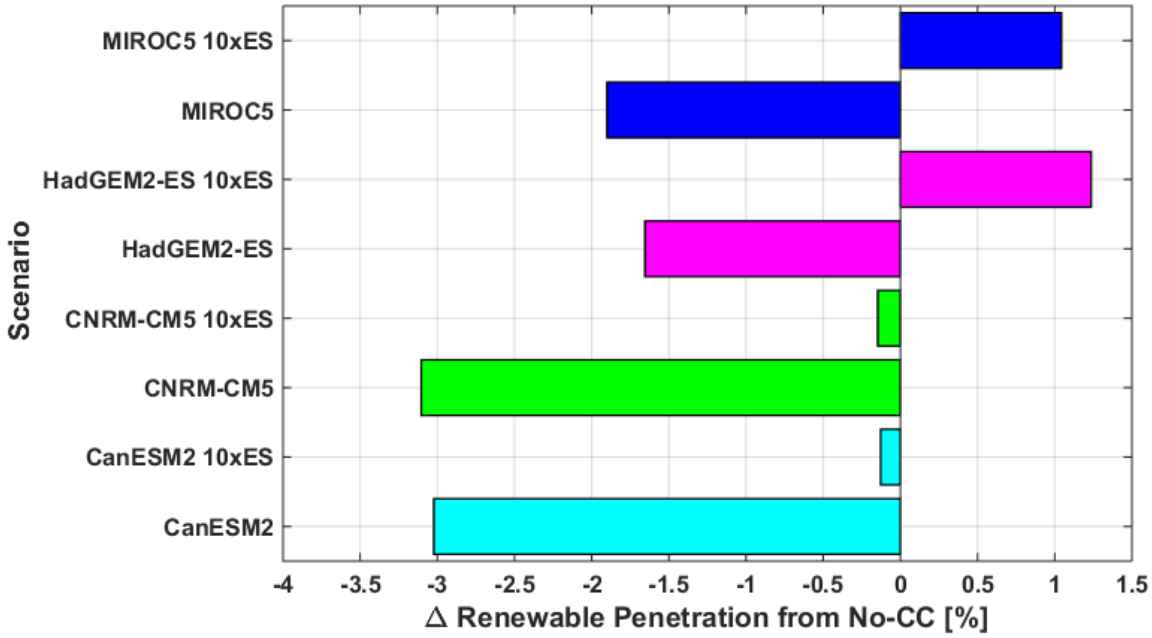

Climate change only vs. climate change + 10x battery storage increase "10xES" represents the cases with a 10x increase in battery energy storage capacity. Renewable Penetration Level without Climate Change = 83.66%

Source: Advanced Power and Energy Program, University of California Irvine

With the increase in battery energy storage capacity, the renewable penetration levels of the electricity system are nominally restored to that of the no-climate-change case, indicating that the tenfold increase in battery energy storage was able to overcome the impacts of climate change on the system. The HadGEM2-ES and MIROC5 models were able to reach higher renewable penetration levels than the no-climate-change case, increasing to 1.3% and 1.05% above the no-climate change-case on average, respectively. Thus, slightly less than a tenfold increase in storage would be sufficient. The CanESM2 and CNRM-CM5 models exhibited renewable penetration levels of 0.18% and 0.2% below the no-climate change-case, which is only

a small deviation. From the 10-year perspective, the HadGEM2-ES and MIROC5 models consistently exhibit higher renewable penetration levels than the no-climate-change case, where the CanESM2 and CNRM-CM5 models exhibit certain years above and certain years below the no-climate-change case.

The increase of energy storage capacity allows the electricity system to capture larger peaks in otherwise curtailed renewable generation and store a given amount of energy for a longer period. This allows greater use of otherwise curtailed renewable energy than the fivefold increase case was able to accomplish. In the CanESM2 and CNRM-CM5 models, however, since hydropower generation is increased and cannot be offset, the margin for using more otherwise curtailed renewable generation is smaller.

The breakdown of projected California delivered electricity by resource to meet the electric load demand in 2050 is presented in Figure 59 as the difference in delivered electricity by resource from the no-climate-change case.

Figure 59: Projected Change in California Delivered Electricity Distribution by Resource in 2050 From Climate Change and 10x Increased Battery Energy Storage

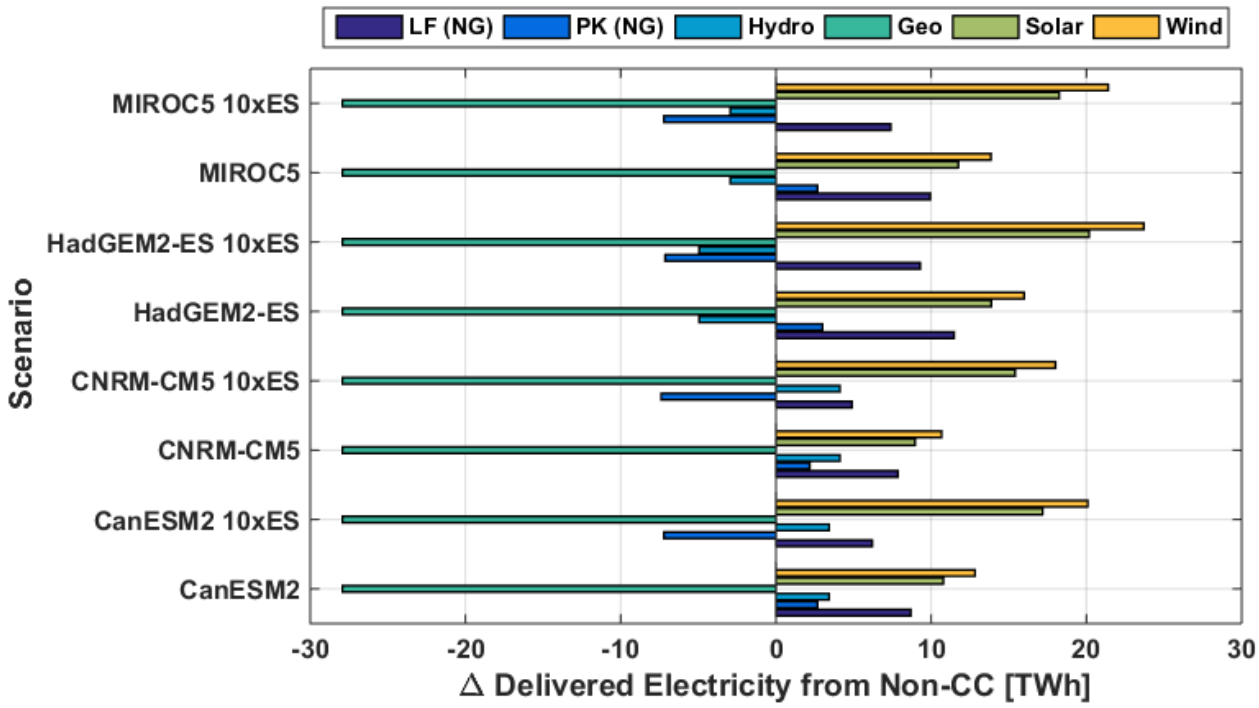

"10xES" represents the cases with a 10x increase in battery energy storage capacity.

Source: Advanced Power and Energy Program, University of California Irvine

By increasing the battery energy storage capacity to 10 times that in the base case, the same qualitative trends shown by the fivefold increase case occur but to larger extents. Comparing these results to those presented for the 5x increase case previously, increased use of wind and solar generation occurs, as well as larger decreases in peaking power plant generation. Furthermore, these results for each climate model show decreases in the reliance on natural gas

load-following power plants relative to the respective cases without the energy storage increase. The decrease in peaking power plant, as well as natural gas load-following power plant generation, contributes to larger GHG emissions reductions compared to the 5x case. An example of this can be seen in the time series snapshot of the generation profile presented in Figure 60. Note the near-complete elimination of peaking power plant generation.

Figure 60: Time Series Snapshot of Projected California Generation Profiles for the CanESM2 Model (2050)

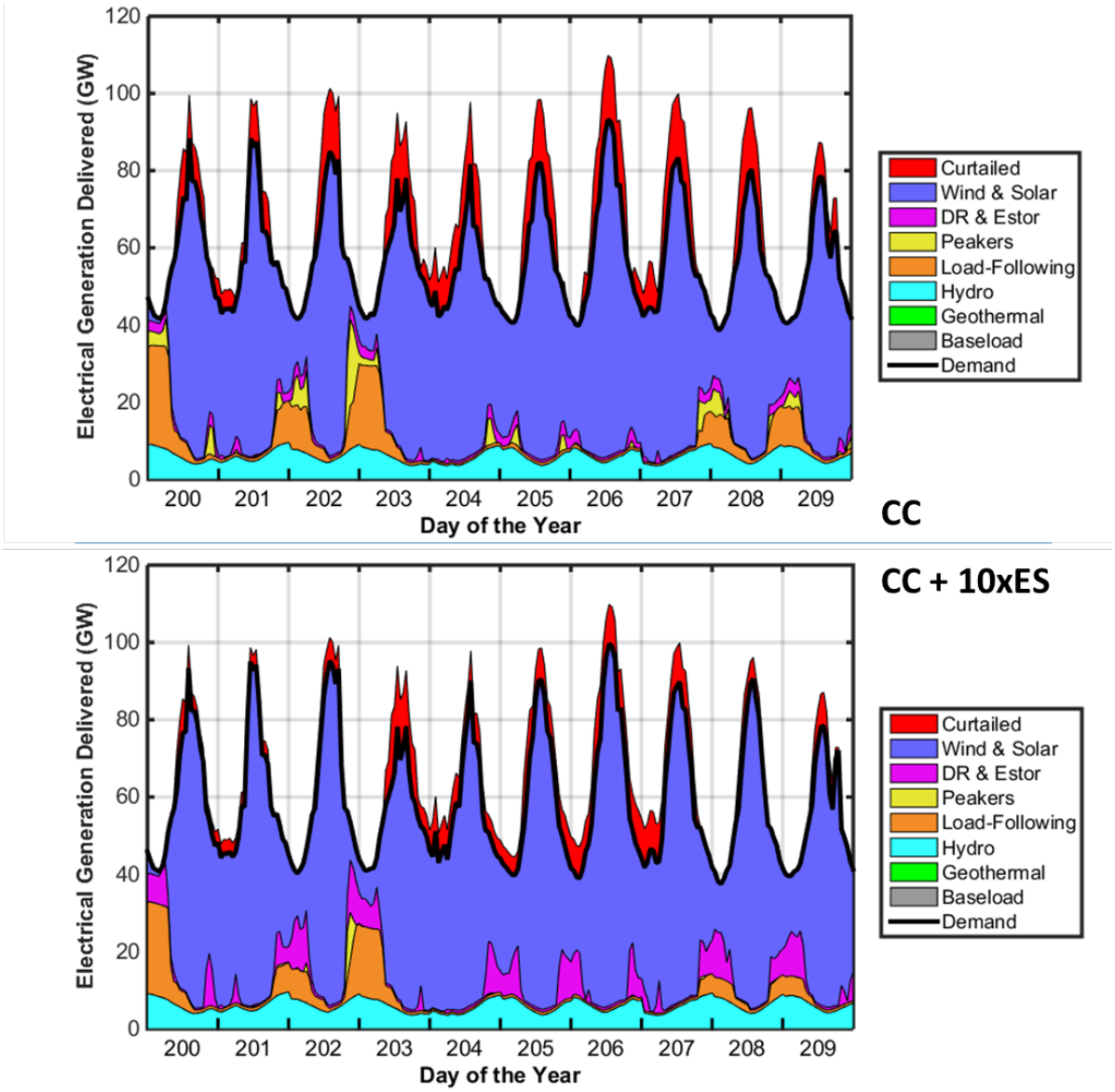

Climate change only vs. climate change + 10x battery storage increase CC: Climate Change, CC+10xES = Climate Change w/5x Battery Energy Storage Capacity.

Source: Advanced Power and Energy Program, University of California Irvine

These results also indicate that a tenfold increase in battery energy storage capacity allows the system not only to have the capability to address net load peaks, but to manage slower load-

following power plants to reduce emissions. Overall, without any other further strategies implemented relative to the base case, a tenfold increase in battery energy storage capacity is sufficient to compensate fully for the effects of climate change on the electricity system in terms of greenhouse gases and renewable resource penetration. Further analysis would be required to determine the precise level of battery energy storage that would completely offset climate change impacts.

6.2.3 Enabling Vehicle-to-Grid Operation of Electric Vehicle Charging

The impact of enabling vehicle-to-grid management of electric vehicle charging on electricity GHG emissions is presented in terms of the difference from the no-climate change case in Figure 60. Each color represents a different climate model. The label "V2G" denotes the cases with vehicle-to-grid charging enabled in Figure 61.

Figure 61: Projected California Electric Grid Greenhouse Gas Emissions Difference From Historical (2001-2010) Climate Conditions – 10-Year Average - Year 2050

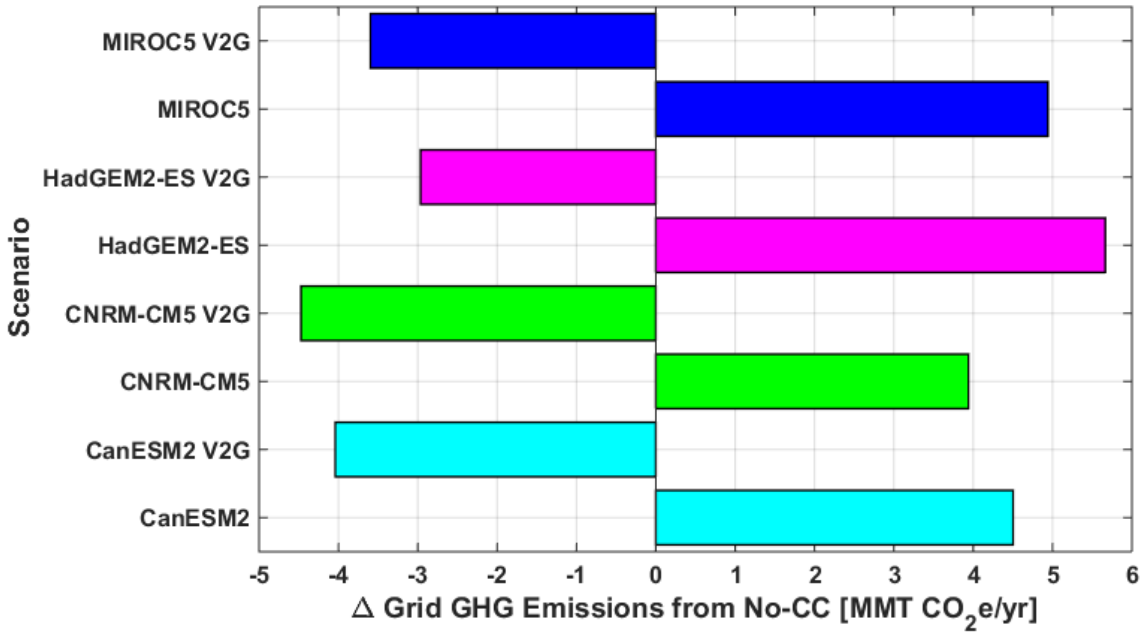

Climate change only vs. climate change + vehicle-to-grid electric vehicles. "V2G" represents the cases with vehicle-to-grid charging management of electric vehicles enabled. Emissions Level without Climate Change = 18.04 MMT CO_2e/yr

Source: Advanced Power and Energy Program, University of California Irvine

Enabling V2G management of electric vehicle charging significantly reduces GHG emissions from the electricity system. This option, when enabled for the entire fleet of light-duty electric vehicles statewide, causes the GHG emissions to drop below the no-climate-change case. On average, enabling V2G operation accounts for a reduction of about 8.5 MMT CO_2e/yr in GHG. This magnitude offsets the impacts of climate change on GHG emissions and improves beyond the no-climate-change case.

The enabling of V2G operation performs essentially the same function as using stationary energy storage. In the model, electric vehicles operate in a smart charging mode to add load when renewable generation is available or in excess but discharges electricity back to the system to reduce grid loads and corresponding dependence on nonrenewable generation to the extent possible, while maintaining the state of charge needed to meet consumer travel patterns. This strategy, if practically realized to the extent here, is advantageous to the use of stationary energy storage in three key ways. First, previous work by Tarroja et al. [25] has shown that V2G can be more efficient in providing energy storage functions than stationary energy storage by limiting the amount of energy that must pass through the system. Second, this option makes use of hardware (electric vehicle batteries) that will already be deployed as part of the energy portfolio, minimizing production and use of additional hardware, and, therefore, may help reduce the environmental footprint of the system from a life-cycle standpoint. Third, the effective capacity of the electric vehicle fleet providing V2G services is very large compared to the battery capacities used even in the tenfold stationary battery energy storage case because most of the light-duty fleet would be plug-in vehicles. For example, the base case for 2050 has 25.86 million BEVs deployed in California, dominating the light duty vehicle fleet. With a 200 mile range corresponding to approximately a 50 kWh capacity per vehicle, this places the raw energy capacity of the vehicles at 1293 GWh. The tenfold battery energy storage capacity increase modeled in the previous section corresponds to only 75 GWh.

The impacts of enabling vehicle-to-grid management of electric vehicle charging compared to the base case on the renewable penetration level is presented in terms of the difference from the no-climate-change case in Figure 62. Each color represents a different climate model. The label “V2G” denotes the cases with vehicle-to-grid charging.

Figure 62: Projected California Electric Grid Renewable Penetration Level Difference From Historical (2001-2010) Climate Conditions – 10-Year Average Representing the Year 2050

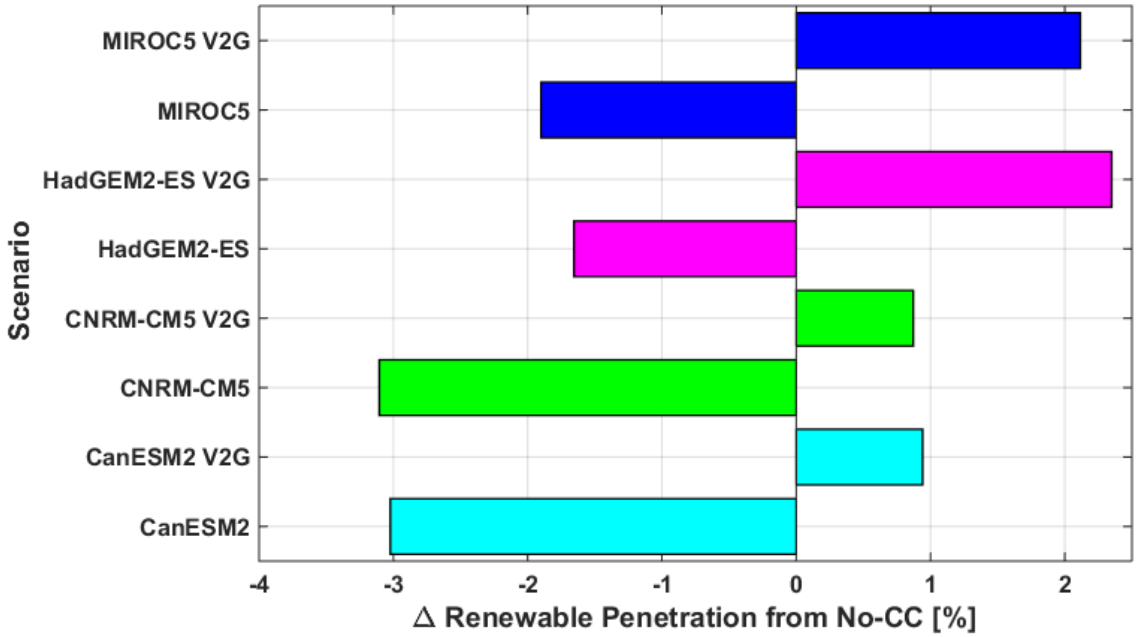

Climate change only vs. climate change + vehicle-to-grid electric vehicles. "V2G" represents the cases with vehicle-to-grid charging management of electric vehicles enabled. Renewable Penetration Level without Climate Change = 83.66%

Source: Advanced Power and Energy Program, University of California Irvine

Similar to the results for GHG emissions, enabling V2G management of electric vehicle charging is projected to enable a significant increase in the renewable penetration level. The increase provided by enabling V2G overcomes the decreases caused by climate change effects, resulting in a net increase in the renewable penetration level compared to the case without climate change. On average, enabling V2G is projected to account for a renewable use improvement of about 4%. On absolute bases, the renewable energy levels in 2050 are increased to between 84% and 86%, up from 83.66% in the no climate change case. This improvement occurs for the same reasons described for the improvement in GHG emissions from V2G use. Using V2G to the extent in this study will not only offset the detrimental impacts of climate change on electricity system performance, but will improve the system overall.

The breakdown of projected California delivered electricity by resource to meet the electric load demand in 2050 is presented as the difference in delivered electricity by resource from the no-climate-change case in Figure 63.

Figure 63: Projected Change in California Delivered Electricity Distribution by Resource in 2050 (including models of the V2G case) Compared to the No-Climate-Change Case

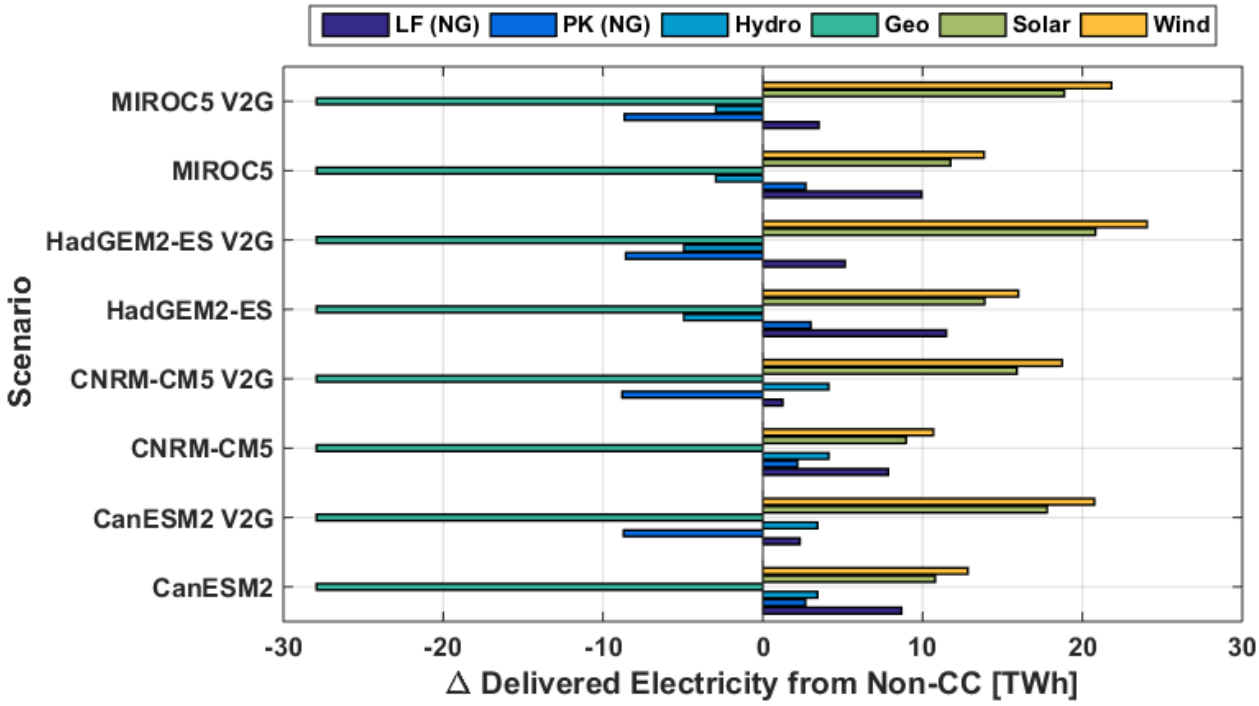

Climate change only vs. climate change + vehicle-to-grid electric vehicles. "V2G" represents the cases with vehicle-to-grid charging management of electric vehicles enabled.

Source: Advanced Power and Energy Program, University of California Irvine

The effect of enabling V2G management of electric vehicle charging has the same qualitative effects as increasing the battery energy storage capacity on the system, but to a larger extent than the case with the tenfold increase in battery energy storage capacity. The ability of the V2G-operating vehicles to capture otherwise curtailed renewable generation to fuel vehicle travel, as well as discharge to meet stationary loads, increases the use of wind and solar generation. The ability of the vehicles to manage and smooth the profile of the net load on the electricity system nearly eliminates the reliance on peaking power plants and reduces the use of load-following generation by reducing the frequency and magnitude of ramps. While V2G does not reduce reliance on load-following generation back to the levels exhibited in the no-climate-change case, it does so relative to the corresponding cases with climate change impacts.

There are a few caveats, however, to achieving these benefits of enabling V2G management of electric vehicle charging. In practice, there are many aspects of V2G that may not be easy to implement. First, the drivers of electric vehicles must be willing to allow their vehicles to participate as grid energy storage, allow them to be dispatched by an external entity, and accept the consequences of that mode of operation on the performance of their vehicles. Second, electric vehicle drivers must also be willing to allow electric grid operators to have some level of access to knowledge of their intended travel plans to schedule optimally the dispatch of their vehicles, which raises privacy concerns. Therefore, the results in this section should be

interpreted as showing the potential of enabling V2G to build resilience to climate change impacts into the electricity system, not a declaration that doing so will automatically build that resilience. In practice, only a fraction of electric vehicle drivers will likely be willing to participate in providing V2G services, and even this segment of drivers will participate only with certain limitations. Nevertheless, the potential benefit of V2G is significant and even partial realization of these benefits in practice can significantly contribute to building a climate change-resilient electricity system in California.

6.3 Conclusions

In this study, the team investigated some options to reduce the impacts of climate change on the electricity system described in Chapter 5. The Chapter 5 analysis determined that climate change can increase greenhouse gas emissions and decrease the renewable penetration level of the electricity system, potentially compromising efforts to meet the state's 2050 greenhouse gas emissions reduction goals. Three options were investigated for the ability to reduce the GHG emissions of the electricity system to the levels complying with California's 2050 goals. These options were 1) increasing the installed capacity of battery energy storage and 2) enabling vehicle-to-grid operation of plug-in electric vehicle charging. The main conclusions of this study are as follows:

1. **Increasing the installed capacity of battery energy storage can build resilience against the projected 2050 impacts of climate change on the California electricity system, but only when appropriately scaled.** Increasing the battery energy storage capacity in the system allowed more use of otherwise curtailed renewable generation to reduce GHG emissions and increase the renewable penetration level. However, the case with fivefold the base case installed battery energy storage capacity did not provide these benefits to the extent necessary to offset the emissions increase and renewable penetration decrease due to climate change. It was found that tenfold the battery energy storage capacity in the base case fully offsets the projected 2050 impacts of climate change on the California electricity system modeled in this study.

2. **Enabling V2G management of electric vehicle charging not only has the potential to offset the impacts of climate change on the California electricity system projected for 2050, but also improve the GHG emissions reduction and renewable penetration of the electricity system.** The option of enabling V2G management of electric vehicle charging for the entire California light-duty vehicle fleet reduced GHG emissions from the electricity sector to below that of the 80 percent below 2050 goal modeled in the study, even when subject to the projected impacts of climate change on California hydropower resources, regional water availability, and electric load demand. This strategy achieved a similar result for the increase in renewable penetration. As modeled, using V2G allows a large effective energy storage capacity to be implemented on the grid with minimal requirements for additional hardware and has the potential to provide significant benefits. These results, however, were obtained under an assumption of full participation of light-duty electric vehicle drivers with electric grid operators,

which is unlikely to occur. Even partial realization of these potential benefits, however, can significantly contribute to building resilience against climate change into the California electricity system.

Overall, there are many available options for increasing the flexibility of the California electricity system. These options allow the electricity system to better use installed renewable resources to meet the variety of load demands on the system and to provide many measures by which the system can respond and be resilient to the impacts of climate change on electricity system operation. In this chapter, these options were investigated individually. In practice, however, combinations of these options will be desired due to potential constraints on each of them that were not modeled here (e.g., drivers of electric vehicles being unwilling to participate in V2G charging). These results do show, however, that energy storage capabilities, whether stationary or mobile, will play an important role in building electricity system resilience in a carbon-constrained context. It may be useful in the future to investigate a wider range of options and simultaneous use of these options.

CHAPTER 7: Conclusions

7.1 Summary Answers to Primary Research Questions

This project was focused on answering two primary research questions:

- How might climate change affect the ability of the future California electricity system to support California's 2050 GHG emissions reduction goal?

- What adjustments can be made in planning the future California electricity system to increase robustness to support long-term GHG emissions reductions in the state?

From the results and the analyses presented in this report, this project provides the following answers to these questions.

The research team found climate change to be only a moderate disruption of the electricity system to support California's 2050 GHG emissions reduction goal (80 percent of 1990 emissions), with a shortfall of about 6 million metric tons. The planning studies that have developed scenarios for the California 2050 electric grid resource mix (such as those by E3) incorporate wind and solar power capacities that give rise to excess renewable generation. The authors of these studies chose this strategy because oversizing the wind and solar capacity was generally deemed a more economical approach to reducing GHGs compared to installing a lower capacity of wind and solar coupled with relatively expensive energy storage systems. The result is that, while climate change does affect the availability of low-/zero-carbon electricity resources and increases electricity demands, about 50% to 70% of these impacts are compensated by additional uptake of otherwise excess renewable generation. For example, increased electric loads occurred under climate change scenarios, but since these load increases typically occurred during times when excess solar generation was available, these additional loads did not translate strongly to increased GHG emissions. The uptake of otherwise excess renewable generation buffers the translation of climate change impacts on electricity generation and demand to GHG emissions from the electric grid and causes the overall impact of climate change on future electric grids to be relatively moderate and manageable.

To address the projected increases in GHG emissions that will occur because of the impacts of climate change in 2050, adjustments to current scenarios for developing the future electricity system should focus on increasing the flexibility of available resources, such as enabling vehicle-to-grid integration of electric vehicles, or on installing additional resources to increase overall system flexibility such as additional energy storage capacity or both. This increase in flexibility will allow the electricity system to use more available, otherwise excess renewable generation to reduce GHG emissions and counteract climate change impacts. Although not specifically studied in this report, increased energy efficiency in all sectors in excess of the improvements specified in current planning studies for the electric system could also help counter climate change impacts by reducing demand.

While climate change impacts on future (2050) California electricity system GHG emissions were found to be moderate, the operational practices of the electricity system will need adjustments to allow the system to be robust in the face of climate change. Projected climate impacts in this study suggest electric grid operators such as the California Independent System Operator and electric utilities must plan the yearly operation of electric grid resources around a more volatile hydropower generation potential and be ready to accommodate extended wet and drought periods. These entities must also increase the ability to obtain electric grid ancillary services from unconventional resources. For example, instead of spinning reserve service being provided by a gas-turbine power plant that increases generation when needed, this service may need to be provided by batteries that have accumulated energy from curtailed renewables and discharge it to the electric grid when needed due to a contingency event. While the results in Appendix B.4 show that this approach will not reduce the GHG emissions impacts of climate change, it is still important for reliable grid operation in the face of decreased provision of spinning reserve from hydropower. Also, projected climate impacts in this study suggest electric utilities must be able to accommodate increased peak loads on distribution circuits from increases to cooling loads caused by climate change in 2050. While these projected load increases did not translate to significantly increased GHG emissions, grid operators still must account for the loads in distribution system capacity planning.

7.2 Summary of Benefits to California

The primary goal of this project was to provide an advisory understanding and information base for California utilities, ratepayers, and government planning agencies on how to build a low-carbon electricity system that can support the state's climate goals when affected by environmental conditions caused by climate change. The research presented in this report achieves this goal.

The first benefit of achieving this goal is the new knowledge necessary for more robust and economic planning of the future California electric grid resource mix in supporting California's GHG emissions reduction goal. By providing the understanding of how climate change affects zero- or low-carbon electricity generation and electric loads, this research enables planning agencies and utilities to make intelligent investments in electricity generation resources that will not be as affected by climate change. For example, understanding that certain resources may be constrained by water availability under climate change could encourage these agencies to increase reliance on other renewable technologies that are not as sensitive to drought. This study also identified infrastructure improvements necessary to operate a low-carbon electricity grid reliably under future climate change conditions. In addition to informing plans for meeting the state's GHG emissions reduction goal, this project also provided insight into how climate change affects electricity system operation. This will allow electric utilities to make targeted investments that will maintain the reliability and resiliency of California electricity service under projected climate change conditions for 2050.

The second benefit provides policy makers and ratepayers with a clear understanding of the mutual benefits of sustainable water resources management for the energy sector. Many of the impacts of climate change on the electricity system from planning and operational standpoints

are imposed through impacts on water resources, and improvements in water resource management can help reduce these impacts. This understanding can inform partnerships between the water and energy sectors working to include climate change in their planning and operations and allow the energy sector to better contribute toward drought resilience in the state.

7.3 Future Research Directions

There are two thematic research directions for future work to build from the outcomes of this project and contribute toward achieving California's climate and energy goals.

The first thematic direction is an in-depth investigation of **how climate change affects the reliability and resiliency of the electricity system from a grid operations standpoint** and how these effects influence low-carbon electricity planning. This project focused on the average impacts of climate change from a GHG reduction perspective and provided some insight into how grid resource operation and the ability to provide reliability services are affected. The response of the system to contingency events caused by extreme climate events, which will be more frequent under climate change, was beyond the scope of this study. Climate change has the potential to affect not only the typical operation of the electric grid, but to cause contingency events through a wide range of various climate extremes. These include, but are not limited to:

- Wildfires damaging transmission and distribution lines.
- Extreme heat events affecting transmission and distribution system capacity.
- Extreme precipitation and overloading of dams, causing flooding of areas housing energy infrastructure elements such as power plants.
- Sea-level rise and coastal storm surges inundating power plants and distribution systems in populated coastal areas.

It is also important to characterize not only these events, but to simulate how the electric grid responds to these occurrences from the perspective of frequency deviation, outages, service restoration time, and economic impacts. This research will require characterizing climate extremes, the types of energy infrastructure that are affected, and the frequency of impacts and simulating these events as sudden disruptions to the operation of a future electric grid configuration.

The second thematic direction is to understand better **how sustainable planning strategies being carried out in the energy and water sectors can be developed in tandem to improve infrastructure resilience against climate change.** In the water sector, efforts to increase the reliability of water supply under climate change are being used, such as installing seawater and brackish water desalination, increasing water reuse, and enacting conservation measures, each of which has impacts on the energy sector. In addition, the energy sector may need to rely on water resources for many components of the energy infrastructure, such as conventional and pumped hydropower facilities, cooling of power plants, steam generation in industrial processes, and others. In addition, the advance of climate change will affect the operations and planning of water and energy sectors simultaneously, and multiobjective optimization of how

these sectors are planned will be critical for ensuring a higher degree of resilience against climate change.

GLOSSARY

Term	Definition
Ancillary Services	Services provided to the electric grid operator focused on maintaining the reliability and resiliency of electricity service.
AR5	Assessment Report 5 – the latest climate change assessment report produced by the IPCC, released in 2013
BEV	Battery-electric vehicle
CEUS	Commercial End-Use Survey – a dataset produced by Itron, Inc. in 2006 to characterize energy usage patterns in the commercial sector
CO_2e	Carbon dioxide equivalent – the greenhouse gas emissions amount in terms of carbon dioxide equivalent of global warming potential
DDNI	Daily direct normal insolation – the component of solar insolation that impacts a given area on Earth's surface normal to the surface orientation
E3	Energy and Environmental Economics – a consulting firm in San Francisco focused on progressive energy system transformations.
EPIC (Electric Program Investment Charge)	The Electric Program Investment Charge, created by the California Public Utilities Commission in December 2011, supports investments in clean energy technologies that benefit electricity ratepayers of Pacific Gas and Electric Company, Southern California Edison Company, and San Diego Gas & Electric Company.
GW	Gigawatt
HiGRID	Holistic Grid Resource Integration and Deployment tool – a modeling platform for capturing the response of electric grid resource dispatch to technological or environmental perturbation, developed at UC Irvine.
IPCC	Intergovernmental Panel on Climate Change – an international panel focused on characterizing climate change and the related impacts on different sectors and countries throughout the world.
LBNL	Lawrence Berkeley National Laboratory – a research institution located in Berkeley, California, funded by the U.S. Department of Energy.
Long-Term Energy Scenarios	The theme of California Energy Commission projects focused on assessing or developing plans to meet California's long-term energy system performance goals.
MMT	Million metric tons

NREL	National Renewable Energy Laboratory - a research institution in Golden, Colorado, funded by the U.S. Department of Energy.
PEV	Plug-in electric vehicle
PHEV	Plug-in hybrid electric vehicle
PNNL	Pacific Northwest National Laboratory - a research institution in Kirkland, Washington, funded by the U.S. Department of Energy.
RCP	Representative Concentration Pathway – a climate scenario representing different radiative forcing levels caused by greenhouse gas emissions
Spinning Reserve	A service provided to the electric grid where additional generation (or reduced load) is provided in the event of a contingency such that the electric grid can maintain the balance between load and generation.
TAF	Thousand acre-feet. One acre-foot is equivalent to 325,851 gallons.
TWh	Terawatt-hour
V2G	Vehicle-to-grid – a scheme for the charging of electric vehicles where vehicles can both draw energy from the electric grid or discharge energy back to the electric grid.

REFERENCES

1. California State Agencies' PATHWAYS Project: Long-Term Greenhouse Gas Reduction Scenarios, 2015, Energy and Environmental Economics (E3).

2. Wei, M., et al.., *Scenarios for Meeting California's 2050 Climate Goals*, 2013, UC Berkeley - Lawrence Berkeley National Laboratory.

3. Stocker, T.F., et al., *IPCC (2013) Climate Change 2013: The Physical Science Basis. Contribution of Working Group I to the Fifth Assessment Report of the Intergovernmental Panel on Climate Change*, 2013, Intergovernmental Panel on Climate Change.

4. *Electric Generation Capacity & Energy*. 2016 [cited 2017 March 22]; Available from http://www.energy.ca.gov/almanac/electricity_data/electric_generation_capacity.html.

5. Chang, M.K., et al. 2013. "Buffering Intermittent Renewable Power With Hydroelectric Generation: A Case Study in California." *Applied Energy*. **112**: p. 1-11.

6. *Addressing the 2000-2001 Western Energy Crisis*. 2001 [cited 2017 March 22]; Available from https://www.ferc.gov/industries/electric/indus-act/wec/enron/data-sets.asp.

7. Madani, K. and J. R. Lund. 2010. Estimated Impacts of Climate Warming on California's High-Elevation Hydropower." *Climatic Change*, **102**(3): p. 521-538.

8. Stewart, I. T., D. R. Cayan, and M. D. Dettinger. 2005. "Changes Toward Earlier Streamflow Timing Across Western North America." *Journal of Climate*, **18**(8): p. 1136-1155.

9. Vicuna, S. and J. A. Dracup. 2007. "The Evolution of Climate Change Impact Studies on Hydrology and Water Resources in California." *Climatic Change*, **82**(3): p. 327-350.

10. "California Drought Leads to Less Hydropower, Increased Natural Gas Generation - Today in Energy." U.S. Energy Information Administration (EIA). 2014 [cited 2017 March 22]; Available from https://www.eia.gov/todayinenergy/detail.php?id=18271.

11. *Market Issues and Performance: 2007 Annual Report*, 2008, California Independent System Operator.

12. Madani, K., M. Guégan, and C. B. Uvo. 2014. "Climate Change Impacts on High-Elevation Hydroelectricity in California." *Journal of Hydrology*, **510**: p. 153-163.

13. Null, S. E. and J. H. Viers. 2012. *Water and Energy Sector Vulnerability to Climate Warming in the Sierra Nevada: Water Year Classification in Non-Stationary Climates*, California Energy Commission and UC Davis.

14. Rheinheimer, D. E., S. M. Yarnell, and J. H. Viers. 2012. "Hydropower Costs of Environmental Flows and Climate Warming in California's Upper Yuba River Watershed." *River Research and Applications,* **29**(10): p. 1291-1305.

15. Vicuña, S., J. A. Dracup, and L. Dale. 2011. "Climate Change Impacts on Two High-Elevation Hydropower Systems in California." *Climatic Change,* **109**(1): p. 151-169.

16. Vicuna, S., et al. 2008. "Climate Change Impacts on High Elevation Hydropower Generation in California's Sierra Nevada: A Case Study in the Upper American River." *Climatic Change,* **87**(1): p. 123-137.

17. *Quantifying the Value of Hydropower in the Electric Grid: Final Report*, 2013, Electric Power Research Institute.

18. Loose, V. W. 2011. *Quantifying the Value of Hydropower in the Electric Grid: Role of Hydropower in Existing Markets*, Sandia National Laboratory.

19. Gaudard, L. and F. Romerio. 2014. "The Future of Hydropower in Europe: Interconnecting Climate, Markets and Policies." *Environmental Science & Policy,* **37**: p. 172-181.

20. Abgottspon, H. and G. Andersson. 2013. "Strategic Bidding of Ancillary Services for a Hydro Power Producer." in *2013 10th International Conference on the European Energy Market (EEM)*.

21. Deng, S.j., Y. Shen, and H. Sun. 2006. "Optimal Scheduling of Hydro-Electric Power Generation With Simultaneous Participation in Multiple Markets" in *2006 IEEE PES Power Systems Conference and Exposition*.

22. Doorman, G. L. and B. Nygreen. 2002. "An Integrated Model for Market Pricing of Energy and Ancillary Services." *Electric Power Systems Research*, **61**(3): p. 169-177.

23. Ehsani, A., A. M. Ranjbar, and M. Fotuhi-Firuzabad. 2009. "A Proposed Model for Co-Optimization of Energy and Reserve in Competitive Electricity Markets." *Applied Mathematical Modelling,* **33**(1): p. 92-109.

24. Mahone, A., et al. 2018. *Deep Decarbonization in a High Renewable Electricity, Biofuels-Constrained Future: Updated Results From the California PATHWAYS Model (forthcoming)*, Energy and Environmental Economics and California Energy Commission: San Francisco, CA, USA.

25. Tarroja, B., et al. 2016. "Assessing the Stationary Energy Storage Equivalency of Vehicle-to-Grid Charging Battery Electric Vehicles." *Energy,* **106**: p. 673-690.

26. *California Hydroelectric Statistics & Data*. 2017 [cited 2017 March 22]; Available from: http://www.energy.ca.gov/almanac/renewables_data/hydro/.

27. *Database of California Power Plants*. 2017. Available from http://www.energy.ca.gov/sitingcases/.

28. *Water Data: Annual Data Reports*. 2011 [cited 2017 March 22]. Available from https://ca.water.usgs.gov/data/waterdata/schematics2007.html.

29. *California Data Exchange Center*. 2017 [cited 2017 March 22]. Available from http://cdec.water.ca.gov/.

30. *National Water Information System*. 2017 [cited 2017 March 22]. Available from https://waterdata.usgs.gov/nwis.

31. Tarroja, B., et al. 2014. "Evaluating Options for Balancing the Water–Electricity Nexus in California: Part 2—Greenhouse Gas and Renewable Energy Utilization Impacts." *Science of The Total Environment,* **497-498**: p. 711-724.

32. Haddeland, I., T. Skaugen, and P. Lettenmaier Dennis. 2006. "Anthropogenic Impacts on Continental Surface Water Fluxes." *Geophysical Research Letters,* **33**(8).

33. Hanasaki, N., S. Kanae, and T. Oki. 2006. "A Reservoir Operation Scheme for Global River Routing Models." *Journal of Hydrology,* **327**(1): p. 22-41.

34. Van Beek, L. P. H., Y. Wada, and F. P. Bierkens Marc. 2011. "Global Monthly Water Stress: 1. Water Balance and Water Availability." *Water Resources Research,* **47**(7).

35. *Record of Decision: Trinity River Mainstem Fishery Restoration Final Environmental Impact Statement/Environmental Impact Report.* 2000. U.S. Department of the Interior.

36. *The Kings River Handbook Handbook.* 2003. Kings River Conservation District.

37. *Hydropower - Oroville Facilities Project Environmental Impact Report.* 2006. Federal Energy Regulatory Commission.

38. *New Melones Unit Project.* 2017; Available from https://www.usbr.gov/projects/index.php?id=365.

39. Bennett, B. and L. Park. California Public Utilities Commission. 2010. *Embedded Energy in Water Studies Study 1: Statewide and Regional Water-Energy Relationship*,

40. *Open-Access Same-Time Information System (OASIS)*, California Independent System Operator.

41. *Protected Areas Database of the United States (PAD-US), Version 1.4 Combined Feature Class.* 2016. U.S. Geological Survey, Gap Analysis Program (GAP).

42. Homer, C. G., et al. 2015. "Completion of the 2011 National Land Cover Database for the Conterminous United States-Representing a Decade of Land Cover Change Information." *Photogrammetric Engineering and Remote Sensing*, **81**(5): p. 345-354.

43. Lopez, A., et al. 2012. *U.S. Renewable Energy Technical Potentials: A GIS-Based Analysis* National Renewable Energy Laboratory.

44. *Concentrating Solar Power Projects in the United States.* 2016. National Renewable Energy Laboratory.

45. *Lower 48 and Hawaii DNI 10km Resolution - 1998 to 2009.* 2012. National Renewable Energy Laboratory.

46. *Piloting the Integration and Use of Renewables to Achieve a Flexible and Secure Energy Infrastructure.* 2014. University of California - Irvine and California Energy Commission.

47. *The Geothermal Prospector.* 2016. National Renewable Energy Laboratory.

48. Williams, C. F., et al. 2008. *Assessment of Moderate- and High-Temperature Geothermal Resources of the United States.* U.S. Geological Survey.

49. Williams, C. F. and J. DeAngelo. 2008. "Mapping Geothermal Potential in the Western United States." *Transactions of the Geothermal Resources Council,* **33**: p. 181-187.

50. Williams, C. F., et al. 2009. "Quantifying the Undiscovered Geothermal Resources of the United States." *Transactions of the Geothermal Resources Council,* **33**: p. 995-1003.

51. *California Water Plan Update 2013 Volume 2: Regional Reports.* 2014. California Department of Water Resources.

52. Macknick, J., et al. 2012. "Operational Water Consumption and Withdrawal Factors for Electricity Generating Technologies: A Review of Existing Literature. *Environmental Research Letters*, **7**(4): p. 045802.

53. *Compliance - Application for Certification for PG&E Geysers Unit (78-NOI-3).* 1979. California Energy Commission.

54. *Salton Sea Geothermal Unit #6 Power Project - Application for Certification (02-AFC-2).* 2003. California Energy Commission.

55. *Abengoa Mohave Solar Project: Licensing Proceedings (09-AFC-05C).* 2014. California Energy Commission.

56. *Residential Building Prototype Models.* 2014. U.S. Department of Energy - Building Energy Codes Program.

57. Taylor, Z. T., V. V. Mendon, and N. Fernandez. 2015. *Methodology for Evaluating Cost-Effectiveness of Residential Energy Code Changes*, Pacific Northwest National Laboratory.

58. *Commercial Building Prototype Models.* 2014. U.S. Department of Energy - Building Energy Codes Program.

59. Hart, R. and B. Liu. 2015. *Methodology for Evaluating Cost-Effectiveness of Commercial Energy Code Changes.* Pacific Northwest National Laboratory.

60. *2016 Building Energy Efficiency Standards for Residential and Nonresidential Buildings*, 2015. California Energy Commission, CEC-400-2015-037-CMF.

61. *EnergyPlus Version 8.5 Documentation - Auxiliary Programs.* 2016. U.S. Department of Energy.

62. Pierce, D. W., D. R. Cayan, and B .L. Thrasher. 2014. "Statistical Downscaling Using Localized Constructed Analogs (LOCA)." *J. Hydrometeorology*, **15**(2558).

63. Liang, X., et al. 1994. "A Simple Hydrologically Based Model of Land Surface Water and Energy Fluxes for General Circulation Models." *Journal of Geophysical Research: Atmospheres*, **99**(D7): p. 14415-14428.

64. *California Building Climate Zone Areas.* 2016. California Energy Commission.

65. *EnergyPlus Weather Data Sources.* 2016. U.S. Department of Energy.

66. *Building Climate Zones by ZIP Code.* 2016. California Energy Commission.

67. *American Fact Finder - 2010 Census.* 2011. U.S. Census Bureau.

68. *2009 Residential Energy Consumption Survey.* 2013. U.S. Energy Information Administration.

69. *California Commercial End-Use Survey (CEUS).* 2006. California Energy Commission, Itron Inc.

70. *2012 Commercial Buildings Energy Consumption Survey (CBECS).* 2016. U.S. Energy Information Administration.

71. Eichman, J. D., et al. 2013. "Exploration of the Integration of Renewable Resources Into California's Electric System Using the Holistic Grid Resource Integration and Deployment (HiGRID) Tool." *Energy,* **50**: p. 353-363.

72. Eichman, J. D. 2012. *Energy Management Challenges and Opportunities With Increased Intermittent Renewable Generation on the California Electrical Grid*, in *Mechanical and Aerospace Engineering.* University of California, Irvine: Irvine, CA.

73. Subin, Z. and A. Mahone. *Personal Communication - E3 Pathways 4/14/2017 Mitigation Scenario Without Climate Change*. 2017.

74. Tarroja, B., B. Shaffer, and S. Samuelsen. 2015. "The Importance of Grid Integration for Achievable Greenhouse Gas Emissions Reductions From Alternative Vehicle Technologies." *Energy,* **87**: p. 504-519.

75. *The 2017 Climate Change Scoping Plan Update: The Proposed Strategy for Achieving California's 2030 Greenhouse Gas Target*. 2017. California Air Resources Board.

76. *California ISO Open Access Same-Time Information System (OASIS)*. 2017. California Independent System Operator.

77. Forrest, K. E., et al. 2016. "Charging a Renewable Future: The Impact of Electric Vehicle Charging Intelligence on Energy Storage Requirements to Meet Renewable Portfolio Standards." *Journal of Power Sources,* **336**: p. 63-74.

78. *Effects of Climate Change on Energy Production and Use in the United States*. 2008. U.S. Department of Energy.

79. Quayle, R. G. and H. F. Diaz. 1979. "Heating Degree Day Data Applied to Residential Heating Energy Consumption." *Journal of Applied Meteorology,* **19**(3): p. 241-246.

80. Lynn, E., et al. 2015, *Perspectives and Guidance for Climate Change Analysis*, F.K. William O'Daly, Jeffrey Woled, Editor California Department of Water Resources (DWR) - Climate Change Technical Advisory Group (CCTAG).

81. Van Vuuren, D.P., et al. 2011. "The Representative Concentration Pathways: An Overview." *Climatic Change,* **109**(1): p. 5.

APPENDIX A:
Description of Analysis Methods

This appendix describes the details of the methods and approaches used to conduct the studies and produce the results described in the main report. Each section corresponds to methods associated with a different chapter in the main report.

A.1. Chapter 2 Analysis Methods

The analysis in Chapter 2 examined the historical contribution of hydropower to electricity generation and ancillary services, using a historical baseline of 2000-2009. Climate change impacts on hydropower, as projected by Representative Concentration Pathways (RCP) 4.5 and 8.5, were investigated, comparing historical conditions to the years 2046-2055. The analysis sought to identify changes in seasonal and annual patterns in hydropower generation and participation in ancillary service markets.

Hydropower plants identified as "large hydropower" by the California Energy Commission were considered for this analysis [26]. Hydropower classified under this heading tends to have a capacity greater than 30 megawatts (MW) and generate electricity on the scale of 10^5 megawatt-hours (MWh) or greater annually.

The following hydropower units in this analysis were previously modeled in Tarroja et al 2014: Don Pedro, Exchequer, Folsom, New Melones, Oroville (Edward C. Hyatt), Pine Flat, Pyramid (Castaic), Shasta, and Trinity. This work incorporates the reservoir model developed in the previous study, building off the established framework for the remainder of the reservoirs examined in this work. A complete list of the hydropower plants included in this study can be found in Table A-1:

Table A-1: Complete List of Hydropower Plants Included in Study

Power Plant	Capacity (MW)	Head (m)	Latitude	Longitude	Service Area [27]	Storage Capacity for Closest Reservoir(s) [28] (TAF)
Balch #1&2	139	725	36.91	-119.09	PG&E	1.2, after Haas
Belden	125	235	40.01	-121.25	PG&E	<1, after Caribou
Big Creek 1	82.9	586	37.20	-119.24	SCE	89.8
Big Creek 2	67.1	499	37.20	-119.31	SCE	after Big Creek 1
Big Creek 2A	98.5	671	37.20	-119.31	SCE	136

Big Creek 3	177	233	37.15	-119.00	SCE	<1, downstream from Mammoth Pool and Big Creek 8
Big Creek 4	100	118	37.14	-119.49	PG&E	35,030
Big Creek 8	64.5	209	37.21	-119.33	SCE	after Big Creek 2A
Bucks Creek	65	780	39.91	-121.33	PG&E	1, downstream from Bucks Lake (101)
Butt Valley	41	80	40.18	-121.19	PG&E	1,175
Camino	154	304	38.83	-120.54	PG&E	<1
Caribou #1&2	195	351	40.09	-121.15	PG&E	49.9
Castaic	1247	319	34.59	-118.66	SCE	172
Chicago Park	44	146	39.18	-120.89	PG&E	<1
Colgate	315	398	39.33	-121.19	PG&E	961
Collierville	263	668	38.15	-120.38	PG&E	1.93
Cresta	70	88.4	39.83	-121.41	PG&E	4.40
Devil Canyon	276	427	34.21	-117.33	SCE	75.0
Dion R Holm	165	640	37.90	-119.97	PG&E	274
Don Pedro	203	170	37.70	-120.42	PG&E and MID	2,030
Donnells	72	351	38.25	-120.03	PG&E	64.7
Drum #1&2	103.5	420	39.26	-120.77	PG&E	74.7
Edward C Hyatt	819	187	39.54	-121.49	PG&E	3,540
Electra	98	388	38.33	-120.67	PG&E	1.17
Exchequer	94.5	133	37.58	-120.27	PG&E	1,030
Folsom	198.7	91	38.71	-121.16	SMUD	977
Forbestown	39.7	242	39.55	-121.28	PG&E	<1

Haas	144	745	36.93	-119.02	PG&E	129 (Wishon), 123 (Courtright Reservoir)
James B Black	172	340	40.99	-121.98	PacifiCorp	24.2 (Iron Canyon), 35.2 (Lake McCloud)
Jaybird	154	450	38.83	-120.53	PG&E	2.61, downstream from Union Valley
Judge F Carr	154	155	40.65	-122.63	PG&E	14.7, downstream from Trinity
Kerckhoff 2	155	128	37.07	-119.56	PG&E	4.20
Keswick	117	26.5	40.61	-122.45	PG&E	23.8, downstream from Shasta
Kings River	52	243	36.89	-119.16	PG&E	<1
Loon Lake	74.1	335	38.98	-120.32	PG&E	76.2
Mammoth Pool	187	306	37.22	-119.34	PG&E	123
Middle Fork	116	590	39.02	-120.60	PG&E	208
Mojave Siphon	32.7	24.7	34.31	-117.32	SCE	N/A
New Melones	300	150	37.95	-120.53	PG&E	2,420
Parker	144	72	37.48	-120.44	SCE	646
Pine Flat	165	129	36.83	-119.34	PG&E	1,002
Pit #1	61	129	40.99	-121.50	PG&E	3.21
Pit #3	70	138	41.00	-121.75	PG&E	41.9
Pit #4	95	92.8	40.99	-121.85	PG&E	1.97
Pit #5	160	162	40.99	-121.98	PacifiCorp	1.04
Pit #6	80	47.2	40.92	-121.99	PacifiCorp	15.9, downstream from James B. Black
Pit #7	112	62.5	40.85	-121.99	PG&E	34.6
Poe	120	149	39.72	-121.47	PG&E	1.15
Ralston	79	400	39.00	-120.73	PG&E	<1

Rock Creek	112	163	39.91	-121.35	PG&E	4.66
Salt Springs 2	33	645	38.50	-120.22	PG&E	52.0
Shasta	676	100	40.72	-122.42	PG&E	4,440
Spring Creek	180	173	40.63	-122.47	PG&E	241
Stanislaus	91	463	38.14	-120.37	PG&E	downstream from Beardsley (98.5)
Tiger Creek	58	372	38.45	-120.49	PG&E	<1
Trinity	140	130	40.80	-122.76	Trinity PUD	2,440
Union Valley	46.7	420	38.86	-120.44	PG&E	266
White Rock	230	238	38.77	-120.79	PG&E	13.4
William E. Warne	75	219	34.69	-118.79	SCE	N/A
Woodleaf	55	444	39.55	-121.20	PG&E	5.92

Source: Advanced Power and Energy Program, University of California Irvine

A.1.1 Historical Data

Historical hydrological data were retrieved from the California Data Exchange Center [29], the United States Geological Survey (USGS) [30], and Pacific Gas and Electric Co. (PG&E). Water data are temporally resolved at the day scale. Available USGS gauges for inflow, outflow, and reservoir data were determined from USGS schematics [23]. In cases where inflow data, Q_{in}, were unavailable or incomplete, inflow was calculated as follows:

$$Q_{in}=dS+ Q_{out,tot}$$

Where dS is the differential change in reservoir storage. This approach was taken from the equations PG&E provided for its hydropower plants.

Gaps in available data were addressed in the following way: day gaps were filled by averaging the day before and the day following the gap. Longer-term gaps on the month or year scale were addressed by applying the data for the same time frame from the most closely matched year.

A hydropower unit was not modeled if it had significant data gaps, such as more than three years of reservoir and flow data were missing, so that inflow could not be calculated and the reservoir profile could not be matched. The large hydropower plants that were ultimately not

included in this analysis due to lack of available data and/or incongruence between historical water data and historical electricity generation are Eastwood (pumped storage), Gianelli (pumped storage), Helms (pumped storage), Kern River 3, Kirkwood, Moccasin, Narrows 2, and Thermalito (pumped storage).

The following parameters were taken from historical data for each hydropower unit: total reservoir capacity, hydraulic head, power capacity, instream water demands, water delivery constraints, and minimum/maximum flow constraints. Many of these values were taken directly from the previous 2012 Energy Commission study [13] and Tarroja et al. (2014) [31].

A.1.2. Reservoir Model

The reservoir model used in this analysis was developed by Tarroja et al (2014) [31], based on previous work [32-34]. A complete description of the model and previous application can be found in Tarroja et al. (2014). The following is a description of the key components of the model relevant to this study.

The reservoir model is temporally resolved at the day scale. The model inputs are inflow, reservoir demand, initial fill level, maximum discharge rate, and minimum/maximum fill level limits.

The reservoir state for each time step (S_i) is calculated as:

$$S_i = S_{i-1} + \int_{i-1}^{i} \dot{Q}_{in} - \dot{Q}_{out} - \dot{Q}_{add},$$

Where:

- $\dot{Q}_{in}$= inflow input
- $\dot{Q}_{out}$ = the outflow corresponding to demand
- $\dot{Q}_{add}$ = any additional release required for management of water levels

Reservoir released outflow is represented as:

$$\dot{Q}_{out} = \ max(min(\dot{Q}_d, \dot{Q}_{lim}), F(s) * \dot{Q}_{avg}),$$

Where:

- $\dot{Q}_d$ = outflow demand, taking into consideration storage capacity constraints (S_{min} is the minimum storage limit):

$$\dot{Q}_d = \ min\left(1, \frac{S_{i-1}}{S_{min}}\right) * Demand_i,$$

- $F(s)$ = the ratio of available storage at the current time step to the maximum dispatchable storage:

$$F(s) = min\left(1, max\left(0, \frac{S_{i-1} - S_{min}}{S_{max,o} - S_{min}}\right)\right).$$

The second outflow variable, $\dot{Q}_{add}$, in the reservoir state equation represents additional releases above demand, associated with managing water levels and flood:

$$\dot{Q}_{add} = max\left(0, \frac{S_{i-1} - S_{max,o}}{S_{max} - S_{max,o}} (\dot{Q}_b - \dot{Q}_{out})\right) + max(0, S_{i-1} - S_{max}),$$

Where:

- $\dot{Q}_b$ = bankfull discharge

This reservoir model was developed for hydropower units with a large storage capacity. For this study, the reservoir model was applied to all hydropower units with reservoirs with greater than 16,000 acre-feet of dispatchable capacity were modeled as dispatchable (i.e., inflow can be retained within the reservoir and dispatched with demand beyond the day scale. Also, outflow throughout the day may be adjusted to respond to changes in electricity demand). Hydropower units are identified as dispatchable or nondispatchable based the size of the most proximate reservoir. Some hydropower units in this analysis have reservoirs with a total capacity greater than 16,000 acre feet; however, the high minimum storage requirements of these reservoirs make the associated *dispatchable* capacity less than the required 16,000 acre-feet. They were, therefore, not simulated as dispatchable hydropower. Hydropower units with reservoirs that do not meet the above limitation or do not have associated reservoirs were considered nondispatchable and vary directly with changes in inflow.

Dispatchable reservoirs were calibrated to match the associated historical profiles. A selection of historical profiles are in Figure A-1. The following parameters were adjusted: reservoir demand, bankfull discharge, and minimum storage capacity. Spill was minimized, corresponding to historical patterns for each reservoir. Minimizing spilling, within flood management and reservoir level constraints, minimizes lost water and potentially lost energy revenue. This assumption is supported by the previous study [13].

Figure A-1: Example Reservoir Profiles, Historical Versus Model

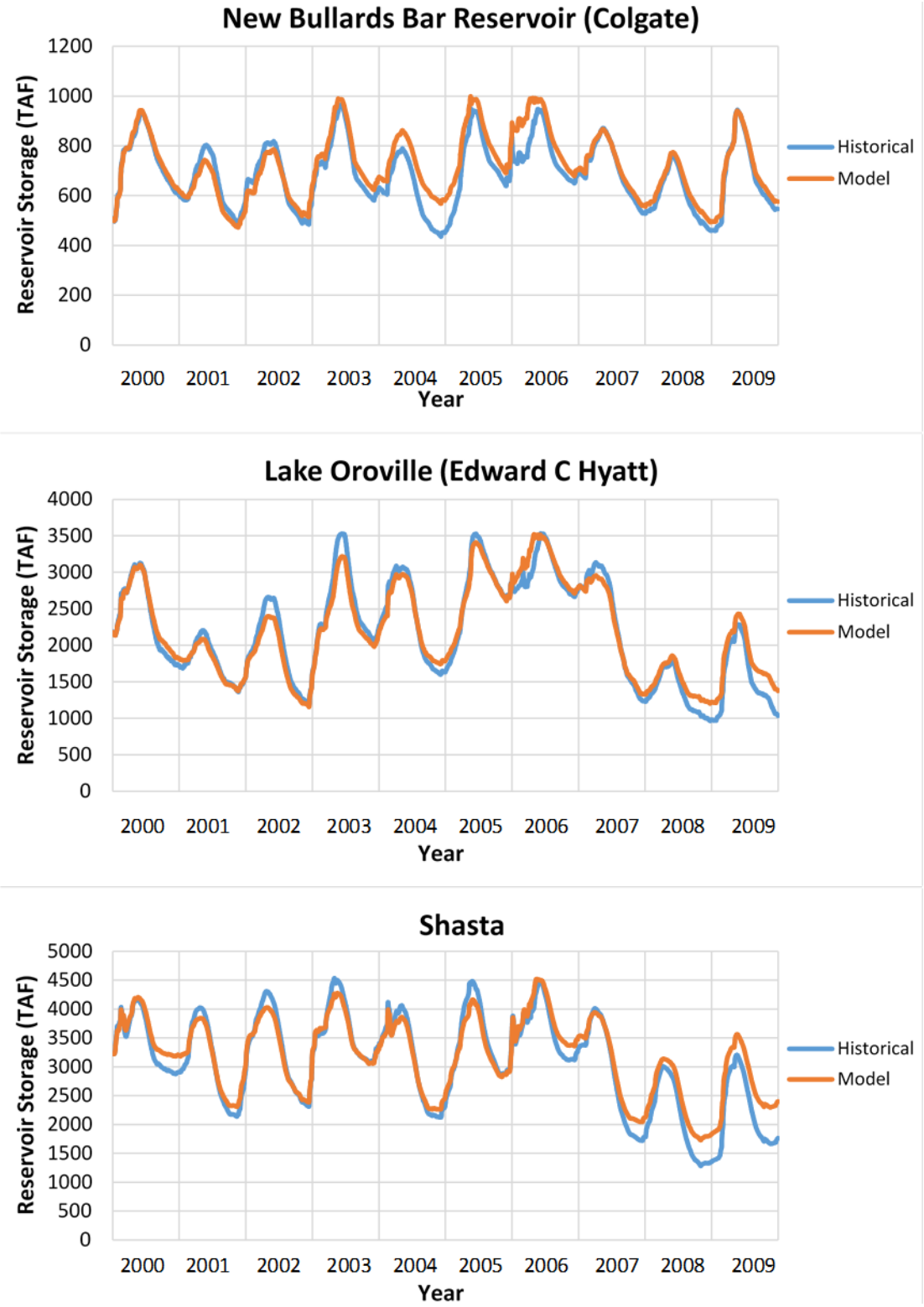

Source: Advanced Power and Energy Program, University of California Irvine

A.1.2.1. Instream Demands and Additional Water Constraints

Most large hydropower stations provide several services, only one of which is electricity generation. A given unit may support water supply (e.g., irrigation, urban use, fisheries, etc.), flood control, or recreation or a combination. This study assumed that dispatch was optimized for electricity generation with the limitation that instream water demands and general water delivery requirements were first met. It is assumed that historical demands remain consistent into the future. This analysis does not make a distinction between water year types for instream water requirements. Where wet and dry year values differ, a median value is taken.

The research team calculated averages for total auxiliary water demands based on measured daily historical data, when available [29, 30]. For some hydropower units, requirements detailed in government reports or previous studies were applied [35-39] (Table A-2). Some hydropower units experience variable water demands between years, so the research team calculated an average value for the relevant hydropower units.

Table A-2: Auxiliary Water Requirement Estimates Obtained From Reports

Reservoir/Hydropower Unit	Historical Range
Oroville/Hyatt	700-1000 TAF/year [37]
Don Pedro	248-330 TAF/year [39]
New Melones	35-155 TAF/year [38]
Trinity	369-647 TAF/year [35]
Pine Flat	36-72 TAF/year [36]

Source: Advanced Power and Energy Program, University of California Irvine

Power plant maintenance and potential changes in water management decisions are outside the scope of this study. Because this study uses the average value for auxiliary water demands, some variance is to be expected for hydropower units with variable seasonal and annual demands.

A.1.3. Power Generation Model

Power generation from nondispatchable and dispatchable hydropower units was evaluated using different approaches. Generation from nondispatchable hydropower is assumed to be a direct function of inflow and is resolved at the day scale, in line with water flow data available, because verifiable assumptions about hourly operations for these facilities could not be drawn:

$$P_i = \eta * min(P_{cap}, \rho g h * \max(0, \dot{Q}_{in} - \dot{Q}_s)),$$

where:

- η = the efficiency of the hydropower unit (assumed to be 90 percent for all power plants)
- P_{cap} = the rated capacity

- h = the hydraulic head
- $\dot{Q}_s$= the auxiliary water demands such as instream requirements and water deliveries

On the other hand, dispatchable hydropower units consider inflow through the turbines to be the outflow from the reservoir model, modified to account for auxiliary water demands. The equation is the same except Q_{in} becomes Q_{res}, where Q_{res} is total outflow from the reservoir.

Dispatchable hydropower units were assumed to be dispatchable at the hourly timescale (Figure A-2) and participate in spinning reserve markets, requiring an optimization based on price. This optimization problem is described in Section A.1.4. In this study, all hydropower units were modeled as fixed head units since the fill vs. head profiles for each reservoir were unavailable. The hydraulic head used for each reservoir can be found in Table A-1.

Figure A-2: Example Days of Hourly Dispatch of Hydropower Units for Each Season

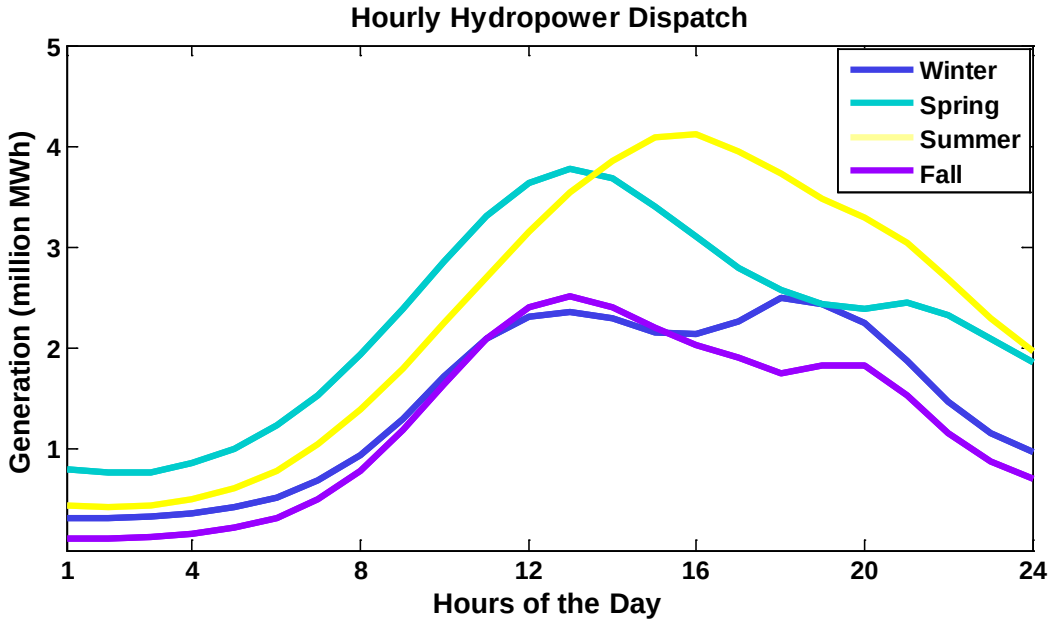

Source: Advanced Power and Energy Program, University of California Irvine

A.1.4. Bidding Optimization Module

Dispatchable hydropower is assumed to participate simultaneously in the energy market and ancillary service markets for spinning reserve throughout the day. The bidding optimization model has the hydropower unit select the optimal service based on price and under a set of constraints.

The optimization acts to maximize water reservoir revenue in each day:

$$\min \ -\text{sum}\left(R_{gen}(t) + R_{SP}(t) + R_{reg}(t)\right)$$

Where $R_{gen}(t)$, $R_{SP}(t)$, and $R_{reg}(t)$ are the revenues in dollars from providing generation (energy), spinning reserve, and frequency regulation respectively, calculated at each hour t within a given day. The bid commitments for generation, spinning reserve, and regulation are the optimization

variables. Generation revenue is calculated from the hydropower unit generation bid (P_{gen}) during a given hour in MW and data on the market clearing price (MCP) as a function of net load (P_{NL}) in $/MWh.

$$R_{gen}(t) = P_{gen}(t) \cdot MCP(P_{NL}(t))$$

Spinning reserve revenue is calculated from the hydropower unit spinning reserve bid (P_{SP}) in MW and the price of spinning reserve (C_{SP}) in $/MW.

$$R_{SP}(t) = P_{SP}(t) \cdot C_{SP}(t)$$

Regulation revenue is calculated from the hydropower unit regulation bid (P_{reg}) in MW and the price of regulation service (C_{reg}) in $/MW.

$$R_{reg}(t) = P_{reg}(t) \cdot C_{reg}(t)$$

Historical data regarding the market-clearing price, net load, prices of spinning reserve and regulation on an hourly basis were obtained from the California ISO OASIS database for 2015. These data were used for the per-unit service prices in this analysis.

The optimization process takes place within the following constraints. First, the total bid from a hydropower unit must not exceed the total power capacity of that unit:

$$P_{gen} + P_{SP} + P_{reg} \leq P_{cap}$$

Second, the total outflow calculated by the power generation module over the day must be equal to the daily outflow calculated by the water reservoir model for the corresponding hydropower unit:

$$sum(Q_{out}(t)) = Q_{day}$$

The outflow calculated by the power generation module is related to the bids during each hour, which correspond to physical releases of water. Generation and frequency regulation are the only services that actually release water from the reservoir; spinning reserve is a contingency service that does not release water unless called upon to respond to a contingency.

$$Q_{out}(t) = \frac{P_{gen}(t) + P_{reg}(t)}{\eta \rho g h}$$

Third, the maximum spinning reserve bid is limited by the amount of water stored at any given time. A hydropower unit cannot bid to provide more spinning reserve at a given hour than is allowed by the amount of energy available to discharge, which is directly related to the amount of water stored:

$$P_{SP}(t) \leq \eta \rho g h \cdot V_{available}(t)$$

Where $V_{available}$ is the difference between the volume of water stored and the minimum water storage level for the corresponding reservoir.

Price curves for spinning reserves were obtained from the California ISO OASIS Database [40]. This study does not modify electricity demand between the historical and future scenarios. The historical pricing for spinning reserve are also retained – that is, no assumption for the change

in the markets for spinning reserve are made. The electricity markets are under rapid transformation, and the value of spinning reserve is subject to change in the future, but specifically how that change will occur is abstract.

The power generation was validated using annual generation data for each hydropower unit obtained from the CA almanac **[26]** and directly from PG&E. The aggregate electricity generation profile was also verified compared to available historical data. The aggregate error for each historical year is in Table A-3.

Table A-3: Historical Aggregate Error for Hydropower Generation Calculations

Year	2000	2001	2002	2003	2004	2005	2006	2007	2008	2009
Aggregate Error	-0.1%	5.6%	1.5%	0.8%	0.7%	1.8%	-1.1%	2.1%	3.7%	2.2%
Standard Deviation	10.1%	7.1%	13.4%	11.7%	12.6%	10.8%	8.4%	10.7%	10.8%	13.7%

Source: Advanced Power and Energy Program, University of California Irvine

The research team performed a second cursory check, examining the available data on monthly trends. As seen in Figure A-3, hydropower tends to peak between May and July, with the lowest generation occurring between November and February [10]. Modeled generation for the baseline years 2000-2009 followed this historical trend, showing a similar range distribution (Figure A-4).

Figure A-3: EIA Data on California Hydropower Generation Range and Mean for 2004-2013

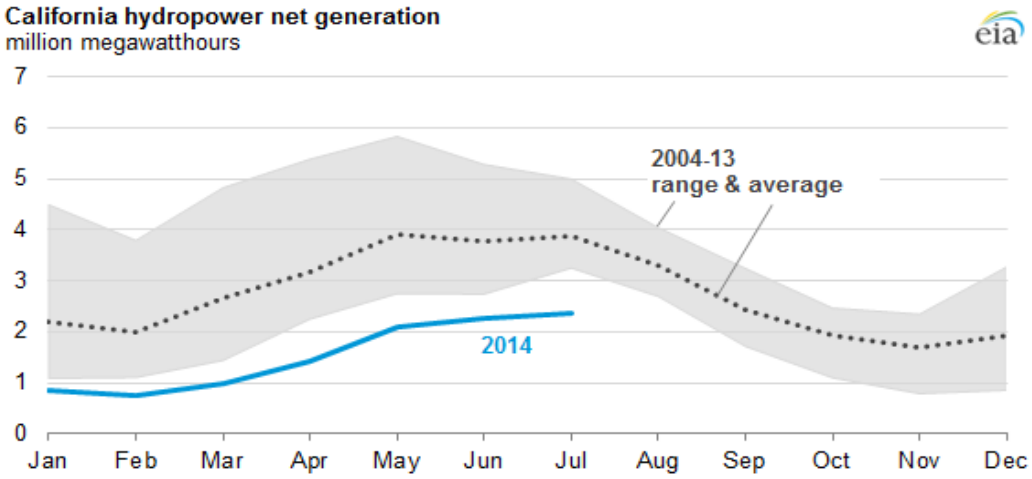

Source: Advanced Power and Energy Program, University of California Irvine

Figure A-4: California Historical Generation for Hydropower Units in Current Study, Mean and Range for 2000-2009

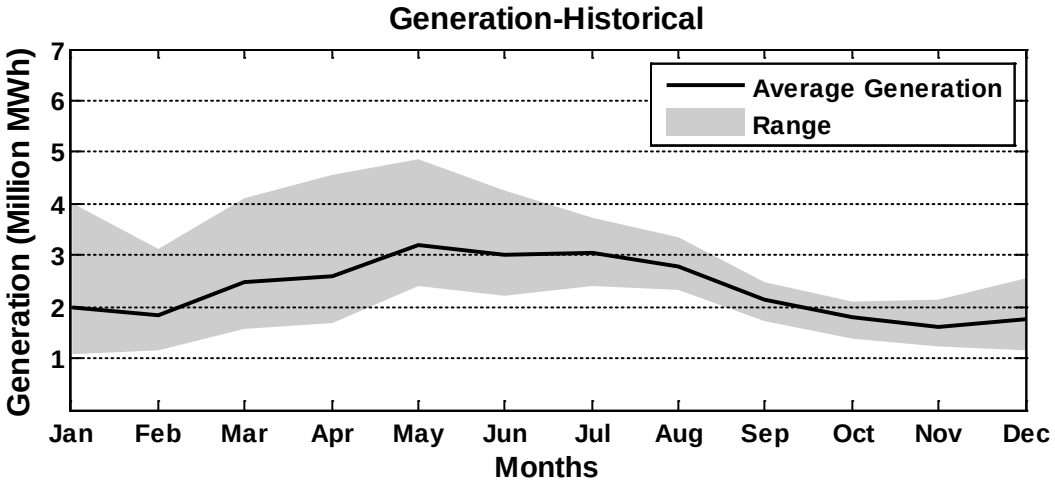

Source: Advanced Power and Energy Program, University of California Irvine

The upper bound is driven by the year 2006, featured in both the reference graph and the modeled data. The difference in magnitude, both for the range and mean, can be accounted for: this study examines a subset of total California hydropower, about 75-80% of total instate hydropower generation for the period investigated.

The research team examined the distribution of historical bidding potential to establish a baseline for historical participation in spinning reserve markets. Comparing spinning reserve bidding and generation bidding can help identify the relative contribution to generation versus spinning reserve, as well as the frequency of days where operational constraints limit participation.

The upper bound of Figure A-5 characterizes days where outflow and bidding constraints did not prevent any hydropower units from full participation in the markets. Days falling below this line are characterized by a fraction of the available hydropower being limited in participation in the spinning reserve market, such that the total bid (electricity generation + spinning reserve) that day was lower than the rated power capacity. Over the 10 years, there were numerous days in which one or more reservoirs experienced constraints on bidding, resulting in spinning reserve bids lower than the maximum possible. The change in the frequency of these days and the magnitude of effect will be examined for the climate change scenarios.

Figure A-5: Aggregated Daily Bidding for Dispatchable Hydropower for the 10-Year Historical Period 2000-2009

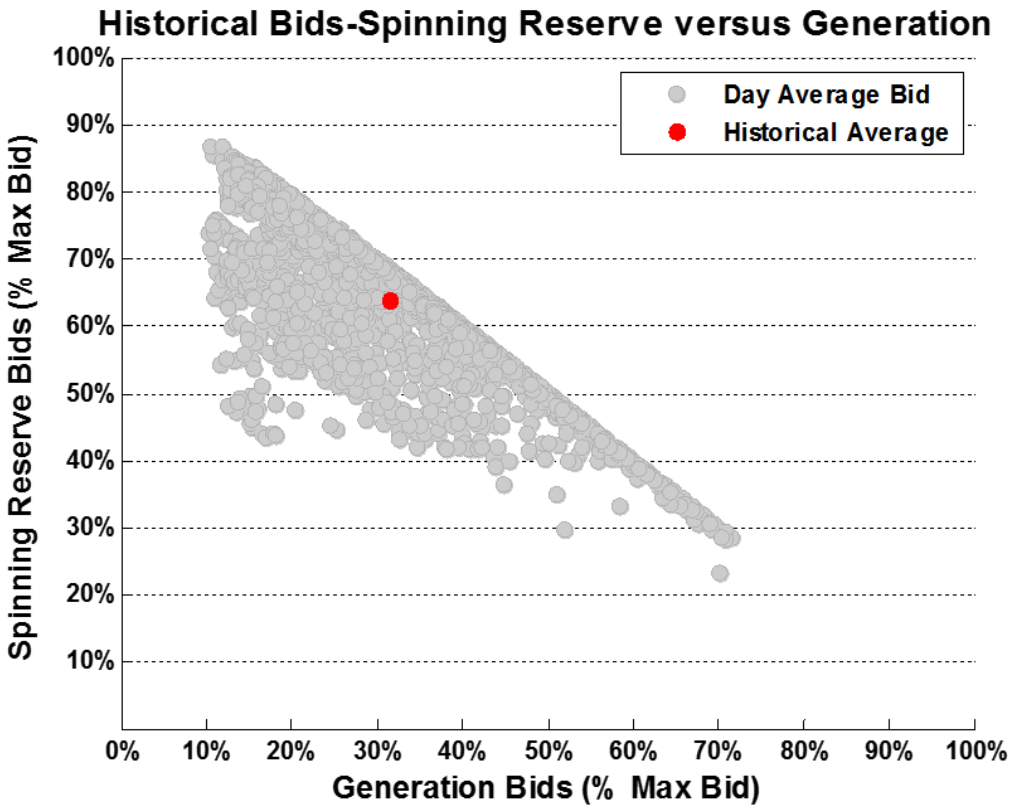

Source: Advanced Power and Energy Program, University of California Irvine

A.1.5. Climate Models

This study uses the climate models described the previous chapter. This analysis considers RCP 4.5 and RCP 8.5, applying the following models: CanESM2, CNRM-CM5, HadGEM2-ES, and MIROC5. These were selected as representative of wetter (CanESM2, CNRM-CM5) and drier (HadGEM2-ES) climate models.

The climate-affected inflows for the following hydropower units were calculated in Tarroja et al 2014: William E. Warne, Castaic, Don Pedro, Exchequer, Folsom, New Melones, and Shasta. Inflow into Mojave Siphon and Devil Canyon were approximated from inflow upstream calculated for San Luis for the same study. These hydropower units relied on routed inflow data using the Scripps Variable Infiltration Capacity (R-VIC) hydrological model.

The remainder of the inflow vectors were perturbed using gridded runoff as described in Appendix B.1. A bias correction was applied to convert changes to runoff to future inflow changes, with negative values calculated for future inflow rounded to zero:

$$I_f = I_h + \propto (R_f - R_h)$$

where:

I_f = future inflow

I_h = historical inflow

$$\propto = \frac{\text{mean}(I_h)}{\text{mean}(R_h)}$$

R_f = future runoff

R_h = historical runoff

The research team conducted a follow-up analysis to examine an extended period of drought under climate change conditions to determine how hydropower may respond to longer droughts. For this analysis, a 10-year period modeled for HadGEM2-ES under the RCP 8.5, where total runoff was lower than the historical baseline was selected from the late 21st century as an example. While *most* hydropower units experience decreased runoff for the drought period selected, not all hydropower units do. This results in some hydropower units experiencing increased inflow compared to the historical baseline. Nevertheless, the overall trend observed from the long drought scenario is a net decrease in runoff and inflow into hydropower units across the 10-year period, which results in lower reservoir levels and decreased bidding for generation and ancillary services. Because routed streamflow was not available for this analysis, all drought-affected inflows were calculated using the bias correction method. For the aqueduct-connected reservoirs, the change in runoff is calculated across the two hydrologic basins defined by the U.S. Geological Survey Hydrologic Unit Map as HUC 180201 and HUC 180400. This is for capturing the drainage area at the source of the aqueduct and was applied to the inflow into the connected reservoirs.

First, the potential installable capacity of solar thermal and geothermal resources is calculated based on energy potential, unconstrained by water availability limits in each of California's hydrologic regions. Second, the available supply of water is calculated based on a water balance of each hydrologic region. Third, the available water supply is used with data for the water consumption intensity for solar thermal and geothermal power plants using different cooling systems to determine the water-constrained installable capacity for each resource under different climate scenarios and cooling system configurations. The details of each step are presented in the following sections.

A.2. Chapter 3 Analysis Methods

A.2.1. Calculating Water-Unconstrained Solar Thermal and Geothermal Capacity

A.2.1.1. Solar Thermal Land Exclusions

For the analysis in Chapter 3, the team starts with calculating the maximum capacity potential for solar thermal resources if all suitable lands are allowed for development. To determine this potential, an analysis in ArcGIS is performed that excludes various types of land cover from solar thermal development due to either physical or legal constraints. In practice, however, there will be more constraints than these and the water constraints that is the focus of the Chapter 3 analysis that can constrain solar thermal development.

The land exclusions considered for this analysis are:

- **U.S. Federal Protected Lands**: These are contained in a dataset that encompasses all of the land areas that are protected from development by federal law. The dataset was obtained from the U.S. Geological Survey (USGS) includes land areas by GAP status code (1-3), which refer to areas which are protected for specific reasons as defined by the USGS [41]. This dataset includes National Parks and Landmarks and is presented in Figure A-6:
    - *GAP 1 Lands* are defined as "an area having permanent protection from conversion of natural land cover and a mandated management plan in operation to maintain a natural state within which disturbance events (of natural type, frequency, intensity, and legacy) are allowed to proceed without interference or are mimicked through management."
    - *GAP 2 Lands* are defined as "an area having permanent protection from conversion of natural land cover and a mandated management plan in operation to maintain a primarily natural state, but which may receive uses or management practices that degrade the quality of existing natural communities, including suppression of natural disturbance."
    - *GAP 3 Lands* are defined as "(an) area having permanent protection from conversion of natural land cover for the majority of area. Subject to extractive uses of either broad, low-intensity type or localized intense type. Confers protection to federally listed endangered and threatened species throughout the area."

Figure A-6: Federal Protected Lands by GAP Code

Source: U.S. Geological Survey

- **Unsuitable Land Cover**: The term refers to land areas on which solar thermal power plants cannot be built due either to current use for other purposes or due to physically being unsuitable for construction. Land cover data were obtained from the Multi-Resolution Land Characteristics Consortium (MRLC) for different categories using the National Land Cover Database Version 2011 (NLCD 2011) [42]. Of the land cover types in the NLCD 2011, the following are assumed unsuitable land areas for constructing solar thermal power plants. Descriptions are from the NLCD documentation. This analysis did not assume any changes in land cover from that displayed in the NLCD 2011 database [42]. The dataset is presented in Figure A-7:

- *Wetlands*: Woody wetlands and emergent herbaceous wetlands
- *Open Water*
- *Developed Land*: Open, low intensity, medium intensity, and high intensity. This includes urban areas
- *Forests*: Deciduous forest, evergreen forest, and mixed forest
- *Agricultural Lands*: Pasture/hay and cultivated crops

Figure A-7: Excluded Land Cover Types From NLCD Database

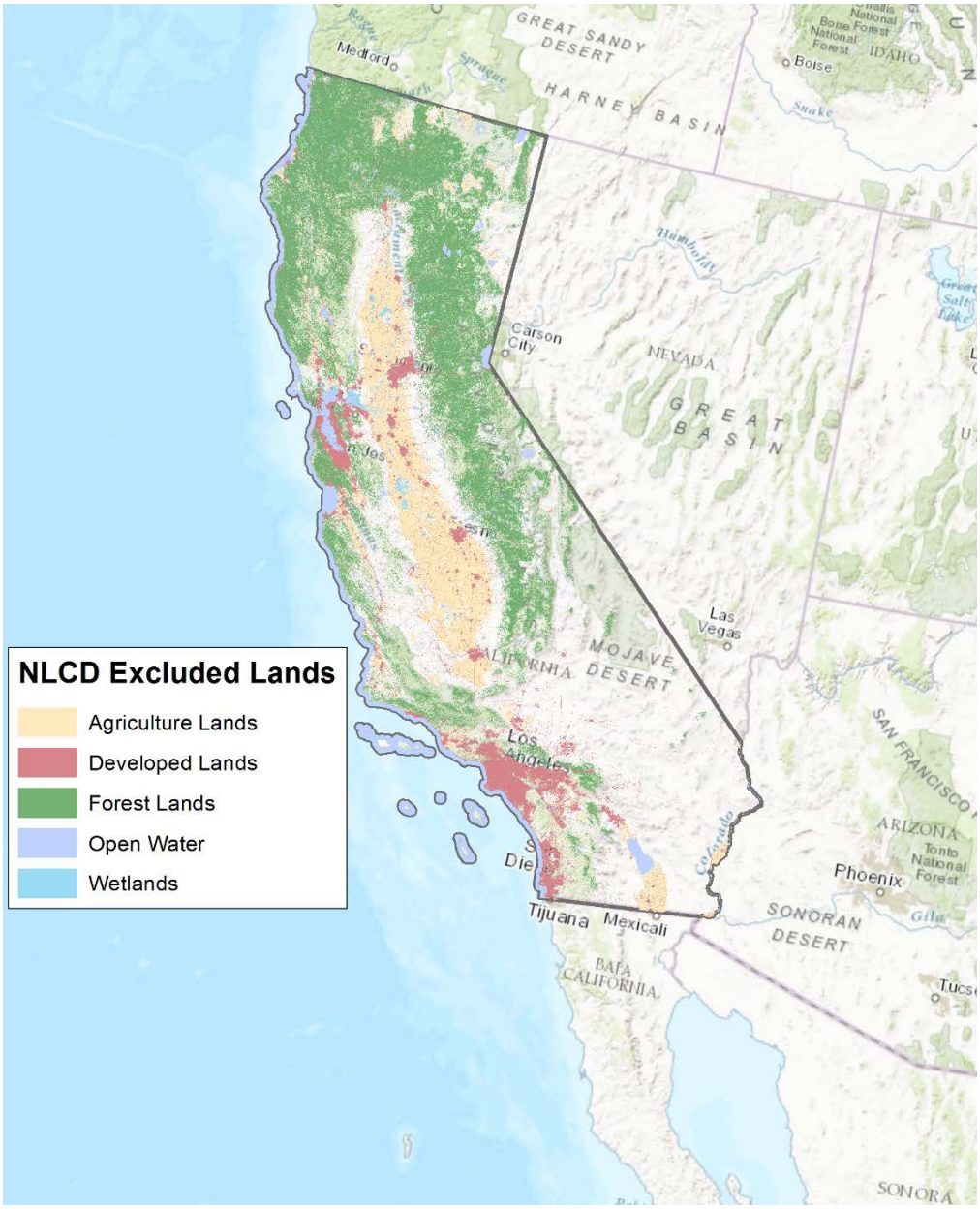

Source: National Land Cover Database

- **Land with Slope > 3% Grade**: This refers to land surfaces that exhibit higher than a 3.5% grade. This exclusion was included due to the need for relatively flat ground to maintain

alignment for large solar collectors, especially with trough systems. This assumption was also used by the National Renewable Energy Laboratory assessment of technical renewable potential [43]. These land areas were calculated from raster elevation data from the USGS National Elevation Dataset (NED) [1], using datasets that cover California. These elevation datasets were processed in ArcGIS to obtain spatially resolved slope information.

Some additional exclusions were applied to the remaining land areas produced after applying the aforementioned exclusions. These additional exclusions are:

- **Contiguous Areas < 1 sq. km**: This refers to remaining land area polygons that have an area of less than 1 square kilometer. These areas were excluded as they were deemed too small to accommodate solar thermal power plants, which require relatively large land areas for the placement of collectors to reach a reasonable capacity. This assumption was also used by the National Renewable Energy Laboratory assessment of technical renewable potential [43].

- **Daily Direct Normal Insolation (DDNI) < 7.0 kWh/m^2/day**: This refers to areas with a daily direct normal insolation value of below 7.0 kilowatt-hours per square meter per day (kWh/m^2/day). This exclusion was included based on the characteristics of currently operating solar thermal power plants in California, all of which are sited in areas with a DDNI greater than 7.0 kWh/m^2/day, according to data from NREL Concentrating Solar Power Projects database [44]. These areas were determined by overlaying 10 km resolution direct normal insolation data from NREL [45] on the remaining land area and excluding the intersecting areas that have a DDNI below 7.0 kWh/m^2/day.

Once these exclusions are applied, the remaining land area is deemed suitable for deploying solar thermal power plants.

A.2.1.2. Water-Unconstrained Installable Solar Thermal Capacity Potential Calculation

With spatially resolved data for the land areas suitable for solar thermal power plant deployment and the daily direct normal insolation, the potential installable capacity unconstrained by water availability can be calculated. For each of the remaining land areas, the calculation of installable capacity is as follows:

First, the annual energy obtained from a solar thermal power plant installed on each land area is calculated:

$$E_{gen,i} = DDNI_i \cdot \frac{365\ d}{1\ yr} \cdot A_{factor} \cdot \eta_{STE} \cdot A_i$$

Where:

- $E_{gen,i}$ = The annual energy obtained from a solar thermal power plant deployed on land area i
- $DDNI_i$ = The Daily Direct Normal Insolation on land area i
- A_{factor} = The aperture-to-total-land-area ratio of a solar thermal power plant.

    - This factor is used to account for the fact that solar collectors will not take up all the available land area due to needs for collector spacing and land area used for other components of the power plant – i.e., steam turbine, etc. Therefore, only a fraction of the land area collects insolation and counts toward the power plant output.
- η_{STE} = The solar-to-electrical efficiency of the power plant.
    - This combines the collector efficiency along with the power block efficiency.
- A_i = The area value of land area i

From the annual energy output, the power capacity can be calculated:

$$P_{cap,i} = \frac{E_{gen,i}/\Delta t}{CF}$$

Where:

- $P_{cap,i}$ = The unconstrained installable solar thermal capacity on land area i
- $E_{gen,i}$ = The annual energy obtained from a solar thermal power plant deployed on land area i
- Δt = The period over which $E_{gen,i}$ is produced
- CF = The capacity factor of the power plant

The power capacities are then summed for land areas in each California hydrologic region.

For this analysis, the following values are assumed for the parameters of this calculation (Table A-4).

Table A-4: Parameter Value Assumptions for Solar Thermal Installable Capacity Calculation

Parameter	Value	Justification	Reference (if applicable)
A_{factor}	0.2	This value was extracted from information regarding the total land area and aperture area of solar thermal power plants installed in California as catalogued by NREL.	[44]
η_{STE}	0.15 (15%)	This value was extracted from information regarding the design energy production and total solar energy collected for solar thermal power plants in California as catalogued by NREL.	[44]
CF	0.28 (28%)	This value was extracted from the capacity factors of solar thermal power plant production calculated in the HiGRID model, without storage.	[46]

Source: Advanced Power and Energy Program, University of California Irvine

An additional assumption in this analysis is that solar thermal collector type is assumed not to significantly affect the aforementioned parameters.

Performing this calculation for each hydrologic region and with the described assumptions yields the following installable capacities for solar thermal power plants in each hydrologic region of California, as presented in Table A-5. Certain regions have zero installable capacity primarily due to the insolation limits that are used for land exclusions in this analysis, in addition to unsuitable terrain in terms of slope preventing installation of large solar collectors.

Table A-5: Water Unconstrained Installable Solar Thermal Capacity by Hydrologic Region

Hydrologic Region	Water-Unconstrained Installable Solar Thermal Capacity [MW]
North Coast	0
San Francisco Bay	0
Central Coast	162.2
South Coast	339.9
Sacramento River	0
San Joaquin	0
Tulare Lake	841.9
North Lahontan	682.7
South Lahontan	123,995.5
Colorado River	73,626.4
Sum	**199,648.6**

Source: Advanced Power and Energy Program, University of California Irvine

A.2.1.3. Water-Unconstrained Installable Geothermal Capacity Potential Calculation

The water-unconstrained installable geothermal capacity potential was determined using data from studies conducted by USGS. This potential capacity has two components: identified hydrothermal resources and unidentified hydrothermal resources. *Identified hydrothermal resources* refer to geothermal reservoirs that have been explored and determined suitable for use in geothermal power production. *Unidentified hydrothermal resources* refer to areas that are likely suitable for use in geothermal power production based on several geographic factors, but these sites have not been explored for suitability.

For identified hydrothermal resources, the spatially resolved dataset was downloaded from the NREL Geothermal Prospector [47] and corresponds to a study from the USGS to assess geothermal capacity potential in 2008 [48]. This dataset was constructed for the entire United States, but the data were filtered to include only sites in California for this analysis and grouped by California hydrologic region. Included in the data set are the site name, location (latitude and longitude), and the potential geothermal capacity in MW with 95% probability, mean probability (50%), and 5% probability. For this analysis, the mean probability datasets were selected to be conservative. The included sites, associated locations, and capacities are presented in Table A-6.

Table A-6: Identified Hydrothermal Resource Capacities From USGS

Name	Identified Hydrothermal Potential (MW)– Mean Probability
Fort Bidwell	9.1
Lake City Hot Springs	100.7
Leonards Hot Sps./Seyferth HS	10
Medicine Lake (Glass Mt.)	365.6
Surprise Valley HS	7.8
Kelly HS	9.5
Canby (I'SOT)	9.4
Little Hot Spring (Fall River)	3.9
West Valley Reservoir	12.6
Kellog HS	5.4
Big Bend HS	4.9
Wendel	11.4
Amedee	7.8
Indian Valley Hot Springs	3.5
Marble Hot Well	3.5
Sierra Valley	3.5
Brockway Hot Springs	2
Wilbur Springs	29.3
Clear Lake (Sulphur Bank mine)	29.2
Geysers	519.7
Geysers Hi T Reservoir	517.9
Carson River	15.7
Grovers HS	2.9
Calistoga HS	16.9
Fales HS	2.9
Boyes HS	8.4

Sonoma Mission Inn	6.3
Travertine HS	2.8
North Shore Mono Lake (Black Rock Point HS)	2.3
Long Valley caldera - deep	47.5
Long Valley shallow	15
Tassajara HS	3
Coso area	419.2
Tecopa HS	9
Paso Robles	3.4
Randsburg area	6.6
Sespe HS	10.7
Arrowhead HS	7.1
Imperial Spa	3
Salton Sea area	2209.9
North Brawley	138
East Brawley	358.5
South Brawley (Mesquite)	42.3
Dunes	18.5
East Mesa (Deep)	60.3
East Mesa (Shallow)	142.4
Heber Deep	34.5
Heber Shallow	125.1
Mt. Signal	14.7
Total Identified Hydrothermal	**5393.6**

Source: Advanced Power and Energy Program, University of California Irvine

For unidentified hydrothermal resources, the geothermal favorability approach applied in the USGS 2008 resource assessment [49, 50] was adapted to the hydrologic regions that are the focus of this report. In the 2008 assessment, USGS assessed undiscovered geothermal resources in 13 western states (Alaska, Arizona, California, Colorado, Hawaii, Idaho, Montana, Nevada,

New Mexico, Oregon, Utah, Washington, and Wyoming), based on a series of Geographic Information Systems (GIS) statistical models for the spatial correlation of geological factors that promote the formation of geothermal systems. The mean estimated power production potential from undiscovered geothermal resources for those 13 western states is 30,033 MW, with a 95% probability of 7,917 MWe and a 5% probability of 73,286 MWe. These undiscovered resource results were also reported on a state-by-state basis, but no assessment was performed at a finer level of resolution.

For this report, the statewide undiscovered resource results for California (11,340 MW) were reanalyzed for each hydrologic region through a geospatial model for the favorability of occurrence for geothermal systems. The approach uses information on relationships between characteristics of the identified geothermal resources compared to the undiscovered, geologic constraints on the formation of geothermal systems, observations of the spatial coverage of geothermal exploration to date, and evaluations of the effectiveness of those exploration efforts [49, 50]. Results from the new modeling effort are reported by hydrologic region in Table A-9. Regions of significant geothermal potential (>400 MW) include the North Coast, San Francisco Bay and Central Coast, Sacramento River, North Lahontan, South Lahontan, and Colorado River. As indicated by the distribution of identified geothermal systems in Table A-8, geothermal resources in California are concentrated east of the Sierra Nevada crest in the Basin and Range physiographic province, on the Modoc Plateau in the north, within the Coast Ranges, and in the Imperial Valley in the south.

Combining the resource potential from identified and unidentified geothermal resources, the total potential capacity of geothermal resources considered in this study by hydrologic region is presented in Table A-7.

Table A-7: Total Geothermal Potential Capacity by Hydrologic Region

Hydrologic Region	Identified Potential Capacity	Unidentified Potential Capacity	100% Potential Capacity Total
	MW	MW	**MW**
North Coast	1037.6	344	**1381.6**
San Francisco Bay	31.6	134	**165.6**
Central Coast	6.4	273	**279.4**
South Coast	17.8	110	**127.8**
Sacramento River	480.3	622	**1102.3**
San Joaquin	0	19	**19**
Tulare Lake	0	30	**30**
North Lahontan	173.1	253	**426.1**
South Lahontan	499.6	504	**1003.6**
Colorado River	3147.2	9051	**12198.2**
Sum	**5393.6**	**11340**	**16733.6**

Source: Advanced Power and Energy Program, University of California Irvine

To obtain the annual energy obtained for geothermal power plants, a capacity factor of 85% is assumed for these systems. This is based in the notion that geothermal power plants operate in a baseload manner since they are based in slow-ramping steam-turbine power blocks:

$$E_{gen,geo,i} = P_{cap,geo,i} \cdot CF \cdot \Delta t$$

A.2.1.4. Solar Thermal and Geothermal Resource Mapping

The locations of solar thermal and geothermal resources based on the analyses in this section are presented in Figure A-8.

Figure A-8: Eligible Solar Thermal Lands and Identified Geothermal Sites in California

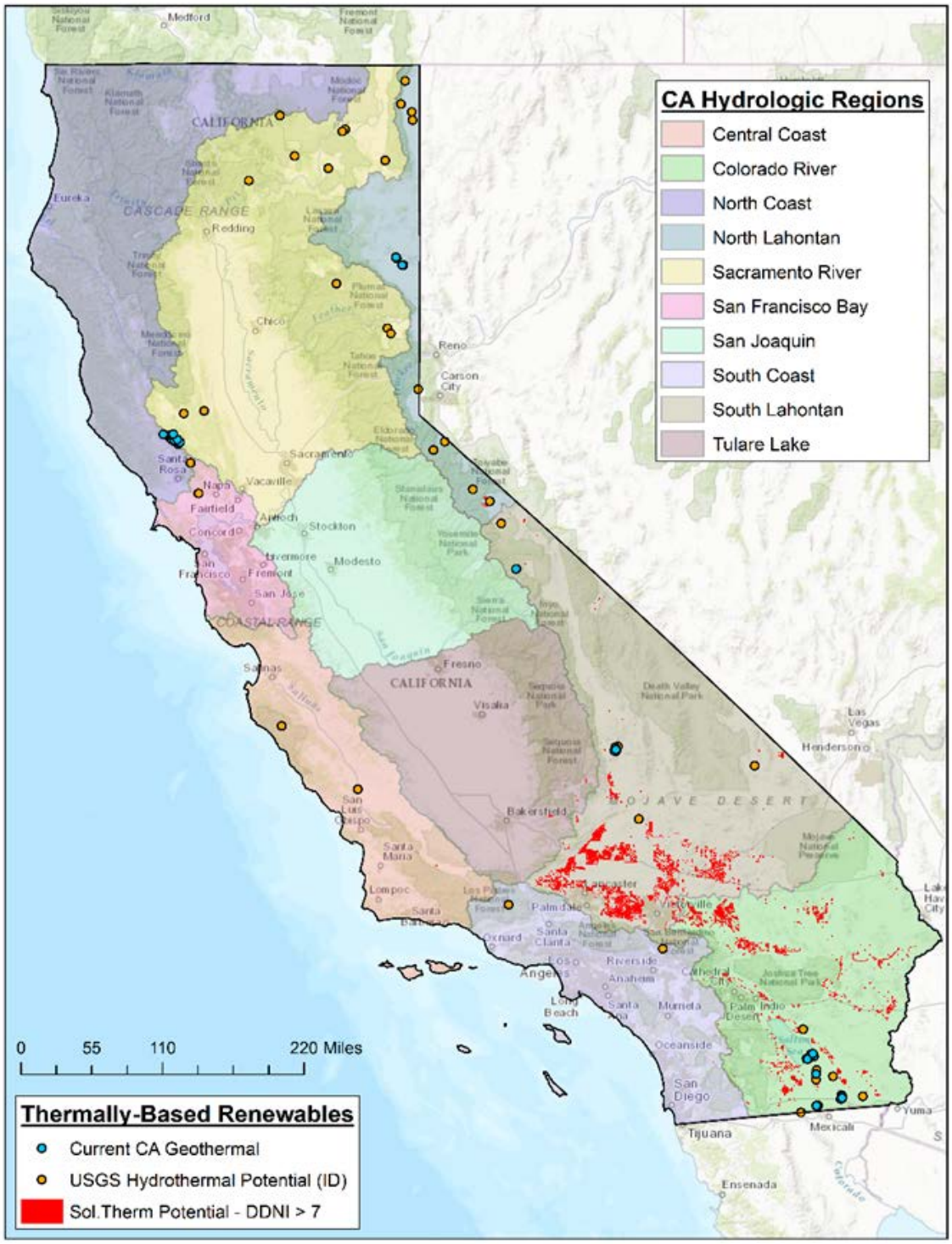

Source: Advanced Power and Energy Program, University of California Irvine

A.2.2. Calculating Net Available Water Supply for Each Hydrologic Region

This step involves performing a water balance on each hydrologic region:

$$\frac{\partial S}{\partial t} = Q_{\text{in}} - Q_{\text{out}}$$

$$Q_{in} = P + F_{in}$$

$$Q_{out} = D + F_{out} + ET$$

Where:

- $\frac{\partial S}{\partial t}$ = change in water storage (surface and subsurface) in the region over time
- Q_{in} = water entering the region including precipitation (P) and streamflow
- Q_{out} = Outflows, evapotranspiration and consumption demand in the region
- P = precipitation over the given region
- F_{in} = Inflow into the region from other regions
- D = consumptive water demand in each region
- F_{out} = water outflows from the region
- ET = evapotranspiration

For this analysis, the team imposes the constraint that there will be no net change in mean water storage for each hydrologic region since this analysis is performed on a representative basis. Any water is characterized that would have contributed to a positive change in storage as available for supporting the water needs of thermally based renewables. This quantity is then termed the *net available storage* (NAS):

$$NAS = mean(\Delta S | \Delta S(t) > 0))$$

Where t is the time step (year) in the baseline and projection period. NAS is the available amount of water in each hydrologic region that is available for supporting the water needs of solar thermal and geothermal resources. Precipitation data are the same as those used in the Chapter 2 analysis, described in Appendix A.1.

The climate change-affected scenario is represented by the years 2046-2055 and compared to a historical baseline of 2001-2010. The baseline water balance data were obtained from the California Water Plan Update 2013 Volume 2 [51], which provided a breakdown of water entering and leaving each hydrologic region. A summary of the data for each hydrologic region is presented in Tables A-8 and A-9.

Table A-8: Water Entering Each Hydrologic Region, 2001-2010, in Thousand Acre-Feet

Year/Region	2001	2002	2003	2004	2005	2006	2007	2008	2009	2010
North Coast	32244	51517	54306	48436	65207	74963	44286	45449	41838	56227
San Francisco Bay	5780	7011	6696	7235	9222	10054	4793	5805	6016	7893
Central Coast	12028	8922	8990	12506	13879	14084	5594	10603	8300	14302

South Coast	11833	8133	12237	14944	17790	11424	6570	12003	9474	13995
Sacramento River	36595	51555	56431	51400	73914	85242	37762	39352	45649	54774
San Joaquin	20692	24596	25929	25911	35642	36029	18768	19179	22025	29929
Tulare Lake	15260	14260	17311	16780	22848	23079	11465	13521	12649	20641
North Lahontan	3759	5755	6563	6135	8995	9717	4247	5046	5854	6350
South Lahontan	10807	4965	12281	16299	18887	12838	7324	9402	8811	13208
Colorado River	10122	7019	10173	13550	14101	8136	7054	10581	8838	11836

Source: California Water Plan Update 2013

Table A-9: Water Leaving Each Hydrologic Region, 2001-2010, in Thousand Acre-Feet

Year/Region	2001	2002	2003	2004	2005	2006	2007	2008	2009	2010
North Coast	32882	51755	54133	48852	65222	75207	44983	46087	42319	55785
San Francisco Bay	5989	6962	6584	7119	9043	9693	5049	5872	6070	7777
Central Coast	12921	10045	9688	13530	14133	14596	6917	11458	9326	14798
South Coast	12901	9356	13353	15980	17990	12459	7890	13264	10816	14750
Sacramento River	40155	52174	55628	45302	72157	86469	42659	43452	46953	54155
San Joaquin	23387	26424	26921	28887	34119	37804	24334	23190	23810	30667
Tulare Lake	19516	18348	20113	20981	22274	23350	16026	18849	18011	22721
North Lahontan	4296	5998	6589	6386	8767	9379	4694	5393	6025	6142
South Lahontan	11107	5290	12514	16604	19022	13043	7709	9736	9069	13474
Colorado River	10301	6940	10407	13418	13904	8304	7093	10690	8985	11814

Source: California Water Plan Update 2013

The climate change-affected scenario is represented by the years of 2046-2055 and compared to a historical baseline of 2001-2010. For each climate model and hydrologic region, precipitation and evapotranspiration data were extracted. The difference between these model

values was applied to perturb the actual historical data of these parameters to obtain future precipitation and evapotranspiration data to be used in the water balance:

$$\Delta P_{cc}(t) = P_{m,2046-2055}(t) - P_{m,2001-2010}(t)$$

$$\Delta ET_{cc}(t) = ET_{m,2046-2055}(t) - ET_{m,2001-2010}(t)$$

$$P_{cc}(t) = P_{a,2001-2010}(t) + \Delta P_{cc}(t)$$

$$ET_{cc}(t) = ET_{a,2001-2010}(t) + \Delta ET_{cc}(t)$$

Where:

- $\Delta P_{cc}(t)$ = The difference in precipitation between the future periods and historical periods
- $P_{m,2046-2055}(t)$ = Modeled precipitation in 2046-2055 for each model
- $P_{m,2001-2010}(t)$ = Modeled precipitation in 2001-2010
- $P_{a,2001-2010}(t)$ = Actual data precipitation in 2001-2010
- $\Delta ET_{cc}(t)$ = The modeled difference in evapotranspiration between the future periods and historical periods
- $ET_{m,2046-2055}(t)$ = Modeled evapotranspiration in 2046-2055 for each model
- $ET_{m,2001-2010}(t)$ = Modeled evapotranspiration in 2001-2010
- $ET_{a,2001-2010}(t)$ = Actual data precipitation in 2001-2010
- $P_{cc}(t)$ = Projected precipitation in each hydrologic region used as input for the water balance model
- $ET_{cc}(t)$ = Projected evapotranspiration in each hydrologic region used as input for the water balance model

The water balance will also be affected by changes in water demand in each hydrologic region between 2006 and 2050. These changes will depend on projected changes in population growth and density in each region and will affect the urban water demand and agricultural water demand in each region. The research team used projections for changes in urban and agricultural water demand based on scenarios for population growth and density from the California Water Plan Update 2013 [51]. This dataset includes demand change scenarios that vary with a range of climate scenarios; however, the team used projections for water demand growth that assume a continuation of the historical climate. This is to ensure that the impacts of climate change are not double-counted, since they are captured explicitly and separately from the demand. The data used for changes in urban and agricultural water demand for each region used in this analysis are presented in Tables A-10 and A-11, respectively. The supply of treated wastewater was not included in the analysis.

Table A-10: Urban Water Demand Change by Hydrologic Region From 2006-2050 in Thousand Acre-Feet per Year

Population Trend/ Region	**Low Pop.**			**Current Trends Pop.**			**High Pop.**		
Population Density Trend	Low Density	Current Trends Density	High Density	Low Density	Current Trends Density	High Density	Low Density	Current Trends Density	High Density
North Coast	1	0.9	0.6	16.2	16.1	15.7	69.7	69.2	67.8
San Francisco Bay	-27.2	-28.7	-33.1	233.1	228.8	218.4	695.3	676	641.7
Central Coast	30	29	28	70	69	67	198	198	190
South Coast	-56	-76	-112	564	535	483	1932	1845	1698
Sacramento River	343	339	327	538	532	512	883	871	832
San Joaquin River	393	391	378	490	488	473	797	793	768
Tulare Lake	317	307	282	522	508	469	737	715	659
North Lahontan	13	13	13	18.2	18.2	18.1	28.1	28	27.9
South Lahontan	140	136	129	201	196	186	401	386	360
Colorado River	36	34	31	176	174	169	324	321	312

Source: California Water Plan Update 2013

Table A-11: Agricultural Water Demand Change by Hydrologic Region From 2006-2050 in Thousand Acre-Feet per Year

Population Trend/ Region	**Low Pop.**			**Current Trends Pop.**			**High Pop.**		
Population Density Trend	Low Density	Current Trends Density	High Density	Low Density	Current Trends Density	High Density	Low Density	Current Trends Density	High Density
North Coast	-103.7	-102.8	-101.9	-110.1	-108.7	-107.9	-133.6	-129	-124.3
San Francisco Bay	-6.3	-5.4	-4.6	-14.2	-12.4	-11.8	-28	-25.6	-22.9
Central Coast	-160	-157	-155	-201	-198	-195	-264	-254	-244
South Coast	-254	-245	-236	-323	-310	-296	-431	-406	-381
Sacramento River	-248	-230	-213	-349	-320	-295	-531	-473	-419
San Joaquin River	-878	-837	-794	-1019	-971	-922	-1247	-1154	-1067
Tulare Lake	-1043	-1005	-965	-1247	-1183	-1121	-1397	-1302	-1213
North Lahontan	-22	-22	-21.6	-21.8	-21.5	-21.5	-25.1	-24.1	-23.5
South Lahontan	-37.8	-38.1	-38.4	-40.7	-39.4	-39.1	-57.3	-54	-53.7
Colorado River	-1687	-1682	-1678	-1719	-1711	-1704	-1766	-1750	-1737

Source: California Water Plan Update 2013

These demand changes are applied to alter the Water Leaving the Region term in the water balance to capture the impacts of water demand on net available supply for supporting thermally based renewables. In addition, a scenario with no demand change is also analyzed for comparison.

A.2.3. Calculating the Water-Constrained Installable Solar Thermal and Geothermal Capacity

With the net available water supply calculated for each hydrologic region under climate change, the water-constrained installable solar thermal and geothermal capacity can be calculated. To accomplish this, the research team obtained data for the water consumption intensity of solar thermal and geothermal power plants equipped with different cooling systems from the National Renewable Energy Laboratory (NREL) via a survey of actual water consumption of these types of systems [52]. The dataset presented includes minimum, median, and maximum values for each type of power plant and cooling system. For this analysis, the team used the median values for each type that are presented in Table A-12.

Table A-12: Water Consumption Factors for Solar Thermal and Geothermal Resources by Cooling Type

Power Plant Type	Cooling System	Median Water Consumption Factor [gal/MWh]
Solar Thermal - Trough	Wet (Tower)	865
	Hybrid	338
	Dry	78
Geothermal - Dry Steam	Wet (Tower)	1796
Geothermal - Flash	Wet (Tower)	2583
	Dry	5
Geothermal - Binary	Wet (Tower)	3600
	Dry	135

Source: National Renewable Energy Laboratory

For solar thermal resources, the water consumption is represented by that for solar thermal trough systems. Solar power towers have slightly less water consumption (786 gal/MWh), and solar Fresnel systems have slightly higher water consumption (1,000 gal/MWh); however, the trough systems have the largest amount of data available and fall near the middle of the range bounded by the different collector types. Power plant cooling is not the only use of water in solar thermal and geothermal power plants. Cooling is often the dominant water use, but the switch to dry cooling systems does not completely eliminate water use in these power plants. Water is also needed for working fluid make-up in the steam turbine power blocks, miscellaneous facilities for the workers, and cleaning of solar collectors, when necessary.

These factors are applied with the calculated Net Available Supply to determine the water-constrained annual energy obtained for each resource in each hydrologic region:

$$E_{gen,wc,i} = NAS_i \cdot \frac{1000\ AF}{1\ TAF} \cdot \frac{325851\ gal}{1\ AF} \cdot C_{factor} \quad , \quad (E_{gen,wc,i} > 0)$$

Where:

- $E_{gen,wc,i}$ = The annual energy obtained from solar thermal or geothermal resources in hydrologic region i
- NAS_i = The calculated net available supply in hydrologic region i
- C_{factor} = The water consumption factor corresponding to the type of power plant and cooling type combination being analyzed

The water-constrained installable capacity for a given power plant type and cooling type combination is then calculated from the annual obtained energy, similar to the method in Section A.2.1.2. These capacities are compared with the unconstrained capacities to determine

the impact of climate change-impacted water availability on the installable solar thermal and geothermal resources.

Energy production is available only if the net available water supply is positive. Since net available supply cannot be negative, regions that have a negative water balance cannot support the water needs of solar thermal and geothermal development, and the installable capacity corresponding to that configuration is determined to be zero. While it is possible for water to be imported from other regions explicitly to support a solar thermal and geothermal power plant, this possibility is excluded for two reasons. First, solar thermal and geothermal power plants are not often sited near water conveyance and distribution pathways and typically use groundwater to meet the needs of these plants [53-55]. Second, importing water by truck or measures other than tapping into existing conveyance or distribution infrastructures adds costs to the power plant and requires large on-site water storage.

A.3. Chapter 4 Analysis Methods

To carry out the analysis presented in Chapter 4, the following general approach is taken. Representative building prototypes for residential and commercial buildings are obtained from the U.S. Department of Energy Building Energy Codes Program, developed by Pacific Northwest National Laboratory (PNNL) and the National Renewable Energy Laboratory (NREL) for the EnergyPlus simulation platform. Downscaled climate data are obtained for each of the California building climate zones and converted to EnergyPlus weather perturbations. The building prototypes were then simulated under both historical conditions and climate change-impacted conditions in each climate zone using the EnergyPlus building simulation platform to obtain the response of their electric load profiles and energy demands to climate change. The details of these steps are presented in this section. The overall methods are visualized in A-9.

Figure A-9: Overall Methods Overview for Chapter 4

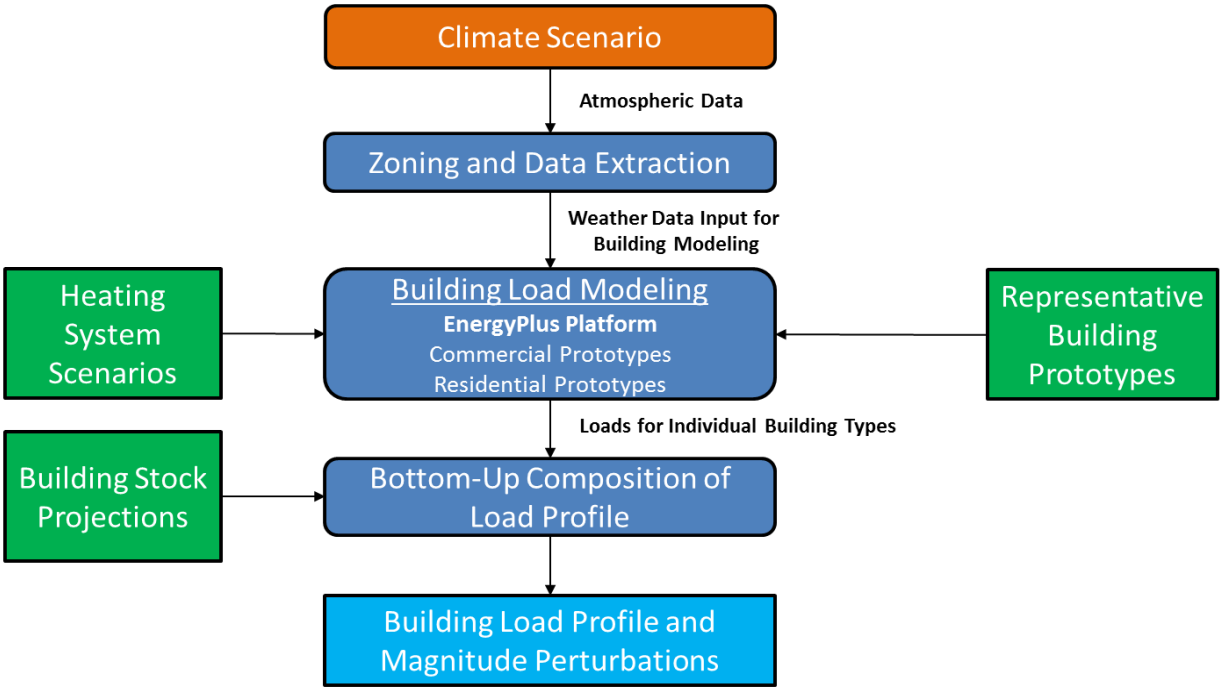

Source: Advanced Power and Energy Program, University of California Irvine

A.3.1. Representative Building Prototypes – Residential

For residential buildings, representative prototypes have been developed by PNNL for use in the U.S. Department of Energy Building Energy Codes Program and obtained from the program database [56]. These building prototypes were developed for use in the EnergyPlus building simulation platform and are used to assess the effectiveness of revisions to building codes for new construction of residential buildings in terms of reducing energy usage and energy costs. The building prototype set includes EnergyPlus models to represent single-family and multifamily homes, with different configurations for building foundation type and building heating system type. The different configurations represented by the set of EnergyPlus models are presented in Table A-13.

Table A-13: Residential Building Prototype Configuration Options

Categories	Configuration Options
Dwelling Type	Single-Family Multifamily
Building Foundation Type	Slab Unheated Basement Heated Basement Crawlspace

Building Heating System Type (Used for both space heating and water heating)	Electric Resistance Gas Furnace Heating Oil Furnace Electric Heat Pump

Source: U.S. Department of Energy

The characteristics of the single-family prototypes are described in detail by PNNL for the Building Energy Codes Program Methodology [57] and are summarized in Table A-14 as follows.

Table A-14: Residential Building Prototype Characteristics

Characteristics	Single-Family	Multifamily
Conditioned Floor Area (Sq. ft)	2,376	21,600 (1,200 per dwelling, 18 dwellings per building)
Area above unconditioned space (Sq. ft)	1,188	1,200 on ground-floor units
Area below roof/ceilings (Sq. ft)	1,188	1,200 on top-floor units
Perimeter (ft)	152	370
Gross Exterior Wall Area (Sq. ft)	2,584	5100
Window Area (Sq. ft)	15% of conditioned floor area	23% of gross exterior wall area
Door Area (Sq. ft)	42	378 (21 per dwelling)
Internal Energy Gains (Btu/day)	86,761	984,024 (54,668 per dwelling)
Footprint and Height	54 ft x 22 ft	120 ft x 65 ft
Stories (#)	2	3 (whole building)
Cooling System	Central electric air conditioning	Central electric air conditioning

Source: U.S. Department of Energy

The residential building prototype set includes 32 EnergyPlus building models. Each building prototype is used for the analysis, and the prototypes are aggregated in each zone by distribution in the total building stock, as described in Section A.3.4.

The Building Energy Codes Program archives residential building prototypes for different revisions of the International Energy Conservation Code (IECC). The oldest available vintage for EnergyPlus models is the 2006 IECC version. For this analysis, the prototypes that were developed for the 2012 IECC codes are used as representative of the average building in 2050 and such that it is as consistent as possible with the vintage years for the commercial building prototypes used in this study.

This represents the major assumption of this study: the average representative building in 2050 is assumed to be represented by a building that complies with the 2012 IECC codes. In the actual building stock, there are a wide variety of buildings distributed across different vintages, and the turnover of the building stock is relatively slow. Buildings that were constructed up to 100 years ago are still in operation, as well as buildings that were recently constructed. Many older buildings have had retrofits that reduce energy use as well. Given this variability, if one wanted to represent the energy consumption of an average operating building of a particular type, such a building would have energy consumption profiles that are larger than those of recently constructed buildings are and smaller than those of older legacy buildings. In general, however, obtaining exact data for the building stock and vintage distribution in the Title 24 Building Climate Zones used for this study is very difficult, and further EnergyPlus model prototypes for each of those vintages are not available. The development of new building prototype models is beyond the scope of this study.

Determining the exact distribution by vintage for residential buildings is a subject for future work. This analysis represents an average 2050 building of each particular type with the corresponding prototype building that complies with the 2012 IECC building codes.

A.3.2. Representative Building Prototypes – Commercial

For commercial buildings, representative prototypes have also been obtained from those developed for the U.S. Department of Energy Building Energy Codes Program [58]. These commercial building prototypes are used to assess the effectiveness of building code revisions on energy usage and energy cost, similar to the analyses for residential buildings. The commercial building dataset contains representative building prototypes developed for use in the EnergyPlus building simulation platform. In contrast to the models for residential buildings, the commercial building prototypes are not configurable with different characteristic options. The types of commercial buildings characterized in this dataset and related characteristics are described by PNNL [59] and are partially repeated for reference in Table A-15.

Table A-15: Commercial Building Prototype Characteristics

Building Type	Floor Area (sq. ft)	# of floors
Small Office	5,500	1
Medium Office	53,630	3
Large Office	498,640	12
Standalone Retail	24,690	1
Strip Mall	22,500	1
Primary School	73,970	1
Secondary School	210,910	2
Outpatient Healthcare	40,950	3
Hospital	241,410	5
Small Hotel	43,210	4
Large Hotel	122,120	6
Warehouse	52,050	1
Quick-Service Restaurant	2,500	1
Full-Service Restaurant	5,500	1
Mid-Rise Apartment	33,740	4
High-Rise Apartment	84,360	10

Source: U.S. Department of Energy

The Building Energy Codes Program archives commercial building prototypes for different revisions of two sets of building codes: the IECC building codes and the ASHRAE 90.1 building standards. For this analysis, the prototypes that were developed for the 2013 ASHRAE 90.1 building standards are used, due to the alignment of California nonresidential standards with this standard set [60] and because the 2013 ASHRAE standards are the latest vintage for which these prototypes have been developed. Therefore, for commercial buildings, the average representative building of the stock in 2050 is assumed to be one that complies with these codes. The selection of this code year also makes it consistent with that used for residential buildings.

A.3.3. Calculation of Climate-Impacted Weather Conditions for EnergyPlus Simulations

The previously described building prototypes are simulated in the EnergyPlus building simulation platform, which captures the effect of weather on building energy usage through a weather input file. The EnergyPlus weather input file is hourly resolved over one year and uses

weather parameters that are relevant to the heat transfer and thermodynamics of the building shell with the surrounding environment. Overall, EnergyPlus can use up to 29 weather parameters, but only 11 of these parameters are required for EnergyPlus to perform building energy calculations [61]. These parameters are listed in Table A-16.

Table A-16: Used EnergyPlus Weather Parameters

EnergyPlus Weather Parameters	Units
Dry Bulb Temperature	Celsius
Dew Point Temperature	Celsius
Relative Humidity	%
Atmospheric Pressure	Pascal
Horizontal Infrared Radiation Intensity	Wh/m^2
Direct Normal Radiation	Wh/m^2
Diffuse Horizontal Radiation	Wh/m^2
Wind Direction	Deg
Wind Speed	m/s
Snow Depth	Cm
Liquid Precipitation Depth	Mm

Source: U.S. Department of Energy

To represent climate change-impacted weather conditions in EnergyPlus, the research team obtained spatially resolved downscaled climate data from the Localized Constructed Analogs (LOCA) climate model simulations [62] and VIC hydrological models [63] similar to that used in the Chapter 2 and Chapter 3 analyses. The data for each relevant parameter were averaged by California Title 24 Building Climate Zones as presented by the California Energy Commission [64].

Figure A-10: California Title 24 Building Climate Zones

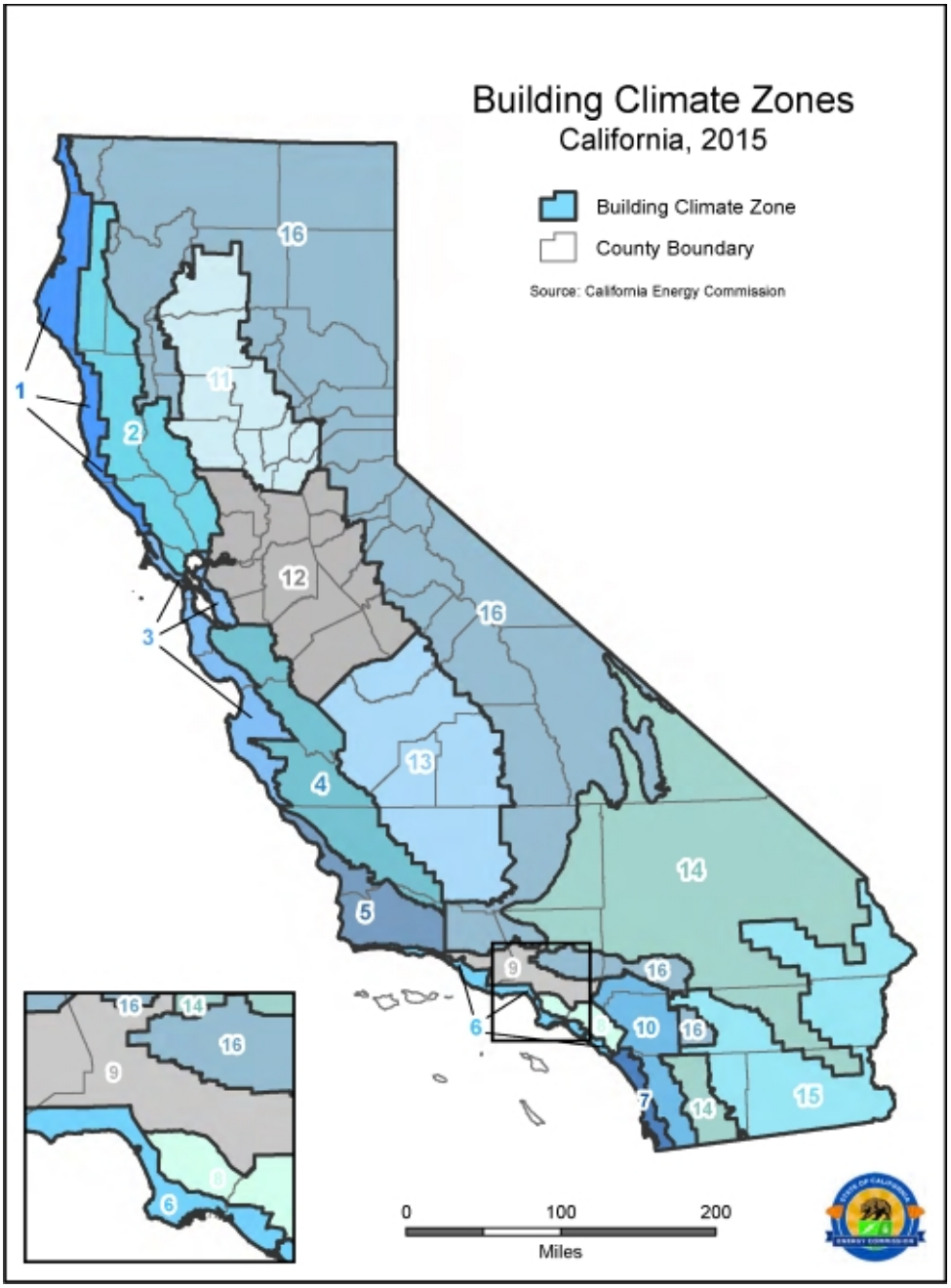

Source: California Energy Commission

The research team obtained historical representative weather data for each of the Title 24 Building Climate Zones in EnergyPlus format from the California Energy Commission and downloaded them from the EnergyPlus Weather Database [65]. The outputs of the climate models are not necessarily the same parameters as those used in the EnergyPlus weather files. For this analysis, climate perturbations are captured by five key parameters that align between EnergyPlus and the downscaled LOCA climate models in Table A-17.

Table A-17: Correspondence Between EnergyPlus and Climate Model Parameters, Daily Temporal Resolution

EnergyPlus Weather Parameter	Climate Model Output Data Type	Units
Dry Bulb Temperature	Air Temperature	Celsius
Relative Humidity	Relative Humidity	%
Dew Point Temperature	N/A (Calculated from air temperature and relative humidity)	Celsius
Wind Speed	Wind speed	m/s
Liquid Precipitation Depth	Precipitation	Mm

Source: Advanced Power and Energy Program, University of California Irvine

All other weather parameters in EnergyPlus are treated as unchanged from the representative historical values in this analysis. While climate change may technically impact other weather parameters such as atmospheric pressure and radiation inputs, the parameters listed in Table A-19 represent the major parameters that are key drivers for building electric loads. The climate change-affected scenario is represented by 2046-2055 and compared to a historical baseline of 2001-2010. For each Title 24 Building Climate zone, the difference between these model values is then applied to perturb the actual historical data each of these parameters to obtain climate change-affected weather parameters to compose a representative climate-impacted weather files for use in EnergyPlus:

$$\Delta T_{cc} = T_{mavg,2046-2055} - T_{mavg,2001-2010}$$

$$T_{cc} = T_{aavg,2001-2010} + \Delta T_{cc}$$

$$\Delta RH_{cc} = RH_{mavg,2046-2055} - RH_{mavg,2001-2010}$$

$$RH_{cc} = RH_{aavg,2001-2010} + \Delta RH_{cc}$$

$$\Delta Td_{cc} = Td_{mavg,2046-2055} - Td_{mavg,2001-2010}$$

$$Td_{cc} = Td_{aavg,2001-2010} + \Delta Td_{cc}$$

$$\Delta v_{cc} = v_{mavg,2046-2055} - v_{mavg,2001-2010}$$

$$v_{cc} = v_{aavg,2001-2010} + \Delta v_{cc}$$

$$\Delta P_{cc} = P_{mavg,2046-2055} - P_{mavg,2001-2010}$$

$$P_{cc} = P_{aavg,2001-2010} + \Delta P_{cc}$$

Where the variables represent the following parameters:

- T = Dry Bulb Temperature
- RH = Relative Humidity
- Td = Dew Point Temperature

- v = Wind Speed
- P = Precipitation Depth

The subscripts assigned to each variable represent, for each variable:

- Δx_{cc} = The modeled difference in parameter x between the future periods affected by climate change and historical periods
- $x_{mavg,2046\text{-}2055}$ = Modeled average parameter x value for the period spanning 2046-2055 affected by climate change for each model.
- $x_{mavg,2001\text{-}2010}$ = Modeled average parameter x value for the period spanning 2001-2010.
- $x_{aavg,2001\text{-}2010}$ = Actual parameter x value for the period spanning 2001-2010.

This process yields climate-impacted EnergyPlus weather files for each Title 24 building climate zone (16), climate model (4), and climate scenario (2) for 128 weather files. Each residential and commercial building prototype is then simulated in EnergyPlus using representative weather files for historical conditions and climate change-impacted conditions. This provides the hourly resolved electric load profile, annual fuel usage by type, and annual energy demand by end use for each building type in each climate zone, for each climate model and climate scenario for each prototype. These data are then used to build up the aggregate residential and commercial load and demand profiles for each region, as described in the next section.

A.3.4. Bottom-Up Composition of Residential and Commercial Building Electric Load and Energy Demands

With the electric load and energy demand profiles for each building prototype obtained, information about the stock distribution of buildings by type in California are used to compose the zonal and statewide electric load and energy demands profiles for the residential and commercial sectors. Different databases are available for residential and commercial building stocks by type.

For residential buildings, the distributions by heating system type and foundation system type are provided by PNNL for U.S. Census divisions [57] for new construction of single-family and multifamily houses in 2014. While these distributions represent the breakdown for new construction, this is consistent with the assumption used for the building codes of representing the average 2050 building fleet with the characteristics of current-day new construction. For California, the distributions are used for the Pacific census division, which encompasses California, Oregon, Washington, Alaska, and Hawaii, since distributions for California alone were unavailable. The Pacific region distribution is assumed to be representative since California accounts for most of the residences in the Pacific census region. The distribution of residential buildings by heating type is presented in Table A-18 and by foundation type in Table A-19.

Table A-18: Heating System Distribution for Residential Buildings

Heating System Type	Single-Family	Multifamily
Electric Heat Pump [%]	34	14.9
Gas Heating [%]	62.9	84.2
Oil Heating [%]	0.2	0.2
Electric Resistance Furnace [%]	2.9	0.8

Source: Pacific Northwest National Laboratory

Table A-19: Foundation Type Distribution for Residential Buildings

Foundation Type	Single-Family	Multifamily
Slab [%]	37	37
Heated Basement [%]	8.9	8.9
Unheated Basement [%]	3.1	3.1
Crawlspace [%]	51	51

Source: Pacific Northwest National Laboratory

These distributions are treated as being the same in each of the Title 24 building climate zones. While there is likely variability in heating system type and foundation type among residential buildings in the different climate zones, however, existing data for what these distributions are by climate zone and category are unavailable. In composing the aggregate residential electric load and energy demand profiles, the contribution of each climate zone to the total is weighted by the associated population. The research team determined the population in each climate zone by combining data from the California Energy Commission for the zip codes encompassed by each climate zone [66] with data for the population by zip code in California from the U.S. Census American Fact Finder [67]. This results in the following population distribution by climate zone as presented in Table A-20.

Table A-20: Population Distribution by Title 24 Building Climate Zone

Title 24 Building Climate Zone	Percentage of Total Population [%]
1	0.483
2	2.461
3	10.139
4	5.323
5	1.245

6	7.686
7	6.017
8	12.376
9	15.990
10	10.750
11	2.848
12	12.502
13	6.291
14	2.367
15	1.760
16	1.763

Source: Advanced Power and Energy Program, University of California Irvine

Data was obtained from the U.S. Energy Information Administration Residential Energy Consumption Survey (RECS) 2009 [68] for the total number of housing units in the California by single-family and multifamily. According to this source, California has 12.2 million total housing units, with 8.0 million single-family homes and 3.9 million multifamily residences. The remaining 0.4 million housing units are mobile homes and are not considered in this analysis. Maintaining the distributions by heating system type, foundation system type, and population, the single-family and multifamily building prototype load profiles are aggregated and scaled up using the number of housing units to obtain statewide profiles for electric loads and energy demands:

$$l_{CZ,SF} = \left[\sum L_{ij} \cdot w_i \cdot w_j\right]_{SF} \cdot Pop_{dist,CZ}$$

$$l_{CZ,MF} = \left[\sum L_{ij} \cdot w_i \cdot w_j\right]_{MF} \cdot Pop_{dist,CZ}$$

$$L_{SF} = \sum l_{CZ,SF} \cdot N_{SF}$$

$$L_{MF} = \sum l_{CZ,MF} \cdot N_{MF}$$

$$L_{CA,res} = L_{SF} + L_{MF}$$

Where:

- $l_{CZ,SF}$ = the electric load of a representative single-family building from climate zone CZ to the total residential electric load. This takes into account the distributions by heating type and foundation type and creates a representative building for the zone.

- $l_{CZ,SF}$ = the electric load of a representative multifamily building from climate zone CZ to the total residential electric load. This takes into account the distributions by heating type and foundation type and creates a representative building for the zone.
- L_{ij} = The electric load profile for the residential prototype building with heating system i and foundation type j
- w_i = The fraction of residential buildings with heating type i
- w_j = the fraction of residential buildings with foundation type j
- $Pop_{dist,CZ}$ = the fraction of total population in each climate zone
- N_{SF} = the number of single-family housing units
- N_{MF} = the number of multifamily housing units
- L_{SF} = The total statewide electric load profile for single-family residences
- L_{MF} = The total statewide electric load profile for multifamily residences
- $L_{CA,res}$ = Total statewide electric load profile for the residential sector

This process is also carried out to obtain the fuel usage and total site-level energy demands, under historical and climate change-affected conditions. Once these are obtained, the output for the historical condition case is scaled to actual historical data to have the correct scale for the absolute results in the analysis. The reason why this occurs is that the building prototypes used in this study are not necessarily representative of the characteristics of homes in California in terms of sizing. In particular, the square footage of the single-family and multifamily dwelling prototypes is on average larger than actual buildings in California. For example, the single-family prototype has a conditioned square footage of 2,376 square feet, whereas the average single-family home in California is 2,163 square feet for detached homes and 1,465 square feet for attached homes. Therefore, the initially calculated loads will be larger than those in historical data. This analysis scales the outputs of the historical conditions case to match 2010 residential electricity consumption and obtain a scaling factor, which is then applied to the climate change condition outputs.

For commercial buildings, data on the building stock by type were obtained from two sources: 1) the California Commercial End-Use Survey (CEUS) [69] and 2) the U.S. Energy Information Administration Commercial Buildings Energy Consumption Survey (CBECS) [70]. The CEUS database provides information for floor space of different commercial building types in the state. The categories provided in the CEUS database, however, are slightly different from the types of prototype buildings used in this study. Therefore, data from CBECS for the West census region were used to supplement the CEUS data regarding the distribution between building types that the CEUS database aggregates. A listing of the CEUS categories used in this study, the correspondence with the ASHRAE commercial building prototypes, and the ratios of the ASHRAE commercial building types in the CEUS categories are presented in Table A-21.

.

Table A-21: Distribution of Commercial Building Types for California Used in This Analysis

CEUS Category	Floor Space (kSq. Ft)	ASHRAE Building Prototype	Ratio in Category by Floor Space	Source
Health	232,606	Hospital	0.56870229	EIA CBECS West
		Out-Patient Care	0.43129771	EIA CBECS West
Large Office	660,429	Office Large	1	N/A
Lodging	270,044	Apartment High-Rise	0.25	Assumed
		Apartment Mid-Rise	0.25	Assumed
		Hotel Large	0.25	Assumed
		Hotel Small	0.25	Assumed
Refrigerated Warehouse	95,540	Warehouse	1	N/A
Restaurant	148,892	Restaurant Fast Food	0.5	EIA CBECS West
		Restaurant Sit-Down	0.5	EIA CBECS West
Retail	702,053	Retail Stand-alone	0.474769012	EIA CBECS West
		Retail Strip Mall	0.525230988	EIA CBECS West
School	445,106	School Primary	0.5	Assumed
		School Secondary	0.5	Assumed
Small Office	361,584	Office Medium	0.5	Assumed
		Office Small	0.5	Assumed
Warehouse	554,166	Warehouse	1	N/A

Source: California Commercial End-Use Survey

The share of floor space among the ASHRAE commercial building prototypes in the categories of Lodging, School, and Small Office are assumed since data for this breakdown are unavailable for California. Moreover, the CEUS database included the categories of Colleges, Grocery, and Miscellaneous, which are not captured by the set of commercial building prototypes used in this analysis. The categories captured in this analysis account for 70.5% of the total commercial

floor space in California. For this analysis, this set of commercial buildings is taken to represent the entire commercial sector.

The distribution of commercial buildings by type is assumed to be the same in each Title 24 building climate zone similar to the assumption for residential buildings, and the contribution of each climate zone to the total is weighted by population. Scaling up of the commercial building loads to represent statewide levels is done to match total commercial floor space instead of number of buildings. The process of calculating the statewide commercial electric loads and energy demands is described as follows:

$$l_{CZ,Com} = \left[\sum L_k \cdot w_k\right]_{Com} \cdot Pop_{dist,CZ}$$

$$A_{CZ,Com} = \left[\sum A_k \cdot w_k\right]$$

$$L_{CA,com} = \sum l_{CZ,Com} \cdot \frac{A_{total}}{A_{CZ,Com}}$$

Where:

- $l_{CZ,Com}$ = the electric load of a representative commercial building from climate zone CZ to the total residential electric load. This takes into account the distributions by commercial building type used in each zone.
- w_k = The fraction of commercial building type k in the total by floor space.
- $Pop_{dist,CZ}$ = the fraction of total population in each climate zone
- $A_{CZ,Com}$ = the area of the representative commercial building from climate zone CZ to the total residential electric load. This takes into account the distributions by commercial building type used in each zone. Since the team is considering the distributions by building type in each zone as consistent between zones, this term is the same in all climate zones.
- A_k = The area of commercial building type k in the total by floor space (sq.ft)
- A_{total} = The total floor space of commercial buildings in California (sq.ft)
- $L_{CA,Com}$ = Total statewide electric load profile for the commercial sector

This process is also carried out to obtain the fuel usage and total site-level energy demands, under historical and climate change-affected conditions.

A.4. Chapter 5 Analysis Methods

To carry out this analysis, the following general approach is taken. A base case scenario representing the mix of technologies used to satisfy the 2050 greenhouse gas reduction goal of 80% below 1990 levels is established before taking into account the impacts of climate change on the electricity system. This scenario was provided by Energy and Environmental Economics (E3) using the PATHWAYS model [1] and provides electricity load demands for different sectors, as well as installed capacities for electric grid technologies and resources in the year 2050, for a system that satisfies the 2050 greenhouse gas goal. The model as configured for this study meets California's electric load demand using instate resources, with the exception of a fixed amount of unspecified imports that are used throughout all of the scenarios. These inputs are

simulated in the HiGRID electric grid balancing model [71] to obtain a base case greenhouse gas emissions and renewable utilization values. Subsequently, a new scenario is simulated that accounts for the impacts of climate change on the electricity system that were characterized in earlier chapters. This allows the research team to determine how much of the differences between the E3 base case and the final scenario were due to the difference in models and how much was due to climate change impacts.

HiGRID is a temporally resolved multimodule platform that determines the operation and dispatch of electric grid resources in response to the integration of renewable and advanced technologies. Specifically, the HiGRID model has three key technical modules and one economic module, the latter of which is not used in this study. An overview of the HiGRID model as applied in this study is presented in Figure A-11.

Figure A-11: HiGRID Model Flowchart as Applied to the Analysis of Climate Change Impacts on the Electricity System

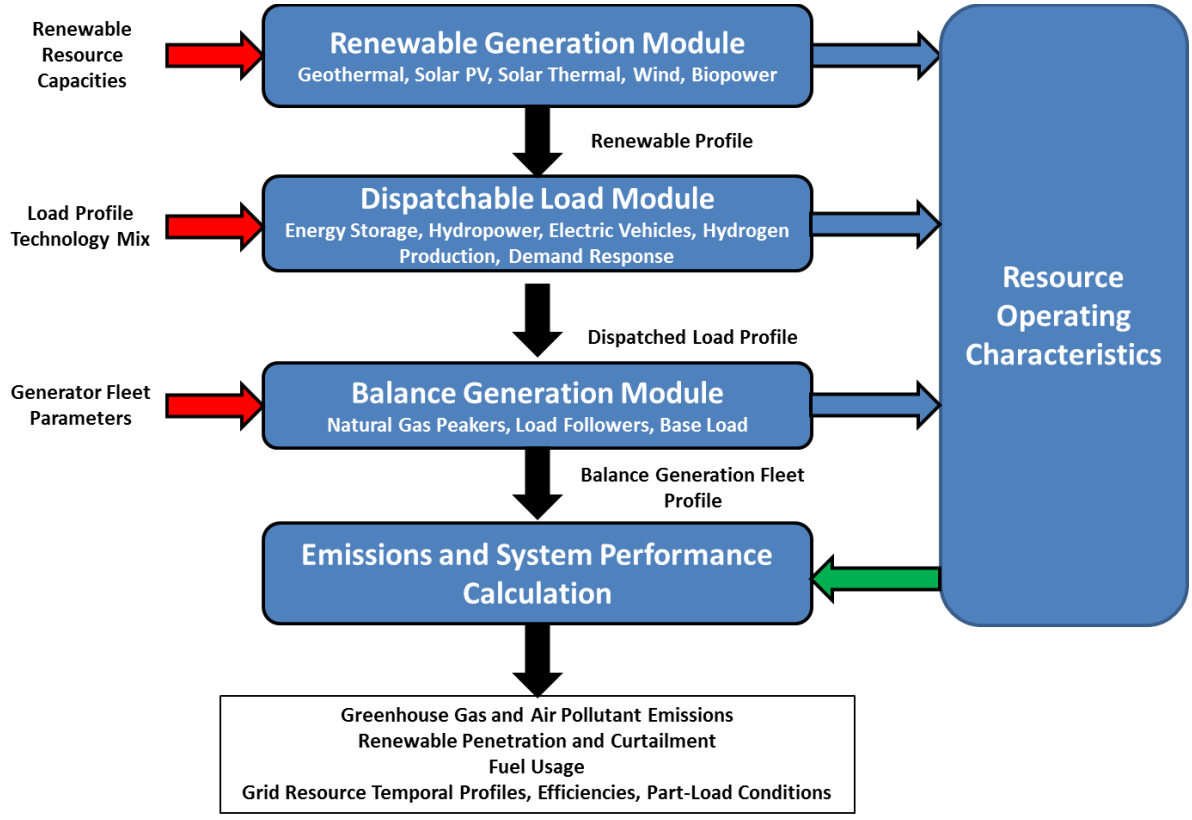

Source: Advanced Power and Energy Program, University of California Irvine

The first component is the renewable generation module, which uses models of renewable technologies and spatially resolved wind data and solar insolation data to determine the temporal profile of renewable generation for an input mix of renewable capacities. The second is the dispatchable load module, which dispatches resources that can alter the net load profile to respond to the impacts of renewable generation on the net load and consists of models for measures including, but not limited to, hydropower, energy storage, electric vehicles, and demand response. The third is the balance generation module, which dispatches conventional

resources such as natural gas power plants and others to meet the remainder of the net load demand and required reliability services to keep load and generation robustly balanced. This module also determines the required curtailment of renewable generation based on grid constraints. The HiGRID model contains an energy storage modeling component as part of the dispatchable load module. This model dispatches the charging and discharging of a gridwide energy storage system based on the net load profile, acting to shave peaks and fill valleys. The operation of the system is constrained by limits on power capacity, energy capacity, and charge-to-discharge power ratios, ramp rates, and round-trip efficiency parameters. These parameters can be configured to represent different energy storage technologies. Details on the HiGRID energy storage model are available from Eichman [72].

Subsequently, the impacts of climate change on hydropower generation, solar thermal and geothermal capacity deployment, and residential and commercial building loads are integrated individually and simultaneously into the scenario and simulated in the HiGRID model to determine how they affect electricity system greenhouse gas emissions and renewable utilization values. The future period is represented by simulations for 2046-2055, centered on 2050. The details of these steps are presented in this section.

A.4.1. Description of the 2050 Greenhouse Gas Goal Compliant Scenario Without Climate Change

The base case scenario to which climate change impacts are applied on this study is provided by Energy and Environmental Economics (E3) from the PATHWAYS model [73]. The PATHWAYS model uses an economywide approach to accounting for greenhouse gas emissions and, therefore, includes many elements that are not part of the electricity sector. The developed scenario is based on cost-preferred technology portfolios that need to be deployed in various economy sectors to meet the 2050 greenhouse gas goal. Since this study focuses on the electricity sector, only the inputs from the PATHWAYS scenario that are relevant to the electricity sector are used and assess the impacts of climate change as differences in electricity sector emissions. Specifically, this includes installed renewable and carbon-free generation capacities by type, electricity subsector load demands (magnitudes and profiles unless otherwise noted), and complementary technology capacities (i.e., energy storage). The E3 scenario includes loads due to technologies implemented to electrify certain energy end uses such as transportation (e.g., electric vehicles, electrolysis to produce hydrogen fuel). The California statewide load demands by electricity subsector for the no-climate-change scenario for 2050 are presented in Table A-22.

Table A-22: Electricity System Annual Loads in 2050 - No Climate Change Compliance Scenario

Electricity System Sector	Load Magnitude [GWh]
Residential Buildings	116683
Commercial Buildings	135336
Transportation – Electric Vehicles	42191
Transportation – Hydrogen Production	12104
Industrial, Agriculture, and Other Transportation (Marine, Air, Rail)	115926
Total	**422,240**

Source: Energy and Environmental Economics

These load demands take into account the impacts of population growth between 2015 and 2050, as well as advances in energy efficiency associated with subsectors within each category that are expected to be implemented between 2015 and 2050. Transportation demands are based on the projected deployment of battery electric vehicles for on-road transportation including light-duty, medium-duty trucking, heavy-duty trucking, and buses.

In addition to the magnitudes of these loads used as inputs to the HiGRID model, the load shapes for these loads are also used to be consistent with the E3 base case scenario with two exceptions. First, the load profile for electric vehicle charging is developed within HiGRID utilizing grid-responsive smart charging optimization constrained by vehicle travel patterns, trip data, and charging infrastructure parameters such as locations and charging power limits [25, 74]. Therefore, the profile from PATHWAYS is not used. Second, the electrolysis load profile is also developed in HiGRID based on hydrogen infrastructure parameters and grid responsive dispatch [74]. Therefore, this profile from PATHWAYS is not used.

The installed renewable and carbon free capacities for the no-climate-change scenario for 2050 is presented in Table A-23. The E3 no-climate-change compliance scenario did not rely on solar thermal so it does not appear in this table.

Table A-23: Renewable and Carbon Free Generation Installed Capacities in 2050 - No-Climate-Change Compliance Scenario

California Electricity System Resource	Installed Capacity [MW]
Nuclear	0
Hydropower (Total)	15,615
Biopower	0
Geothermal	4,857
Solar (Centralized PV)	66,015
Solar (Rooftop PV)	41,500
Wind	99,748
Unspecified Imports	12,620

Source: Energy and Environmental Economics

In contrast to the load demands, the generation profiles from PATHWAYS for these resources are not used in HiGRID. The HiGRID model takes as an input the installed capacity of these resources and develops internally the profiles for these resources based on dispatch rules and streamflow for hydropower, operational rules for base load generation, and spatially distributed atmospheric conditions combined with first principles models for wind and solar devices [71, 72]. In this case, the centralized PV solar is assumed to be one-axis tracking, while the rooftop PV is fixed axis. The input for the installed capacity of natural gas balancing power plants is not taken from the PATHWAYS results. This is because the HiGRID model produces the installed capacity of natural gas balancing power plants (combined cycle, peaker) as an output based on the needs to balance the net load and meet grid reliability conditions [71, 72].

In addition to load demands and generation resources, the PATHWAYS scenario also includes the installation of complementary technologies and load management strategies. These elements and a comparison of how they are implemented in HiGRID are presented in Table A-24.

Table A-24: Complementary Technology/Resource Implementation in PATHWAYS and HiGRID

Resource	PATHWAYS Implementation	HiGRID Implementation
Energy Storage	2.4 GW Pumped hydro	2.4 GW Pumped hydro
	0.5 GW 2-hr batteries	0.5 GW 2-hr batteries
	0.5 GW 5-hr batteries	0.5 GW 5-hr batteries
	0.3 GW 8-hr flow batteries	0.3 GW 8-hr flow batteries

Electric Vehicle Charging Dispatch	90% flexible, maximum lead or delay time of 12 hours	Grid-communicative smart charging, constrained by vehicle travel patterns, trip data (i.e. NHTS for light-duty), and charging location parameters.
Hydrogen Electrolysis Dispatch	Flexible dispatch in response to grid, set at 25% capacity factor, 1 week of hydrogen storage	Flexible dispatch in response to grid, capacity factor variable, storage in natural gas pipeline equivalent to 7% of annual demand
Nontransportation Demand Response	80% flexible loads for commercial and residential sector (water heating, space heating, air conditioning, refrigeration), maximum lead/delay time of 2-3 hours.	Event-responsive turndown of lighting, ventilation, and air conditioning loads in commercial buildings; magnitude and duration limited by occupant comfort tolerances.

Source: Advanced Power and Energy Program at University of California, Irvine; and Energy and Environmental Economics

Overall, PATHWAYS and HiGRID implement different resources and loads in slightly different ways and have slightly different models for characterizing the behavior of these resources, since each model has different resources available and different approaches taken for each aspect. This study has attempted to represent the no-climate-change compliance scenario from PATHWAYS as best as possible for the electricity sector in HiGRID. This scenario represents the base to which the impacts of climate change will be applied.

A.4.2. Application of the Impacts of Climate Change

This section will describe the application of the impacts of climate change on hydropower generation, solar thermal and geothermal capacity, and electric load demands to the base compliance scenario.

A.4.2.1. Impacts on Hydropower Generation

The full description of the hydropower model developed to characterize the impacts of climate change on hydropower generation is in Chapter 2. As a summary, 71 large hydropower plants (P > 30 MW) and the corresponding water reservoirs or stream systems are characterized. The first component of the model is a water reservoir model that captures the dispatch of water reservoir releases. The second component of the model uses the output of the water reservoir model of daily water releases as constraints on the hourly dispatch of the hydropower plants to provide generation and ancillary services. The dispatch of this component is based on price signals for energy and ancillary services that are affected by grid conditions such as the integration of renewable resources.

The results of the hydropower analysis determined that climate change leads to increased risk of reservoir spill and overflow events, a temporal shift (seasonally) in hydropower generation to an earlier parts of the year, and a decrease in spinning reserve bidding potential. For the RCP 8.5 scenario, overall inflow and generation tended to increase on average.

The difference between the analysis in Chapter 2 and the application of the model here is that in this case, the hydropower model will be responding to electric grid conditions corresponding to the high renewable, low-carbon compliance scenario by E3 instead of historical grid conditions. Instead of using historical price signals for generation and ancillary services, the price signals will be based on the net load demand as an output from HiGRID. The provision of generation ancillary services from hydropower resources is then subtracted from the overall grid requirement to be met by other resources in HiGRID.

A.4.2.2. Water Constraints on Solar Thermal and Geothermal Capacity

The full description of the methods to assess how water availability constraints affect the deployable capacity of solar thermal and geothermal resources is described in Chapter 3. As a summary, the deployable potential for solar thermal and geothermal resources without water constraints was calculated from USGS data, land use and geographical data, and insolation data in 10 hydrologic regions across California. The available water resources for each of these regions were determined via a water balance analysis and used as a constraint on the deployable capacity of solar thermal and geothermal resources using different power plant cooling systems.

The Chapter 3 analysis determined that the water-constrained deployable capacity of solar thermal and geothermal resources depended much more on whether the areas of high or increased precipitation spatially aligned with the regions that exhibited high solar thermal or geothermal energy potential. This factor mattered more than the cooling system used by solar thermal and geothermal power plants: dry cooling systems allowed more deployable capacity for a given amount of available water in a given region, but if a region had no net available supply after meeting other water demands, cooling system selection had no effect. This analysis found that most of the increases in precipitation occurred in the northern regions of the state, while the vast majority of the energy potential for solar thermal and geothermal is in the southeastern regions of the state. Combined with high water demands in the southeastern regions, it was found that without reductions in other water demands, water availability can significantly constrain the deployment of solar thermal and geothermal capacity in the state.

The results from the Chapter 3, however, showed that installable solar thermal and geothermal capacities ranged between zero and the full energy potential capacity depending on the RCP scenario and climate model, with the results dominated by whether significant precipitation was available in the Colorado River and South Lahontan hydrologic regions. Therefore, because there is a wide range of values for maximum installed capacity, the application of these results here is to assume that no geothermal and solar thermal capacity can be installed. The E3 no-climate-change compliance scenario did not rely on solar thermal to begin with; therefore, assuming zero solar thermal has no effect. The geothermal capacity, however, is decreased

from 4.857 GW to zero as a conservative, bounding assumption to account for climate change impacts on water availability.

A.4.2.3. Impacts on Residential and Commercial Building Electric Loads

The methods to assess how climate change-altered weather conditions (temperature, humidity, wind speed, etc.) affected commercial and residential building energy use is described in Chapter 4. As a summary, residential and commercial building prototypes representing the entire residential sector and 80% of the commercial sector floor space were obtained from the U.S. Department of Energy Building Energy Codes Project for use in the EnergyPlus building simulation model. Daily climate data for each of four climate models – CanESM2, CNRM-CM5, HadGEM2-ES, and MIROC5, as well as historical condition data – were obtained for each of the California Title 24 building climate zones. Each of the building prototypes was simulated in EnergyPlus under historical and climate change-affected weather conditions.

Chapter 4 determined that climate change increased residential and commercial electric demands through increases in space cooling loads, with larger effects in the commercial sector. While electricity demands increased, the total energy usage of residential buildings remained essentially the same and only increased slightly for commercial buildings. This was due to decreases in heating demands, which tend to be met by natural gas. The specific results varied slightly among climate models and RCP scenarios, with RCP 8.5 scenario and CanESM2 climate model exhibiting the highest electricity demand increases.

Since this analysis focuses on electricity sector emissions, application of the Chapter 4 results will focus only on the changes in electric loads due to climate change. Furthermore, this study focuses on the RCP 8.5 scenario only, to be consistent with the other types of impacts. The annual magnitudes representing 2050 under current and climate change-altered weather conditions is presented in Table A-25. The year 2015 loads are slightly different than the historical case in Chapter 4, since it was scaled to match the load magnitude in the E3 no-climate-change compliance case. The percentage increases for each climate model are applied to that base.

Table A-25: Year 2050 Projected California Residential and Commercial Electric Loads: With and Without Climate Change (RCP 8.5 Scenario)

	Year 2015 [GWh]	Year 2050 [GWh]	Year 2050 [GWh]	Year 2050 [GWh]	Year 2050 [GWh]	Year 2050 [GWh]
	No CC	No CC	CanESM2	CNRM-CM5	HadGEM2-ES	MIROC5
Residential Load	89,776.54	116,683.70	121,701.10	119,484.11	121,584.42	119,600.79
Commercial Load	106,971.55	135,336.56	141,020.70	138,584.64	141,291.37	139,261.32

Source: Advanced Power and Energy Program, University of California Irvine

Moreover, the shifts in the load profiles for residential and commercial loads are captured by replacing the original normalized load shapes with those generated from the EnergyPlus models under climate change.

A.5. Chapter 6 Analysis Methods

To carry out this analysis, the following general approach is taken. The electric grid resource mix is altered in three ways compared to that specified in the base case of Chapter 6, which is the 2050 case that meets the 80% reduction in greenhouse gas emissions from 1990 levels. This scenario was provided by Energy and Environmental Economics (E3) using the PATHWAYS model [1] and provides electricity load demands for different sectors, as well as installed capacities for electric grid technologies and resources in 2050, for a system that satisfies the 2050 greenhouse gas goal. The altered configurations are then simulated in the HiGRID electric grid balancing model [71] to obtain greenhouse gas emissions and renewable penetration performance, as well as details of system operation. These metrics are then compared with the base case and the case without mitigation measures but including climate change to assess how effective the alterations could be in counteracting the impacts of climate change.

An overarching theme of the options investigated is that each can increase the flexibility and dispatchability of the electricity system. The option of changing the mix of renewable resources installed in the electricity system was not investigated since some level of optimization based on costs and resource potential was conducted by E3 to select the renewable mix in the base case [1]. At the high levels of renewable resources installed in the base case, certain resources such as wind are near capacity for easily accessible generation. In addition, increasing the installed capacity of resources such as solar generation would be ineffective, since solar power is already in excess of the load on most days even in the base case.

The details of the three mitigation options (increasing the installed capacity of battery energy storage, allowing ancillary services to be met by renewable resources, and enabling vehicle-to-grid operation of battery electric vehicles) are presented as follows:

A.5.1. Increasing the Battery Energy Storage Capacity

The first mitigation option investigated is to increase the installed capacity of battery energy storage. The base case exhibited a relatively sizeable level of curtailed renewable generation due to the high capacity of installed wind and solar power, with 66.015 GW of centralized PV and 41.500 GW of rooftop PV. This generation, combined with occasional wind generation during the daytime, causes generation to exceed the daytime load demand on many days throughout the year. The base case does implement dispatchable resources, such as smart charging of electric vehicles, dispatchable hydrogen production, and building demand response, but these were unable to eliminate curtailed renewable generation.

Energy storage is a part of the electric resource portfolio in the base case, but only in small amounts. The installed capacity in the base case is 3.7 GW on a power basis, being composed of a mix of pumped hydropower, 2-hr and 5-hr conventional batteries (assumed to be lithium -ion in this case), and 8-hr flow batteries. These amounts are tied to the level of storage assumed in the California Air Resources Board Scoping Plan to meet the state's energy storage mandate [75]. Therefore, this case will analyze increasing the installed capacity of battery energy storage by 5 times and 10 times the level in the base case as follows in Table A-26.

Table A-26: Installed Energy Storage Capacities for Chapter 6 Analysis

Battery Type	Base Case Installed Capacity [GW]	5x Energy Storage Case [GW]	10x Energy Storage Case [GW]
2-hr Lithium Ion	0.5	2.5	5.0
5-hr Lithium Ion	0.5	2.5	5.0
8-hr Flow Battery	0.3	1.5	3.0

Source: Advanced Power and Energy Program, University of California Irvine

For this sensitivity analyses, the installed capacity of pumped hydropower energy storage is held constant. Pumped hydropower systems are geographically constrained in capacity and are not easily scaled up to larger capacities compared to battery energy storage. Therefore, only the installed capacity of batteries is increased in this scenario.

The cases of increased battery energy storage are then simulated in the HiGRID model [71] with all the climate change impacts applied. The metrics of greenhouse gas emissions and renewable penetration level, as well as details of system operation and the generation mix, are then determined. These are compared to the corresponding metrics for the case without climate change impacts and the case with climate change impacts but no resource alterations to determine the effectiveness of these strategies.

A.5.2. Enabling Renewable Resources to Meet Ancillary Services

The second mitigation option involves allowing renewable resources to provide ancillary services, namely spinning reserve. Traditionally and in the base case as modeled by the HiGRID model, ancillary services are provided only by dispatchable resources, specifically hydropower and natural gas combined-cycle power plants. The ability of hydropower to provide ancillary services is somewhat constrained by water availability and the need to meet water demands for environmental, agriculture, and urban uses. The analysis in Chapter 6 showed that for this scenario, the amount of spinning reserve provided by hydropower is similar under climate change. Therefore, even under climate change, a significant amount of spinning reserve services must still be provided by natural gas power plants. To provide spinning reserve services, these power plants must be on-line at all times of the day and operate at part load with slightly decreased efficiency. The provision of ancillary services by natural gas power plants contributes to greenhouse gas emissions and increases renewable curtailment, since these power plants are meeting a portion of the load while being on-line.

This scenario investigates the impact of allowing renewable and nongenerating resources to be capable of satisfying the spinning reserve requirements on the electric grid. *Nongenerating resources* refer to grid resources that do not by themselves provide generation to meet the load demand but can alter the net load demand in various ways (e.g., load shifting), and includes energy storage and demand response.

Renewable resources are modeled to be able to provide spinning reserve during the hours when renewable curtailment exists. When renewable generation is being curtailed, the natural gas

power plants are allowed to turn down or shut down to allow renewable curtailment to “firm” the generation portfolio at that time and provide spinning reserve services. The limit on the turndown of natural gas power plants providing spinning reserve is bounded by the maximum renewable curtailment at each given hour of the year. This approach is taken since in this case, if a grid contingency occurs where additional reserve generation must be called upon, instead of turning up natural gas power plants, additional use of otherwise curtailed renewable generation occurs to compensate for the contingency shortfall.

In this case, the ancillary service requirements are not altered from historical levels. Traditionally, the spinning reserve requirement has been set by the capacity of the maximum contingency that can occur on the system at any given time. Data for the spinning reserve requirements were obtained from the California ISO OASIS database [76] for 2015 and assumed to be unchanged in the future case.

A.5.3. Enabling Vehicle-to-Grid Charging of Electric Vehicles

An additional strategy for increasing the flexibility of the electricity system and allowing additional use of otherwise curtailed renewable generation to offset the additional greenhouse gas emissions due to the impacts of climate change is to enable electric vehicles to operate in a vehicle-to-grid charging mode. In the base case as modeled in HiGRID, the electric vehicles deployed on the system are already allowed to operate using smart charging, where the profile of vehicle charging is optimally shaped in response to grid conditions within the constraints of vehicle dwell time, charging power, vehicle travel pattern needs, and charging infrastructure location. In this capacity, electric vehicle charging is managed as dispatchable electric loads when these vehicles are plugged in.

Vehicle-to-grid (V2G) enables a further step in electric vehicle charging management where not only are electric vehicle charging loads allowed to be set in time and magnitude in response to the grid, but the electric vehicles are allowed to discharge energy back to the grid in response to grid conditions. In this way, the electric vehicles act as variable capacity energy storage that can both charge using renewable energy and discharge any energy that is not needed to meet the vehicle travel needs back to the grid. This aids in increasing renewable penetration and reducing greenhouse gas emissions of the electric system.

The base case for 2050 already includes the deployment of a significant number of electric vehicles across multiple vehicle classes. Specifically, these are presented in Table A-27.

Table A-27: Base Case Plug-In Electric Vehicle Stock in 2050 (E3)

Vehicle Class	Plug-In Electric Vehicle Stock
Light-Duty	• **PHEV25**: 390,000 • **BEV**: 25,860,000
Medium-Duty	• **BEV**: 137,360
Heavy-Duty	• No plug-in electric vehicles deployed
Buses	• **BEV**: 73,740

PHEV25 refers to Plug-in Hybrid Electric Vehicles that have a 25-mile all electric range.

Source: Energy and Environmental Economics

Therefore, enabling V2G operation of these vehicles is an option to increase the flexibility of the electric system with minimal deployment of additional hardware relative to the base case, in contrast to the option of increasing the capacity of stationary energy storage. For this analysis, only the light-duty vehicle sector is enabled to operate in V2G modes. The operation of other vehicle classes in V2G mode is an option for future work; however, these classes have very different travel patterns, and the related constraints on smart charging while providing V2G need further investigation. Moreover, the light-duty vehicle sector accounts for the largest fraction of the total electric load due to electric vehicles. Therefore, capturing the impact of light-duty electric vehicles providing V2G services will be qualitatively representative of the effectiveness of this option.

The electric vehicles providing V2G services are still subject to the same constraints as regular smart charging. The charging of each vehicle is optimized over the dwell time of the vehicle at each location, subject to the constraints of needing to unplug at the end of each dwell window, having enough charge to meet each vehicles' next series of trips before charging, the maximum rate of charging at any given location (charging power), and the limitations on vehicle battery capacity for discharging electricity back to the grid. A description of the methods used to model V2G operation of electric vehicle charging is presented by Tarroja and Zhang [25]. These methods have been implemented in the HiGRID model to study the stationary energy storage equivalency of V2G charging electric vehicles [25] and how V2G charging can reduce the requirements for stationary energy storage capacity to reach high renewable penetration levels [77].

APPENDIX B:
Supporting Results

This section presents supporting results that have been produced from the analyses in each chapter but are not central to the main takeaways and outcomes of the project analyses.

B.1. Summary of Climate Change Impacts on Atmospheric Conditions

These results focus on climate change impacts on atmospheric conditions and describes Localized Constructed Analogs (LOCA) model simulations for temperature and precipitation in each climate division in California from 1950 to 2099 [62]. This chapter provides simple evaluations of the trends in the atmospheric variables. Because local climate affects energy generation and demand, this chapter reports changes in heating and cooling degree days (HDD and CDD, respectively) in the climate divisions as a measure of changing energy demand [78]. Heating and cooling degree days were calculated in degrees Celsius, with a baseline of 18 degrees Celsius. Daily HDD and CDD are calculated by the difference between the average daily temperature and the baseline [79]. Thus, if the daily temperature is 19 degrees, the daily CDD would be 1, while if the daily temperature is 17 degrees, the daily HDD would be 1. The nonparametric Mann-Kendall trend test was used to evaluate whether climate divisions would experience significant trends in the studied variables.

Ten climate models were selected for *California's Fourth Climate Change Assessment*: ACCESS1.0, CanESM2, CCSM4, CESM1(BGC), CMCC-CMS, CNRM-CM5, GFDL-CM3, HadGEM2-CC, HadGEM2-ES, and MIROC5 [80]. Four of these models were chosen as priorities (CanESM2, CNRM-CM5, HadGEM2-ES, and MIROC5), with the other six encouraged for analyses conducted under this program. This section presents the average of the 10 model simulations are reported for all variables and indices driven by two representative concentration pathways (RCPs): RCP 4.5, which assumes intermediate emissions and a future impact of 4.5 watts per square meter by the end of the 21st century, and RCP 8.5, which reaches an impact of 8.5 watts per square meter in a future with no reduction in the world's emissions trajectories [81]. The average of the climate models for each RCP was used for each pathway analysis.

B.1.1 Statewide Results

The seven climate divisions of California based on hydrologic drainage basins designated by the U.S. National Oceanic & Atmospheric Administration (NOAA) are presented in B-1. These are used to analyze hydrological behavior in distinct areas of the state.

Figure B-1: NOAA Climate Divisions of California

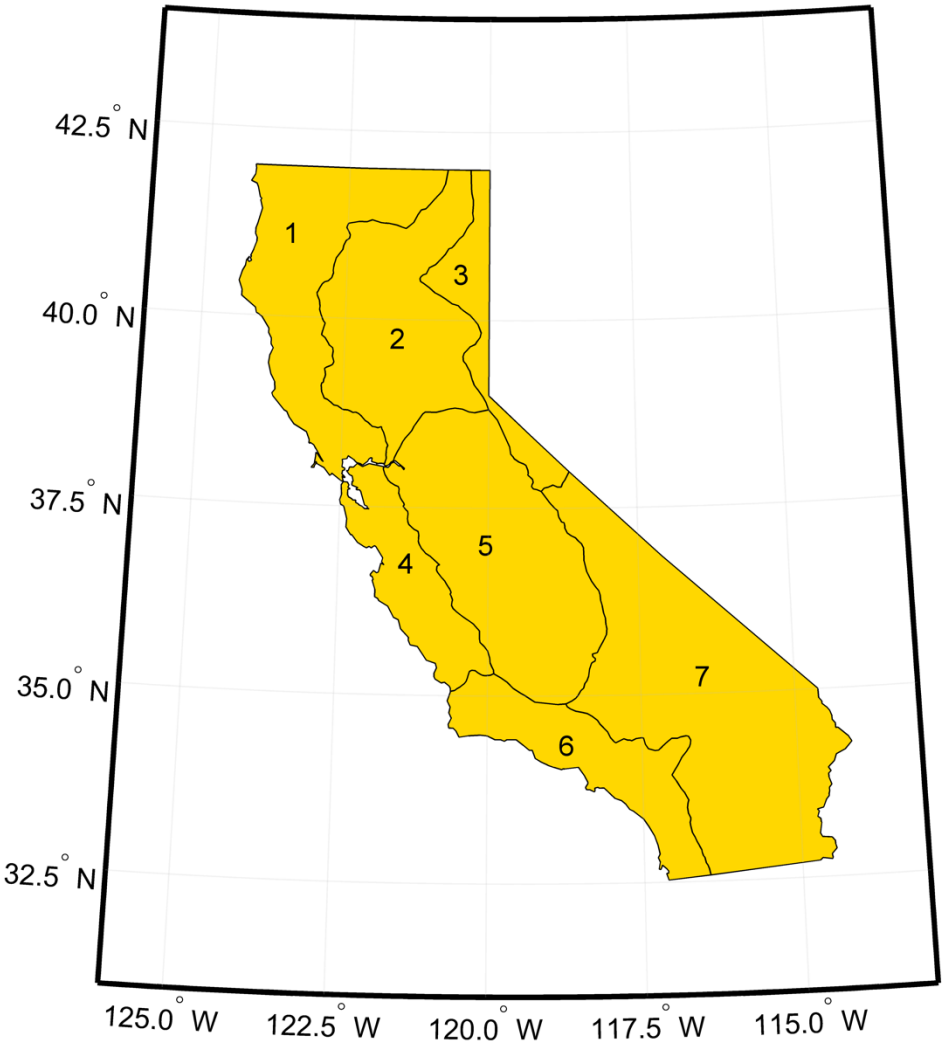

Source: National Oceanic and Atmospheric Administration

Figure B-2 displays the projected annual precipitation in 2010-2020 and 2045-2055 using the RCP 8.5 scenario, averaged among the 10 climate models and averaged temporally over each 10-year period. In comparison to the reference 2010-2020, the mid-21st century experiences significant increases in precipitation for Climate Divisions 1, 2, and 3 in upper Northern California. Climate Divisions 4 and 5, in the midlatitudes of California, experience little to no changes in precipitation between the two periods. Climate Divisions 6 and 7 in Southern California show slight nonsignificant decreases in precipitation compared to the reference period.

Figure B-2: Annual Precipitation by Climate Division (2010-2020 and 2045-2055)

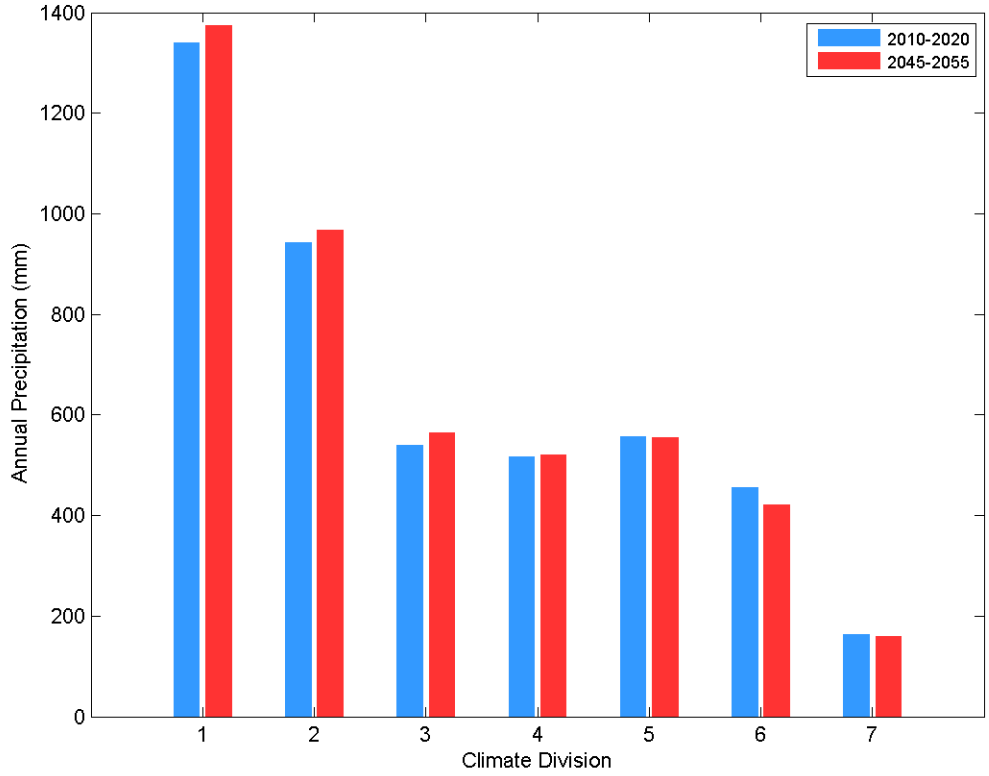

Source: Advanced Power and Energy Program, University of California, Irvine

Figure B-3 examines the projected shift in daily temperatures in 2010-2020 and 2045-2055 using the RCP 8.5 scenario. Although there is variability in reference period temperatures, all climate divisions experienced similar increases in daily temperatures in the later period.

Figure B-3: Average Daily Temperature by Climate Division (2010-2020 and 2045-2055)

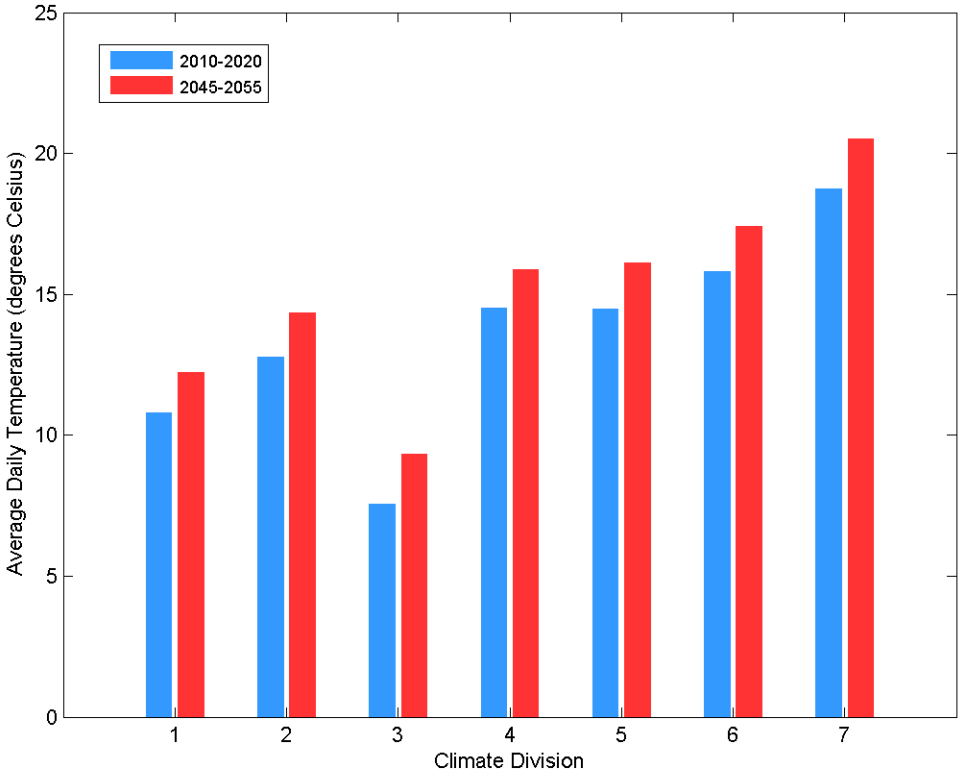

Source: Advanced Power and Energy Program, University of California, Irvine

Figure B-4 shows declines in the annual HDD index across all climate divisions in California from the baseline period to 2045-2055. The statewide decline in annual HDD can be easily attributed to the increase in average daily temperatures, reducing the number of days where temperature conditions are lower than the baseline temperature of 18 degrees Celsius. Climate Division 3, in the inland northeastern region of California, experienced the largest decline in the annual HDD index.

Figure B-5 shows increases in the annual CDD index across all climate divisions. Climate Division 7, in the inland southeastern part of California, experienced the largest increase in the annual CDD index.

Figure B-4: Annual Heating Degree Days by Climate Division (2010-2020 and 2045-2055)

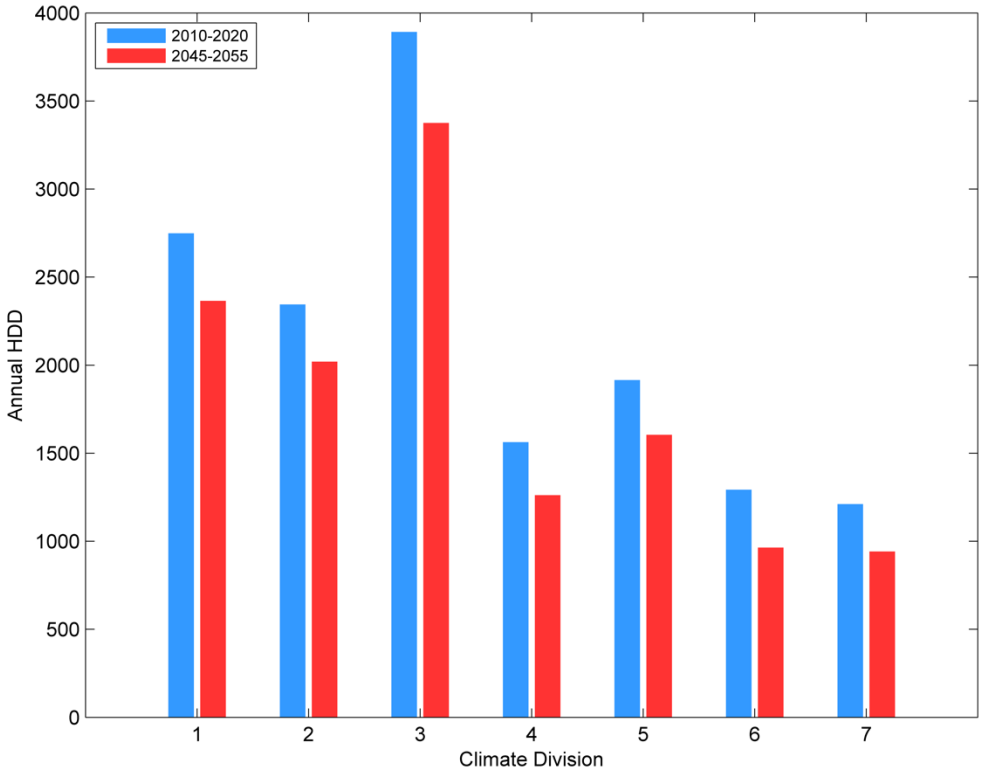

Source: Advanced Power and Energy Program, University of California, Irvine

Figure B-5: Annual Cooling Degree Days by Climate Division (2010-2020 and 2045-2055)

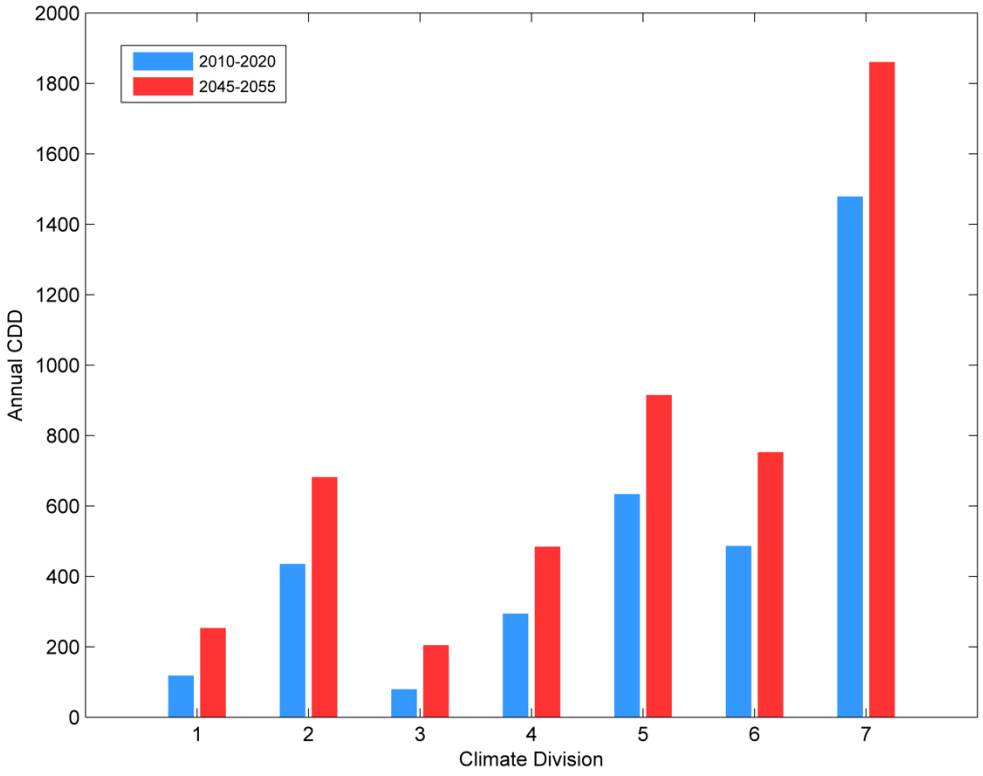

Source: Advanced Power and Energy Program, University of California, Irvine

Daily extremes also show shifts similar to those seen from annual values. Figure B-6 displays declines across the climate divisions in the 90th percentile of the daily HDD index, calculated from a 30-year rolling window of values. Figure B-7 displays the corresponding increase in the 90th percentile of the daily CDD index.

Figure B-6: 90th Percentile Daily HDD 30-Year Running Statistic (2010-2020 and 2045-2055)

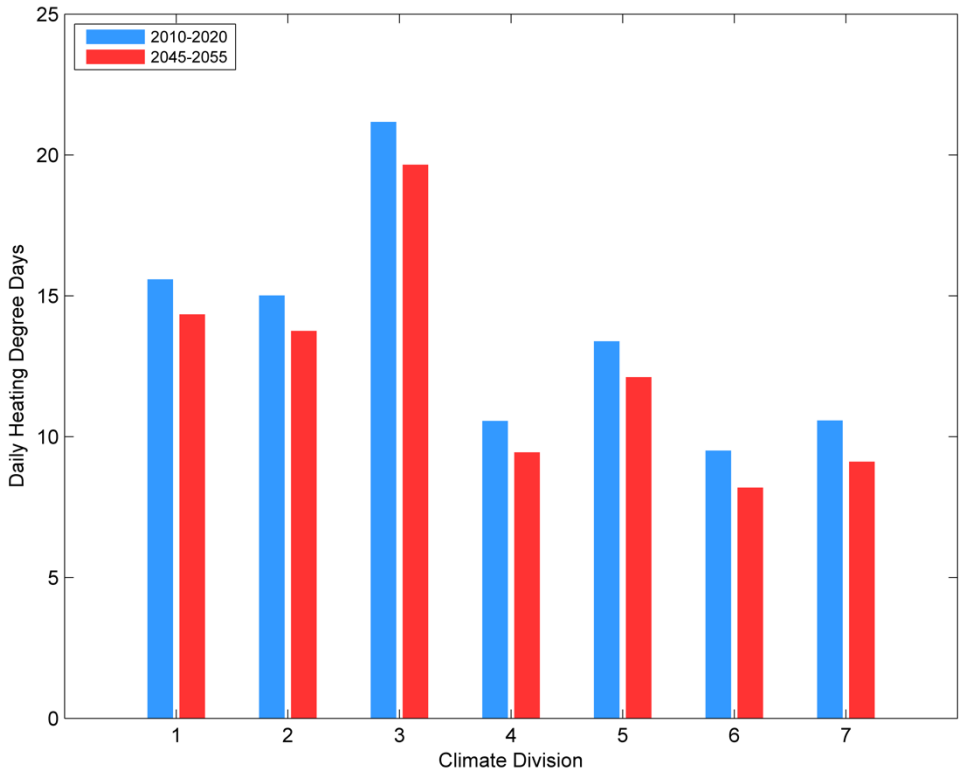

Source: Advanced Power and Energy Program, University of California, Irvine

Figure B-7: 90th Percentile Daily CDD 30-Year Running Statistic (2010-2020 and 2045-2055)

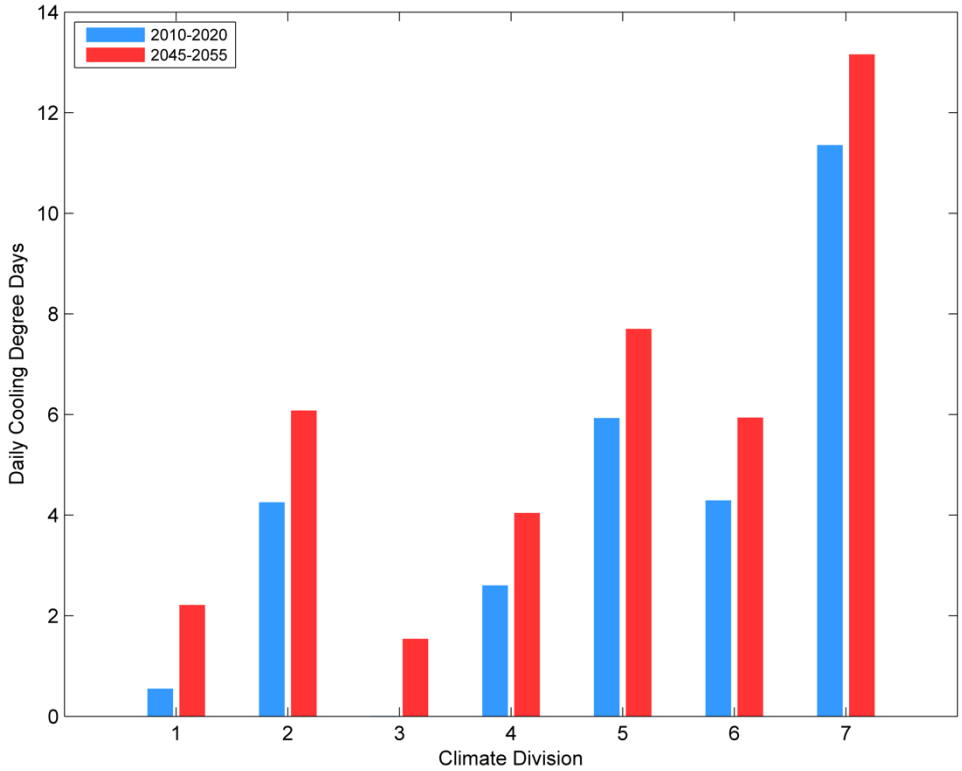

Source: Advanced Power and Energy Program, University of California Irvine

B.1.2. Summary of Results for Individual Climate Zones

Table B-1 summarizes the results for the changes in annual and extreme precipitation, as well as annual and extreme temperatures, for individual climate zones is presented here.

Table B-1: Summary Results for Individual Climate Zones

Climate Division	Climate Scenario	Metric	Trend	p-value
1	RCP 4.5	Annual Precipitation	Increase	0.0121
		Extreme Precipitation	Increase	<0.001
		Annual Temperature	Increase	<0.001
		Extreme Temperature	Increase	<0.001
	RCP 8.5	Annual Precipitation	Increase	<0.001
		Extreme Precipitation	Increase	<0.001
		Annual Temperature	Increase	<0.001
		Extreme Temperature	Increase	<0.001
2	RCP 4.5	Annual Precipitation	Increase	0.0254
		Extreme Precipitation	Increase	<0.001
		Annual Temperature	Increase	<0.001
		Extreme Temperature	Increase	<0.001
	RCP 8.5	Annual Precipitation	Increase	0.0011
		Extreme Precipitation	Increase	<0.001
		Annual Temperature	Increase	<0.001
		Extreme Temperature	Increase	<0.001
3	RCP 4.5	Annual Precipitation	Increase	0.0022
		Extreme Precipitation	Increase	<0.001
		Annual Temperature	Increase	<0.001
		Extreme Temperature	Increase	<0.001
	RCP 8.5	Annual Precipitation	Increase	<0.001
		Extreme Precipitation	Increase	<0.001
		Annual Temperature	Increase	<0.001
		Extreme Temperature	Increase	<0.001
4	RCP 4.5	Annual Precipitation	None	0.0868
		Extreme Precipitation	Decrease	0.0049
		Annual Temperature	Increase	<0.001
		Extreme Temperature	Increase	<0.001
	RCP 8.5	Annual Precipitation	Increase	<0.001
		Extreme Precipitation	Decrease	0.001
		Annual Temperature	Increase	<0.001
		Extreme Temperature	Increase	<0.001
5	RCP 4.5	Annual Precipitation	None	0.5806
		Extreme Precipitation	Decrease	0.0025
		Annual Temperature	Increase	<0.001
		Extreme Temperature	Increase	<0.001
	RCP 8.5	Annual Precipitation	None	0.0929
		Extreme Precipitation	Decrease	<0.001

		Annual Temperature	Increase	<0.001
		Extreme Temperature	Increase	<0.001
6	RCP 4.5	Annual Precipitation	None	0.8607
		Extreme Precipitation	Decrease	<0.001
		Annual Temperature	Increase	<0.001
		Extreme Temperature	Increase	<0.001
	RCP 8.5	Annual Precipitation	None	0.7183
		Extreme Precipitation	Decrease	<0.001
		Annual Temperature	Increase	<0.001
		Extreme Temperature	Increase	<0.001
7	RCP 4.5	Annual Precipitation	None	0.9896
		Extreme Precipitation	Decrease	<0.001
		Annual Temperature	Increase	<0.001
		Extreme Temperature	Increase	<0.001
	RCP 8.5	Annual Precipitation	None	0.6213
		Extreme Precipitation	Decrease	<0.001
		Annual Temperature	Increase	<0.001
		Extreme Temperature	Increase	<0.001

Source: Advanced Power and Energy Program, University of California, Irvine

B.1.3. Analysis of the Results

Model simulations of annual precipitation showed a mixture of significant and nonsignificant trends. The climate divisions showing significant positive trends of annual precipitation in both emissions scenarios also showed positive trends in extreme precipitation. Climate divisions associated with nonsignificant trends of annual precipitation showed negative trends in extreme precipitation. This indicates that extreme daily precipitation shapes the significance of annual precipitation trends. More rapid increases in annual precipitation were observed in higher latitudes, which agree with larger-scale predictions [3].

Annual average temperatures and extreme daily temperatures experienced significant increases across all climate divisions, which were reflected in trends in the heating and cooling degree days. Changes in heating and cooling degree days were naturally associated with current climate conditions in each division. For example, Climate Division 7, the Southeast Desert Basin, which is in inland Southern California, would experience the largest increase in cooling degree days.

The predicted shifts in total degree days, the research team's proxy for total energy demand, implies that most divisions in California will demand less energy in the mid-21st century in comparison to the early 21st century. This is given the assumptions: each degree day demands the same energy cost across the spectrum of temperature; heating and cooling degree days demand the same energy cost. Further, more detailed examination of the impacts of climate conditions on energy demands will be presented as the focus of Chapter 4, which will evaluate how effective the use of total degree day shifts will be in evaluating energy demand changes.

B.2. Chapter 2 Auxiliary Results

This section presents auxiliary results for the Chapter 2 analysis. While the main text of Chapter 2 and the subsequent analyses focus on the RCP 8.5 climate scenario, results for the climate change impacts on hydropower for the RCP 4.5 climate scenario are presented here.

B.2.1. Inflow Change for RCP 4.5 Climate Scenario

Looking at the state aggregated inflow, the average annual inflow into hydropower units increases compared to the historical period for all scenarios for RCP 4.5. CNRM-CM5 had the largest increase in annual inflow, about 80% higher than the historical average. CanESM2 and MIROC5 predict annual inflow increases by 30% on average, and HadGEM2-ES increases 40% on average. Increases in inflow did not occur uniformly across the year (Figures B-8 and B-9). Average inflow increased in winter for all RCP 4.5 scenarios, and CNRM-CM5 showed the greatest increase in average inflow for every season.

Figure B-8: Average Seasonal Inflow as a Percentage of Historical Inflow (100%) for All RCP 4.5 Scenarios

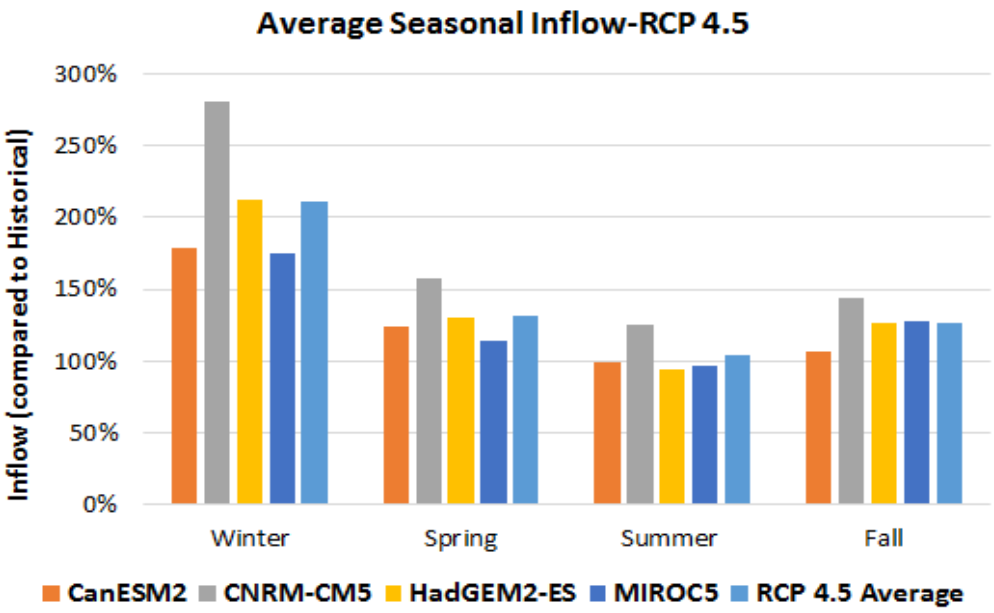

Source: Advanced Power and Energy Program, University of California, Irvine

Peak inflow shifts from midspring to earlier in the year for all RCP 4.5 scenarios (Figure B-9). All scenarios show a net state-level increase in inflow during January through April and little to no change in inflow during late summer to early fall. The RCP 4.5 scenarios are split on inflow during December, with CNRM-CM5 and HadGEM2-ES showing increased inflow on average, and CanESM2 and MIROC5 predicting decreased inflow on average.

Figure B-9: Average Monthly Inflow for Historical and All RCP 4.5 Scenarios

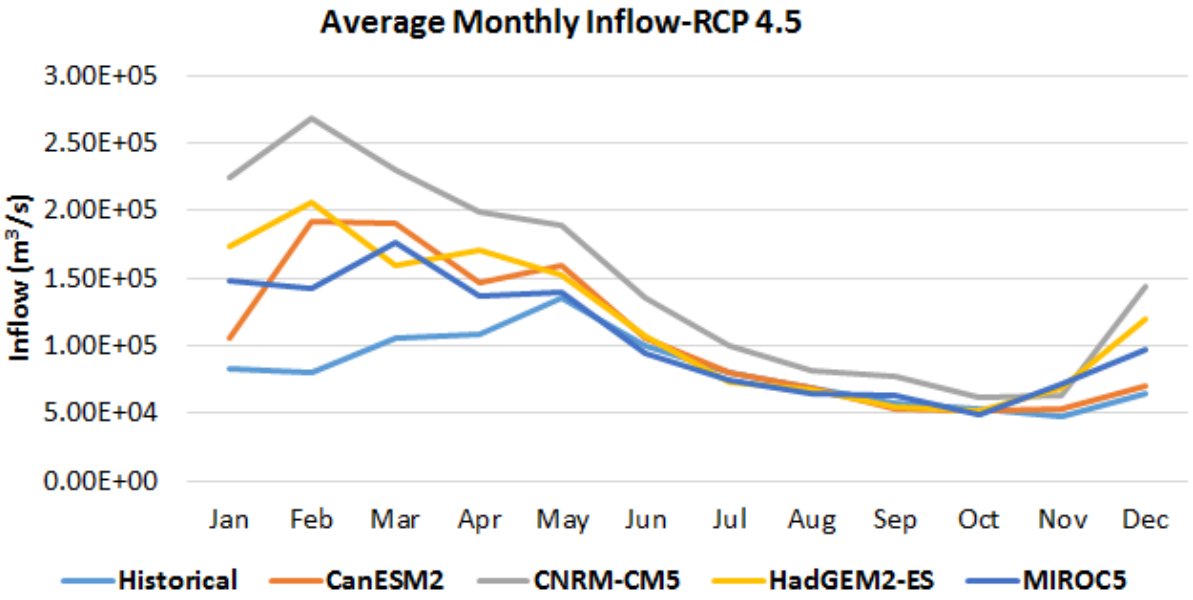

Source: Advanced Power and Energy Program, University of California, Irvine

Historically, inflow into California hydropower units can vary significantly between years. Similarly, seasonal inflow varies for all RCP 4.5 scenarios. This variability is represented in Figure B-10.

Figure B-10: Boxplots for Historical Inflow and Inflow for All RCP 4.5 Scenarios

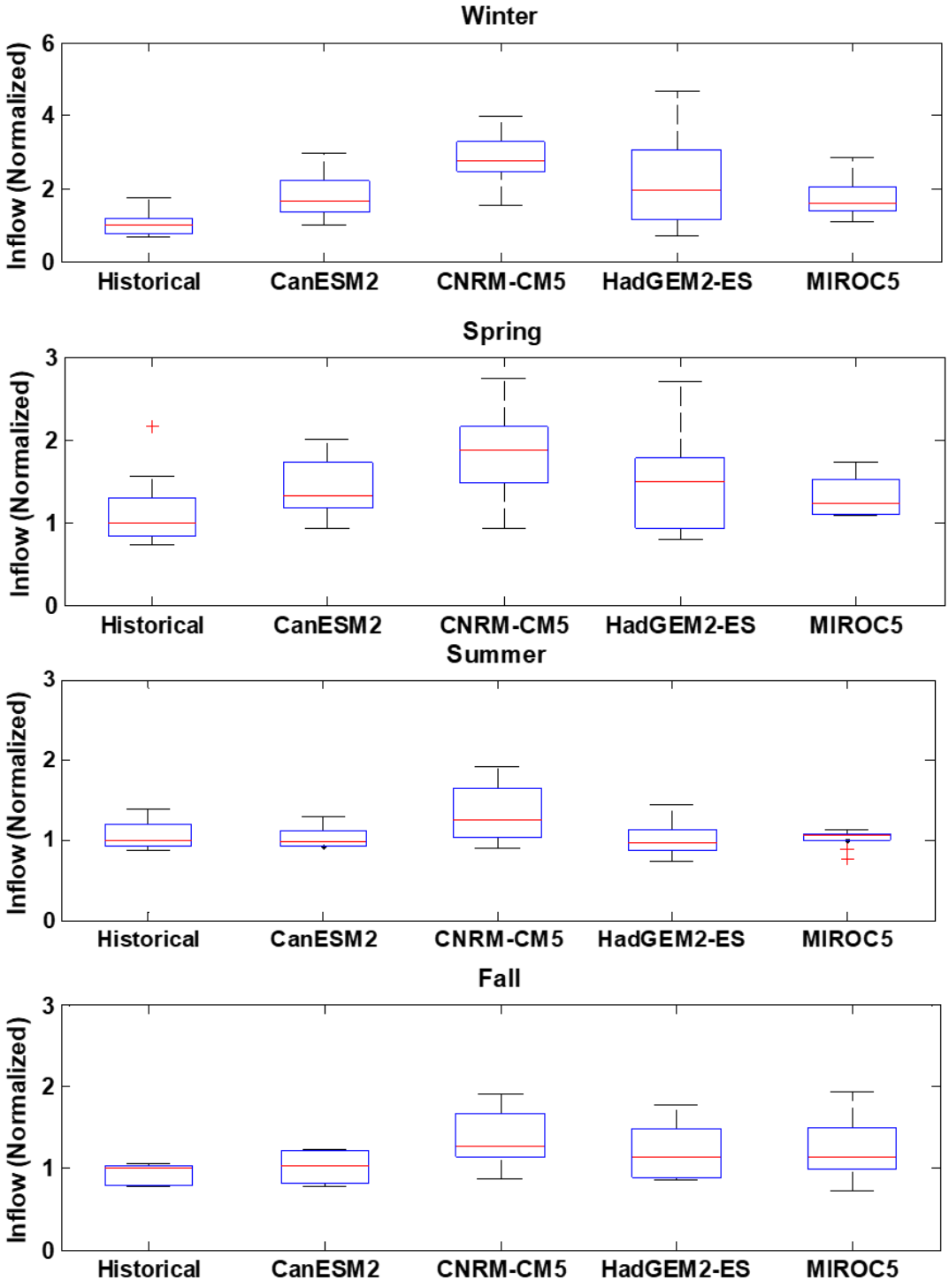

Each season is normalized based on the historical median for that season.

Source: Advanced Power and Energy Program, University of California, Irvine

For the historical period 2000-2009, it was found that the driest year received 73% of the 10-year average annual inflow, while the wettest year received 160%. Examining inflow variability at the seasonal scale, inflows during winter and spring are more variable from year to year compared to summer and fall, with the range for winter 2000-2009 being 65% to 170% of the 10-year average and for spring 87% to 255%. For all RCP 4.5 scenarios, interannual variability in inflow during winter and fall increases. Half of the scenarios—CNRM-CM5 and HadGEM2-ES—show increased variability for all seasons.

B.2.2. Generation Trends for RCP 4.5 Scenarios

Average annual generation increases for all models compared to the historical period: about 2% higher for CanESM2 and MIROC5, 8% for HadGEM2-ES, and 25% for CNRM-CM5 (Figure B-11). While total inflow increases, there is also increased spilling, which results in a more subdued generation response to increased precipitation and the resultant reservoir inflow. As discussed, inflow increases are not uniform across the year. Higher inflows during winter and spring result in increased spilling during those months, affecting the water available for hydroelectric generation in summer when inflow is low and hydropower units rely more heavily on stored capacity to provide power. The net impact is a significant difference between actual generation and the theoretical generation based solely on total flow through the hydropower unit (excluding auxiliary water demands).

Figure B-11: RCP 4.5 Generation Comparison to Historical Generation (100%) for Theoretical Generation Based on Total Inflow Versus Net Generation

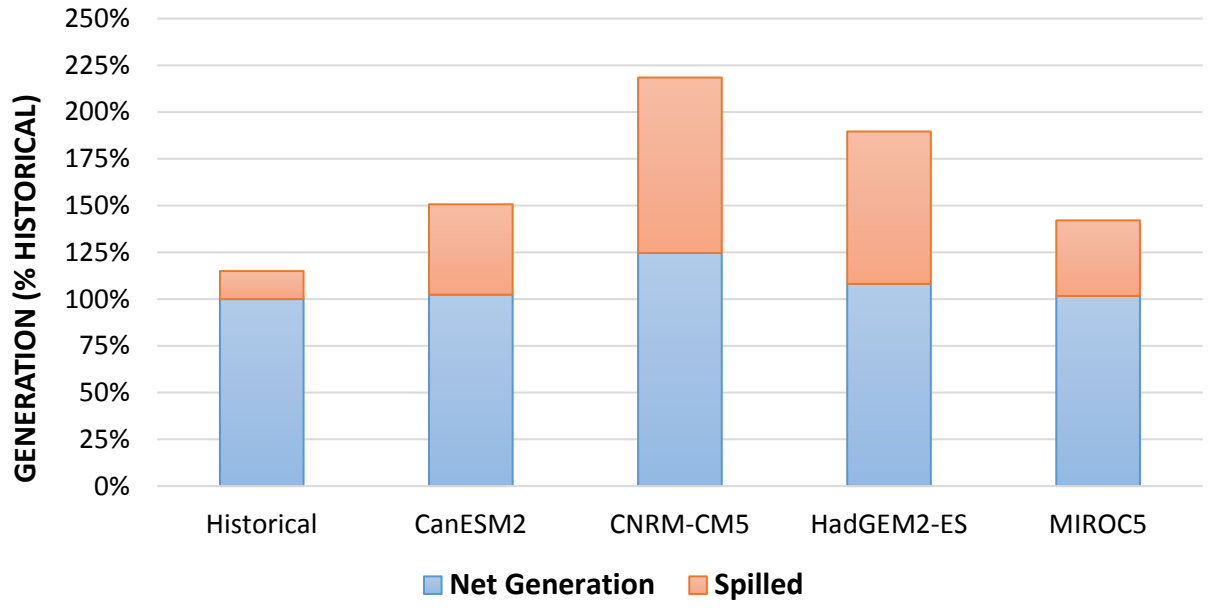

Spilled is the amount of generation lost due to spills. The sum of net generation and spilled is the total theoretical generation if available inflow was utilized for electricity generation.

Source: Advanced Power and Energy Program, University of California, Irvine

Examining the change in generation compared to historical levels by season, the amount by which generation changes is not uniform across the year. All RCP 4.5 scenarios indicate that generation will increase during the winter and spring. The climate models are divided whether this increase will persist through the summer and fall, with CanESM2 and MIROC5 showing slightly lower (less than 3%) generation during the summer and generation during the fall comparable to historical (Figure B-12).

Figure B-12: Average Seasonal Generation for All RCP 4.5 Scenarios Compared to Historical (100%)

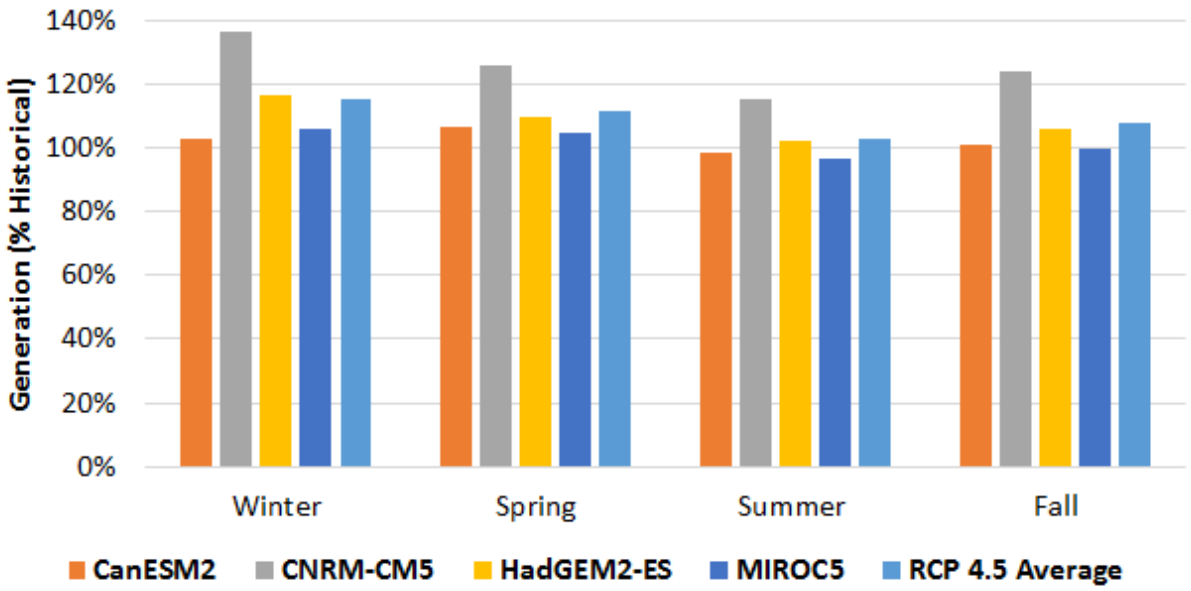

Source: Advanced Power and Energy Program, University of California, Irvine

Due to the variability of generation within a given season and across the 10 years, the research team also examined monthly trends were (Figure B-13). The average monthly generation for all models was higher than historical levels, with the exception of August through October for CanESM2 and July through October for MIROC5. The decrease for these months for CanESM2 and MIROC5 was less than 5% compared to historical. February through April had the highest increases in generation compared to historical for each model. Peak generation still occurs around May on average; however, all RCP 4.5 scenarios had higher average peak value for May compared to the historical period, ranging from 4% to 20% higher.

Figure B-13: Monthly Generation for All RCP 4.5 Scenarios-Mean and Range for 2046-2055

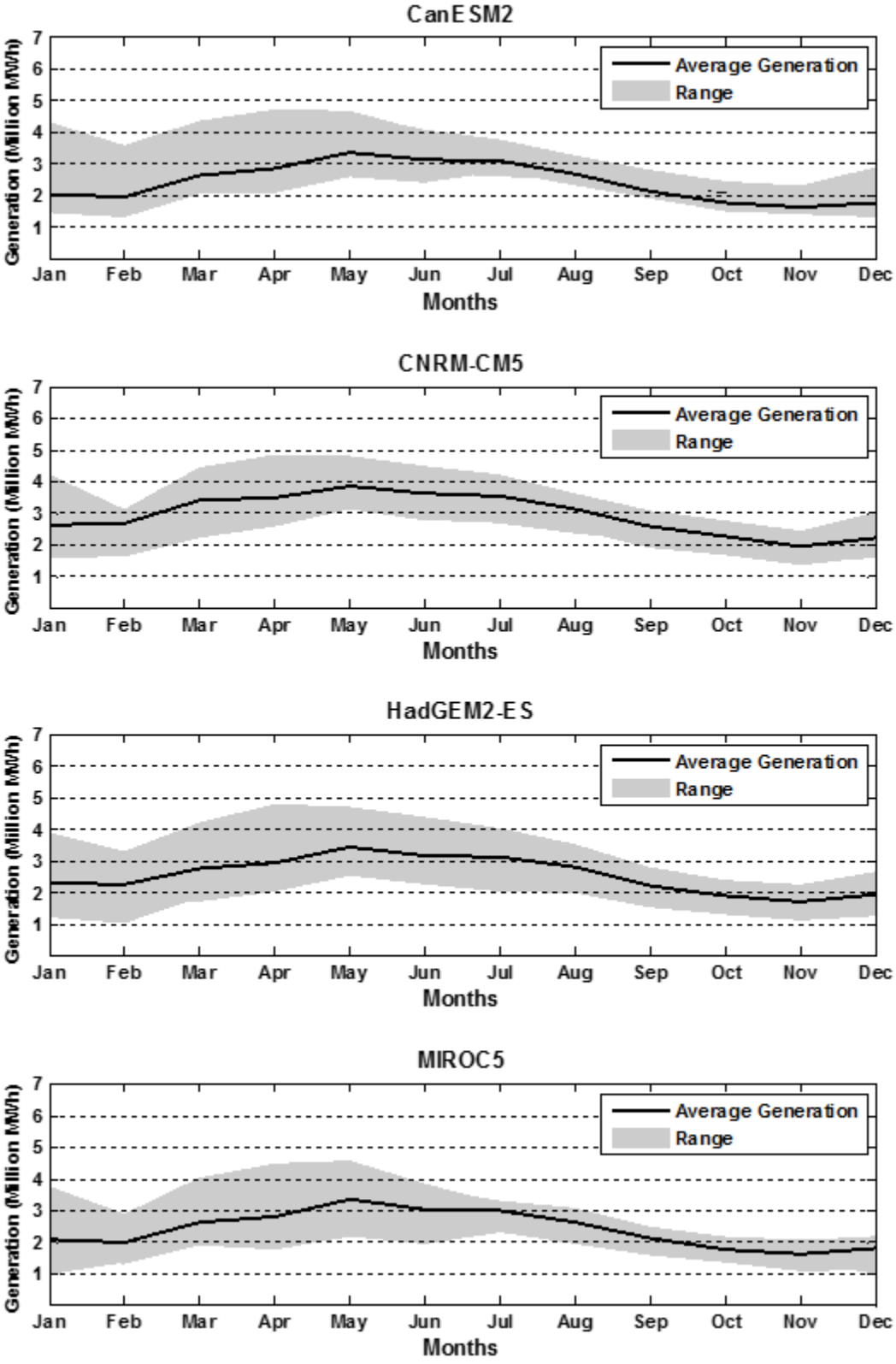

Source: Advanced Power and Energy Program, University of California, Irvine

The research team also investigated average monthly generation compared to average peak generation (Figure B-14). The average generation for each month across the 10-year period was divided by highest average monthly value (the month of May for all scenarios). This metric allows a comparison of scenarios with higher and lower monthly generation means to identify potential overarching trends. Historically, hydropower tends to peak in May, with generation staying high through August, around 90-95% of peak generation. Generation then tends to decrease in fall, reaching a minimum around November and staying low through February, at which point it begins increasing again.

Figure B-14: Average Monthly Generation Compared to the Annual Peak for Historical and All RCP 4.5 Scenarios

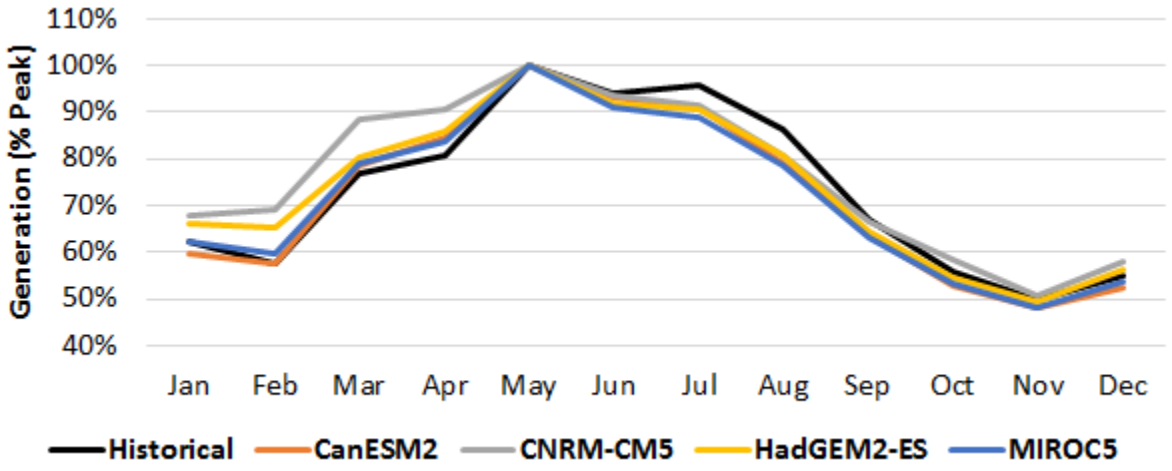

Source: Advanced Power and Energy Program, University of California, Irvine

Examining the RCP 4.5 model projections for 2046-2055, generation compared to peak during fall remains near historical levels. In winter and spring, generation compared to peak is higher than the historical pattern for all scenarios. This shift can be attributed to increased average inflow during these months, with each scenario showing an increase correlated with the average increase in inflow. For example, CNRM-CM5, which has the highest average inflow increase compared to historical, shows the greatest increase in generation compared to the peak. (It also has the largest overall peak.)

For all RCP 4.5 scenarios, peak generation is not sustained throughout the summer, dropping down to about 80% of peak by August (6% lower than historical). This shift is the result of higher winter and spring inflow followed by summer inflow around historical levels: peak generation increases, while generation during summer remains around the historical average, resulting in a lower ratio. The one exception is CNRM-CM5, which experiences higher average generation for all months compared to historical. For CNRM-CM5, the greatest increases are experienced in the winter (up 43%) and the lowest increase in August (12%).

Despite increased precipitation earlier in the year, hydropower units are not able to retain it until summer. Higher inflow during the winter and spring results in increased spilling. Therefore, not enough of the increased inflow is retained into summer to overcome the

relatively lower summer inflow values, and generation appears lower in the summer compared to peak. The net result of the changes between months is that a greater portion of a given year's hydropower generation is produced earlier in the year, and less of the year's generation is produced during the summer months.

B.2.3. Spinning Reserve Bidding Under RCP 4.5

Average annual spinning reserve bidding decreases by about 14%, with average bidding decreasing for all seasons for all RCP 4.5 scenarios (Figure B-15). All scenarios show the same seasonal trend: spring experiences the greatest average reduction (-25% to -15% compared to historical) for all RCP 4.5 scenarios, with the remaining seasons experiencing spinning reserve bidding reduction by -17% to -9%. Of the four scenarios, CNRM-CM5 has the greatest reduction in spinning reserve bidding. This result was expected, given that CNRM-CM5 had the greatest increase in generation and the two types of bidding are inversely related. If a hydropower chooses to bid into the energy market, that dedicated capacity is no longer available for spinning reserve, and vice versa. This relationship was seen in the historical baseline.

Figure B-15: Average Spinning Reserve Bidding Compared to Historical for RCP 4.5 Scenarios

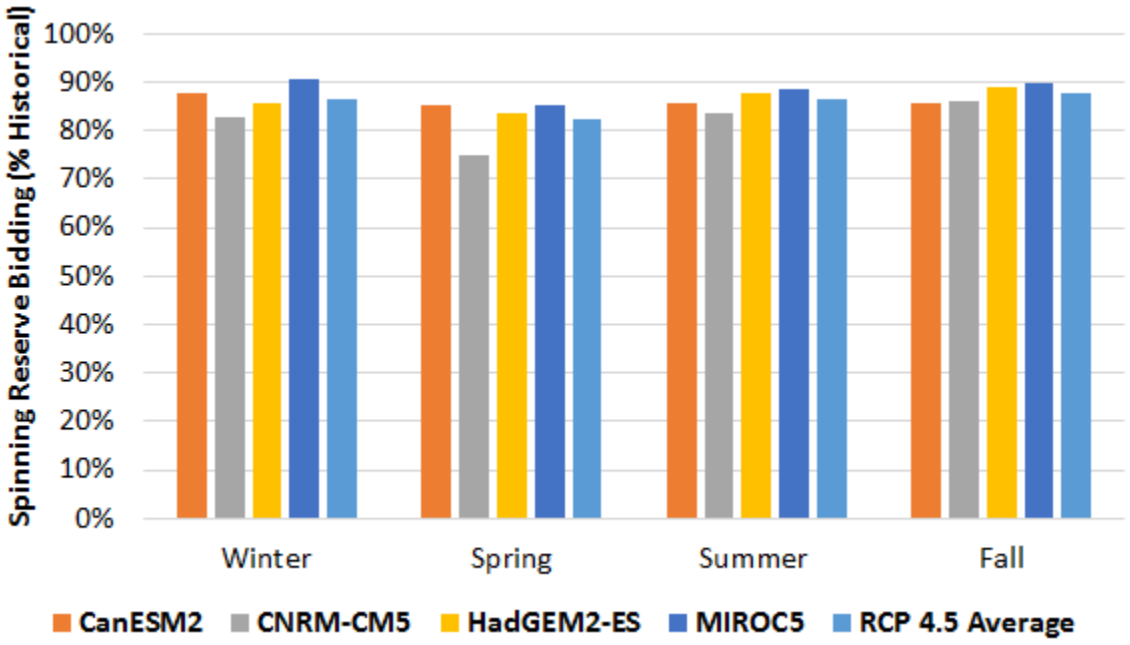

Source: Advanced Power and Energy Program, University of California, Irvine

Yet, there is another factor that contributed to the average decline in spinning reserve bids observed for all the RCP 4.5 scenarios. In addition to spinning reserve bidding being secondary to generation bids, spinning reserve bids occur after reservoir outflow demand is satisfied, and therefore, under flood and drought conditions, outflow and reservoir level constraints may restrict spinning reserve bidding.

A comparison between generation commitments and spinning reserve bidding for the RCP 4.5 scenarios versus the historical scenario is made in Fibure B-15 to illustrate the two factors

contributing to decreased spinning reserve potential. Firstly, Figure B-16 shows that the average total generation bid is larger compared to the historical baseline. The increase in capacity bid as generation results in a lower potential for spinning reserve bidding. This difference is most significant for CNRM-CM5. Secondly, it shows that all RCP 4.5 scenarios experience an increased number of days where dispatchable hydropower units bid below the associated rated capacity. These two changes result in an overall decrease in spinning reserve potential for all RCP 4.5 scenarios.

Figure B-16: Daily Average Spinning Reserve Bids Versus Generation Bids for All RCP 4.5 Scenarios

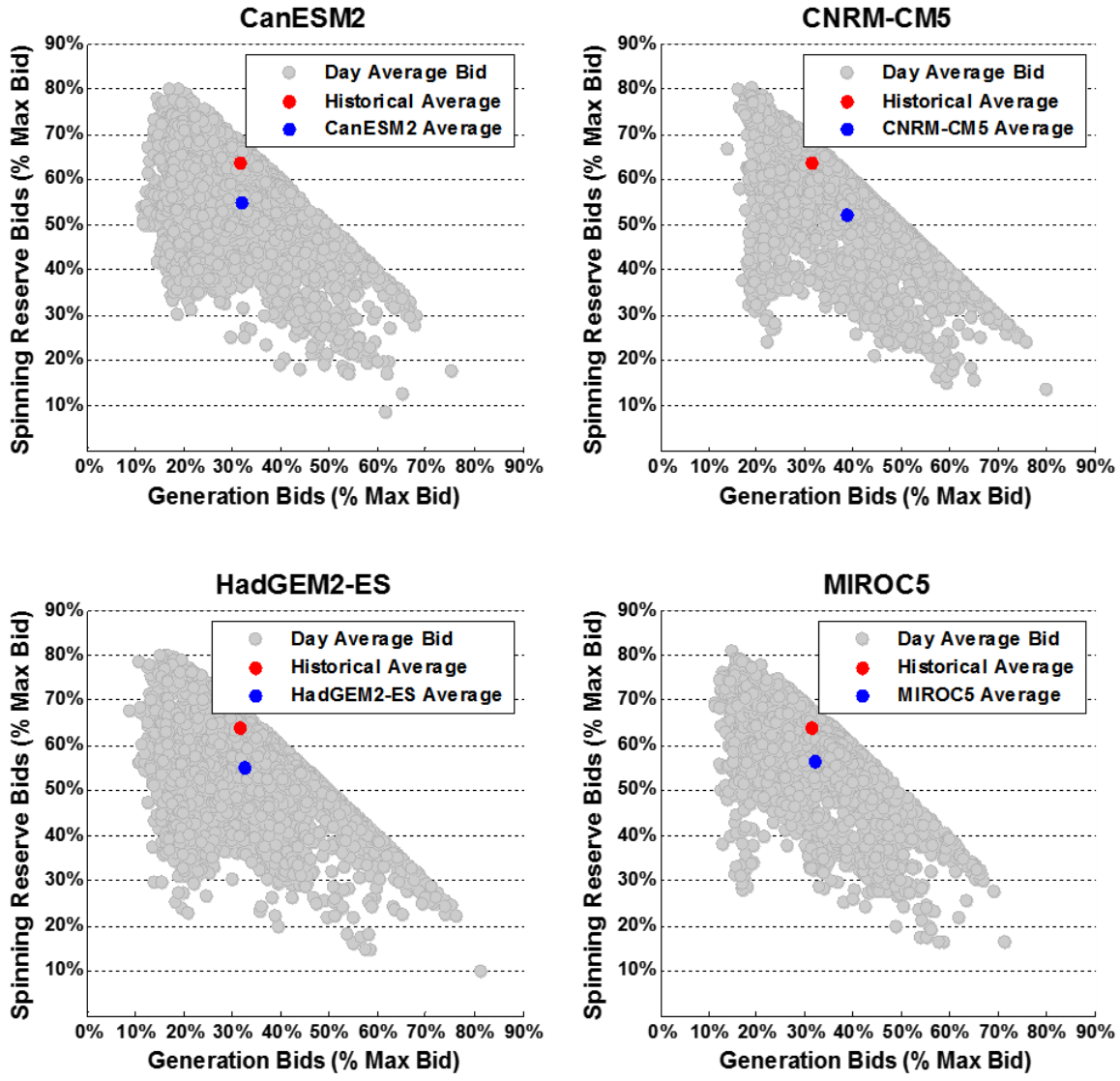

Year 2000-2009 for historical, 2046-2055 for climate change.

Source: Advanced Power and Energy Program, University of California, Irvine

B.3. Chapter 4 Auxiliary Results

This section presents auxiliary results for the Chapter 4 analysis. While the main text of Chapter 4 and the subsequent analyses focus on the combined residential and commercial sector results, the individual results for residential and commercial sectors are presented here.

B.3.1. Residential Sector Impacts

The impact of climate change conditions on the annual electric load demand of the residential sector is presented in Figure B-17 for percentage change between the climate change conditions and the historical conditions (Base) and in Figure B-18 for absolute magnitude of the load.

Figure B-17: Climate Change Impacts on Annual Electric Load Demand in Percentage Change From the Base Case for Different Climate Models and Climate Scenarios

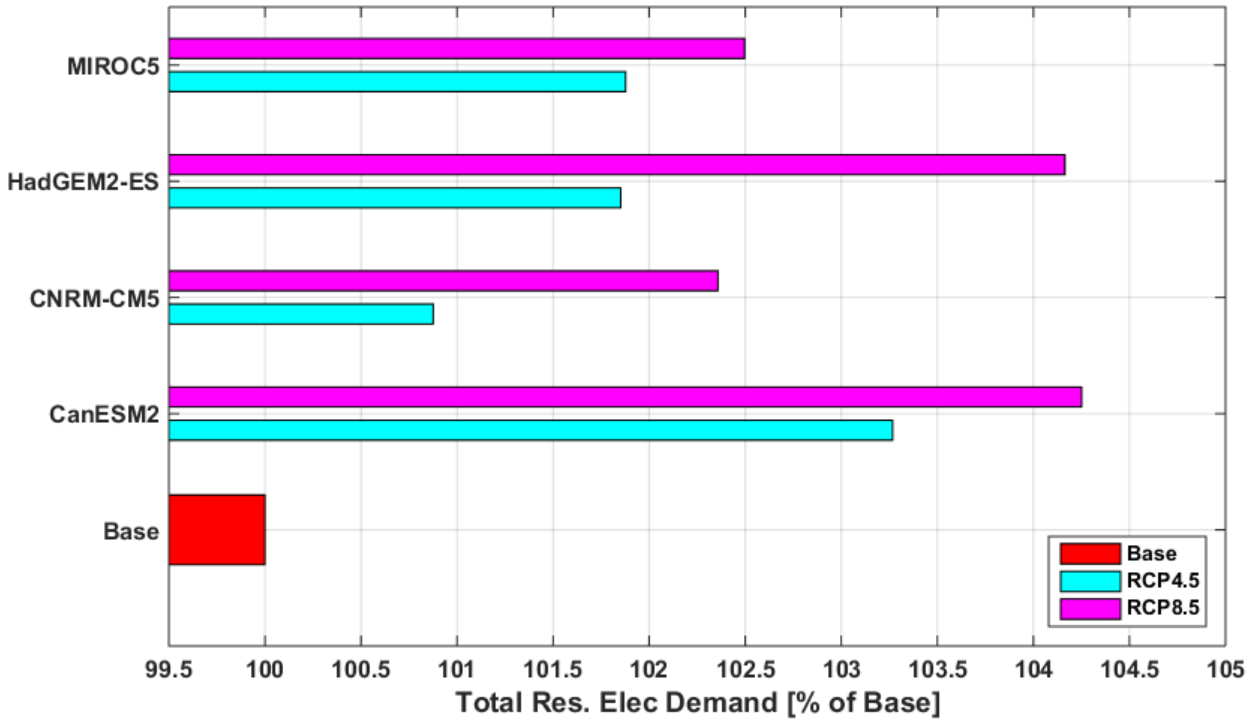

Source: Advanced Power and Energy Program, University of California, Irvine

Figure B-18: Climate Change Impacts on Annual Electric Load Demand in Absolute Magnitude for Different Climate Models and Climate Scenarios

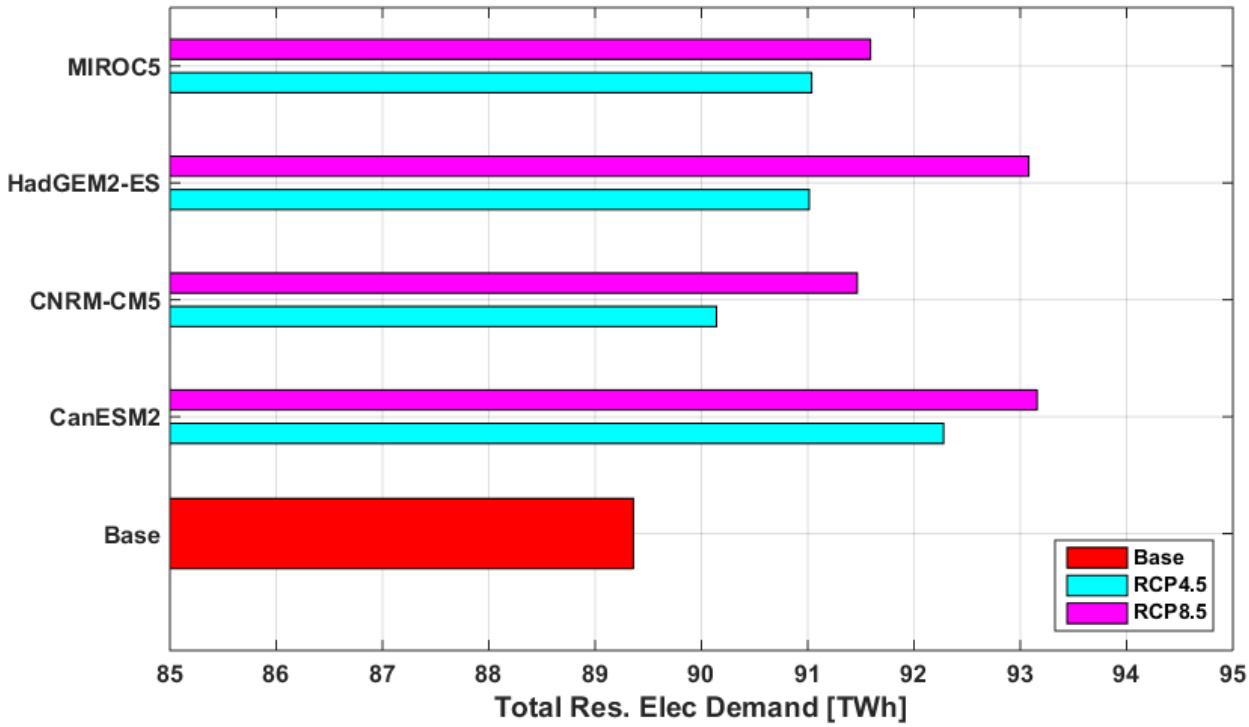

Source: Advanced Power and Energy Program, University of California, Irvine

For the residential sector, the electric load demand increases due to climate change by between 0.9 to 3.3% for the RCP 4.5 climate scenario and 2.4% to 4.3% for the RCP 8.5 climate scenario, depending on climate model. In absolute terms, this translates to increases of between 0.78 to 2.92 TWh for the RCP 4.5 cases and between 2.11 to 3.80 TWh for the RCP 8.5 cases. The RCP 8.5 scenarios have increased temperatures relative to the RCP 4.5 cases due to larger greenhouse gas concentrations and radiative forcing in the atmosphere, resulting in higher temperatures. Across climate models within a given climate scenario, the CanESM2 climate model tends to have the highest increases in electric loads temperatures, and the CNRM-CM5 climate scenario has the lowest increases for the RCP 4.5 and RCP 8.5 climate scenarios. These increases are linked exclusively to increases in space cooling loads due to increased temperatures, which occur across all the building climate zones in California because space cooling loads are met entirely through electric energy input. The change in cooling degree days between the historical and climate change conditions corresponding to each building climate zone is presented in Figure B-19 for the RCP4.5 and in Figure B-20 for RCP 8.5. These results represent the average across the climate models for each climate scenario, and the cooling degree days are calculated using a reference temperature of 18˚C.

Figure B-19: Shift in Annual Cooling Degree Days by Climate Zone - RCP 4.5 Scenario

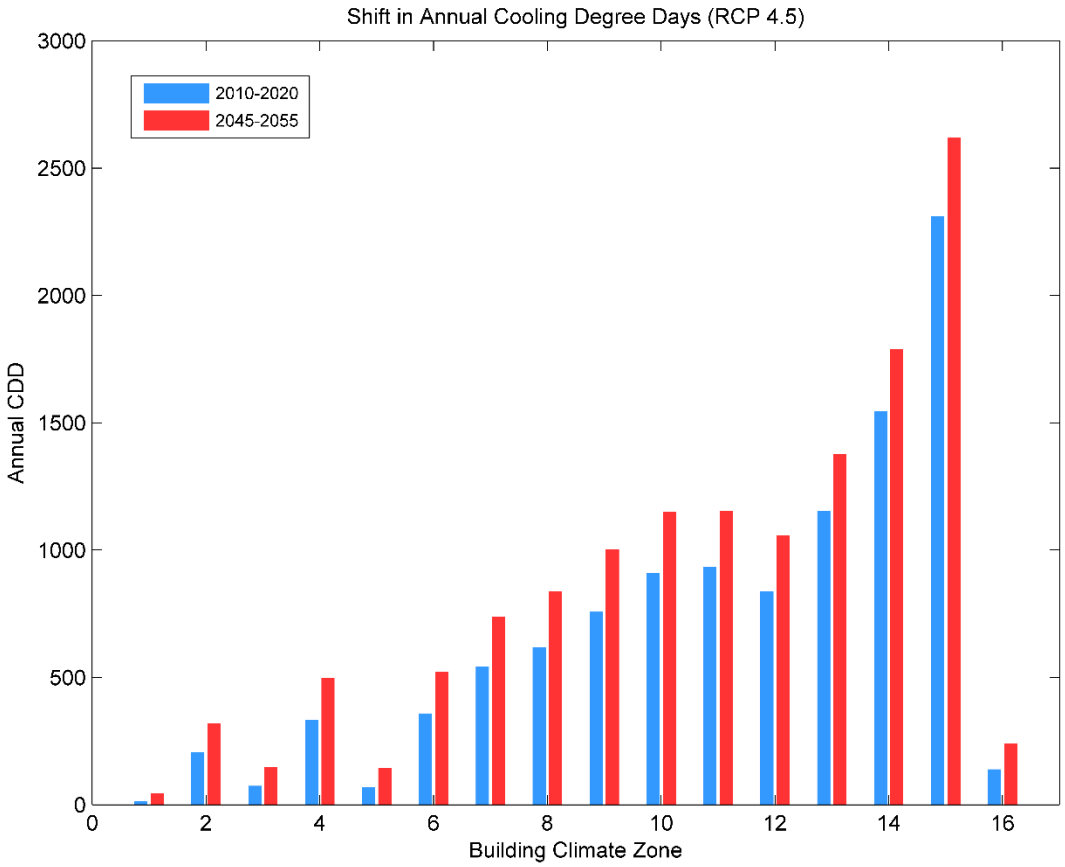

Source: Advanced Power and Energy Program, University of California, Irvine

Figure B-20: Shift in Annual Cooling Degree Days by Climate Zone - RCP 8.5 Scenario

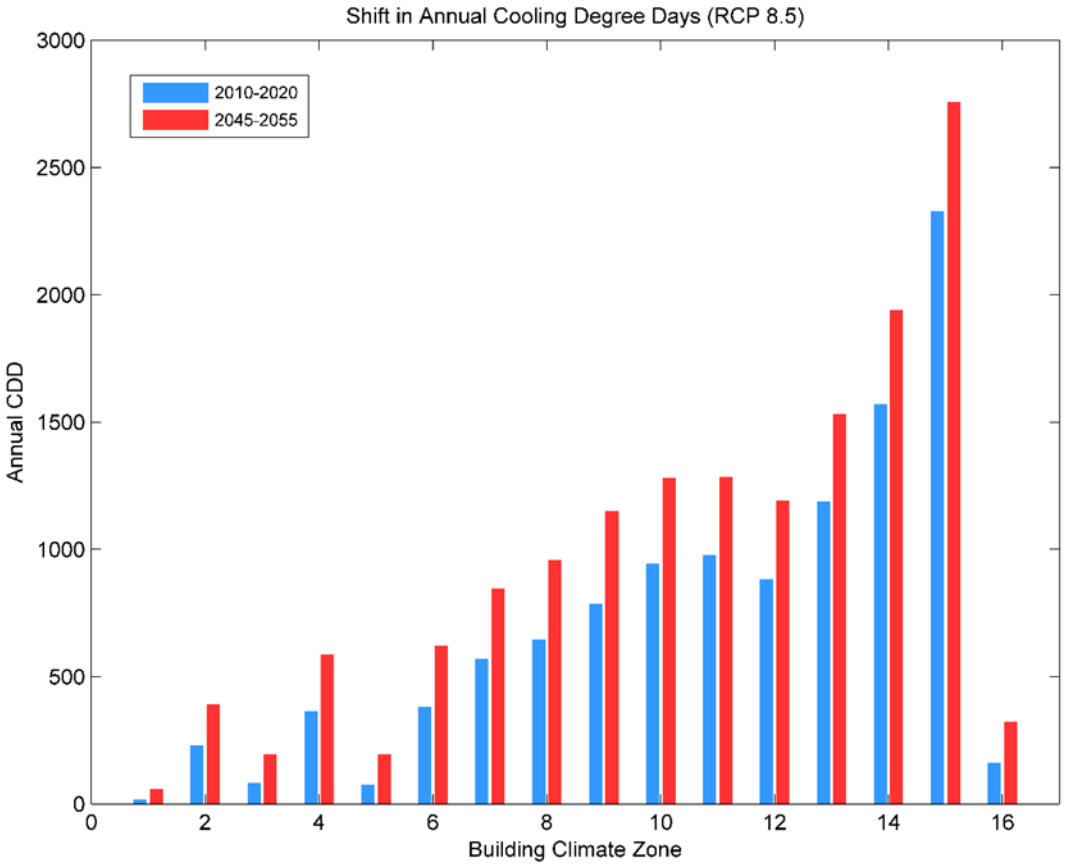

Source: Advanced Power and Energy Program, University of California, Irvine

The increase in temperatures that drive increases in space-cooling loads also affect peak electric loads in residential buildings. For this sector, the highest loads tend to occur during the early evening hours, when people return home from work between 5 and 7 p.m. During the summer, this period still falls within the daylight hours and exhibits the use of residential cooling systems. Therefore, increased temperatures due to climate change also manifest in increased peak electric loads due to the increased energy use of residential cooling systems during the time of residential load peaks. A time series snapshot of the electric load profile of residential buildings under historical climate and climate change-impacted conditions for the RCP 8.5 climate scenario is presented in Figure B-21 for each climate model and in Figure B-22 for the climate model average.

Figure B-21: Residential Sector Electric Load Profiles Under Climate Change for Each Climate Model Under the RCP 8.5 Climate Scenario

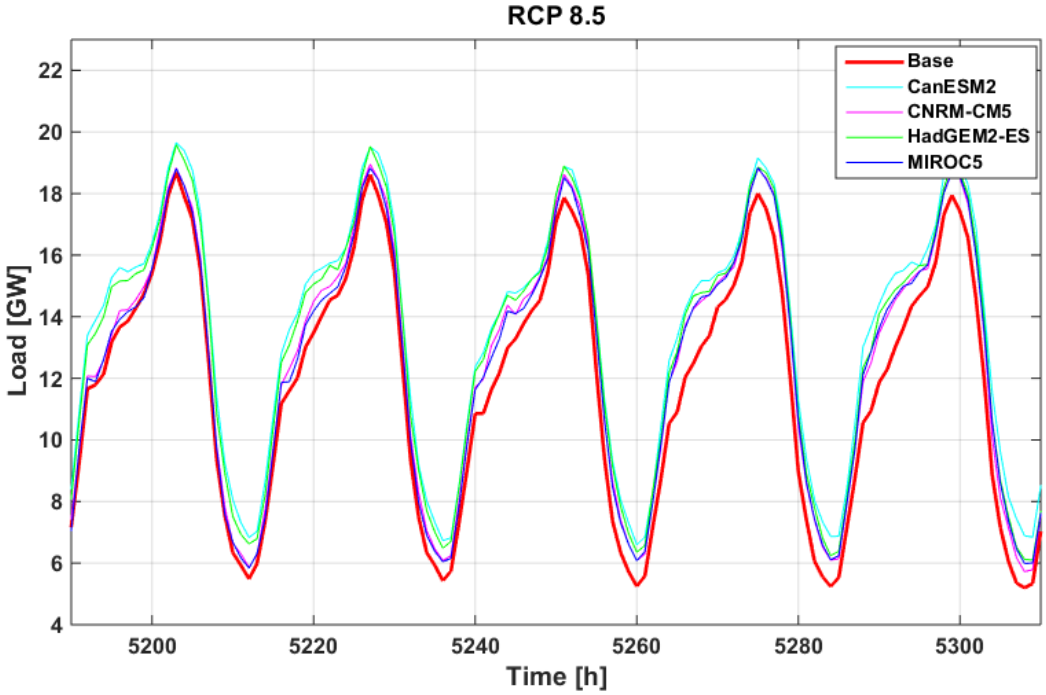

Source: Advanced Power and Energy Program, University of California, Irvine

Figure B-22: Residential Sector Electric Load Profiles Under Climate Change for the Climate Model Average Under the RCP 8.5 Climate Scenario

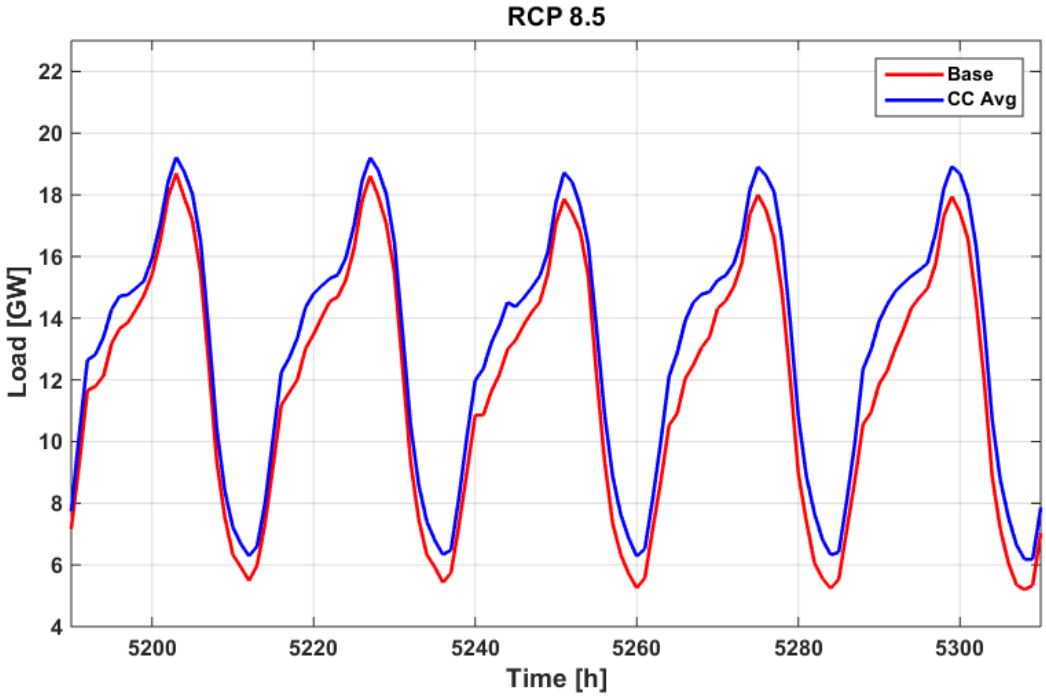

Source: Advanced Power and Energy Program, University of California, Irvine

These snapshots are during the summer, where cooling systems tend to be running the entire day in certain climate zones due to heat waves. Therefore, increases in cooling loads are present to varying extents the entire day. The impact of climate change-affected temperatures on typical residential sector peak hourly electric loads are presented in Figure B-23 for percentage change from historical conditions (Base) and in Figure B-24 for absolute magnitudes. Because the climate conditions are derived from an average between 2046 and 2055 in the climate models to derive a *representative* 2050 profile, these are termed as *typical hourly peak electric demands*.

Figure B-23: Climate Change Impacts on Peak Hourly Electric Load Demand in Percentage Change From the Base Case for Different Climate Models and Climate Scenarios

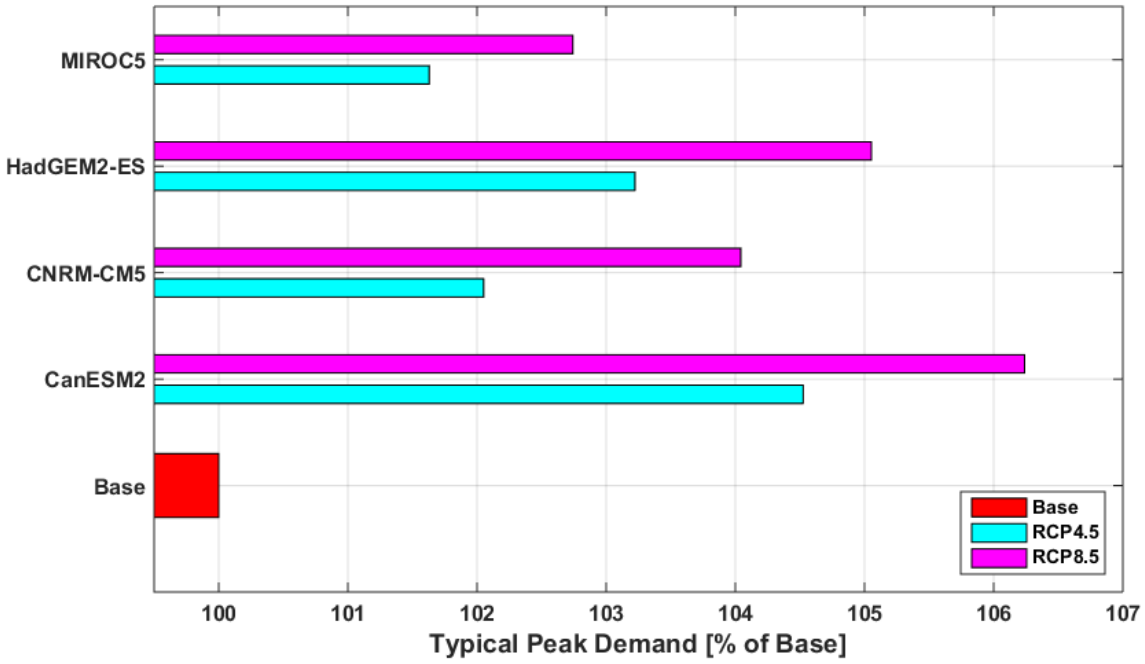

Source: Advanced Power and Energy Program, University of California, Irvine

Figure B-24: Climate Change Impacts on Peak Hourly Electric Load Demand in Absolute Magnitude for Different Climate Models and Climate Scenarios

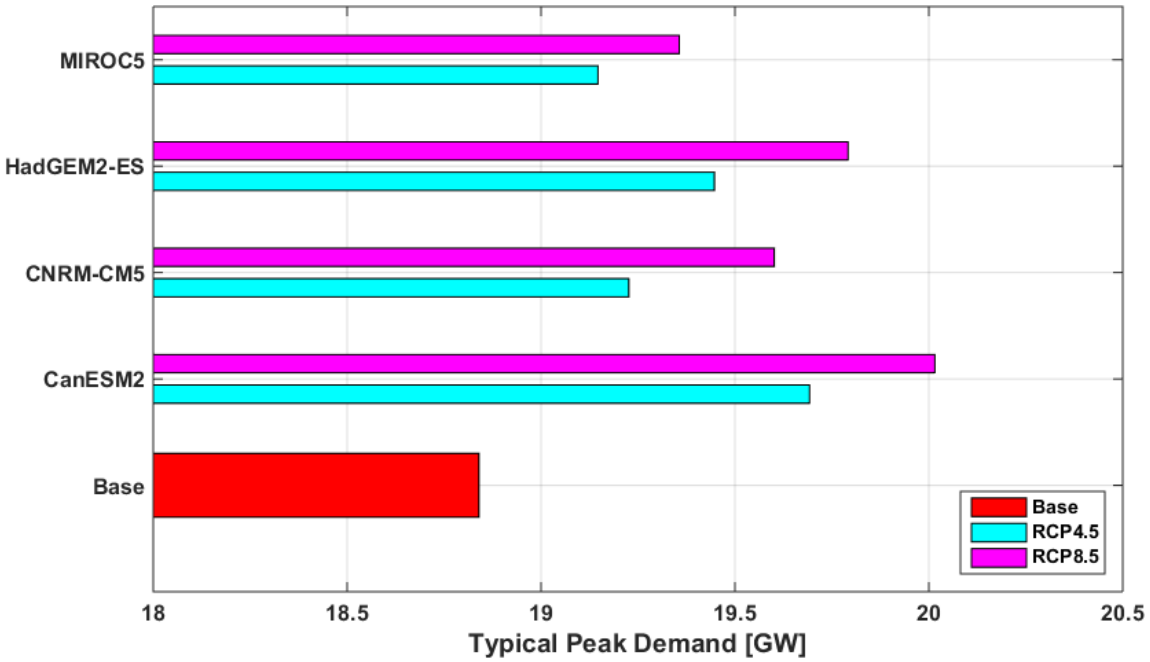

Source: Advanced Power and Energy Program, University of California, Irvine

For the residential sector, the electric load demand increases due to climate change by between 1.6% to 4.5% for the RCP 4.5 climate scenario and 2.7% to 6.2% for the RCP 8.5 climate scenario, depending on climate model. In absolute terms, this translates to increases of between 0.31 to 0.85 GW for the RCP 4.5 cases and between 0.52 to 1.18 GW for the RCP 8.5 cases. As expected, the RCP 8.5 cases have higher peak electric loads due to higher temperatures, and the CanESM2 climate model tends to have the highest peak load increases. In contrast to the results for annual electric demand, however, the MIROC5 climate model tends to have the lowest increases in peak loads.

The impact of climate change conditions not only affects the electric load shapes and magnitudes of the residential sector, but the site-level energy demands that may use energy inputs other than electricity. Residential buildings in California can use natural gas or fuel oil for water heating and space heating in addition to electricity, and the impacts of climate change affect these end uses as well. Therefore, to obtain a sense of how climate change impacts the overall energy footprint of the residential sector, it is important to characterize the impacts on energy demands by end use and fuel type. For the residential sector, the annual site-level energy use under historical climate conditions and climate change-impacted conditions by end use is presented in Figure B-25. The end uses considered are space cooling, space heating, and water heating. The “other” category refers to other loads within residential buildings such as appliances and plug loads, which do not vary significantly with external building conditions.

Figure B-25: Annual Site Level Residential Energy Demand in Million MMBTU by End Use

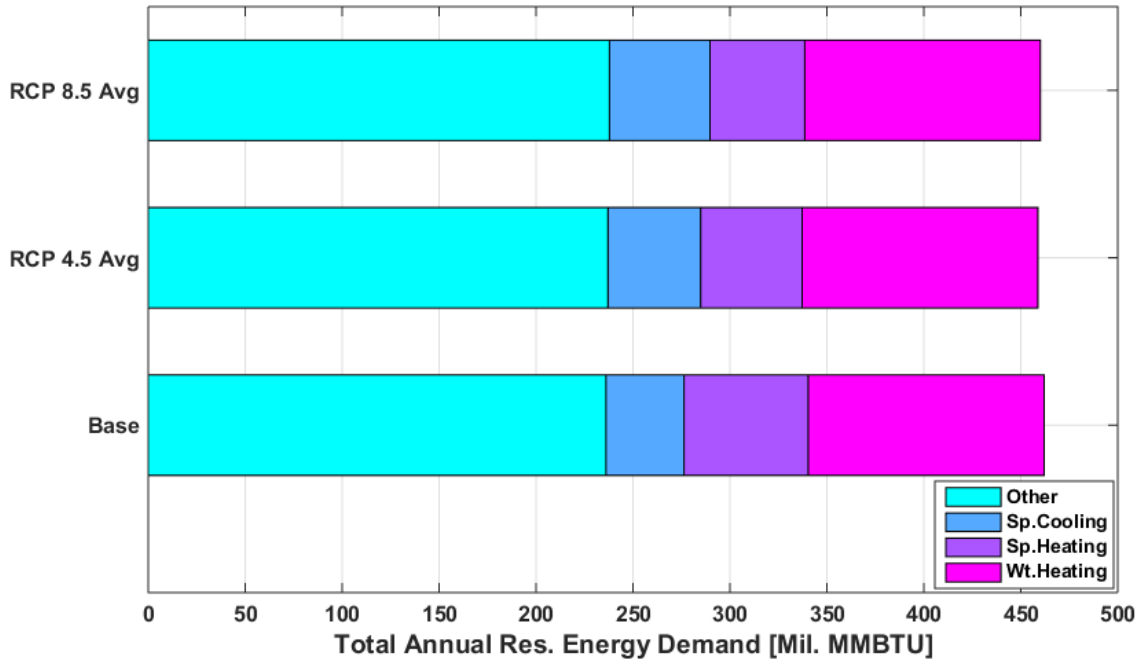

Sp. Cooling = Space Cooling, Sp. Heating = Space Heating, and Wt. Heating = Water Heating.

Source: Advanced Power and Energy Program, University of California, Irvine

Relative to the historical climate conditions, the onset of climate change actually reduces the overall site-level energy footprint of the residential sector. While the increased temperatures will increase electric energy consumption due to increased space cooling loads, especially during the summer season, the increased demand end up being offset by the decrease in space heating energy demands, which occur typically during the winter seasons. The overall effect is to decrease slightly the annual site-level residential energy demand under climate change compared to the base case. The values from the individual climate models were averaged with equal weight to provide a representative climate change effect. In general, the hotter models (CanESM2 and HadGEM2-ES) showed larger decreases in space heating demands and increases in space cooling demands compared to the average. This effect occurs because the energy needs for providing a given unit of cooling are lower than those for providing a given unit of heating due to the systems used to provide heating as compared to cooling. In California, the vast majority of the space heating energy demands are met using natural gas boilers. Natural gas boilers convert fuel input to heat with an efficiency of about 85%. Space-cooling needs, however, are met using vapor compression cooling cycles with a coefficient of performance (COP) typically of about 3. This means that one unit of electric energy input meets three units of space cooling energy demand, whereas one unit of natural gas fuel input meets 0.85 units of space heating demand. Therefore, reductions in heating demand have a larger impact on site-level energy demand than a similar magnitude increase in cooling energy demand. This refers to site-level energy demand, not source-level energy demand. The impact on source-level energy

demand will depend on the primary energy resources used to produce the electric energy inputs to the cooling system.

The change of site-level energy demand by end use under climate change is presented in Figure B-26 in percentage change from base and in Figure B-27 for absolute magnitude changes.

Figure B-26: Climate Change Impacts on Annual Site-Level Energy Demand by End Use in Percentage Change From the Base Case for Different Climate Scenarios

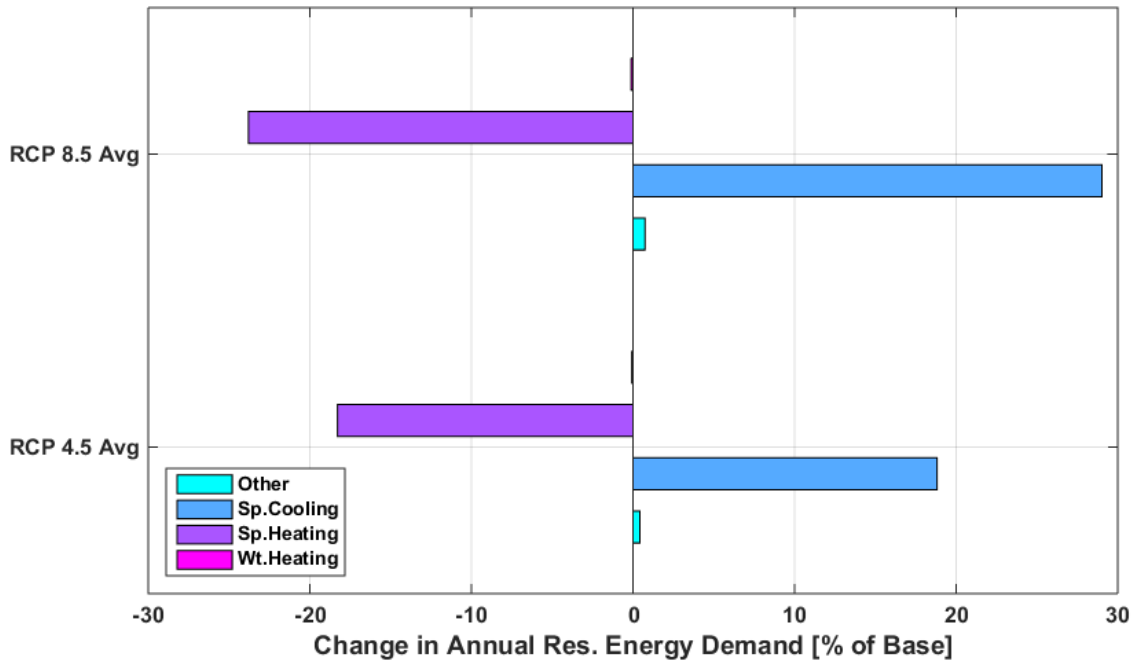

Source: Advanced Power and Energy Program, University of California, Irvine

Figure B-27: Climate Change Impacts on Annual Site-Level Energy Demand by End Use in Absolute Magnitude From the Base Case for Different Climate Scenarios

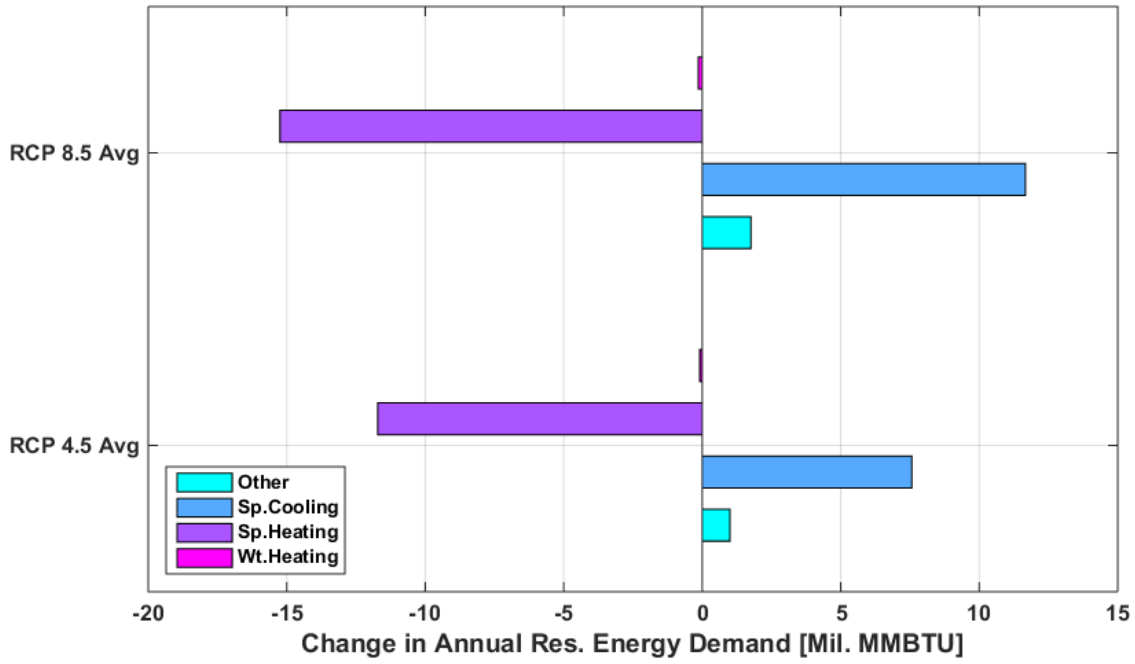

Source: Advanced Power and Energy Program, University of California, Irvine

By examining the end-use changes, the research team finds that the residential sector exhibits decreases in space-heating energy demand, increases in space-cooling energy demand, slight increases in other energy demands, and very small decreases in water-heating energy demands. The decreases in space-heating demands are larger than the increases for space-cooling demands in absolute terms. Relative to the respective base case values, space-cooling loads are increased between 18.82% and 29.02%, and space-heating loads are decreased between 18.29% and 23.79%.

The increase in space-cooling energy demands and the decrease in space-heating and water-heating demands have the effect of shifting the distribution of energy use by fuel type toward electricity. The annual site-level energy demand for the residential sector is presented in Figure B-28.

Figure B-28: Climate Change Impacts on Annual Site-Level Energy Demand by Fuel Type in Absolute Magnitude From the Base Case for Different Climate Scenarios

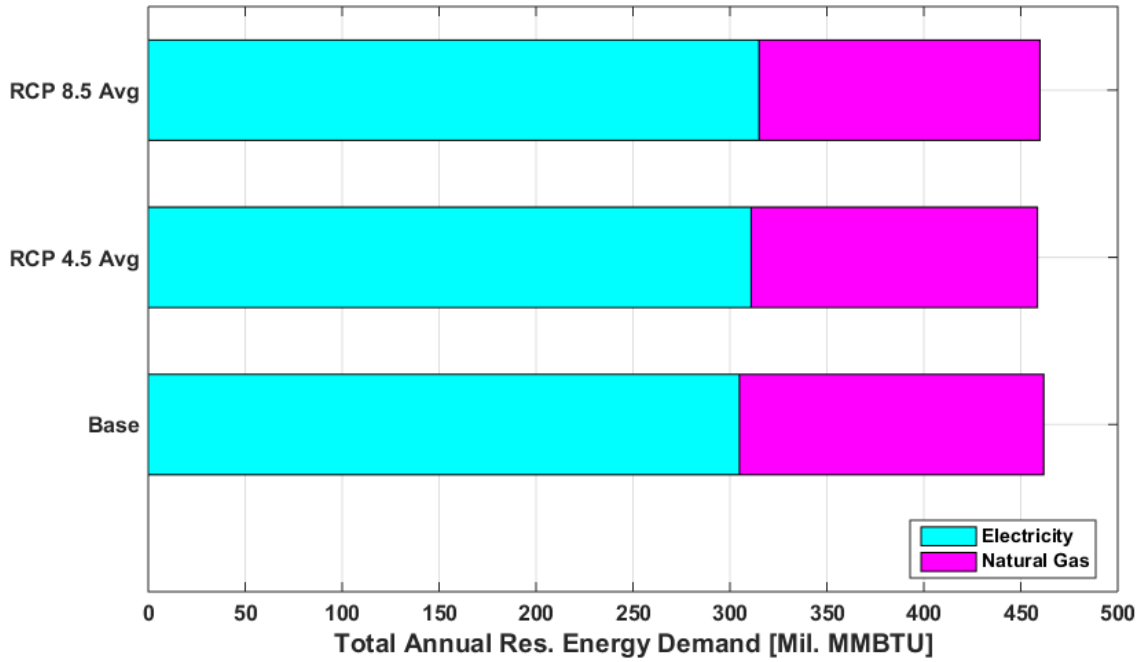

Source: Advanced Power and Energy Program, University of California, Irvine

The effect is slight, but the onset of climate change causes homes to increase reliance on electricity and decrease reliance on natural gas. Fuel oil is not plotted here because it is a negligible fraction of the energy use in the residential sector in this analysis.

In addition to the statewide impacts of climate change on the residential sector, the impacts of climate change vary across climate zone and location. The annual residential electricity demand by climate zone is presented in Figure B-29, and the change from historical climate conditions (Base) is presented in Figure B-30.

Figure B-29: Annual Residential Electric Demand by Climate Zone Under Climate Change - Absolute Magnitude

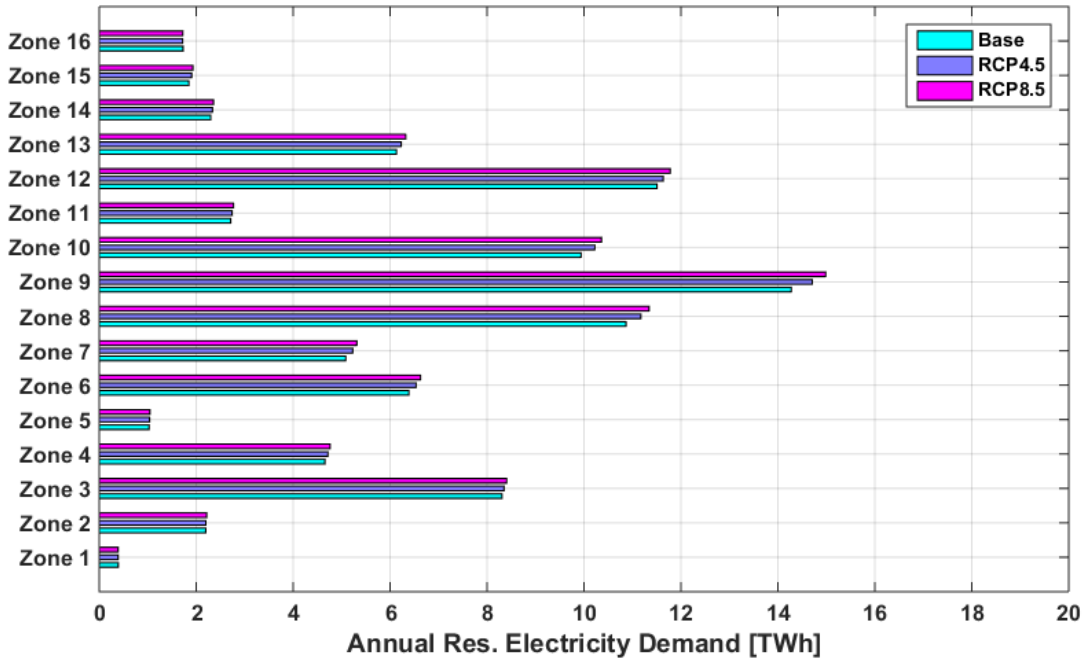

Source: Advanced Power and Energy Program, University of California, Irvine

Figure B-30: Annual Residential Electric Demand by Climate Zone Under Climate Change - Percentage Change From Base

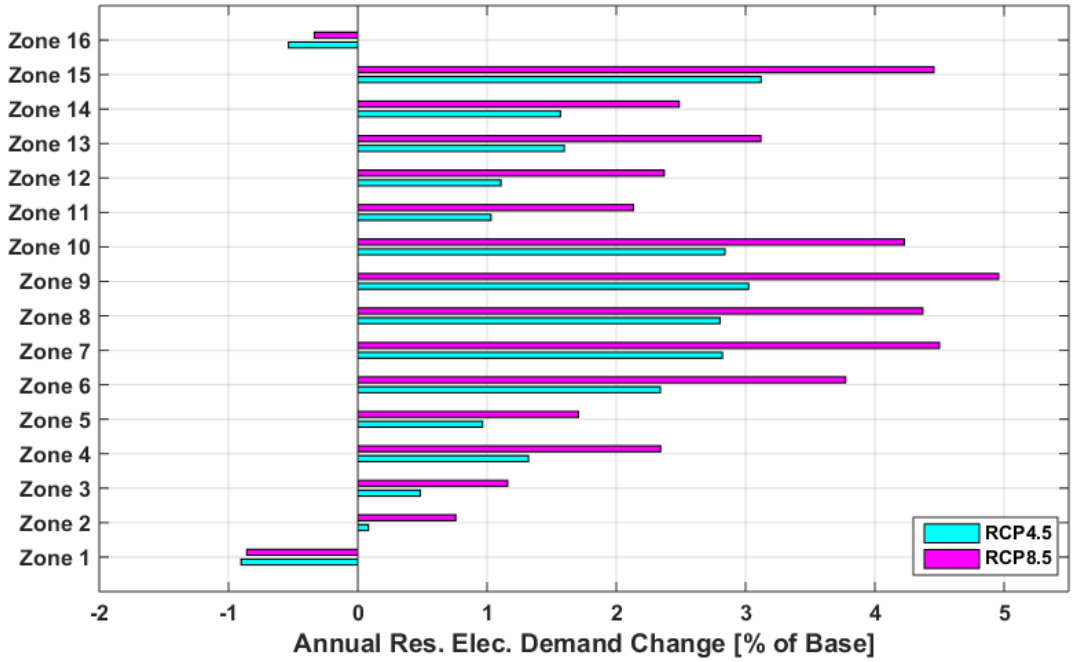

Source: Advanced Power and Energy Program, University of California, Irvine

The largest percentage increases in electricity demand occur in Climate Zones 6, 7, 8, 9, 10, and 15 for both RCP 4.5 and RCP 8.5 climate scenarios. Climate Zones 6-10 are all in Southern California, encompassing the heavily populated coastal and slightly inland areas of the state. These zones have high absolute electricity demand due to population. Climate Zone 15 is California's southeastern desert regions, which have low absolute population but are subjected to extreme heat waves which that cause high-percentage increases in electricity demand. There are two climate zones – Zone 1 (the North Coast) and Zone 16 (mountainous areas) – that exhibit decreases in electricity consumption. Overall, however, these results show that the largest increases in electricity demand, even on a percentage change basis, will occur in heavily populated areas of the state, focused in Southern California.

B.3.2. Commercial Sector Impacts

The impact of climate change conditions on the annual electric load demand of the commercial sector is presented in Figure B-31 for percentage change between the climate change conditions and the historical conditions (Base) and in Figure B-32 for absolute magnitude of the load.

Figure B-31: Climate Change Impacts on Annual Electric Load Demand in Percentage Change From the Base Case for Different Climate Models and Climate Scenarios

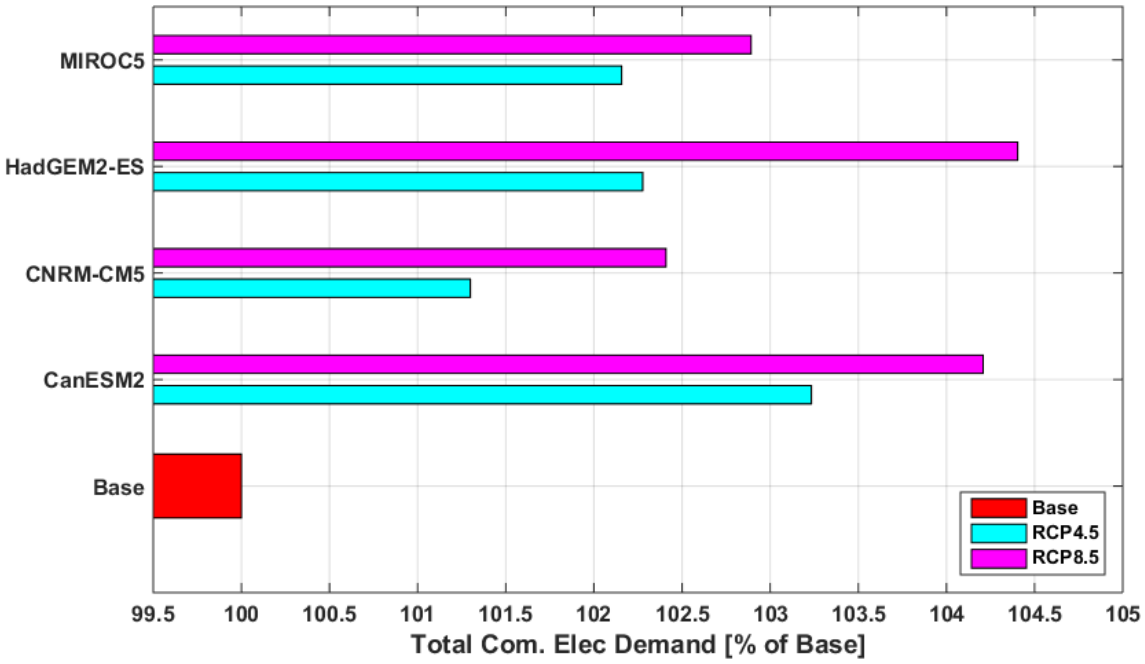

Source: Advanced Power and Energy Program, University of California, Irvine

Figure B-32: Climate Change Impacts on Annual Electric Load Demand in Absolute Magnitude for Different Climate Models and Climate Scenarios

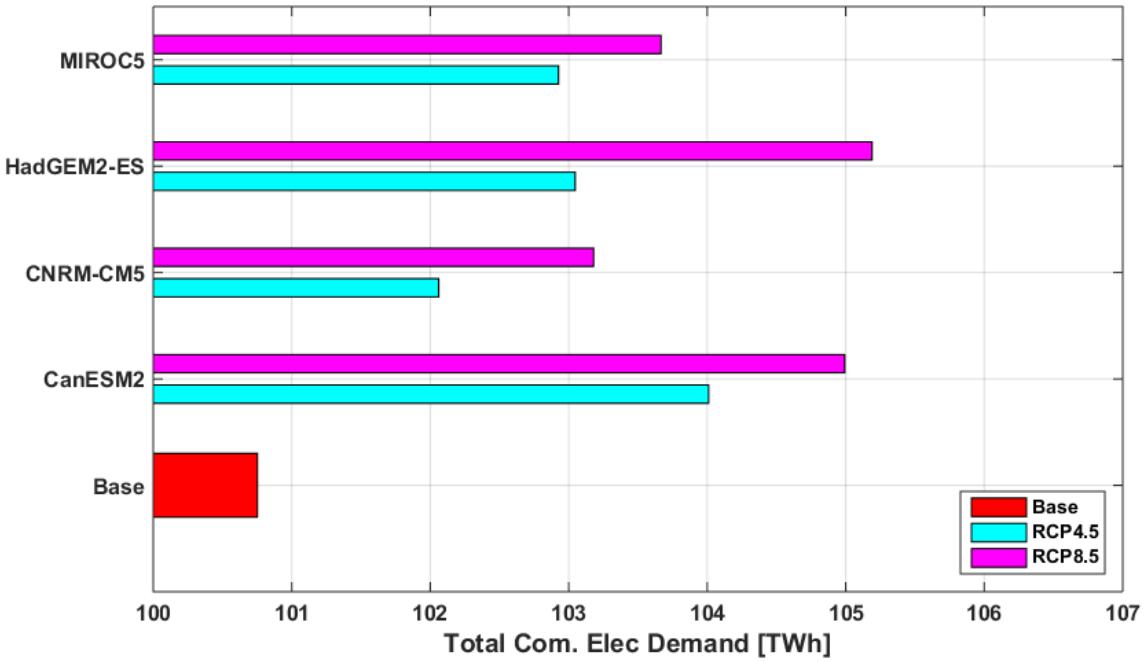

Source: Advanced Power and Energy Program, University of California, Irvine

For the commercial sector, electric load demand increases between 1.3% and 3.2% due to climate change for the RCP 4.5 climate scenario and between 2.4% and 4.4% for the RCP 8.5 climate scenario, depending on climate model. In absolute terms, these load demand increases translate to increases between 1.30 and to 3.20 TWh for the RCP 4.5 cases and between 2.40 and 4.40 TWh for the RCP 8.5 cases. The RCP 8.5 scenarios have increased temperatures relative to the RCP 4.5 cases due to larger greenhouse gas concentrations and radiative forcing in the atmosphere, resulting in higher temperatures. The CanESM2 climate model tends to have the highest increases in electric loads in the RCP 4.5 climate scenario; however, the HadGEM2-ES climate model exhibited the highest increases in electric loads in the RCP 8.5 scenario. The CNRM-CM5 climate scenario has the lowest increases in average temperatures for the RCP 4.5 and RCP 8.5 climate scenarios.

Similar to the residential sector, these increases are generally linked to increases in cooling loads, which are met exclusively by electricity. However, the difference between which climate model exhibited the highest increases in electric load demand between the commercial and residential sectors shows that the increases are not only linked to the average temperatures exhibited by different climate models, but also the interaction between the seasonality of the temperature increases and the residential and commercial load demand shapes.

The increase in temperatures that drive increases in space-cooling loads also affect peak electric loads in commercial buildings. In the commercial sector, the peak loads during peak commercial activity between noon and 3 p.m., which corresponds to the times where the

cooling loads are the highest. Therefore, increased temperatures due to climate change also manifest in increased peak electric loads due to the increased energy use of commercial cooling systems during commercial load peaks. A time series snapshot of the electric load profile of commercial buildings under historical climate and climate change-impacted conditions for the RCP 8.5 climate scenario is presented in Figure B-33 for each climate model and in Figure B-34 for the climate model average.

Figure B-33: Commercial Sector Electric Load Profiles Under Climate Change for Each Climate Model Under the RCP 8.5 Climate Scenario

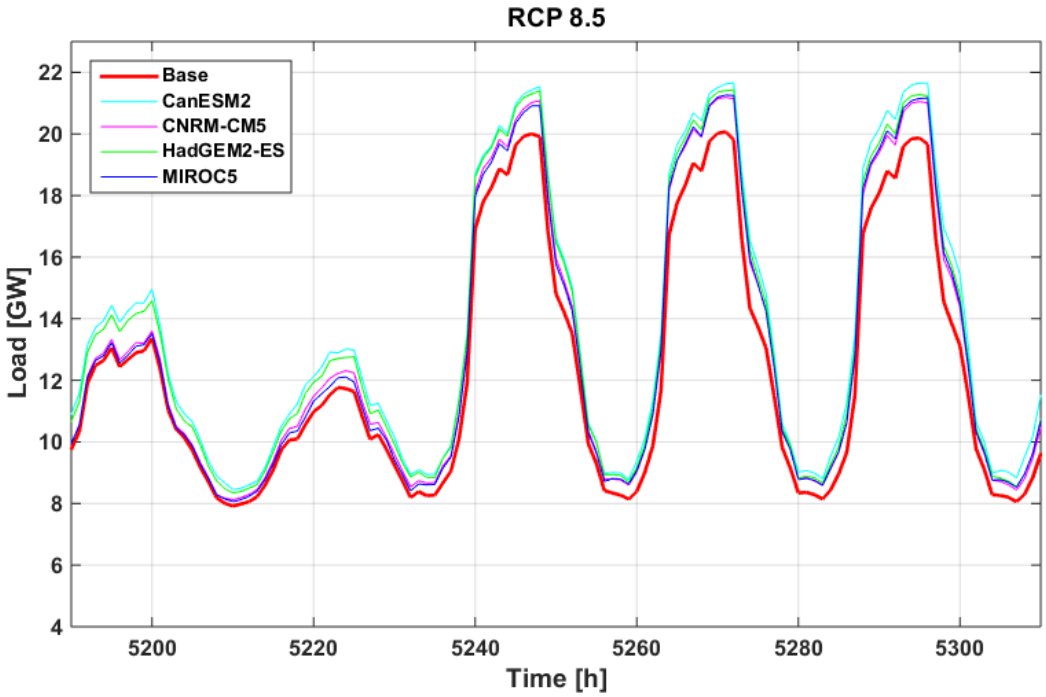

Source: Advanced Power and Energy Program, University of California, Irvine

Figure B-34: Commercial Sector Electric Load Profiles Under Climate Change for the Climate Model Average Under the RCP 8.5 Climate Scenario

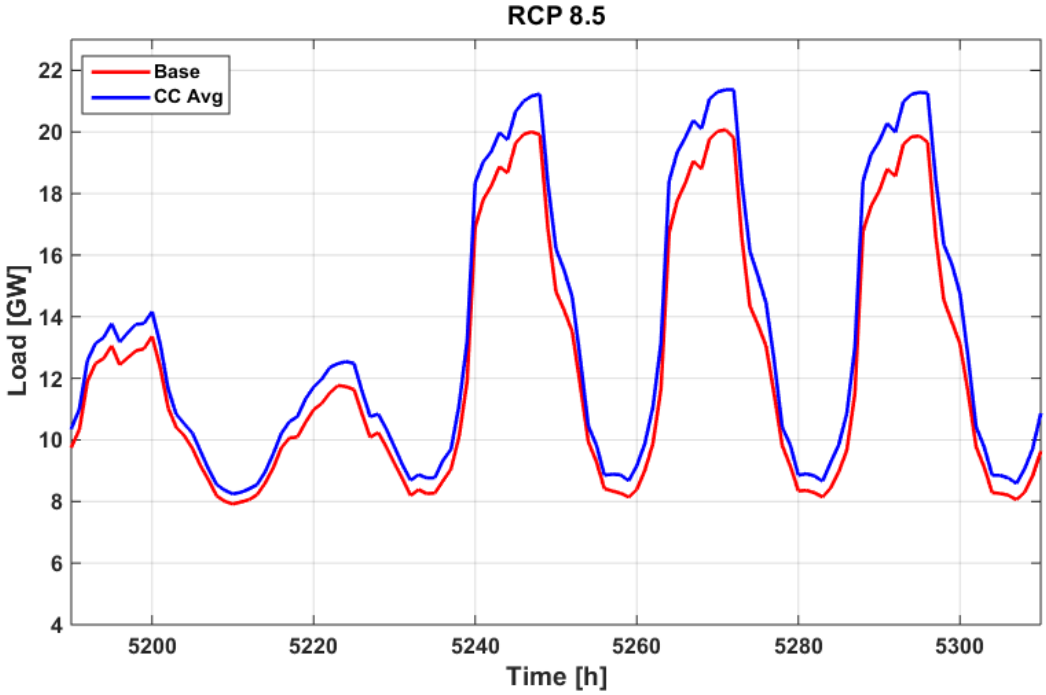

Source: Advanced Power and Energy Program, University of California, Irvine

The first two days in the snapshots represent weekend electric load profiles, while the following days represent weekday electric load profiles. The largest increases occur during the daytime on top of the current peak load demand. The impact of climate change-affected temperatures on typical commercial sector peak hourly electric loads are presented in Figure B-35 for percentage change from historical conditions (Base) and in Figure B-36 for absolute magnitudes. Because the climate conditions are derived from an average between 2046 and 2055 in the climate models to derive a *representative* 2050 profile, these are termed as *typical hourly peak electric demands*.

Figure B-35: Climate Change Impacts on Peak Hourly Electric Load Demand in Percentage Change From the Base Case for Different Climate Models and Climate Scenarios

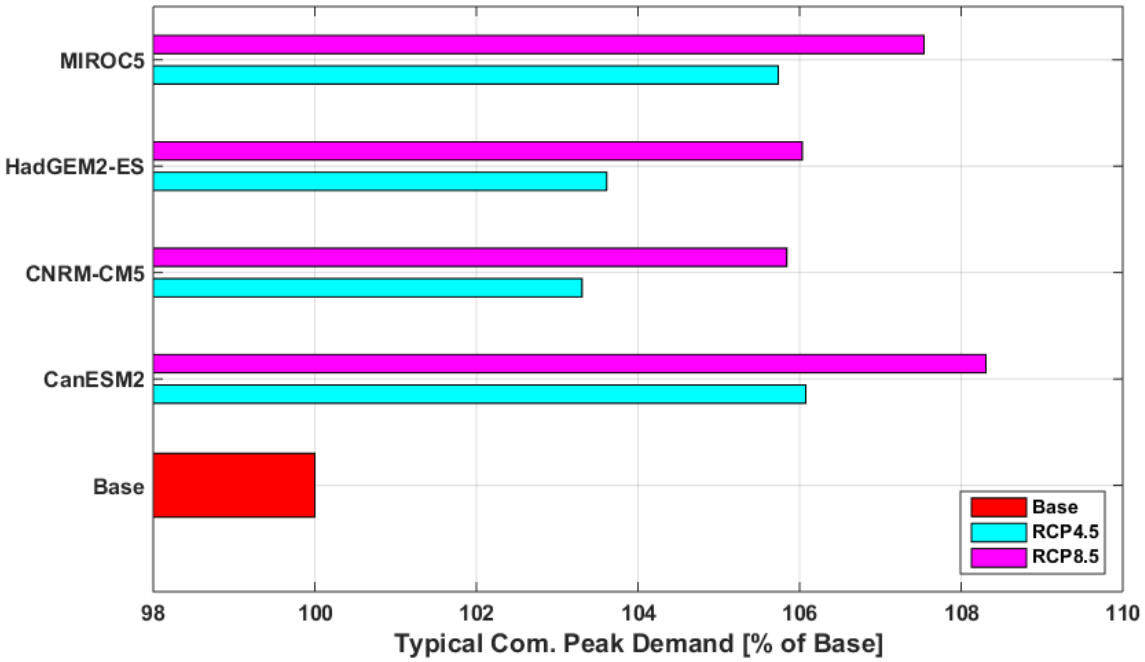

Source: Advanced Power and Energy Program, University of California, Irvine

Figure B-36: Climate Change Impacts on Peak Hourly Electric Load Demand in Absolute Magnitude for Different Climate Models and Climate Scenarios

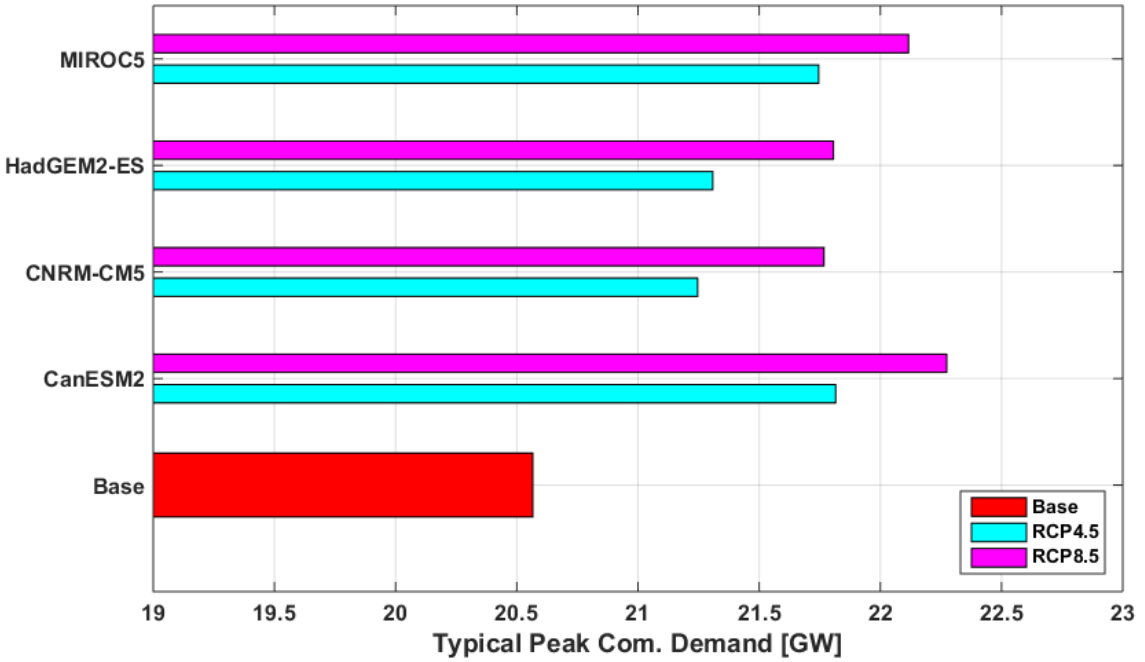

Source: Advanced Power and Energy Program, University of California, Irvine

For the commercial sector, the peak electric load demand due to climate change increases between 3.3% and 6.1% for the RCP 4.5 climate scenario and between 5.8% and 8.3% for the RCP 8.5 climate scenario, depending on climate model. In absolute terms, these increases translate to increases of between 0.68 and 1.00 GW for the RCP 4.5 cases and between 1.20 and 1.70 GW for the RCP 8.5 cases. As expected, the RCP 8.5 cases have higher peak electric loads due to higher temperatures, and the CanESM2 climate model tends to have the highest peak load increases. These increases, even on a percentage change basis, are significantly larger than those experienced by the residential sector. These increases occur because peak cooling loads for the commercial sector occur during the middle of the day, as opposed to the late afternoon/early evening for the residential sector. During the middle of the day, commercial activity is at the highest, and cooling systems must balance larger internal heat gains. Ambient temperatures are at the highest during this period, which increase loads on cooling systems and cause them to operate with decreased efficiency.

For the commercial sector, the annual site-level energy use under historical climate conditions and climate change-impacted conditions by end use is presented in Figure B-37. The end uses considered are space cooling, space heating, water heating, and other, as described in the results for the residential sector.

Figure B-37: Annual Site Level Commercial Energy Demand in Million MMBTU by End Use

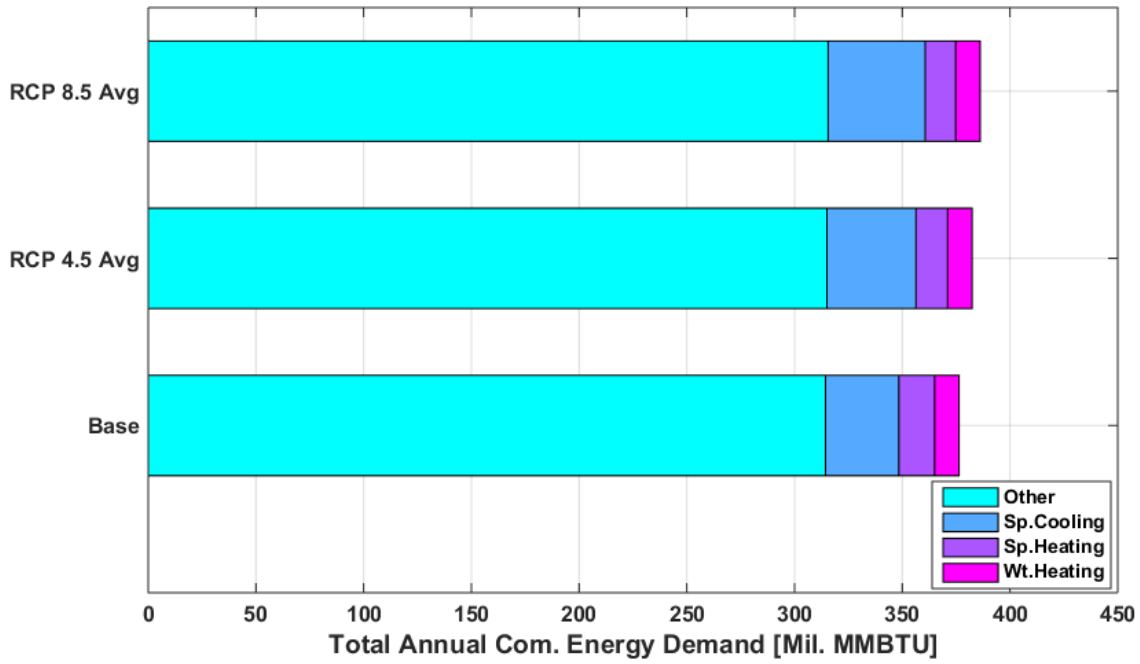

Sp. Cooling = Space Cooling, Sp. Heating = Space Heating, and Wt. Heating = Water Heating.

Source: Advanced Power and Energy Program, University of California, Irvine

Relative to the historical climate conditions, the onset of climate change slightly increases the site-level energy footprint of the commercial sector, in contrast to the results for the residential

sector. This occurs because space-heating demands are a smaller component of the commercial energy demand breakdown relative to space cooling. This is in contrast to the residential sector, where space-cooling and space-heating energy demands were about the same magnitude. The energy demands in the commercial sector occur during the day, which is when temperatures are the highest and space-heating loads are minimal. During the nighttime when temperatures are lower, commercial activity is decreased. Therefore, while the effects of decreased space heating loads do occur due to temperature increases, these decreases are small relative to the increases in space-cooling loads. The increases in space-cooling loads drive increases in the total site-level energy demand for commercial buildings. Another key characteristic to note, however, is that energy demands for uses other than space cooling, space heating, or water heating is a significantly larger component of commercial energy demand compared to residential energy demand. Commercial buildings have a more diverse array of equipment, such as plug loads and other equipment, which are not very sensitive to external temperature. The primary impact on the "other" category from temperature is due to effects on commercial building transformers due to increased electricity loads.

Again, this refers to site-level energy demand, not source-level energy demand. The impact on source-level energy demand will depend on the primary energy resources used to produce the electric energy inputs to the cooling system.

The change of site-level energy demand by end use under climate change is presented in Figure B-38 in percentage change from base and in Figure B-39 for absolute magnitude changes.

Figure B-38: Climate Change Impacts on Annual Site-Level Energy Demand by End Use in Percentage Change From the Base Case for Different Climate Scenarios

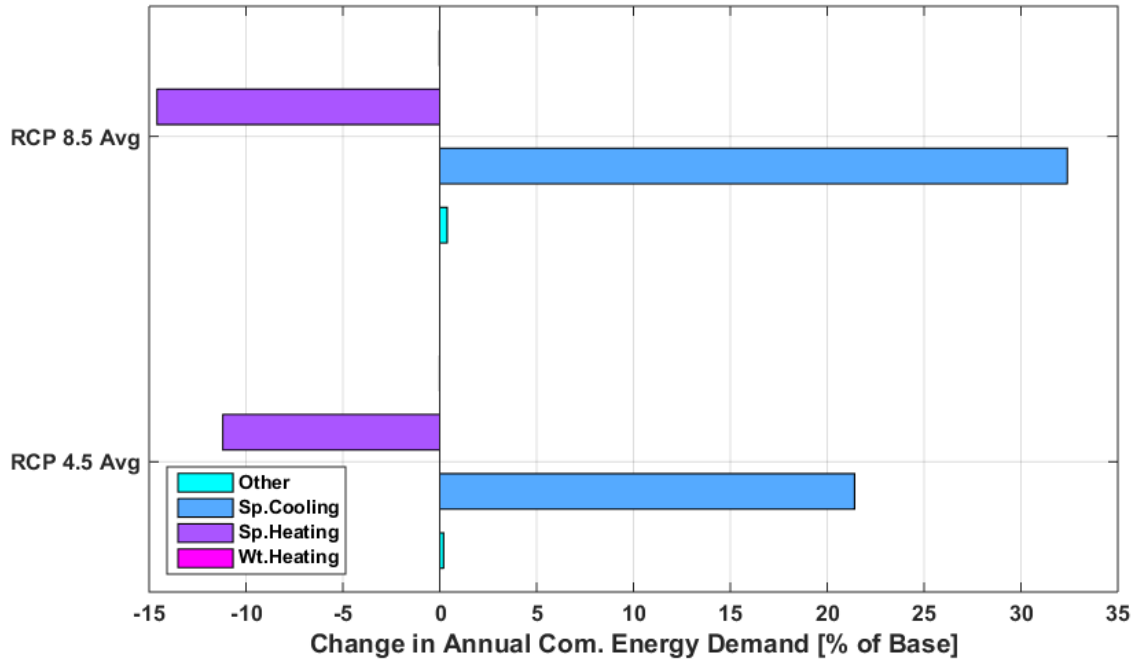

Source: Advanced Power and Energy Program, University of California, Irvine

Figure B-39: Climate Change Impacts on Annual Site-Level Energy Demand by End Use in Absolute Magnitude From the Base Case for Different Climate Scenarios

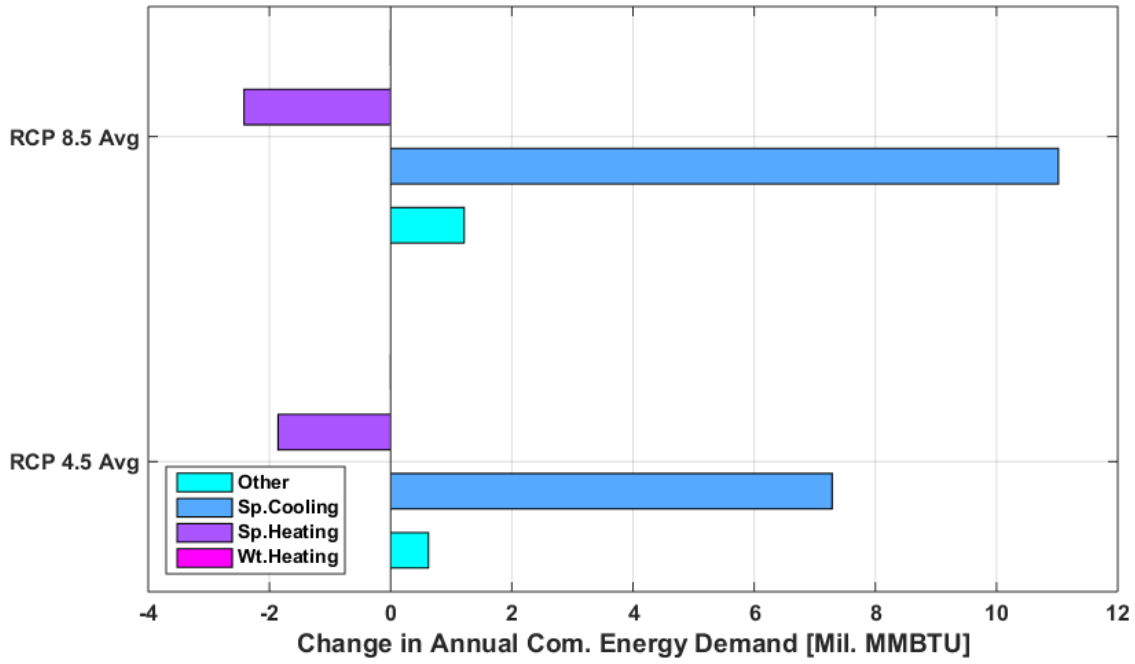

Source: Advanced Power and Energy Program, University of California, Irvine

By examining the end-use changes, the research team finds that the commercial sector exhibits increases in space-cooling energy demand (+21.41% to +32.39%), slight increases in other energy demands (+0.18% to +0.38%), decreases in space-heating demands (-11.20% to -14.59%), and no change in water heating demand. In absolute terms, the decrease in space-heating energy demand is smaller than the increase in space cooling demands, causing overall site-level energy demand to increase.

The increase in space-cooling energy demands and the decrease in space-heating and water-heating demands that do occur, however, still have the effect of shifting the distribution of energy use by fuel type toward electricity similar to the residential sector. The annual site-level energy demand for the commercial sector is presented in Figure B-40.

Figure B-40: Climate Change Impacts on Annual Site-Level Energy Demand by Fuel Type in Absolute Magnitude From the Base Case for Different Climate Scenarios

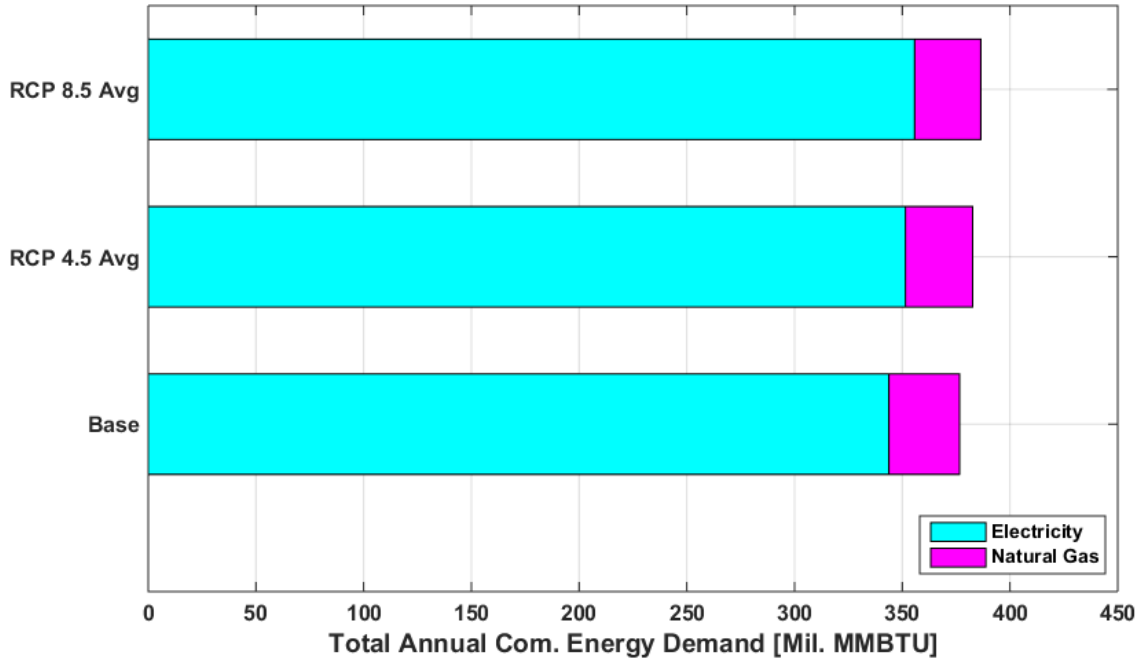

Source: Advanced Power and Energy Program, University of California, Irvine

The effect is slight, but the onset of climate change causes commercial buildings to increase reliance on electricity and decrease reliance on natural gas. Fuel oil is not plotted here because it is a negligible fraction of the energy use in the commercial sector in this analysis.

In addition to the statewide impacts of climate change on the commercial sector, the impacts of climate change vary across climate zone and location within the state. The annual commercial electricity demand by climate zone is presented in Figure B-41, and the change from historical climate conditions (Base) is presented in Figure B-42.

Figure B-41: Annual Commercial Electric Demand by Climate Zone Under Climate Change - Absolute Magnitude

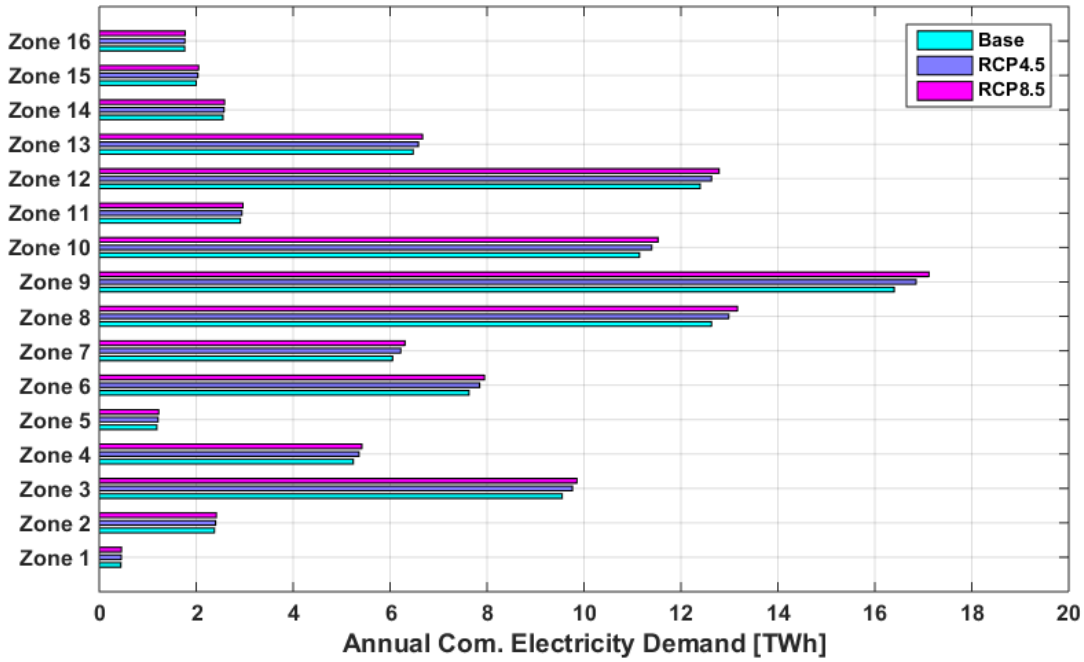

Source: Advanced Power and Energy Program, University of California, Irvine

Figure B-42: Annual Commercial Electric Demand by Climate Zone Under Climate Change - Percentage Change From Base

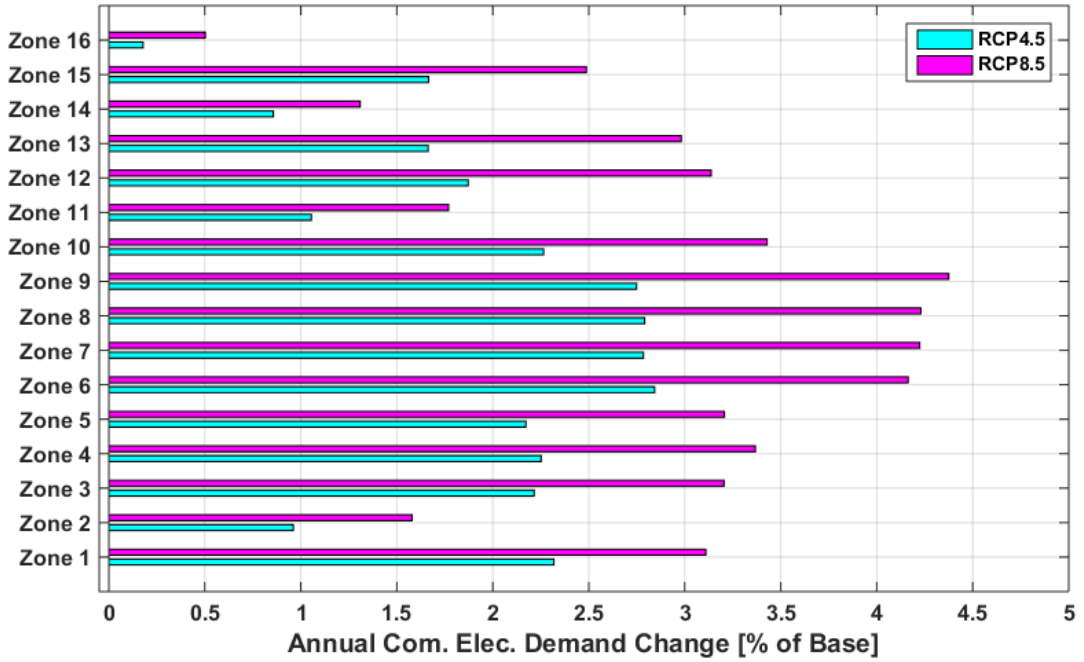

Source: Advanced Power and Energy Program, University of California, Irvine

The largest percentage increases in electricity demands occur in Climate Zones 6-10 for the RCP 4.5 and RCP 8.5 climate scenarios, similar to the results for the residential sector. These climate zones are all in Southern California, encompassing the heavily populated coastal and slightly inland areas of the state. These zones have high absolute electricity demands due to population. These results confer with those for the residential sector, showing that the largest increases in electricity demand even on a percentage change basis will occur in heavily populated areas of the state, focused in Southern California.

B.4. Chapter 5 Auxiliary Results

The main text of Chapter 5 presented the combined impacts of hydropower generation under climate change, geothermal constraints, and load demands on electricity system greenhouse gas emissions and renewable penetration. To better understand the driving factors behind the results presented in the previous section, these supporting results will present the effect of each climate change impact in isolation on the system to provide insight into which of these factors are the strongest contributors to the combined impacts.

B.4.1. Impacts of Hydropower Generation Under Climate Change

The impacts of how climate change affected hydropower alone on electricity system greenhouse gas emissions and renewable penetration are presented in Figure B-43 and Figure B-44, respectively.

Figure B-43: Difference in Electricity System Greenhouse Gas Emissions From Historical Conditions - Hydropower Impact Only

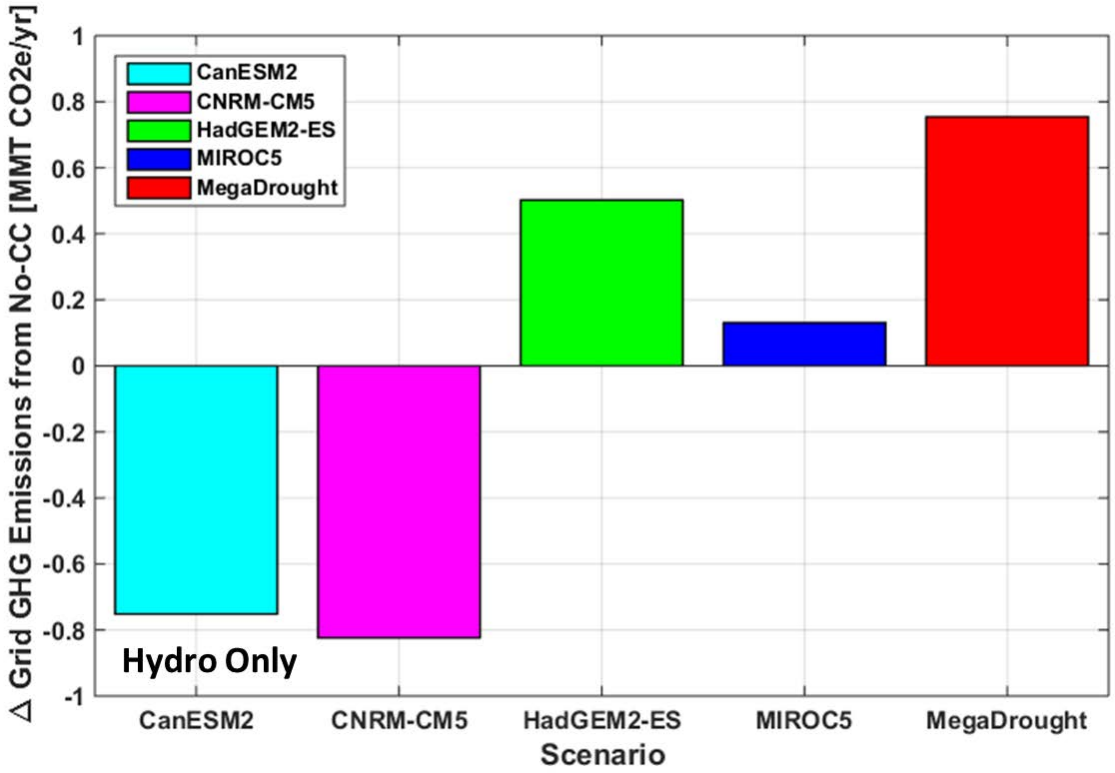

Source: Advanced Power and Energy Program, University of California, Irvine

Figure B-44: Difference in Electricity System Renewable Penetration From Historical Conditions - Hydropower Impact Only

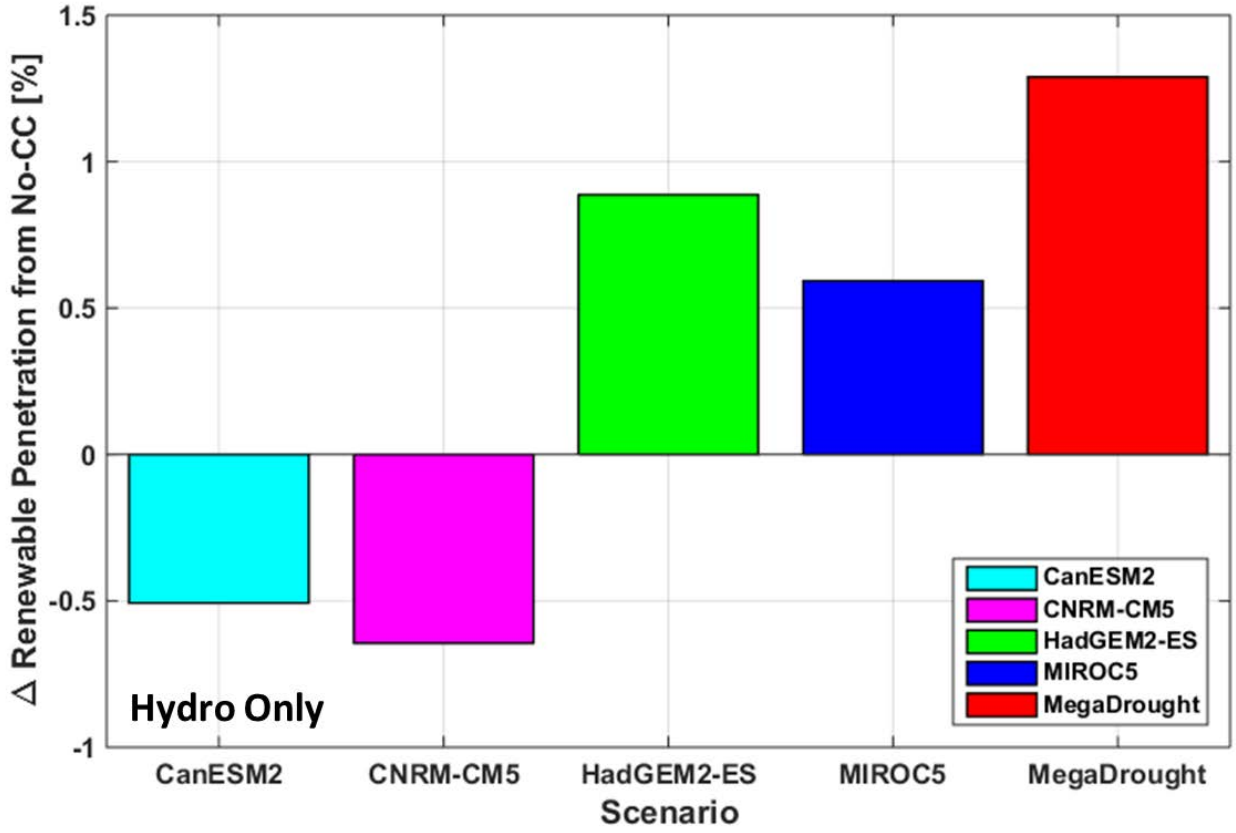

Source: Advanced Power and Energy Program, University of California, Irvine

The two wetter climate models (CanESM2 and CNRM-CM5) exhibit decreases in greenhouse gas emission of 0.75 MMT CO_2e/yr and 0.82 MMT CO_2e/yr, respectively, whereas the two drier climate models (HadGEM2-ES and MIROC5) exhibit increases of 0.50 MMT CO_2e/yr and 0.13 MMT CO_2e/yr respectively. The MegaDrought case exhibits an increase of 0.75 MMT CO_2e/yr. In general, the impact of climate change-affected hydropower alone is relatively small compared to the combined impacts discussed in Chapter 5, indicating that hydropower effects are not the major driver behind the overall emissions impacts of climate change. The wetter models decrease greenhouse gas emissions due to increasing hydropower generation, which is carbon-free in operation, while the drier models exhibit the opposite.

With regard to renewable penetration, the wetter models exhibit decreases in renewable penetration of 0.51% and 0.64%, respectively, while the drier models exhibit increases in renewable penetration of 0.89% and 0.59%, respectively. The MegaDrought case exhibits an increase of 1.29%. This percentage increase occurs because the increased hydropower generation in wetter models is absorbed by the system and displaces wind and solar generation in meeting the same load demand. The drier models exhibit the opposite trend, where the decrease in hydropower generation is compensated by a mix of natural gas-fired generation and additional use of otherwise curtailed wind and solar generation. These effects are presented by the change in the generation profile from historical conditions in Figure B-45.

Figure B-45: Change in Delivered Electricity Distribution by Resource in 2050 Due to Climate Change - Hydropower Impact Only

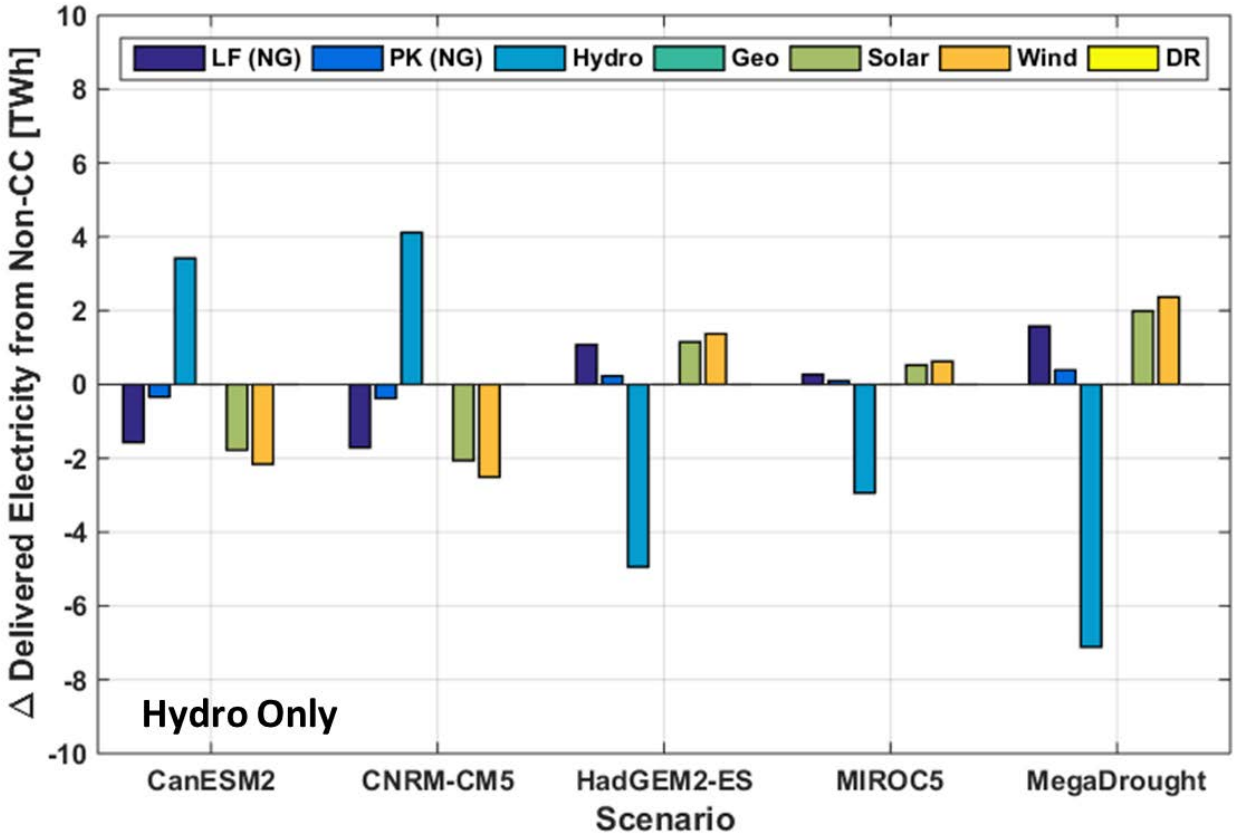

Source: Advanced Power and Energy Program, University of California, Irvine

Overall, under the climate effects predicted by the IPCC AR5 modeling set, hydropower under climate change is not expected to affect the greenhouse gas emissions of the electricity system significantly. This occurs in this case due to the overall wetter climate predicted under the RCP 8.5 pathway, which even with increased spillage still allows hydropower generation to remain close to historical levels on a 10-year average basis. Individual years may vary significantly, however.

B.4.2. Impacts of Climate Change-Constrained Geothermal Resources

The impacts of climate change-constrained geothermal resources alone on electricity system greenhouse gas emissions and renewable penetration are presented in Figure B-46 and Figure B-47, respectively. These results are presented differently than those for hydropower, since the impacts on geothermal resources are similar across climate models. Therefore, one aggregated climate change impact scenario is used to characterize the impact of climate change.

Figure B-46: Electricity System Greenhouse Gas Emissions Under Historical and Climate Change Conditions – Constrained Geothermal Impact Only

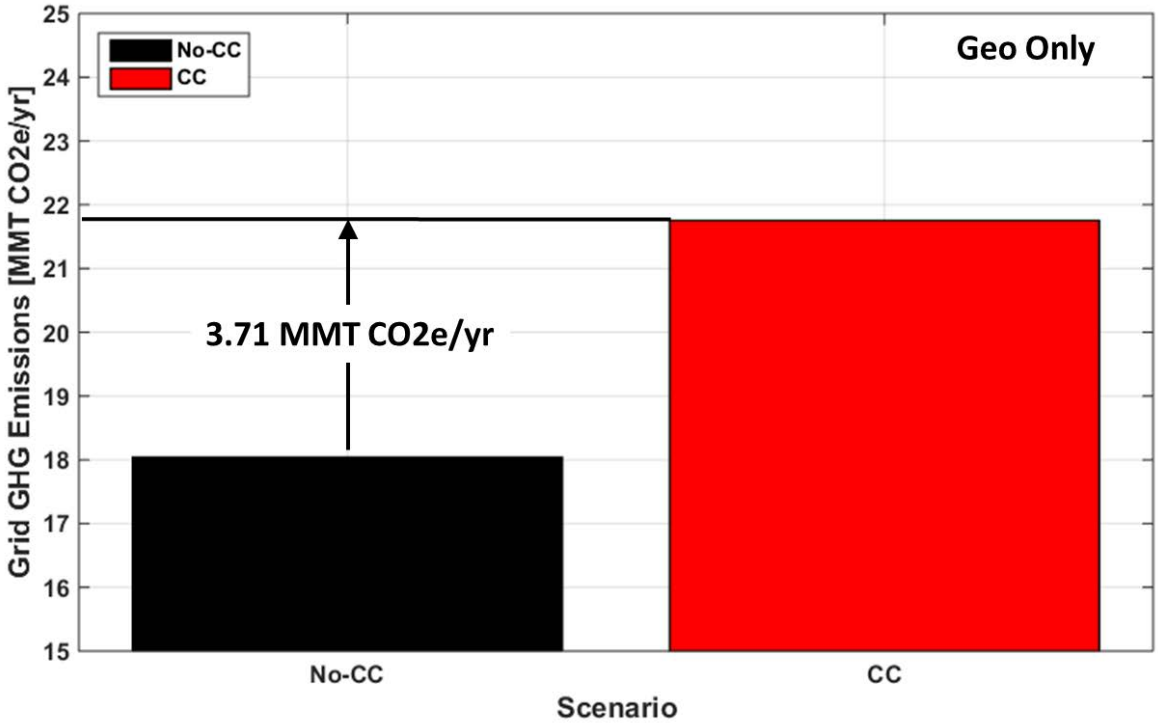

Source: Advanced Power and Energy Program, University of California, Irvine

Figure B-47: Electricity System Renewable Penetration Under Historical and Climate Change Conditions – Constrained Geothermal Impact Only

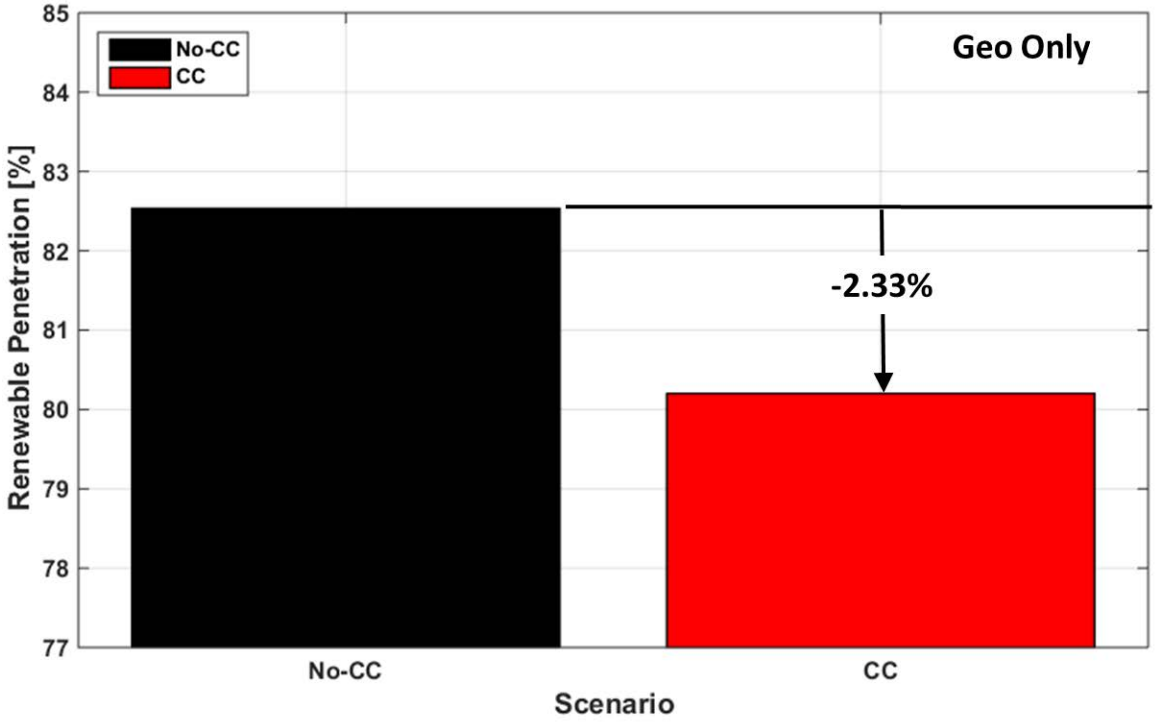

Source: Advanced Power and Energy Program, University of California, Irvine

The impact of limiting geothermal resource usage due to water availability constraints causes an increase in greenhouse gas emissions of 3.71 MMT CO_2e/yr and a decrease of 2.33% in electricity system renewable penetration. When compared to the magnitudes of the results for the combined climate change impacts, the impact of constrained geothermal resources is a large contributor to the overall result. Geothermal resources, while not a large part of the overall resource mix by capacity in 2050, still provide a base load resource that is both carbon-free and counted as renewable, as well as exhibits very high capacity factors and, therefore, provides a nontrivial fraction of the overall resource mix by energy. In the non-climate change compliance scenario, geothermal accounts for about 6.3% of overall delivered electricity. The loss of this resource must be compensated by other resources; however, since otherwise curtailed wind and solar generation is not available at sufficient scale at all hours of the year, natural gas load following and peaking power plants provide the difference. This is exhibited through the change in generation mix presented in Figure B-48.

Figure B-48: Change in Delivered Electricity Distribution by Resource in 2050 Due to Climate Change - Constrained Geothermal Impact Only

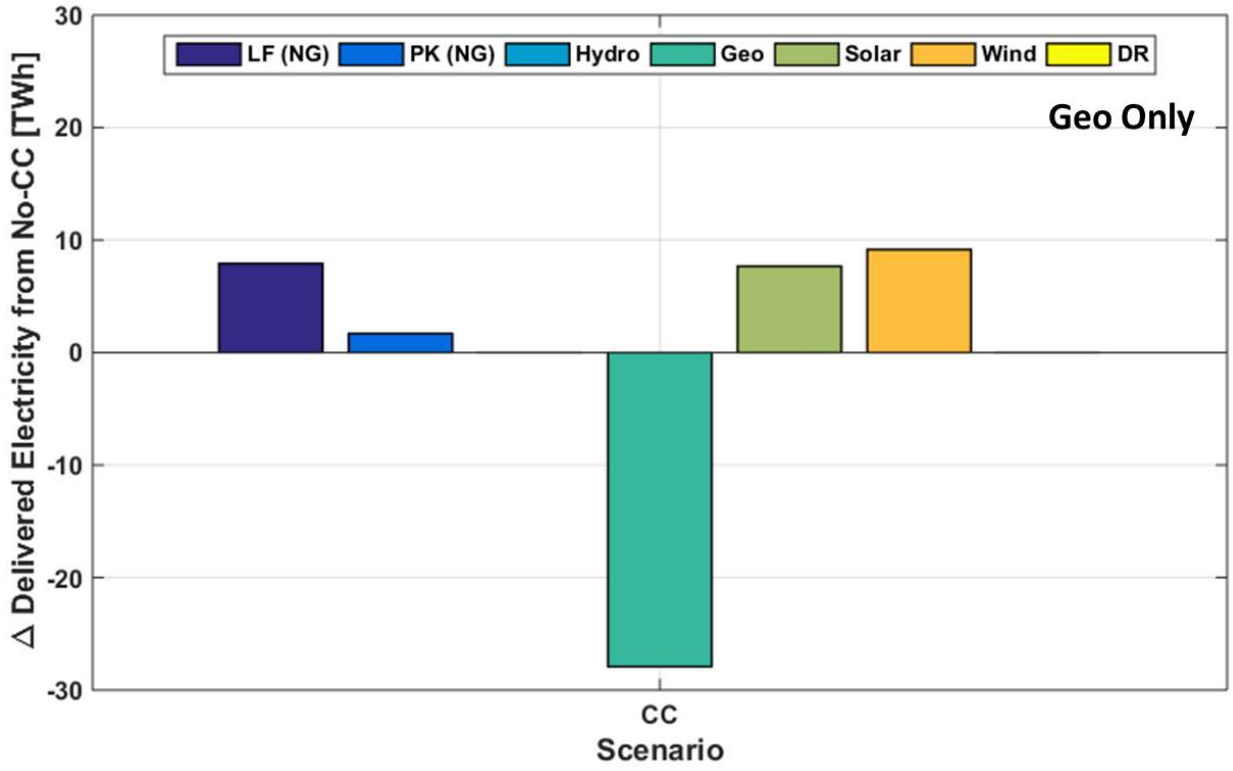

Source: Advanced Power and Energy Program, University of California, Irvine

The presence of otherwise curtailed wind and solar generation during some of the hours of the year to compensate for the loss of geothermal generation limits the magnitude of emissions increase and renewable penetration decreases. In this case, the additional increase in the use of wind and solar resources each are of about the same magnitude as the additional increase in natural gas resources. This finding indicates that without the slight overbuild of renewable resources, the loss of geothermal resources would have caused double the emissions impact.

B.4.3. Impacts of Residential and Commercial Building Electric Loads Under Climate Change

The impacts of climate change affected hydropower alone on electricity system greenhouse gas emissions and renewable penetration are presented in Figure B-49 and Figure B-50, respectively.

Figure B-49: Difference in Electricity System Greenhouse Gas Emissions From Historical Conditions – Electric Load Impact Only

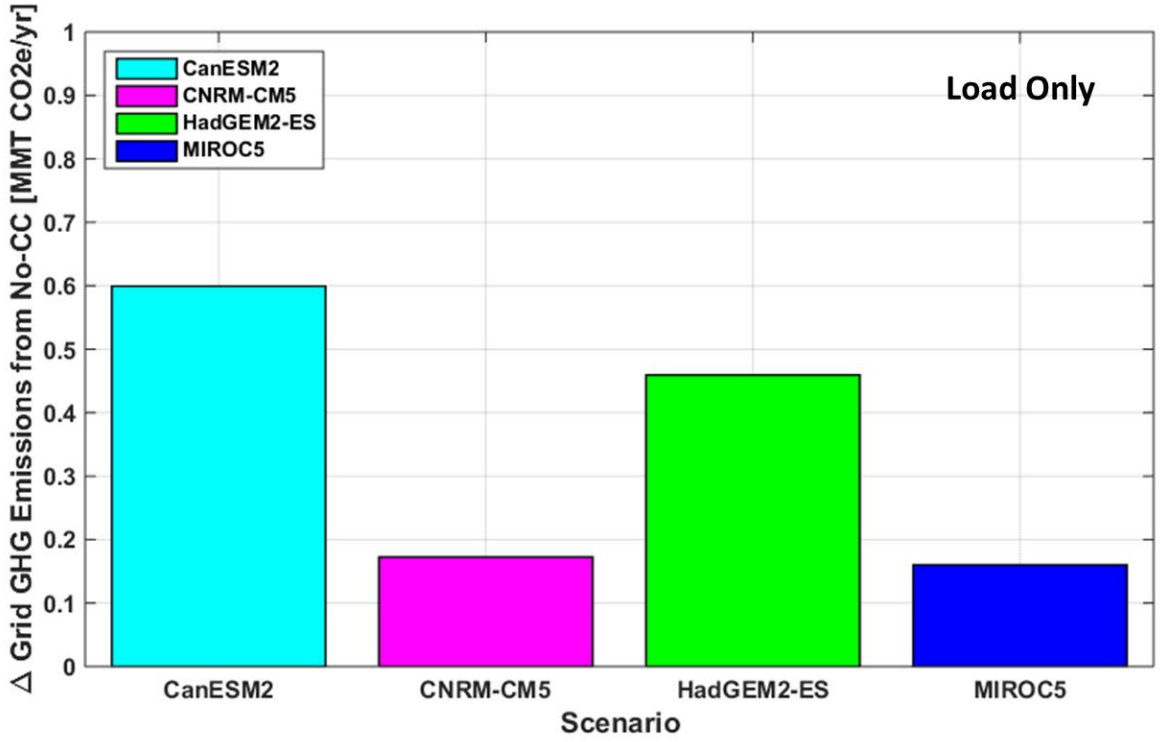

Source: Advanced Power and Energy Program, University of California, Irvine

Figure B-50: Difference in Electricity System Renewable Penetration From Historical Conditions – Load Impact Only

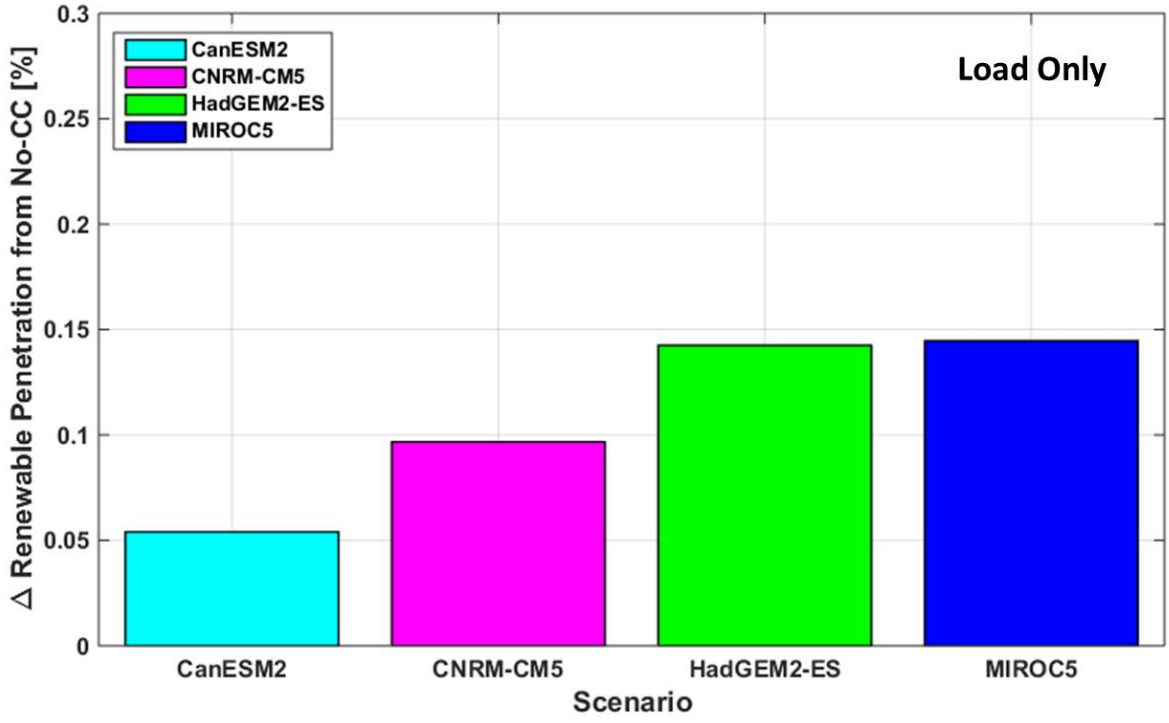

Source: Advanced Power and Energy Program, University of California, Irvine

The CanESM2 and HadGEM2-ES climate models exhibited the highest temperatures and electric load increases, which translate into the highest electricity system greenhouse gas emissions increases of the set of 0.60 MMT CO_2e/yr and 0.46 MMT CO_2e/yr. The CNRM-CM5 and MIROC5 climate models produced emissions increases of 0.17 MMT CO_2e/yr and 0.16 MMT CO_2e/yr, respectively. When compared to the greenhouse gas emissions increases due to the combined impacts, the effect of increased electric loads is a small contributor to the overall impact of climate change.

While climate change does increase electric load demands by a nontrivial amount, especially during the summer months and daytime hours, the bulk of the load increases tend to occur during the middle of the day due to increased space-cooling loads. During these times, however, there is typically a large amount of otherwise curtailed solar generation due to the high capacity of solar resources installed in the non-climate change compliance scenario. Therefore, during heat waves and the summer months, the marginal increase in electric loads is met by solar generation and does not contribute to emissions increases. The emissions increases that occur do so at times when cloud cover is prevalent or during the late afternoon/evening hours, when solar is decreasing, wind has typically not yet picked up, but temperatures are still relatively high. During these events, natural gas power plants meet the marginal load increase.

This impact of using additional solar generation is exemplified by small increases in the renewable penetration level. On this metric, there are differences among the climate models

due to the timing of the load increases slightly differing among the models. The CanESM2 model exhibits the lowest increase in renewable penetration, while the MIROC5 model shows the largest increase. The CanESM2 model shows a large increase in annual electric load magnitude, but a larger portion of the load increases occurs outside hours with excess wind and solar generation compared to HadGEM2-ES, which has a similar load magnitude increase.

The change in the mix of delivered electricity due to the load increases is presented in Figure B-51.

Figure B-51: Change in Delivered Electricity Distribution by Resource in 2050 Due to Climate Change - Load Impact Only

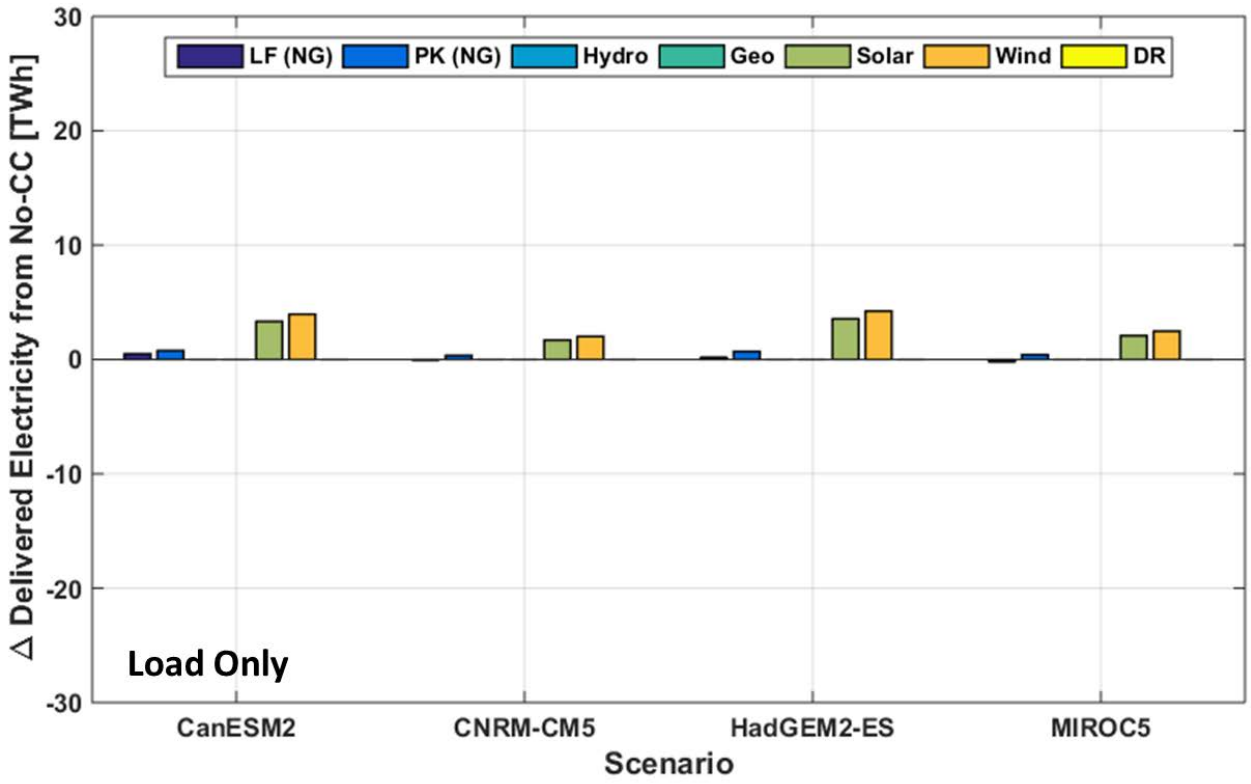

Source: Advanced Power and Energy Program, University of California, Irvine

All the cases show the largest increase in delivered electricity coming from wind and solar generation, as otherwise curtailed generation from these resources is used by the additional loads. In the CNRM-CM5 and MIROC5 models, the timing of load increases and renewables actually causes a small decrease in natural gas-fired load following generation.

B.5. Chapter 6 Auxiliary Results

B.5.1. Enabling Renewable Resources to Provide Spinning Reserve

The impact of allowing renewable resources to provide spinning reserve when excess generation is available on electricity greenhouse gas emissions is presented for the 10-year simulation time frame in Figure B-52, on the 10-year average in Figure B-53, and in terms of the

difference from the no-climate change case in Figure B-54. Each color represents a different climate model. The dotted lines in Figure B-52 denote the cases that allow renewable resources to provide spinning reserve, while the label "RenAS" denotes these cases in Figure B-53 and Figure B-54.

Figure B-52: Electric Grid Greenhouse Gas Emissions under Historical and Climate Change Conditions Over the 10-Year Simulation Time Frame (2046-2055), Centered on 2050

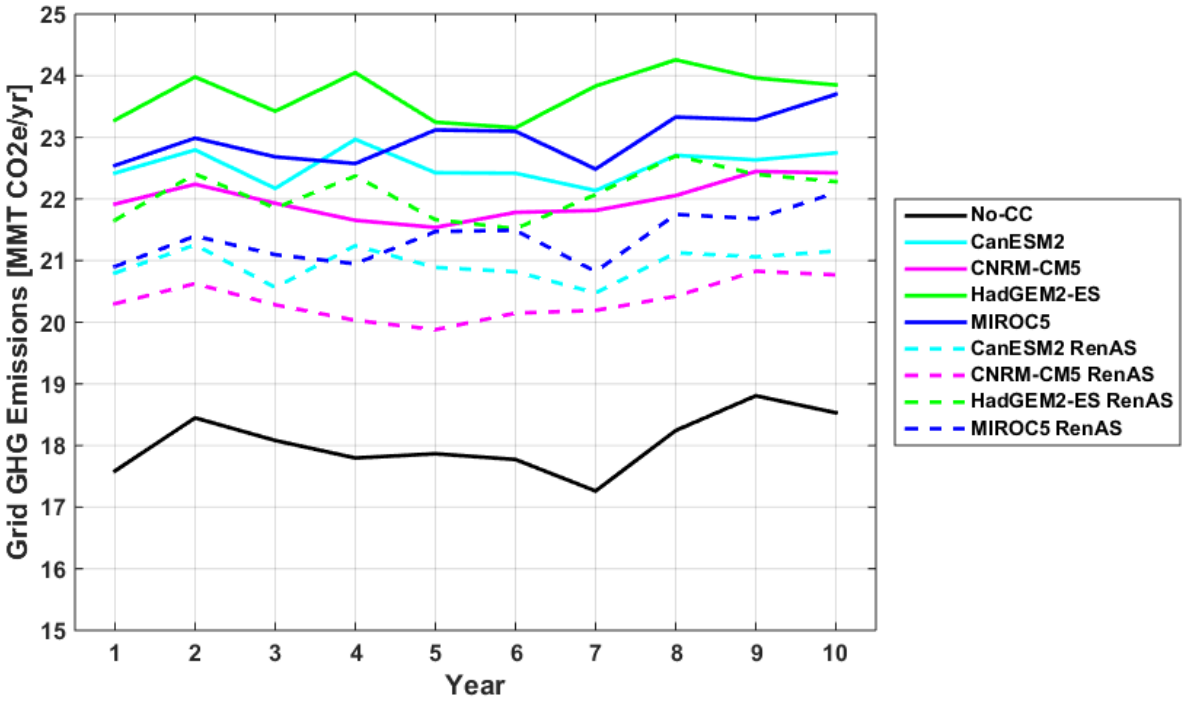

"RenAS" represents the cases where renewable resources are allowed to provide spinning reserve.

Source: Advanced Power and Energy Program, University of California, Irvine

Figure B-53: Electric Grid Greenhouse Gas Emissions Under Historical and Climate Change Conditions – 10-Year Average Representing 2050

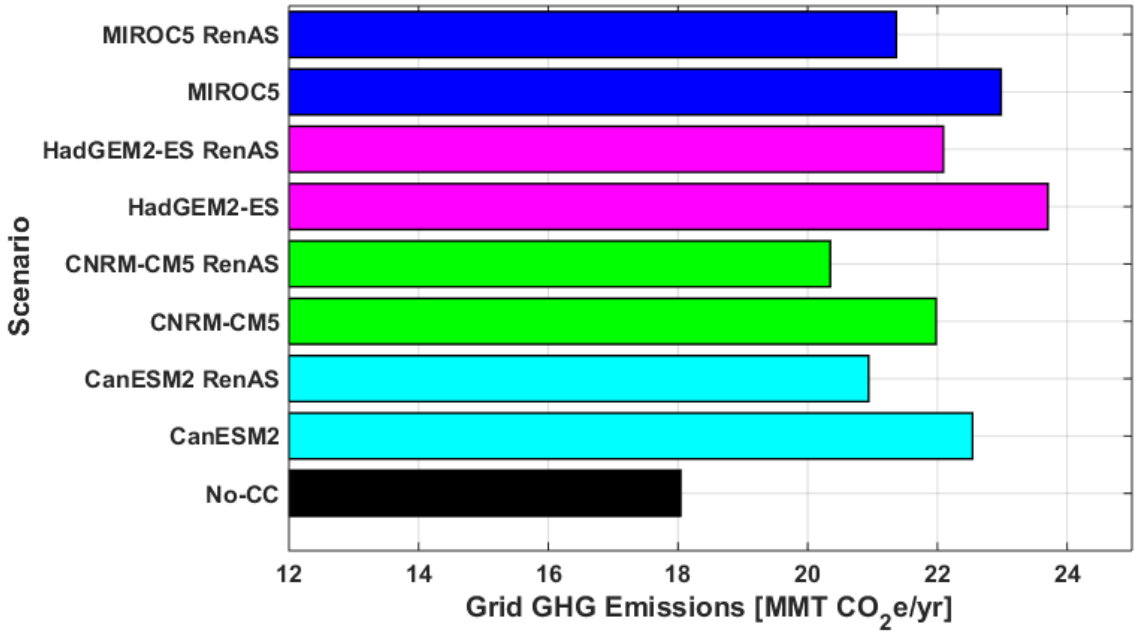

"RenAS" represents the cases where renewable resources are allowed to provide spinning reserve.

Source: Advanced Power and Energy Program, University of California, Irvine

Figure B-54: Electric Grid Greenhouse Gas Emissions Difference From Historical Climate Conditions – 10-Year Average Representing 2050

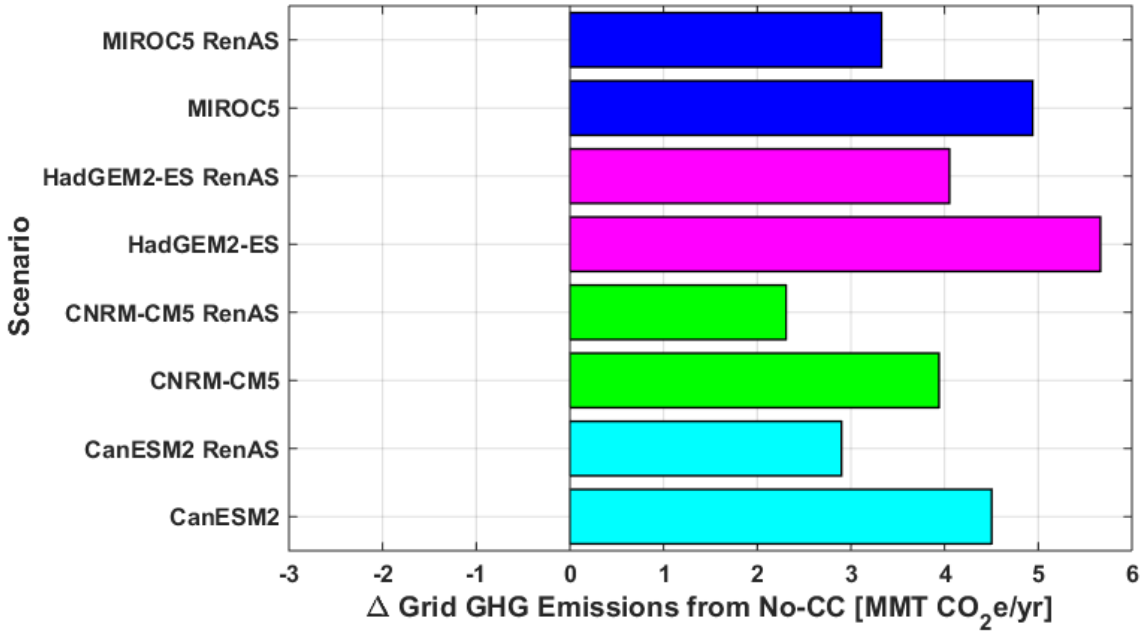

"RenAS" represents the cases where renewable resources are allowed to provide spinning reserve.

Source: Advanced Power and Energy Program, University of California, Irvine

Allowing wind and solar generation to provide ancillary services and turn down or shut off natural gas load-following power plants has a beneficial impact, but it is relatively small and does not allow the system to come close to reducing the greenhouse gas emissions due to climate change impacts on the electricity system. On average, allowing renewable resources to provide spinning reserve services accounts for about a 1.3 MMT CO_2e/yr reduction in greenhouse gases.

While this option does provide some benefit, the emissions reductions are limited due to a few factors. First, the primary use of natural gas load-following generation with the grid resource mixes specified here is to provide generation to ensure that the electric load demand is balanced during the hours in the year when wind and solar generation are low relative to demand. The majority of the greenhouse gas emissions from the electricity system in these cases occur when providing this function. Second, allowing renewable resources to provide spinning reserve using curtailed generation allows natural gas power plants to be turned down only during periods when curtailed renewable generation is available and the amount of natural gas generation is already relatively low.

This option, however, is more of a management change in the system as opposed to a hardware investment and does provide a nontrivial benefit. Therefore, even though by itself it will not build resilience into the electricity system to the impacts of climate change on the ability of the system to meet the state's greenhouse gas emissions reduction goals, it is an option that should be considered in conjunction with one or more of the others investigated in this study.

The impacts of enabling renewable resources to provide spinning reserve compared to the base case on the renewable penetration level is presented for the 10-year simulation time frame in Figure B-55, on the 10-year average in Figure B-56, and in terms of the difference from the no-climate change case in Figure B-57. Each color represents a different climate model. The dotted lines in Figure B-55 denote the cases with renewable spinning reserve, while the label "RenAS" denotes these cases in Figure B-56 and Figure B-57.

Figure B-55: Renewable Penetration Level Under Historical and Climate Change Conditions Over the 10-year Simulation Time Frame (2046-2055), Centered on 2050

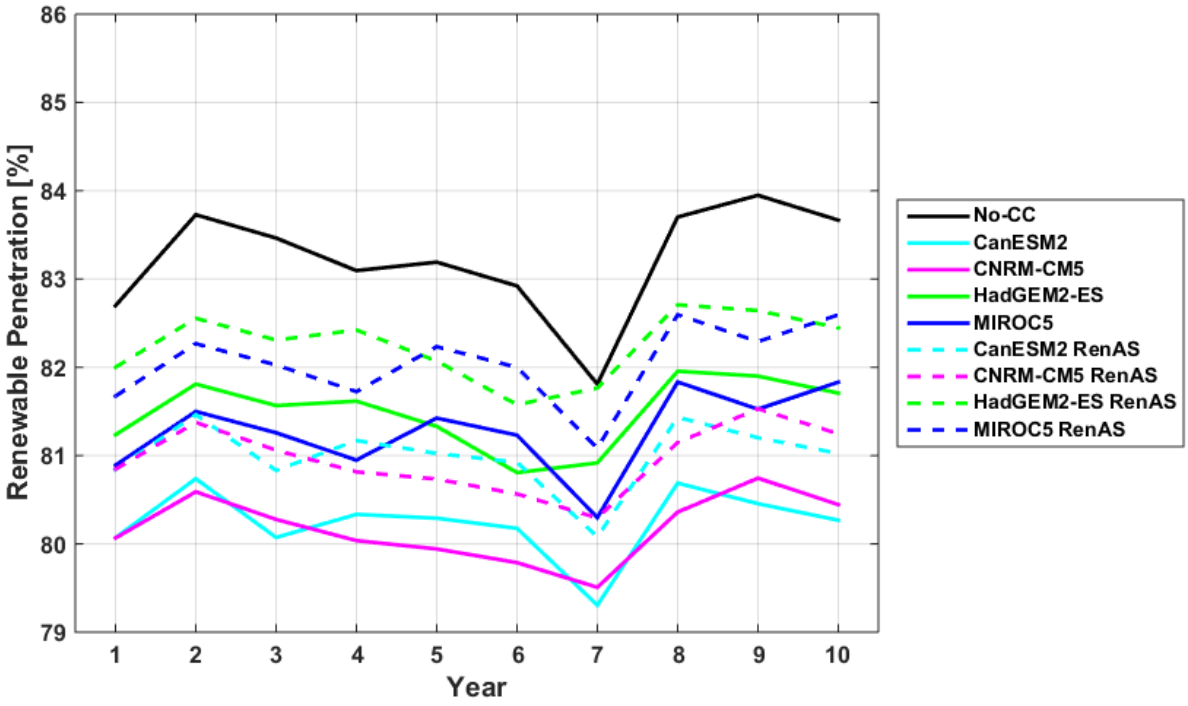

"RenAS" represents the cases where renewable resources are allowed to provide spinning reserve.

Source: Advanced Power and Energy Program, University of California, Irvine

Figure B-56: Electric Grid Renewable Penetration Level Under Historical and Climate Change Conditions – 10-Year Average Representing 2050

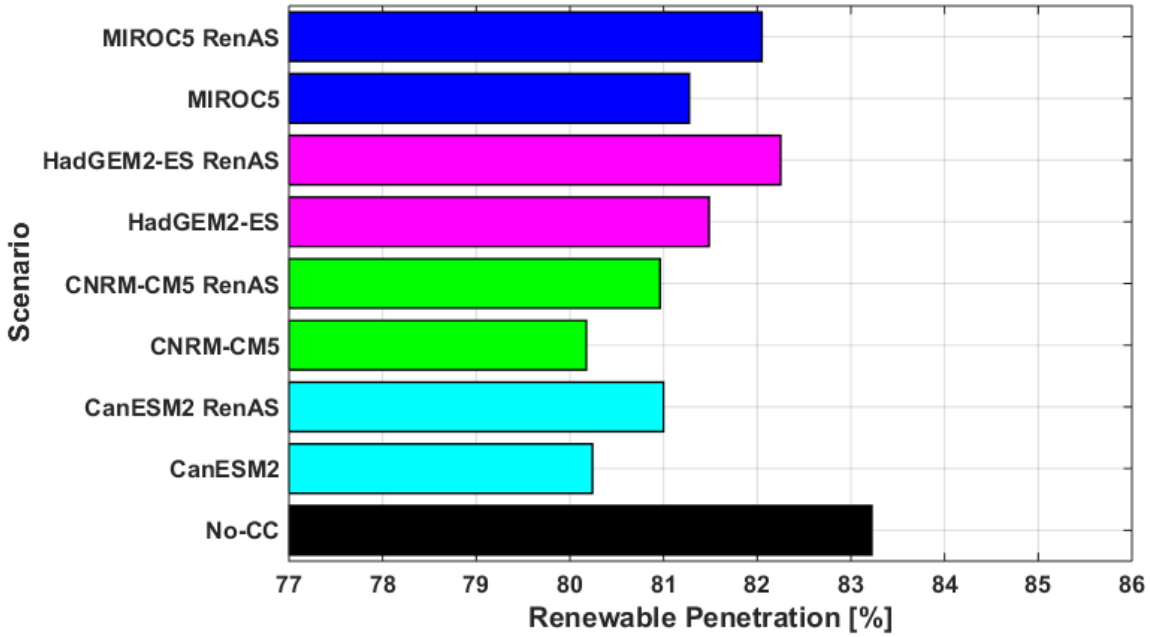

"RenAS" represents the cases where renewable resources are allowed to provide spinning reserve.

Source: Advanced Power and Energy Program, University of California, Irvine

Figure B-57: Electric Grid Renewable Penetration Level Under Historical and Climate Change Conditions – 10-Year Average Representing 2050

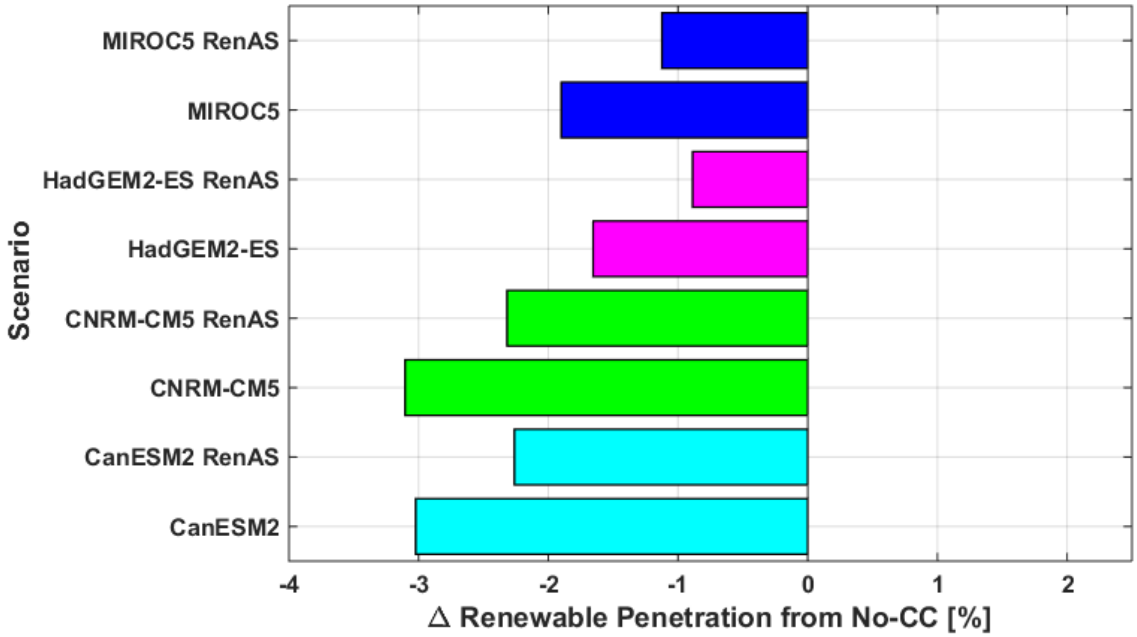

"RenAS" represents the cases where renewable resources are allowed to provide spinning reserve.

Source: Advanced Power and Energy Program, University of California, Irvine

Allowing renewable resources to provide spinning reserve services allows the renewable penetration level to be increased relative to the case without this capability for each climate model. Similar to the results for greenhouse gas emissions, however, this option alone does not allow the system to raise the renewable penetration level to that of the no-climate change case. Overall, allowing renewable supply of spinning reserve accounts for an improvement in renewable penetration of about 0.6% on average.

The breakdown of delivered electricity by resource to meet the electric load demand is presented for each case in Figure B-58, with the difference in delivered electricity by resource from the no-climate change case presented in Figure B-59.

Figure B-58: Delivered Electricity Distribution by Resource in 2050 for Each Climate Model

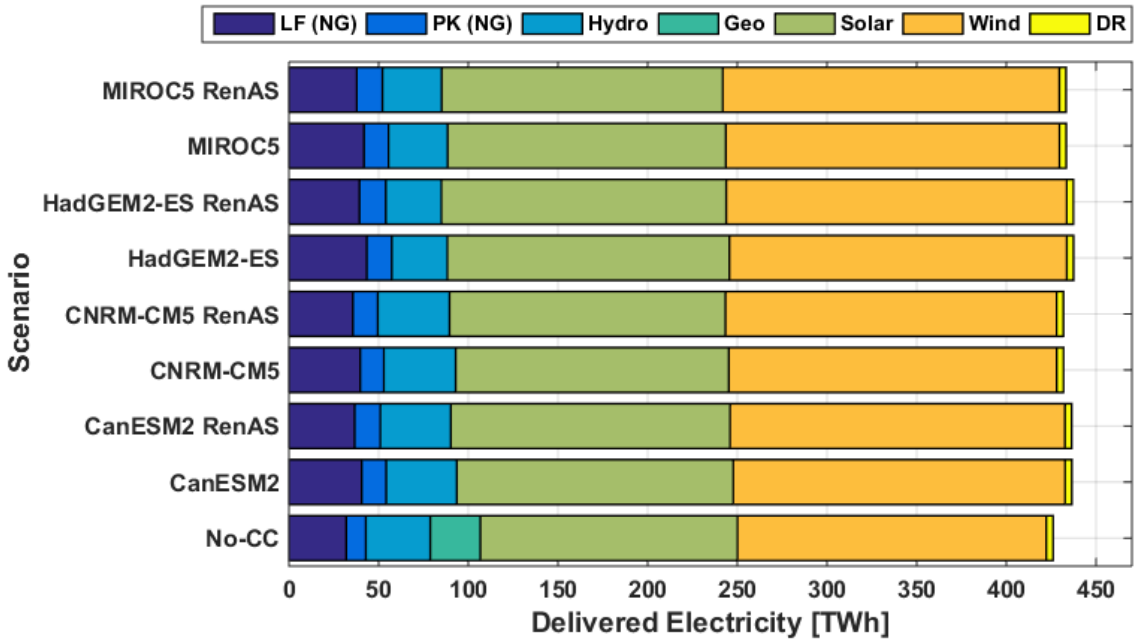

"RenAS" represents the cases where renewable resources are allowed to provide spinning reserve.

Source: Advanced Power and Energy Program, University of California, Irvine

Figure B-59: Change in Delivered Electricity Distribution by Resource in 2050 Due to Climate Change and Increased Battery Energy Storage

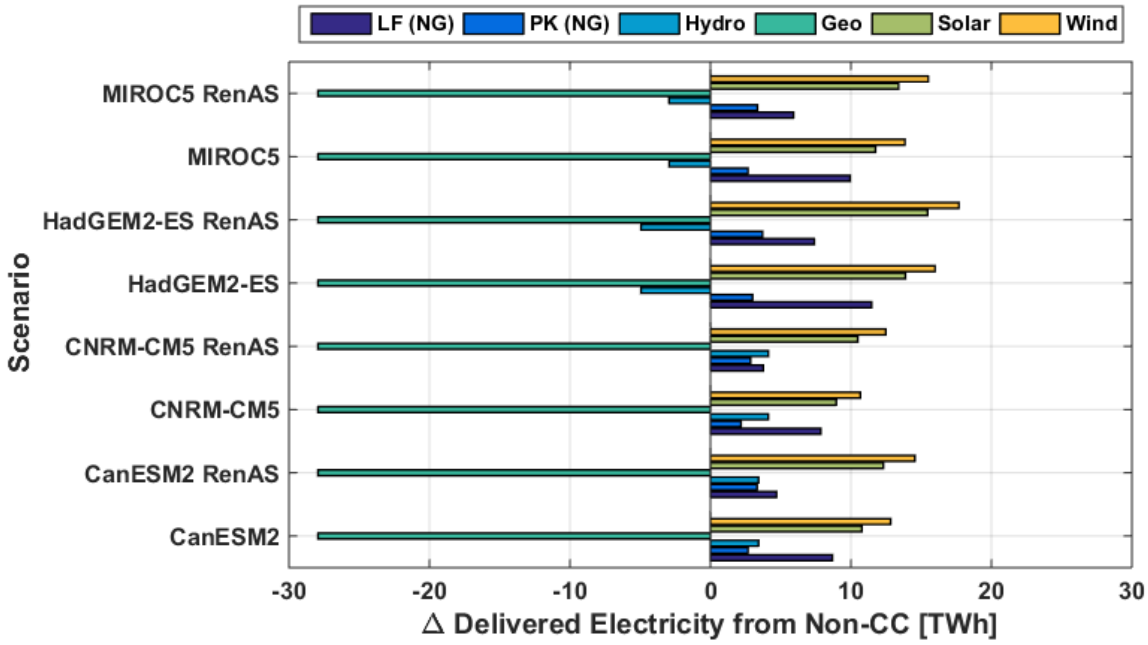

"RenAS" represents the cases where renewable resources are allowed to provide spinning reserve.

Source: Advanced Power and Energy Program, University of California, Irvine

Allowing renewable resources to provide spinning reserve acts mainly to reduce reliance on load-following generation relative to the cases without this capability. Increased uptake of renewable resources occurs due to the turndown of these generators during periods where large amounts of renewable curtailment are available. However, allowing renewable provision of spinning reserve does not reduce peaking power plant generation. This adds another factor to why this option is limited in reducing greenhouse gas emissions. Natural gas load-following power plants are typically large combined-cycle power plants with high design point and part-load efficiencies, while peaking power plants are typically simple-cycle gas turbine power plants with relatively low design and part-load efficiencies. Therefore, allowing renewable resources to provide spinning reserve reduces generation from a resource that emits carbon but is relatively efficient and has relatively low emissions to begin with. The amount of emissions reduction resulting from this is, therefore, limited.

Overall, allowing renewable resources to provide spinning reserve services provides a nontrivial benefit to the system in terms of greenhouse gas emissions reductions and increased renewable resource usage. The extent of these benefits, however, are not sufficient to overcome the impacts of climate change on the electricity system in affecting these metrics. Despite this, implementing this option should still be considered. This study examined the spinning reserve effect with historical spinning reserve requirements. If these requirements increase in the future, this option will become more important.